Influence of Individual Radiosensitivity on Biological Responses to Ionizing Radiation Dose Estimation and the Role of Telomere Maintenance

Grace Shim

UNIVERSITÉ PARIS-SUD

ÉCOLE DOCTORALE 418
DE CANCÉROLOGIE

Laboratoire de Radiobiologie et Oncologie

THÈSE DE DOCTORAT
en

SCIENCES DE LA VIE ET DE LA SANTE

par

Grace SHIM

Influence de la radiosensibilité individuelle sur les réponses biologiques à des rayonnements ionisants, l'estimation de la dose, et le rôle de maintenance des télomères

Date de soutenance : 30 septembre 2015

Composition du jury :

Directeur de thèse :	Laure SABATIER	CEA, Fontenay-aux-Roses, France
Co-directeur de thèse :	Edouard AZZAM	Rutgers University, Newark, NJ, USA
Rapporteurs :	Dietrich AVERBECK Elena GIULOTTO	CEA / IRSN, Fontenay-aux-Roses, France Università di Pavia, Pavia, Italy
Examinateurs :	Michel BOURGUIGNON Christophe BADIE	IRSN, Fontenay-aux-Roses, France Public Health England, London, UK

UNIVERSITÉ PARIS-SUD

ÉCOLE DOCTORALE 418
DE CANCÉROLOGIE

Laboratory of Radiobiology and Oncology

DOCTORAL THESIS
in

LIFE AND HEALTH SCIENCES

by

Grace SHIM

Influence of individual radiosensitivity on biological responses to ionizing radiation, dose estimation, and the role of telomere maintenance

Date of thesis defense: September 30, 2015

Composition of jury:

Director of thesis:	Laure SABATIER	CEA, Fontenay-aux-Roses, France
Co-director of thesis:	Edouard AZZAM	Rutgers University, Newark, NJ, USA
Reviewers:	Dietrich AVERBECK Elena GIULOTTO	CEA / IRSN, Fontenay-aux-Roses, France Università di Pavia, Pavia, Italy
Examiners:	Michel BOURGUIGNON Christophe BADIE	IRSN, Fontenay-aux-Roses, France Public Health England, London, UK

ACKNOWLEDGEMENTS / REMERCIEMENTS

Je tiens à exprimer mes sincères remerciements à Laure Sabatier de m'avoir accueillie en France et dans son Laboratoire de Radiobiologie et Oncologie (LRO) du Commissariat à l'énergie atomique et aux énergies alternatives (CEA), et de m'avoir permis d'effectuer ce travail sous ta direction. Ta confiance et ton soutien m'ont particulièrement motivée.

I would like to sincerely thank Edouard Azzam for encouraging me to continue my studies in France, and for his continued guidance and support through this entire adventure.

I would like to thank all the members of the jury for this thesis who have given me the honor of accepting with enthusiasm to judge my work. Thank you to Dr. Dietrich Averbeck and Professor Elena Giulotto, who have graciously agreed to be the reviewers for my thesis, and to Professor Michel Bourguignon and Dr. Christophe Badie, who have kindly agreed to be examiners of my work.

Je tiens à remercier l'ensemble des personnes du LRO pour leur patience et pour leurs soutiens. Je voudrais remercier Géraldine Pottier, Luc Morat, et Marie Delna Normil pour leur aide dans ma transition dans ma vie française pendant mes premiers mois en France ; à Aude Lenain, Michelle Ricoul, Marion Bellamy, et Radhia M'Kacher pour leurs conseils et aide technique au cours de cette thèse ; à Corina Cuceu, Monika Frenzel, et Laure Piqueret pour leurs bonnes discussions amusantes ; à Annie Vernique pour toutes son aide administrative pendant tout mon séjour en France ; à Isabelle Testard et Muriel Viau pour leurs conseils utiles et leurs bonnes collaborations ; to William Hempel for all of his helpful advice and assistance, and for critically reading my manuscripts ; et à tous les autres qui ont participé à ce travail et/ou qui m'ont soutenu et aidé.

I would also like to thank all the members of Edouard's lab, past and present, for all of their assistance and insightful discussions. Special thanks to Sonia de Toledo for all of her help and guidance in the lab, and to Géraldine Gonon for all of her help with the French translations and for her friendship both in the US and in France.

Je remercie les membres du département de radiobiologie du CEA et de l'Institut de radioprotection et de sûreté nucléaire (IRSN), et également les personnes de Genopole et du CEA Evry qui ont contribué à ma formation scientifique. Je remercie les personnes de l'Unité d'Accueil International du CEA et du Service du Personnel au Faculté de Médecine à l'Université Paris Sud 11 pour leur assistance administrative.

I am extremely grateful to my amazing parents, brother, and the rest of my family for their endless love and support, and to my beloved friends for sticking with me through it all.

Enfin, je voudrais remercier le pays magnifique de France et la ville extraordinaire de Paris pour leur hospitalité. C'était un grand plaisir d'apprendre ta belle langue et d'avoir vu toutes tes merveilles.

ABSTRACT

Exposure to ionizing radiation (IR), from both natural and man-made sources, is an inevitable part of modern life. It is well established that there are considerable inter-individual variations in sensitivity to IR among healthy individuals and cancer patients. However, the mechanisms involved in the heterogeneity of biological responses to IR are not well understood, and a reliable biodosimetric and clinical approach to measure and rank radiosensitivity remains to be established. In this thesis, we study the extent and impact of individual radiosensitivity in healthy individuals in the contexts of emergency dosimetry and radiotherapy, and we explore the roles of telomeres in the prediction of individual radiosensitivity and long-term human health risks following IR exposure (specifically, cardiovascular diseases and/or cancer). First, in the context of dosimetry in the event of an emergency situation (when rapid dose estimates of each individual in an irradiated population are needed), we demonstrate that the impact of individual radiosensitivity can be negligible using global cellular measurements of γH2AX fluorescence via flow cytometry in human fibroblasts and lymphocytes at 4 hours post-irradiation; this method could be an effective and rapid biodosimetry tool that can aid in the medical triage of irradiated individuals in an emergency setting based on individual levels of exposure. Second, we study the extent and influence of individual radiosensitivity on the induction of chromosomal aberrations following a routinely administered dose of 2 Gy during conventional fractionated photon radiotherapy (γ-rays) in lymphocytes of healthy individuals. For these analyses, we define individual radiosensitivity based on the frequency of IR-induced DNA double strand breaks (DSBs), which were calculated from the scoring of chromosomal aberrations visualized with telomere/centromere-fluorescence *in situ* hybridization (TC-FISH). This TC-FISH staining of metaphasic chromosomes enhances the "gold standard technique" of biodosimetry (the dicentric chromosome assay) with the visualization of telomeres and centromeres and thereby provides improved simplicity and sensitivity to the classical cytogenetic assay. We also compare individual radiosensitivity following γ-irradiation to that following carbon irradiation, an up-and-coming ion species currently being used in charged particle radiotherapy. We provide dose response curves for both γ- and carbon irradiations based on the calculated frequency of IR-induced DNA DSBs at a range of doses, and estimate the relative biological effectiveness (RBE) of carbon irradiation relative to γ-irradiation. We then estimate the RBE of a third type of IR also frequently used in charged particle radiotherapy (proton beams) in comparison to γ-irradiation, and compare individual radiosensitivity to each of these three types of IR with different IR energies. Third, we evaluate the roles of telomeres and telomere maintenance in the prediction of individual radiosensitivity; we find that inherent mean telomere length in combination with the IR-

induced change in mean telomere length may be a strong predictor of individual radiosensitivity. Finally, we show how telomeres could be linked to long-term health risks following IR exposure: we demonstrate that telomere shortening could be a new prognostic factor for cardiovascular disease following radiotherapy, and discuss how telomeres could be key players in the process of radiation-induced carcinogenesis. In conclusion, we deliberate the relationships between telomere maintenance, radiation effects, and individual radiosensitivity, and propose a model of how telomeres could play crucial roles in the development of cardiovascular diseases and the process of IR-induced carcinogenesis.

Key words: Ionizing radiation, individual radiosensitivity, telomere maintenance, relative biological effectiveness, biodosimetry, cytogenetics

RÉSUMÉ (FR)

L'exposition aux rayonnements ionisants est une composante inévitable de la vie moderne. Il est bien établi qu'il existe une grande variabilité inter-individuelle de la radiosensibilité chez les individus sains et chez des patients atteints de cancer. Cependant, les mécanismes impliqués dans l'hétérogénéité des réponses biologiques radio-induites ne sont pas encore bien compris, et une approche biologique permettant d'établir de façon fiable le niveau de radiosensibilité reste à développer. Dans cette thèse, nous avons étudié l'ampleur et l'impact de la radiosensibilité individuelle chez les individus sains dans les contextes de dosimétrie d'urgence et de radiothérapie. Nous avons également examiné les différents rôles des télomères dans la prédiction de la radiosensibilité individuelle et des risques pour la santé humaine à long terme (spécifiquement, en ce qui concerne les maladies cardiovasculaires et/ou les cancers) après irradiation. Tout d'abord, dans le contexte de la dosimétrie dans le cas d'une situation d'urgence (lorsqu'il est nécessaire d'estimer rapidement la dose d'irradiation reçu par un individu), nous avons démontré que l'impact de la radiosensibilité individuelle peut être négligeable en utilisant des mesures globales de fluorescence de γH2AX via cytométrie en flux dans des fibroblastes humains et des lymphocytes à 4 heures après exposition ; cette méthode peut être un outil de biodosimétrie efficace et rapide qui peut aider au tri des personnes irradiées dans une situation d'urgence basées sur les niveaux individuels d'exposition. Dans un second temps, nous avons étudié l'ampleur et l'influence de la radiosensibilité individuelle sur l'induction d'aberrations chromosomiques après une irradiation de 2 Gy de rayons γ, correspondant à une fraction de radiothérapie conventionnelle, dans les lymphocytes d'individus sains. Pour ces analyses, nous définissons la radiosensibilité individuelle par rapport à la fréquence des cassures double-brin (CDB) radio-induite, qui ont été calculées à partir de la quantification des aberrations chromosomiques visualisées par hybridation *in situ* des télomères et centromères (TC-FISH). Ce marquage améliore et simplifie la technique « gold standard » de dosimétrie biologique (la quantification des chromosomes dicentriques). Nous avons également estimé la radiosensibilité individuelle à l'irradiation carbone, particules chargées utilisées en radiothérapie, et l'efficacité biologique relative (EBR) des ions carbone par rapport à une irradiation γ. Nous avons fourni des courbes dose-réponse pour ces deux types d'irradiations en fonction de la fréquence des CDB radio-induite par exposition à une gamme de doses. De plus, nous avons estimé l'EBR d'un troisième type de rayonnement également utilisé en radiothérapie de particules chargées (protons) par rapport à une irradiation γ, et nous avons comparé la radiosensibilité individuelle de ces trois types d'irradiation avec énergies différentes. Ensuite, nous avons évalué les rôles des télomères et de leur maintien pour la prédiction de la radiosensibilité individuelle. Nous avons constaté

que la longueur moyenne des télomères, en combinaison avec leurs modifications radio-induites, peuvent être un bon prédicteur de la radiosensibilité individuelle. Enfin, nous avons montré comment les télomères pourraient être liés à des risques sanitaires à long terme après une irradiation: nous avons démontré que le raccourcissement des télomères pouvait être un nouveau facteur de prédiction de maladies cardiovasculaires après radiothérapie, et nous avons discuté par la suite, les télomères comme des acteurs clés dans le processus de cancérogenèse radio-induite. En conclusion, nous proposons un modèle présentant la façon dont les télomères pourraient jouer un rôle crucial dans ces deux pathologies radio-induite, et nous délibérons des relations entre le maintien des télomères, les effets biologiques radio-induites, et la radiosensibilité individuelle.

Mots clefs: Rayonnements ionisants, radiosensibilité individuelle, maintenance des télomères, efficacité biologique relative, biodosimétrie, cytogénétique

LIST OF ORIGINAL PUBLICATIONS INCLUDED IN THIS THESIS

1) Viau M¤, Testard I¤, **Shim G**¤, Morat L, Normil MD, Hempel WM, Sabatier L. *Global quantification of γH2AX as a triage tool for the rapid estimation of received dose in the event of accidental radiation exposure*. Mutation Research - Genetic Toxicology and Environmental Mutagenesis. 2015; 793: 123-131. ¤ co-first authors. doi: 10.1016/j.mrgentox.2015.05.009.

2) M'kacher R, Girinsky T, Colicchio B, Ricoul M, Dieterlen A, Jeandidier E, Heidingsfelder L, Cuceu C, **Shim G**, Frenzel M, Lenain A, Morat L, Bourhis J, Hempel WM, Koscielny S, Paul JF, Carde P, Sabatier L. *Telomere shortening: a new prognostic factor for cardiovascular disease post-radiation exposure*. Radiation Protection Dosimetry. 2015; 164 (1-2): 134-137. doi: 10.1093/rpd/ncu296.

3) **Shim G**, Ricoul M, Hempel WM, Azzam EI, Sabatier L. *Crosstalk between telomere maintenance and radiation effects: A key player in the process of radiation-induced carcinogenesis*. Mutation Research/Reviews in Mutation Research. 2014; 760: 1-17. doi: 10.1016/j.mrrev.2014.01.001.

Original Publications/Book Chapters in Appendix:

4) de Toledo SM, Buonanno M, Li M, Asaad N, Qin Y, Gonon G, **Shim G**, Galdass M, Boateng Y, Zhang J, Azzam EI. *The impact of adaptive and non-targeted effects in the biological responses to low dose/low fluence ionizing radiation: the modulating effect of linear energy transfer*. Health Physics. 2011; 100 (3): 290-292. doi: 10.1097/HP.0b013e31820832d8.

5) Zhang J, Buonanno M, Gonon G, Li M, Galdass M, **Shim G**, de Toledo SM, Azzam EI. (2012) *Bystander effects and adaptive responses modulate in vitro and in vivo biological responses to low dose ionizing radiation*, in Mothershill CE, Korogodina V, Seymour CB (Ed.), Radiobiology and environmental security, Springer, Netherlands.

6) Frenzel M, Cuceu C, **Shim G**, Ricoul M, Sabatier L. (2014) *Telomere*, in H.V. Krieken (Ed.), Encyclopedia of Pathology, Springer-Verlag Berlin Heidelberg.

7) Pottier G, Viau M, Ricoul M, **Shim G**, Bellamy M, Cuceu C, Hempel WM, Sabatier L. *Lead exposure induces telomere instability in human cells*. PLoS One. 2013; 8 (6): e67501.

TABLE OF CONTENTS

LIST OF FIGURES

LIST OF TABLES

LIST OF EQUATIONS

LIST OF ABBREVIATIONS

ALT	alternative lengthening of telomeres
ARS	acute radiation syndrome
ATM	ataxia telangiectasia mutated
A.U.	arbitrary units
CA	chromosomal aberration
CBMN	cytokinesis block micronuclei
CCA	complex chromosomal aberrations
CCTA	coronary CT angiography
CEA	Commissariat à l'énergie atomique et aux énergies alternatives
CHO	Chinese hamster ovary
CT	computed tomography
DC	dicentric chromosome
DDR	DNA damage response
DNA	deoxyribose nucleic acid
DSB	double strand breaks
eV	electron volt
FISH	fluorescent *in situ* hybridization
Gy	Gray
γH2AX	Serine 139-phosphorylated histone H2AX
HR	homologous recombination
IAEA	International Atomic Energy Agency
ICRP	International Commission on Radiation Protection
IR	ionizing radiation
IRSN	Institut de radioprotection et de sûreté nucléaire
ISO	International Organization for Standardization
kb	kilobase
LET	linear energy transfer
LIG1	ligase 1
LIG4	ligase 4
LNT	linear no-threshold
LOH	loss of heterozygosity
LRO	Laboratoire de Radiobiologie et Oncologie
M-FISH	multicolor-fluorescence *in situ* hybridization
NATO	North Atlantic Treaty Organization
NBS	Nijmegen breakage syndrome
NBUD	nuclear buds
NHEJ	non-homologous end joining
Pb	lead
PBL	peripheral blood lymphocytes
PCC	premature chromosome condensation
PHA-M	Phytohemagglutinin M
PNA	peptide nucleic acid
RABiT	Rapid Automated Biodosimetry Technology
RBE	relative biological effectiveness
RNA	ribonucleic acid

ROS	reactive oxygen species
RS2g	radiosensitivity to 2 Gy of γ-rays
RT	room temperature
SCID	severe combined immunodeficiency
SF2	survival fraction at 2 Gy
SNP	single nucleotide polymorphisms
SOBP	spread-out Bragg peak
SSB	single strand breaks
Sv	Sieverts
TC-FISH	telomere/centromere-fluorescence *in situ* hybridization
TELOLOH	LOH induced by telomere loss
TIF	telomere-induced foci
TL	telomere length
u	unit
UNSCEAR	United Nations Scientific Committee on the Effects of Atomic Radiation
US	United States
WHO	World Health Organization

FOREWORD

Exposure to ionizing radiation (IR) is an inevitable part of modern life, especially in the advent of diagnostic radiology, radiation therapy, and military/civilian nuclear technology. It is well established that there are considerable inter-individual variations in sensitivity to IR in the general population. As radiosensitivity can have significant impact on short-term and long-term IR effects, understanding the mechanisms involved in the heterogeneity of biological responses to IR and the development of a reliable clinical and biodosimetric approach to measure and rank radiosensitivity is essential for the refinement of radiation protection protocols, cancer radiotherapy regimens, and overall long-term human health. In this thesis, we study the extent and impact of individual radiosensitivity in healthy individuals in the contexts of emergency dosimetry and radiotherapy, and we explore the roles of telomeres in the prediction of individual radiosensitivity and long-term human health risks following IR exposure. First, we ask whether individual radiosensitivity measured in terms of the induction of γH2AX, a promising candidate as a biomarker for biodosimetry, significantly impacts the development of an effective and rapid biodosimetry tool that can aid in medical triage of irradiated individuals in a large-scale emergency setting. Second, we seek to characterize the extent and influence of individual radiosensitivity on the induction of chromosomal aberrations following a routinely administered dose during conventional fractionated photon (γ-rays) and charged particle (carbon and proton) radiotherapy, and we define the relative biological effectiveness (RBE) of these charged particles, as this remains a major issue in the improvement of modern radiotherapy regimens. For these analyses, we utilize an enhanced version of the dicentric chromosome assay (the "gold standard technique" of biodosimetry) that utilizes telomere/centromere peptide nucleic acid fluorescence *in situ* hybridization (TC-FISH), which provides improved simplicity and sensitivity to the classical cytogenetic assay. Finally, we ask whether telomeres, telomere maintenance, and telomere dysfunction play a role in the prediction of individual radiosensitivity and in the manifestation of long-term health risks following IR exposure (specifically, cardiovascular diseases and/or cancer). Therefore, throughout this manuscript, we describe individual radiosensitivity in healthy individuals and explore how telomeres and their IR-induced modifications could influence this variability and overall long-term human health post-irradiation.

AVANT-PROPOS (FR)

L'exposition aux rayonnements ionisants est une composante inévitable de la vie moderne, en particulier dans l'avènement de la radiologie diagnostique, la radiothérapie, et la technologie nucléaire militaire/civile. Il est bien établi qu'il existe une grande variabilité inter-individuelle de la radiosensibilité dans la population générale. Comme la radiosensibilité peut avoir un impact significatif sur les effets radio-induits à court terme et à long terme, la compréhension des mécanismes impliqués dans l'hétérogénéité des réponses biologiques aux rayonnements ionisants et le développement d'une approche biologique permettant d'établir de façon fiable le niveau de radiosensibilité, sont essentiels pour améliorer les protocoles de radioprotection, les régimes de radiothérapie, et la santé humaine à long terme après exposition. Dans cette thèse, nous étudions l'ampleur et l'impact de la radiosensibilité individuelle chez les individus sains dans les contextes de dosimétrie d'urgence et de radiothérapie. De plus, nous avons examiné le rôle des télomères dans la prédiction de la radiosensibilité individuelle et des risques pour la santé humaine à long terme (pour ce qui est des maladies cardiovasculaires et / ou cancer) après une exposition aux rayonnements ionisants. Tout d'abord, nous nous sommes demandés si la radiosensibilité individuelle, mesurée par l'induction de γH2AX (candidat prometteur en tant que biomarqueur pour la biodosimétrie), a un impact significatif sur le développement d'un outil de biodosimétrie efficace et rapide, ceci afin de faciliter le tri des personnes irradiées lors de situations d'urgence. Dans un second temps, nous cherchons à caractériser l'ampleur et l'influence de la radiosensibilité individuelle sur l'induction d'aberrations chromosomiques à une dose de rayons γ correspondant à une fraction de radiothérapie conventionnelle (rayons γ) et de particules chargées (carbone et protons). Nous définissons également l'efficacité biologique relative (EBR) de ces particules chargées, car cela reste un problème majeur pour l'amélioration de nouvelles techniques de radiothérapie. Pour ces analyses, nous utilisons une version améliorée de la technique « gold standard » de dosimétrie biologique (quantification des chromosomes dicentriques) par hybridation *in situ* des télomères et centromères (TC-FISH), ce qui permet de simplifier et d'améliorer la sensibilité de l'analyse cytogénétique classique. Enfin, nous nous sommes demandés si les télomères et leur maintien peuvent jouer un rôle dans la prédiction de la radiosensibilité individuelle ainsi qu'au niveau des risques pour la santé à long terme après expositions aux rayonnements ionisants (spécifiquement les maladies cardiovasculaires et/ou cancer). Ainsi, au cours de ce manuscrit, nous détaillons la radiosensibilité individuelle chez les individus sains et explorons comment les télomères et leurs modifications radio-induites pourraient influencer cette variabilité et les conséquences sur la santé humaine globale à long terme, post-irradiation.

1 - INTRODUCTION

Exposure to ionizing radiation (IR) is an inevitable part of the environment, and increasingly of modern life. IR is omnipresent in the environment from natural sources (e.g. cosmic rays, terrestrial sources in soil and rock, radon decay products in the air, and various radionuclides found in food and water), and from man-made sources released into the environment (e.g. fallout from nuclear weapons testing, discharges of radioactive waste, and consumer products). Additionally, individuals may be exposed to IR during occupational activities related to nuclear technology, mining, high altitude airline travel, and deep space exploration, as well as during medical procedures (e.g. diagnostic radiology, nuclear medicine, and cancer radiotherapy). Of these, of greatest significance perhaps is the increasing growth in the use of diagnostic radiology, where increasing numbers of individuals are being *repeatedly* exposed to significant doses of IR. This has led to significant increases in levels of human exposure to IR. As it is well established that there are considerable inter-individual variations in sensitivity to IR in the general population (Advisory Group on Ionising Radiation, 2013), these increasing levels of IR exposure may be an important public health issue in the future, particularly for highly radiosensitive individuals (Hall, 1984;UNSCEAR, 2010). A reliable biodosimetric and clinical approach to measure and rank radiosensitivity to identify and better protect these highly radiosensitive individuals still remains to be developed. In this thesis, we characterize the extent of individual radiosensitivity in healthy individuals and the impact of this variability in the contexts of emergency dosimetry and radiotherapy, and we demonstrate that telomeres could be linked to individual radiosensitivity and long-term human health risks following IR exposure (specifically, cardiovascular diseases and/or cancer).

To introduce these various topics in this chapter, we start with a presentation of current general knowledge of telomeres, telomere maintenance, and consequences of telomere dysfunction, followed by an overview of various biological effects of IR exposure (focusing especially on IR-induced telomeric and chromosomal damages and repair, as well as IR-induced chromosomal instability). We then describe a variety of biomarkers that are used to measure these IR-induced biological effects, and, as we focus on cytogenetic methodologies in this thesis, we provide the current status of state-of-the-art cytogenetic biomarker assays that are being used for biodosimetry. Finally, we link these topics in the context of individual radiosensitivity, and provide an overview of the current understanding of the mechanisms, consequences, and prediction of individual radiosensitivity.

1.1 Telomeres

1.1.1 Telomeres and telomere maintenance mechanisms

Telomeres play a critical role as the guardians of genomic stability and integrity. As discussed in detail in **our original paper** (Shim et al., 2014) presented in Section 5.2, telomeres are specialized nucleoprotein structures located at the ends of linear eukaryotic chromosomes (Blackburn et al., 2006). As shown in Figure 1, they consist of a single-stranded DNA portion (3' overhang) composed of G-rich tandem repeats of 5'-TTAGGG-3' sequences that protrudes beyond the double-stranded portion of telomeric DNA, along with six associated proteins, named TRF1, TRF2, TIN2, POT1, TPP1, and RAP1. Together, they form a protective cap called the shelterin complex (de Lange, 2005) that protects chromosome ends from being recognized as DNA double strand breaks (DSBs) and prevents unwanted activation of DNA damage response (DDR) and repair pathways (de Lange, 2005;Doksani and de Lange, 2014).

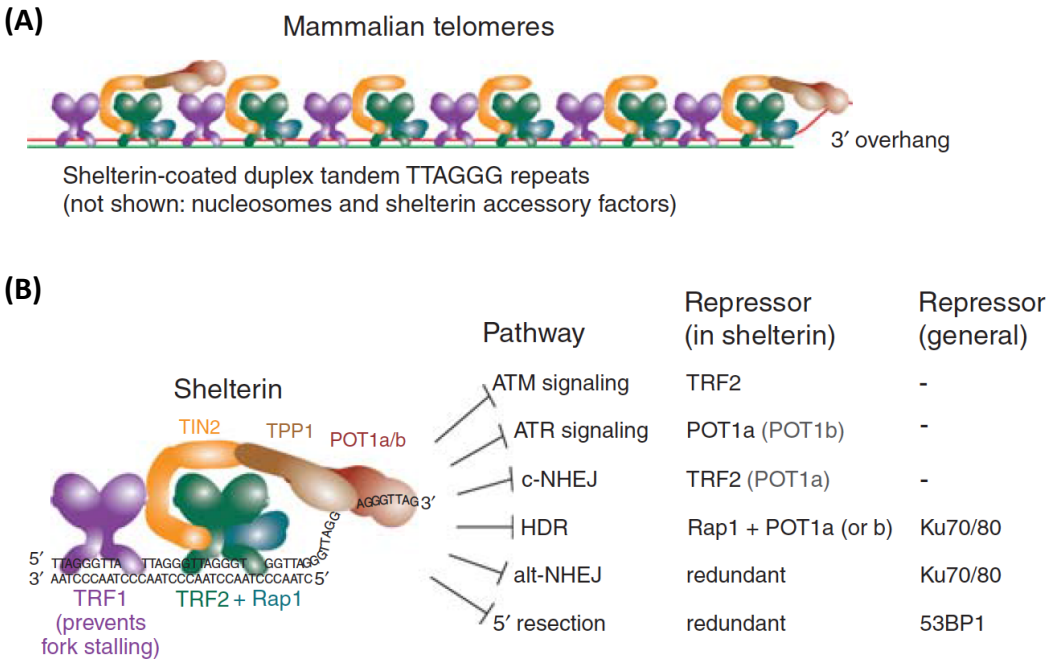

Figure 1. (A) Structure of mammalian telomeres, including the double-stranded telomeric DNA, the single-stranded 3' overhang, and the shelterin complex. (B) Interactions of the six shelterin proteins with DNA, and their repression of six DNA damage response (DDR) pathways that threaten telomere integrity: (1) ATM and (2) ATR signaling, (3) classical and (4) alternative non-homologous end joining (c-NHEJ and alt-NHEJ, respectively), (5) homology-directed repair (HDR), and (6) 5' resection. Removal of TRF2 and POT1a elicit ATM and ATR signaling, respectively. TRF2 blocks c-NHEJ, and Rap1, POT1a/b, and Ku70/80 block HDR. Alt-NHEJ and 5' resection is blocked by multiple shelterin components (or their interacting factors), as well as Ku70/80 and 53BP1, respectively (Adapted from Sfeir and de Lange, 2012;Doksani and de Lange, 2014).

Telomeres can be found in the shape of T-loop structures, formed when the single-stranded telomeric DNA invades the double-stranded portion (Griffith et al., 1999;de Lange, 2004;Palm and de Lange, 2008). The G-rich single-stranded telomeric DNA may also form G-quadruplexes, which are formed from a series of G-quartets each containing four guanine bases arranged in a helical fashion (Huppert, 2008;Lipps and Rhodes, 2009). These structures may serve as an architectural solution to protect telomeres from DDR machinery (Griffith et al., 1999). Additionally, the shelterin proteins were shown to repress the activation of six independent DDR mechanisms at telomeres, indicating that many mechanisms are used to protect chromosomal ends from DNA damage surveillance proteins, as shown in Figure 1B. Namely, shelterin proteins block (1) classical and (2) alternative non-homologous end joining (c-NHEJ and alt-NHEJ, respectively) to prevent chromosome fusions; control (3) homologous recombination (HR) to regulate telomere lengths; prevent activation of (4) ATM (ataxia telangiectasia mutated) and (5) ATR (ATM- and RAD3-related) kinase pathways, which could induce cell cycle arrest; and protect chromosome ends from (6) hyper-resection (Sfeir and de Lange, 2012;Doksani and de Lange, 2014).

Telomere length (TL) varies between organisms; in humans, the length of the double-stranded end can be 2 to 20 kilobases (kb), while the length of the single-stranded G-rich overhang can be 50 to 500 nucleotides. TL also varies on individual chromosome arms (Pommier and Sabatier, 2002), and this inherent heterogeneity of TL is conserved during life (Graakjaer et al., 2003). TL in somatic proliferative tissues naturally declines with each cell replication cycle at a rate of approximately 20–300 base pairs per population doubling (varying with cell type) (Harley et al., 1990) due to the incomplete replication of telomere ends by conventional DNA polymerases, a situation known as the ‘end replication problem’ (de Lange, 2009). After many rounds of cell division, telomeres eventually become critically short and dysfunctional. In normal cells with intact p53 functions and cell cycle checkpoints, these dysfunctional/uncapped telomeres are sensed as DNA damage and trigger DDR pathways, forming telomere dysfunction-induced foci, termed TIFs (Takai et al., 2003). At this point, these DDR signals prevent the cell from further division (d'Adda di Fagagna et al., 2003), and cells enter a stage of permanent growth arrest called *replicative senescence* (Hayflick and Moorhead, 1961). A recent study showed that DDR signals persist long after the onset of senescence, indicating that these signals are important both for senescence establishment and maintenance (Fumagalli et al., 2014). Progressive telomere shortening therefore acts as a 'molecular clock' that limits the number of cell divisions, thereby regulating cellular lifespan and aging (Harley, 1991).

The natural progressive shortening of telomeres during cell replication can be *accelerated* via exposure to DNA damaging agents throughout the cell lifespan, leading to

premature replicative senescence. Indeed, DNA is continuously exposed to endogenous and exogenous damaging agents. Some endogenous DNA damaging factors include point mutations or deletions in genes encoding proteins involved in telomere protection, as well as recombination and epigenetic regulation. Telomere shortening can also be accelerated by external environmental stress and lifestyle factors that cause DNA DSBs or mis-replication of telomeres such as IR and other oxidizing agents, oxidative stress, inflammation, hyperoxia, oncogenes, toxins, chronic viral infections, smoking, alcohol consumption, obesity, stress, and even psychiatric conditions (Jackson and Bartek, 2009;Lin et al., 2012;Price et al., 2013). As will be discussed in Section 1.1.3, reduced TL has been associated with numerous chronic diseases that are generally considered to be diseases of aging, such as diabetes, cancer, and heart disease (Blasco, 2005;Armanios and Blackburn, 2012;Holohan et al., 2014). Furthermore, abnormal and persistent loss of telomeres may contribute to the increased frequency of secondary complications seen in long-term cancer survivors (Shim et al., 2014).

The persistent shortening of telomeres can be offset in different cell types (i.e. normal somatic cells, germ cells, cancer cells) via two mechanisms of telomere elongation: (1) by telomerase, a specialized reverse transcriptase that elongates telomeres by adding TTAGGG DNA sequence repeats to the 3' G-strand overhang at chromosome ends (Greider and Blackburn, 1985; 1987), and/or (2) by homologous recombination (HR) of telomeres via “alternative lengthening of telomeres” (ALT), a pathway independent of telomerase activity (Bryan et al., 1995). Telomerase is primarily expressed in stem cells, germ cells, regenerating tissues, and cancer cells; it is silent in most differentiated cells, such as normal somatic cells (Wright et al., 1996), thereby resulting in telomere shortening after each round of cell division. The enzyme is up-regulated in about 85% of human cancers, suggesting its important role in the process of cellular immortalization and tumorigenesis (Shay and Bacchetti, 1997), and its down-regulation or inhibition has been shown to promote apoptosis in malignant cells (Massard et al., 2006); these properties make telomerase an attractive target for anti-cancer therapies (Olaussen et al., 2006;Mocellin et al., 2013) as telomerase inhibitors would target and sensitize telomerase-positive malignant cancers to cancer treatments while normal somatic cells, which do not express telomerase, are minimally affected (Buseman et al., 2012). However, a significant subset of human tumors (10-15%) employs the telomerase-independent ALT pathway (Bryan et al., 1995;Shay and Bacchetti, 1997).

1.1.2 Telomere dysfunction, telomere fusions, and chromosomal instability

As mentioned above, critically short telomeres due to natural and/or accelerated progressive shortening of telomeres during cell replication become dysfunctional and are sensed as DNA DSBs, which activate DDR pathways without actual presence of DSBs at telomeres. Dysfunctional telomeres can arise due to a number of other factors, including improper functioning of telomere maintenance mechanisms, or the loss or improper functioning of the shelterin proteins, which leads to loss of their protective capping functions (i.e. repression of the six DDR mechanisms at telomeres described above). Telomere dysfunction can also be due to loss or dysfunction of DDR proteins themselves, as these proteins were also shown to be involved in the normal maintenance and protection of telomeres (Ayouaz et al., 2008). Generally, shelterin protein levels were shown to be directly proportional to TL and the level of telomerase inhibition, and inversely correlated with the induction of DDR factors (such as ATM and γH2AX) (Raynaud et al., 2008a;Raynaud et al., 2009;Raynaud et al., 2010).

Upon activation of the DDR pathways, a complex signaling cascade is triggered to activate DNA repair pathways, induce cell cycle arrest to allow time for repair of DNA damage, and in certain cases, initiate senescence or apoptosis. DDR pathways will be discussed in detail in Section 1.2.3. In short, ATM, ATR, and DNA-PK (members of the phosphatidyl inositol 3-kinase-like kinase [PIKK] family) phosphorylate histone H2AX to form γH2AX around the DSB or dysfunctional telomere, which leads to both structural alterations to the chromatin around the damaged site to allow repair proteins access to the damaged regions of the DNA, as well as the recruitment and retention of key DDR factors including MDC1, the MRN complex (MRE11–RAD50–NBS1), 53BP1, and BRCA1. These proteins continue to initiate the phosphorylation and dimerization of checkpoint kinases CHK2/CHK1, which targets effectors including p53, CDC25A, and CDC25C that goes on to activate cell cycle checkpoints or induce apoptosis (Raynaud et al., 2008b;Thompson, 2012). At dysfunctional telomeres, the recruitment of DDR factors such as 53BP1, γH2AX, ATM, and MRE11 induces the formation of TIFs (Takai et al., 2003). An important study suggested that normal human cells are able to tolerate small numbers of dysfunctional telomeres, and cells can continue to proliferate until a threshold of five TIFs per cell is reached (Kaul et al., 2012), at which point senescence is triggered in normal cells with intact p53 functions and cell cycle checkpoints (Hayflick and Moorhead, 1961;d'Adda di Fagagna et al., 2003). The lack of chromosomal fusions in pre-senescent cells may indicate that sufficient levels of shelterin proteins are present at the telomeres to retain their protective roles. However, in cells that are unable to senesce due to the loss of cell cycle checkpoint proteins such as p53 or p16, senescence is temporarily bypassed, and cells continue to proliferate with further

accumulation of TIFs (Kaul et al., 2012) and telomere shortening, until “telomeric crisis” is reached. In virus-immortalized cells undergoing crisis, more than 5 dysfunctional telomeres were found (Kaul et al., 2012) along with massive chromosome fusion and cell death (Counter et al., 1992;Counter et al., 1994;Ducray et al., 1999), perhaps due to extreme telomere shortening and loss of shelterin proteins (Kaul et al., 2012).

Damaged or dysfunctional telomeres, sensed as DNA DSBs, may result in telomeric end-to-end fusions and chromosomal aberrations (CAs) via DNA DSB repair mechanisms. As will be discussed in detail in Section 1.2.3, mammals possess two principle mechanisms of DNA DSB repair – non-homologous end joining (NHEJ) and homologous recombination (HR) repair – with the majority of chromosome fusions in mammalian cells occurring via NHEJ, the major form of DSB repair. Chromosome fusions due to telomere dysfunction from the loss or dysfunction of shelterin or DDR proteins have thus far been shown to occur via two pathways: the classical-NHEJ (c-NHEJ) pathway, or the alternative-NHEJ (alt-NHEJ) pathway. A compilation of published data on this subject is presented in **our original paper** (Shim et al., 2014); however, it should be noted that many conflicting data exist, and the consequences of the dysfunction of these proteins also appear to differ among species. The choice of repair pathway appears to depend on how the telomeres were rendered dysfunctional, as shown in Figure 1B (Sfeir and de Lange, 2012;Doksani and de Lange, 2014); for instance, naturally shortened telomeres and loss of TRF2 result in chromosomal fusions via c-NHEJ, while loss of TPP1–POT1a/b result in chromosomal fusions via alt-NHEJ (Rai et al., 2010;Decottignies, 2013). A recent study indicates a previously undescribed role of BRCA1 and CtIP in fusions of a large fraction of TRF2-depleted cells via alt-NHEJ in conjunction with EXO1, and LIG3; this study further highlights the complexity of telomere protection mechanisms (Badie et al., 2015).

Telomeric regions (and sub-telomeric regions, extending at least 100 kb from the telomere) are particularly sensitive to DSBs, and thus the presence of DNA DSBs near telomeres leads to a higher propensity of chromosome rearrangements. It has been postulated that this is because c-NHEJ repair is repressed by TRF2 along with the inappropriate processing of DSBs in this region as though they are telomeres via alt-NHEJ (Muraki et al., 2012;Muraki et al., 2013); however, a recent study illustrated the c-NHEJ is in fact not deficient at telomeres and that the higher propensity of chromosome rearrangements following DSBs in this region is due to their excessive processing by MRE11 (Muraki et al., 2015). The presence of DNA damage within telomeric repeat sequences hinders telomere replication, leading to telomere shortening or loss, and the deficiency of DSB repair near telomeres has been suggested to play a role in chromosomal instability associated with human cancers (Muraki et al., 2012;Muraki et al., 2013).

Additionally, telomeric sequences can also be found at internal sites of chromosomes and may colocalize with fragile chromosomal sites that are more prone to breakage; these interstitial telomeric sequences could be associated with genomic instability, human disease, and cancers (Desmaze et al., 1999). Meanwhile, DSBs at interstitial chromosomal sites occur primarily through c-NHEJ. Large deletions and gross chromosomal rearrangements (inversions, translocations, dicentric chromosomes) have been observed when DSBs occur near telomeres (Muraki et al., 2012;Muraki et al., 2013) or at interstitial telomeric sequences (Aksenova et al., 2013), whereas small deletions have been found to be the most common CAs when DSBs were induced at interstitial DNA sites (Muraki et al., 2012;Muraki et al., 2013).

To compensate for the increased sensitivity to DSBs near telomeres, chromosome healing, or the *de novo* addition of telomeric repeat sequences at DSB sites, may serve as an alternate mechanism of repair. Chromosomal healing in human cells may or may not involve telomerase, and does not occur at interstitial DSBs in somatic cells (Rebuzzini et al., 2005;Muraki et al., 2012;Murnane, 2012). However, interestingly, strong evidence suggests that telomerase was involved in the insertion of interstitial telomeric sequences during the repair of DSBs in rodents and primates during evolution (Nergadze et al., 2007). Chromosome healing results in terminal deletions, which are less detrimental than gross chromosome rearrangements, and thereby prevents chromosomal instability resulting from DSBs near telomeres. Chromosome healing may be deficient in human cancer cells, and may be responsible for the chromosomal instability observed in these cells (Muraki et al., 2012;Murnane, 2012).

Chromosome fusions result in the formation of dicentric chromosomes, which is an unstable, non-transmissible type of CA and cause cell cycle arrest in normal cells with intact cell cycle checkpoints. However, cells lacking normal checkpoints continue to divide, and chromosomal instability is propagated via breakage-fusion-bridge (B/F/B) cycles. As shown in Figure 2, B/F/B cycles are initiated when a dicentric chromosome is formed when sister chromatids fuse following the replication of a chromosome that has lost a telomere. This dicentric chromosome forms a bridge during anaphase, which breaks at a location other than the site of fusion when the centromeres are pulled in opposite directions during cell division. This results in the transfer of DNA from one chromosome to another, with large inverted repeats at the end of the chromosome in one daughter cell and a terminal deletion at the end of the chromosome in the other daughter cell. Since the chromosomes are still missing a telomere, they will fuse again in the next cell cycle, and the B/F/B cycles continue until each chromosome is stabilized by the acquisition of a new telomere, usually by translocation of the end of another chromosome. The instability is thus transferred to the

chromosome donating the telomere; therefore, the loss of a single telomere can cause chromosomal instability in multiple chromosomes (Murnane, 2012). As continuing chromosomal instability and cell proliferation may be key elements of the initiation and progression of multi-stage carcinogenesis (Sabatier et al., 1995;Raynaud et al., 2008b;Shim et al., 2014), understanding the factors promoting telomere loss and its consequences is important for understanding chromosome instability associated with human cancer.

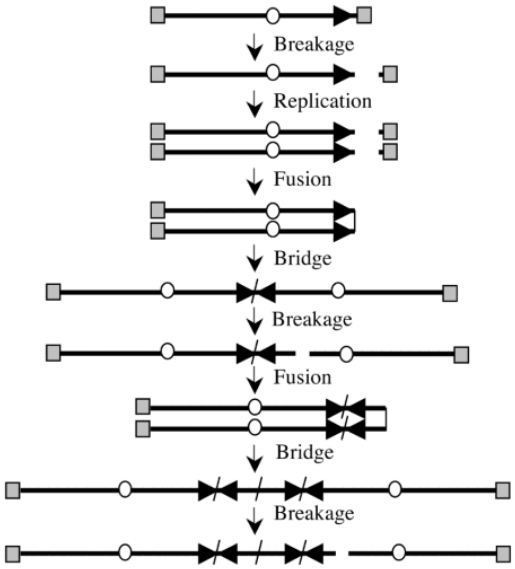

Figure 2. Propagation of chromosome instability via breakage-fusion-bridge (B/F/B) cycles. Telomeres are illustrated as gray squares, centromeres as circles, and the orientation of the sub-telomeric sequences are illustrated as horizontal arrows (Adapted from Murnane, 2012).

The role of telomeres and DDR activation in the multi-stage carcinogenesis process was demonstrated in a previous study in our laboratory in colorectal carcinoma* (Raynaud et al., 2008a). As illustrated in Figure 3, telomere shortening, decreasing levels of TRF1/TRF2, and increasing activation of DDR processes (ATM, CHK2, and γH2AX) occur during the early stages of the carcinogenesis process; this telomere attrition in these early stages may have a protective mechanism against cancer as critically short telomeres induce a cell cycle arrest (i.e. replicative senescence). When the full invasive potential of the tumor has been reached, telomere length and TRF1/TRF2 levels increase with only low levels of DDR

* In this study, 4 types of colon tissue samples representing the major histological steps of colorectal carcinogenesis were obtained from each of 15 patients: normal mucosal epithelia, 2 stages of benign epithelial tumors (low-grade and high-grade adenomas), and invasive (malignant) carcinoma. Telomere length, telomeric protein levels (TRF1 and TRF2), and DDR marker expression (ATM, CHK2, and γH2AX) were evaluated in these consecutive tissue sections from each patient (Raynaud et al., 2008a).

activation, suggesting that cancer cells may avoid apoptosis by impairing DDR (Raynaud et al., 2008a).

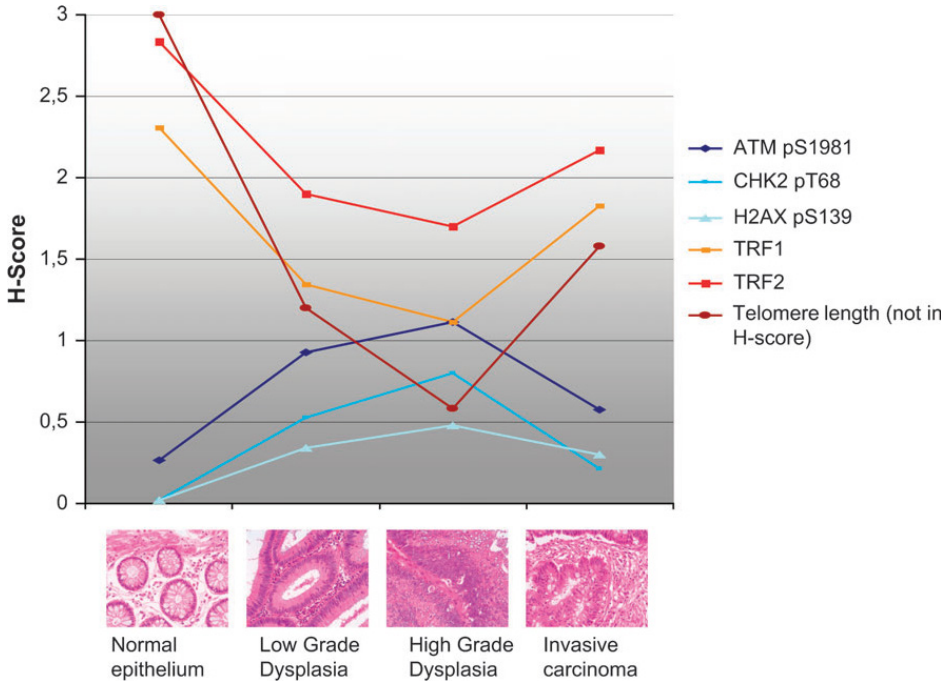

Figure 3. DNA damage response (DDR) activation, TRF1/TRF2 expression levels, and telomere length in the multi-step process of colorectal carcinogenesis. H score, shown on the vertical axis, is a relative measure of protein expression level, and the stages of cancer progression are shown on the horizontal axis. Telomere shortening and decreasing levels of TRF1 and TRF2 with corresponding activation of DDR processes (increasing ATM, CHK2, and γH2AX protein expression levels) occur during the early stages of the carcinogenesis process (from normal mucosal epithelia to low-grade dysplasia and high-grade dysplasia, with attrition and activation peaks, respectively, occurring at the high-grade dysplasia stage; this telomere attrition in these early stages may have a protective mechanism against cancer as critically short telomeres induce a cell cycle arrest (i.e. replicative senescence). When the full invasive potential of the tumor has been reached (invasive carcinoma stage), telomere length and TRF1/TRF2 levels increase with only low levels of DDR activation, suggesting that cancer cells may avoid apoptosis by impairing DDR (Adapted from Raynaud et al., 2008a).

1.1.3 Telomere-related human pathologies

Short telomeres due to defects in telomere maintenance machinery has been linked to a spectrum of age-related human diseases, referred to as “telomeropathies,” “telomere disorders,” “telomere syndromes,” or “impaired telomere maintenance spectrum disorder.” New syndromes are increasingly being identified. Common symptoms of a telomeropathy include idiopathic pulmonary fibrosis (IPF) and bone marrow failure. Increasing evidence indicates that although clinical manifestations of symptoms are diverse, telomeropathies comprise a single spectrum of diseases defined by short telomeres that leads to proliferative failure of a variety of tissues (most importantly lung tissue and hematopoietic stem cells)

(Carroll and Ly, 2009;Diaz de Leon et al., 2010;Armanios and Blackburn, 2012;Holohan et al., 2014).

Table 1. Summary of all genes known to cause telomeropathies when defective, and the telomere/telomerase-relevant complexes these genes participate in. Putative candidate genes and complexes are also presented (not bold) based on their known interactions with genes known to cause telomeropathies (bold) (Adapted from Holohan et al., 2014).

Genes that cause telomere disorders when defective	Process/complex	Diseases	Process/complex including genes that cause telomeropathies	Candidate genes
TIN2	Shelterin, inhibits TRF1 PARsylation	DKC/HHS/ Revesz syndrome	Shelterin	TRF1, TRF2, **TIN2**, RAP1, TPP1, POT1
RTEL1	T-loop dissociation, target of cytosolic iron–sulfur protein assembly (CIA) complex	DKC/HHS	CST complex	**CTC1**, STN1, TEN1
CTC1	CST complex	Coats Plus	Telomerase	**TERT**, **TERC**, **Dyskerin**, **NHP2**, **NOP10**, GAR1
Apollo	Overhang processing	HHS	CIA complex	MMS19, MIP18, CIAO1, IOP1, **RTEL1**
TERT, TERC, Dyskerin, NHP2, NOP10	Telomerase	IPF, DKC, aplastic anemia	Apollo	TRF2, FANCD2, **Apollo**
TCAB1	Cajal body, telomerase assembly	DKC	Cajal body	Coilin, HOT1, **TCAB1**, **Telomerase complex**
			TRF1 regulation	TRF1, TNKS1, **TIN2**, TNKS1BP1

Dyskeratosis congenita (DKC) was the first disorder linked to impaired telomere maintenance. It was originally diagnosed from the "diagnostic triad" of symptoms, namely oral leukoplakia, skin hyperpigmentation, and nail dystrophy. DKC is also associated with other symptoms, most frequently including organ failure (usually in the bone marrow, with some patients encountering pulmonary fibrosis before bone marrow failure), aplastic anemia (a deficiency of all types of blood cells due to bone marrow failure), or specific lymphopenias. The pathology and genetic cause of DKC overlaps significantly with three more severe and extremely rare forms of DKC, each with additional symptoms: Hoyeraal-Hreidersson syndrome (HHS), Coats Plus syndrome, and Revesz syndrome[†]. These severe syndromes present during childhood, with symptoms including bone marrow failure and mucocutaneous abnormalities. Symptoms presenting during adulthood, on the other hand, generally include IPF, liver cirrhosis, aplastic anemia, and acute myelogenous leukemia (AML). However, due to the incomplete penetrance of symptoms and the rarity of HHS,

[†] Other, less frequent symptoms of DKC include failure of a variety of endothelial and epithelial compartments (e.g. enterocolitis, emphysema, liver cirrhosis, premature hair graying, short stature, dental caries, osteoporosis, and esophageal stricture). Patients with HHS syndrome exhibit symptoms of DKC with the addition of intrauterine growth retardation, cerebellar hypoplasia, and microcephaly. Patients with Revesz syndrome present with symptoms of HHS with the addition of exudative retinopathy, while patients with Coats Plus syndrome exhibit symptoms of HHS and Revesz syndrome with the addition of cerebral calcifications. Despite these distinctions, cerebral calcifications and exudative retinopathy have been observed in patients with all three severe forms of DKC (Holohan et al., 2014).

Coats Plus, and Revesz syndromes, these diseases are difficult to distinguish. As they have overlapping symptoms and causes (Table 1), these disorders may in fact represent a single disease entity (not three distinct disorders) with multiple genetic mechanisms for the same pathological conditions (Holohan et al., 2014).

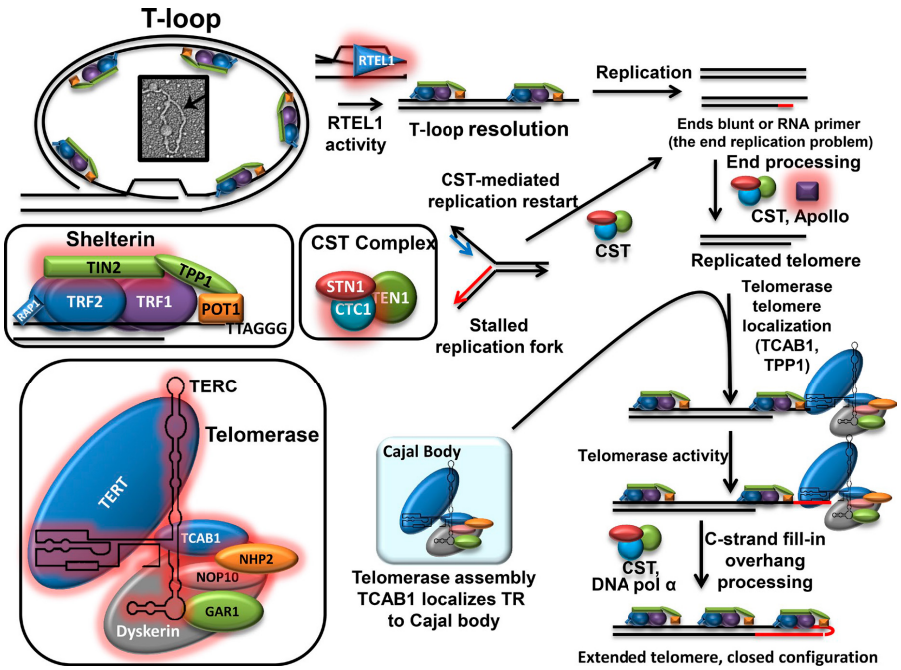

Figure 4. Telomere replication and the molecular biology of telomeropathies. Genes with known disease-causing mutations are denoted in red. Telomeres are configured in a "T-loop" characterized by invasion of the single-strand onto the double-stranded DNA. To initiate telomere replication, the T-loop is resolved by the RTEL1 helicase. The blunt-ended (from leading-strand synthesis) and RNA primer–ended (from lagging strand synthesis) telomere ends created from DNA replication must be processed by the CST complex (composed of CTC1, STN1, and TEN1) and Apollo before telomerase activity. The assembly of telomerase, a complex containing TERT, TERC, and the Dyskerin complex dimer (Dyskerin, NOP10, NHP2, GAR1), is promoted by TCAB1 in the Cajal body. After telomerase assembly, it is localized to the replicated and processed telomere by TCAB1 and TPP1, where it can add new telomere repeats to the G-overhang. After telomerase activity, the CST complex and DNA polymerase-α perform a fill-in reaction and nucleolytic processing that creates an extended telomere that is closed to further action by telomerase (Adapted from Holohan et al., 2014).

Defective genes that have been linked to DKC, HHS, Coats Plus, and Revesz syndromes, IPF, and aplastic anemia are summarized in Table 1. These disorders are associated with gene defects in the shelterin protein TIN2, RTEL1 helicase, CTC1 (a component of the CST complex), Apollo, telomerase components (TERT, TERC, Dyskerin, NHP2, NOP10), and TCAB1 in the Cajal body. These components and their roles in telomere replication and telomerase structure/assembly are illustrated in Figure 4. As shown in Table 1, there are indeed overlaps in the genetic causes of these disorders. However, a substantial portion (~40%) of DKC has no proven monogenic cause, and thus further studies are needed to uncover the genetic mutations and details of telomere maintenance

mechanisms responsible for these disorders. To aid in the search for genes that cause these disorders, candidate genes have been proposed in Table 1 based on their known interactions with the known genetic links to telomeropathies. However, it is possible that telomeropathies are linked to undiscovered components of telomere maintenance, or that some telomeropathies are not due to monogenic defects. Conversely, new human syndromes are expected to be revealed in the future, which may help to reveal more insight into basic telomere biology as well as the full spectrum of these diseases (Holohan et al., 2014).

Telomeropathies are complex to classify, as the manifestation of symptoms and the age of onset of these disorders are highly variable, even with the inheritance of the same genetic mutation. Indeed, successive generations in families with telomere disorders have been shown to exhibit different symptoms, with decreasing age of onset and increasing severity of symptoms, a phenomenon called genetic anticipation. Earlier generations manifest adult-onset symptoms (IPF, liver cirrhosis, aplastic anemia, AML) while later generations show at younger ages DKC/HHS symptoms (bone marrow failure, mucocutaneous abnormalities) (Armanios and Blackburn, 2012;Holohan et al., 2014).

Age of onset of telomeropathies can be explained by a combination of inheritance of telomere length, environmental factors (e.g. environmental air pollution, tobacco exposure, stress, asthma, chronic obstructive pulmonary disease), and differential proliferative capacity and degree of telomere shortening in tissues (e.g. lung tissue and hematopoietic stem cells). As the hematopoietic compartment is a highly proliferative tissue, it is not surprising that telomere-associated disease leads to prominent manifestation in the bone marrow during childhood. On the other hand, in tissues with slower cell turnover such as the lung, additional telomere damage via endogenous or exogenous factors may be needed to accelerate telomere shortening, thereby explaining why telomere-mediated lung disease manifests in adulthood. Additionally, in slowly proliferating tissue, short telomeres can cause gene expression changes that lead to metabolic and mitochondrial dysfunction, as well as endoplasmic reticulum stress that can alter exocytosis in secretory tissues (e.g. pancreas, nervous system) (Armanios and Blackburn, 2012;Holohan et al., 2014).

Though these factors can explain the age of onset of disease, they cannot readily explain genetic anticipation. Indeed, the mechanisms by which genetic anticipation occurs remain uncertain. To explain these generational differences in symptoms of telomere disorders, several models based on various interpretations of data about telomere dynamics in the two most important tissues (lung tissue and hematopoietic stem cells) have been presented: (1) differential rates of telomere shortening in the two tissues, (2) synchronous age-related telomere shortening in the two tissues but with alternative pathological

thresholds for IPF and bone marrow failure, and (3) a blend both possibilities by assuming synchronous age-related telomere shortening punctuated by rapid telomere loss via environmental telomere damage in specific tissues. Determining the mechanisms behind genetic anticipation will require further detailed knowledge of rates of telomere shortening and the sensitivity to shortened telomeres in various tissues (Holohan et al., 2014).

Patients with telomere disorders have been shown to be predisposed to cancer despite conventional interpretation of telomere length as a limit on cellular proliferative capacity. This may be explained by more than one mechanism. Defects in telomere maintenance can lead to persistent DNA damage signals, telomere fusions, and chromosomal instability, all of which can initiate carcinogenesis. Additionally, telomere length can limit the proliferative capacity of the adaptive immune system, leading to immunodeficiency that can in turn lead to a failure in cancer surveillance. However, it is possible that the increased cancer incidence may be a consequence of the organ failure state itself, and not necessary the telomere defect. All in all, accumulating evidence of telomeropathies will not only clarifies their disease mechanisms, but will also contribute to overall knowledge of telomere biology and its influences on human health (Armanios and Blackburn, 2012;Holohan et al., 2014).

1.2 Biological responses to ionizing radiation

1.2.1 Overview of levels of human exposure to ionizing radiation in the modern era

On the global scale, according to the United Nations Scientific Committee on the Effects of Atomic Radiation (UNSCEAR) 2008 Report, the average dose of IR exposure from natural sources is estimated to be 2.4 mSv (milli-Sieverts[‡]) per year, ~50% of which is from natural radionuclides (mainly radon) found in soil and rocks, and ~15% of which is from cosmic radiation (at sea level); the average dose of cosmic radiation at cruising altitudes on commercial flights can range from 0.003 to 0.008 mSv per hour. Meanwhile, the average dose of IR exposure from man-made sources (worldwide) is estimated to be 0.6 mSv per year, with medical diagnostic radiology as the predominant source of exposure (UNSCEAR, 2010). Additional annual dose limits (i.e. excluding natural and medical IR exposure) for the general public and occupational workers are 1 and 50 mSv per year, respectively, as

[‡] Sieverts (Sv) is the unit of effective dose. It is an estimation of the overall harm to a patient caused by the IR exposure. The effective dose provides only an approximate estimate of the true risk (Brenner and Hall, 2007).

advised by several regulatory agencies (ICRP, 2007). Globally, the total number of diagnostic radiological examinations (both medical and dental) is estimated to have risen by ~50% from 2.4 billion per year (in 1991–1996) to 3.6 billion per year (in 1997–2007), and the average dose is estimated to have increased from 0.4 to 0.6 mSv per year. The total number of diagnostic nuclear exams has increased by under 1% since the 1991–1996 survey, and the average annual dose due to nuclear exams is estimated to have increased by ~35%. The frequency of administration of radiotherapy treatments is also estimated to have increased from 4.3 to 5.1 million per year between 1997 and 2007 (UNSCEAR, 2010). According to the World Health Organization (WHO), these numbers have increased further since then worldwide to 37 million nuclear medicine procedures per year and 7.5 million radiotherapy treatments per year (WHO, 2015).

Despite these global estimates, diagnostic radiology (X-ray) examinations in developed countries with high levels of health care (which account for 24% of the global population) are estimated to be over 65 times more frequent than in countries with the lowest levels of health care (which account for 27% of the global population). Thus, in these countries where diagnostic radiology is more readily available and more heavily prescribed, annual doses due to diagnostic radiology alone based on the UNSCEAR 2008 Report can be as high as 2.0 mSv per year (without including radiotherapy); this level of exposure from medical uses is, on average, ~80% of that from natural sources. These numbers continue to rise as the use of radiation in medicine increases due to the major improvements it provides in the diagnosis and treatment of human diseases, as well as due to the increasingly widespread use of new high-dose X-ray technology, particularly CT scanning (UNSCEAR, 2010). Indeed, the use of CT scans has increased in the United States (US) by more than 3-fold since 1993 to ~70 million scans per year (Berrington de Gonzalez et al., 2009), and ~7.6 million CT scans were performed in France in 2007 (Journy et al., 2015a;Journy et al., 2015b). Though CT scans are perhaps the single most important advancement in diagnostic radiology, as they provide three-dimensional views of the organ/region of interest that facilitates disease screening and diagnosis (Brenner and Hall, 2007), they deliver 5–20 times the effective dose of conventional radiology, corresponding to organ doses of up to tens of milli-Grays[§] (mGy) per scan (Journy et al., 2015b). In countries where CT scans are heavily prescribed, their increasing use of the scans, along with the higher doses of IR administered per scan, result in a marked increase in annual doses of IR exposure in the population to those that exceed, for the first time in history, doses from the previously largest

[§] Gray (Gy) is the unit of absorbed dose, or the energy absorbed per unit of mass. One gray is equal to 1 joule of radiation energy absorbed per kilogram. The organ dose will largely determine the risk level to that organ from IR exposure (Brenner and Hall, 2007).

source (natural background IR) (UNSCEAR, 2010). With these increasing levels of medical exposure in addition to exposure from natural sources, individuals may be receiving total annual doses of almost *double* that from natural sources alone.

Exposure to increasing levels of IR can be associated with increased risks of IR-related cancers. As will be discussed further in Section 1.2.5, the health risks of low levels of IR exposure (< 0.2 Gy) remain ambiguous and controversial, as epidemiological studies to evaluate the long-term health effects of exposure to low doses of IR are difficult to conduct and interpret. Thus, estimates of health risks to low doses are extrapolated based on extensive experimental studies of high doses of IR (> 1 Gy), long-term follow-up of survivors of atomic bombings and radiation accidents, and other large-scale epidemiologic studies (Brenner et al., 2003;National Research Council, 2006). It is estimated that the ~70 million CT procedures administered per year in the US may cause as many as 29,000 new cancer cases (Berrington de Gonzalez et al., 2009); as of 2006, ~1.5−2.0% of all cancers in the US may be attributable to the IR from CT studies, a drastic increase from the estimated 0.4% between 1991 and 1996. (Brenner and Hall, 2007). Despite this concern about long-term IR-related health risks, the use of CT scans will undoubtedly continue to increase because of its superior diagnostic value (Amis et al., 2007). While the risk of cancer is not large for any one person, the increasing exposure to IR in the population (especially in children, who are more sensitive to IR than adults (Bakhmutsky et al., 2014)) may be a public health issue in the future. Reducing the population dose from CT scans (and other radiological procedures) and reducing this IR-related cancer risk may be achieved by simply reducing the inappropriate prescription of radiological procedures, which can lead to unnecessary IR doses; indeed, about one third of all CT scans are not justified by medical need, and perhaps 20 million adults and more than 1 million children per year in the US are being irradiated unnecessarily (Brenner and Hall, 2007).

1.2.2 Targeted and non-targeted effects of exposure to ionizing radiation

The biological effects of IR depend on the amount of energy absorbed by living matter (i.e. absorbed dose, measured in Gy[§]) and by the spatial distribution of the absorbed energy, which is related to the linear energy transfer (LET) of the IR. LET, expressed in keV μm^{-1}, is defined as the amount of energy lost per unit length along the path travelled by the radiation; it is an average quantity, as the actual energy deposition has a particular distribution that varies as a function of depth in the target material (Hall, 2006).

As illustrated in Figure 5A, low-LET IR (e.g. X- and γ-rays) deposits exponentially decreasing amounts of energy as a function of penetration depth in the target material. Doses of low-LET IR produce a uniform pattern of distribution throughout the target material.

On the other hand, high-LET IR (e.g. heavy charged particles, protons, neutrons, α-particles) have a well-defined range in matter: a relatively low entrance dose in the target material, followed by a pronounced sharp maximum dose near the end of their range called the *Bragg peak*, and energy close to zero beyond the Bragg peak. This ability to localize a great amount of energy at the Bragg peak is advantageous for use in cancer radiotherapy, as the tumor site can be precisely targeted by placing it at the Bragg peak while the surrounding normal tissues would be minimally exposed to IR (Hall, 2006).

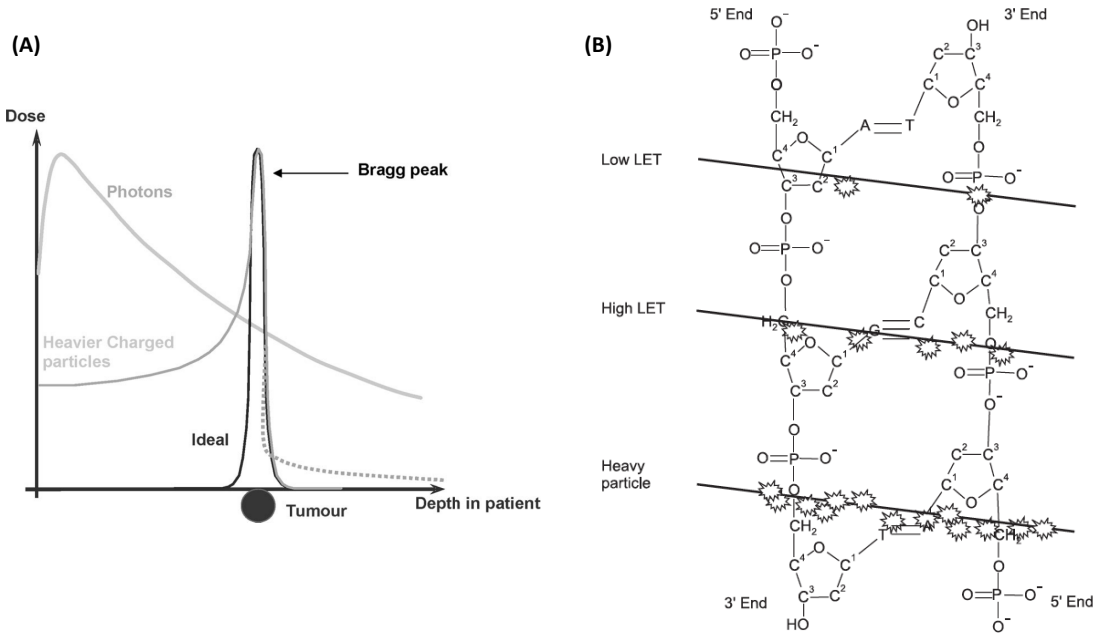

Figure 5. (A) Typical energy loss profiles as a function of the distance traveled in tissue for photons (i.e. X- and γ-rays) and heavy ions (i.e. carbon ions). The exponential tail in the photons curve indicates that they deposit their energy through the entire target with decreasing amounts of energy as a function of penetration depth in the target material. In contrast, heavy ions are characterized by a relatively low entrance dose in the target material, followed by a pronounced sharp maximum dose near the end of their range called the Bragg peak, and energy close to zero beyond the Bragg peak (Adapted from Pijls-Johannesma et al., 2010). (B) Interactions of low-LET IR, high-LET IR, and high-LET heavy charged particles with DNA. Low-LET IR produces ionization events that are sparsely distributed along its traversal path, whereas high-LET IR and heavy charged particles produce ionization events that are more densely concentrated along the particle track. The extent of DNA damage depends on the specific physical characteristics of the IR such as energy and mass (Adapted from Park and Kang, 2011).

When IR is absorbed by living cells, it deposits discrete packets of photon energy that cause the ejection of electrons from molecules along its traversal path. These ionization events cause cellular damage either directly (via direct impact on cellular structures, e.g. DNA, mitochondria) or indirectly (via excess reactive oxygen species [ROS] production from radiolysis of cellular water or mitochondrial dysfunction). The density of these ionization events, and the extent of the resulting biological damage, increases with dose and the LET

of the IR. As shown in Figure 5B, low-LET IR produces ionization events that are sparsely distributed along its traversal path. However, when high-LET IR traverses a target material, it produces ionization events that are more densely concentrated along the track compared to low-LET IR (Hall, 2006); the local dose at the center of a particle track may be thousands of Gy, but a few microns away (e.g. a neighboring cell), the dose may be close to zero (Cucinotta et al., 2000). Because of these characteristics, direct traversal of high-LET IR through cellular DNA induces *clustered* damage along the radiation track that result in DNA DSBs, gene mutations, and other complex chromosomal aberrations (CCAs), with the extent of damage depending on the specific physical characteristics of the IR such as energy and mass (Goodhead, 1994). Direct traversal of low-LET IR through cellular DNA induces lower frequencies of DNA DSBs than high-LET IR; instead, direct traversal of low-LET IR predominantly causes DNA base damage and DNA single strand breaks (SSBs). Because high-LET IR deposits greater amounts of energy per unit length of traversed matter, there is a high possibility that multiple lesions are in close proximity within a short period of time (Cucinotta et al., 2003).

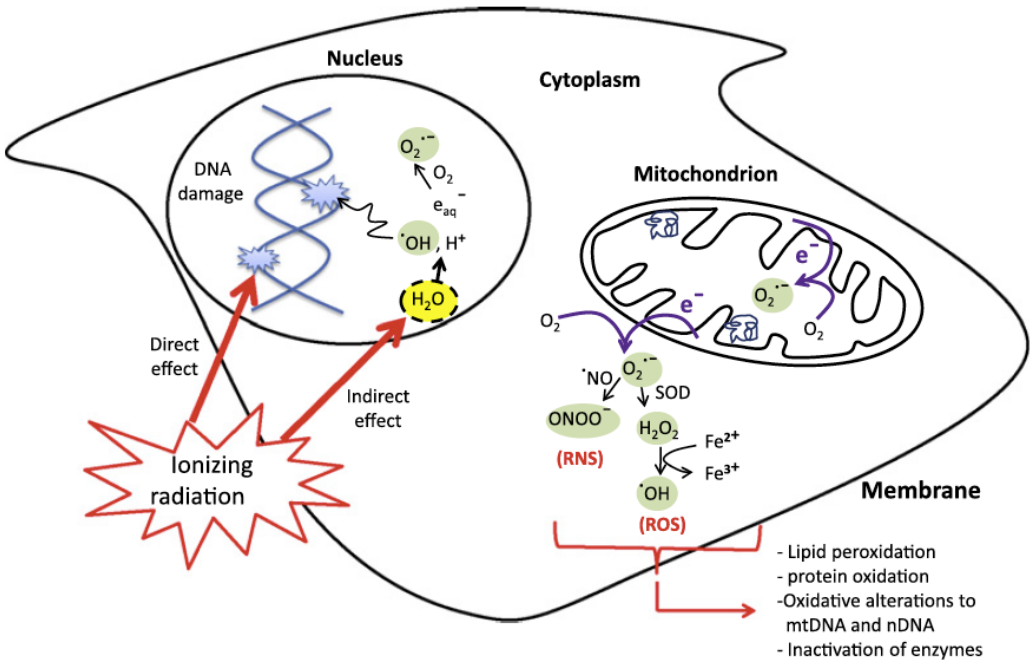

Figure 6. Summary of the direct and indirect cellular effects of IR. Absorption of IR by living cells can induce direct DNA damage through direct interaction with atoms and molecules in DNA. DNA damage can also be induced indirectly through its interaction with atoms, particularly through radiolysis of cellular water and generation of reactive oxygen species (ROS). IR may also disrupt mitochondrial functions, which produces excess ROS and reactive nitrogen species (RNS) by stimulation of oxidases (e.g. SOD) and nitric oxide (NO) synthases. These reactions significantly contribute to persistent alterations in lipids, proteins, nuclear DNA (nDNA) and mitochondrial DNA (mtDNA) (Adapted from Azzam et al., 2012).

As mentioned above, IR-induced cellular damage can also occur indirectly through production of excess ROS from radiolysis of cellular water or IR-induced mitochondrial dysfunction. As shown in Figure 6, radiolysis of water (which makes up ~80% of the cell) generates free radicals (e.g. hydroxyl, superoxide radicals) and other ROS that go on to damage critical targets in the vicinity (e.g. DNA). Sparsely ionizing low-LET IR predominantly induces biological effects through these indirect mechanisms, while densely ionizing high-LET IR induces direct, clustered cellular damage along the radiation track. Moreover, interaction of high-LET IR with water produces significantly higher levels of ROS compared to traversal of low-LET IR: it is estimated that ~2000 ROS per nanogram of tissue are generated within less than a microsecond from a single traversal of a high-LET 3.2 MeV α-particle, whereas ~60 ROS are generated from a hit of low-LET ^{137}Cs γ-rays. Consequently, for the same total absorbed dose, high-LET IR is more damaging than low-LET IR. Such ROS concentrations in the nucleus can obviously cause extensive oxidative injury and significantly modify normal biochemical reactions. ROS can cause other cellular damages, including lipid peroxidation, protein oxidation, oxidative alterations to nuclear and mitochondrial DNA, and inactivation of enzymes (Figure 6) (Hall, 2006;Dianov and Parsons, 2007;Azzam et al., 2012). Though the immediate burst of excess ROS initially produced at the time of irradiation is believed to persist for only microseconds or less, IR-induced oxidative stress in the cell may be prolonged due to persistent long-term effects on oxidative metabolism caused by this initial IR-induced ROS insult (Spitz et al., 2004). Over the last two decades, increasing evidence has been gathered that shows that the long-term effects of IR exposure are due to persisting oxidative stress that causes continuous accumulation of DNA damage. Oxidative stress has been implicated in aging, degenerative diseases (including mitochondrial diseases), as well as cancer (Azzam et al., 2012).

Similar to IR-induced chromosomal damage, IR-induced damage of telomeres can also occur directly (via ionization events via direct traversal of IR within telomere sequences) or indirectly (via post-irradiation telomere uncapping and alterations in telomere maintenance mechanisms) (Ayouaz et al., 2008). Since telomeres make up only a tiny portion (0.02%) of the total human genome (Fumagalli et al., 2012), the probability that a radiation particle will directly traverse a telomeric sequence is infinitesimally small. Therefore, IR-induced damage of telomeres more likely occurs through perturbations of telomere maintenance post-irradiation. The guanine-triplet repeats in telomeric sequences (5′-GGG-3′) were shown to be preferential targets for oxidative damage by ROS (Henle et al., 1999), which are well established to be formed in excess following IR exposure from water radiolysis and IR-induced mitochondrial dysfunction (Azzam et al., 2012), and these damages persist due to deficiencies in DNA repair at telomeres as discussed in Section

1.1.2 (Muraki et al., 2012). The presence of oxidized guanine bases in telomeric nucleotides has been shown to disrupt telomerase activity (Szalai et al., 2002) as well as inhibit the binding of telomeric shelterin proteins, i.e. TRF1 and TRF2 (Opresko et al., 2005). Excess ROS has also been shown to generate other oxidative DNA lesions including oxidized bases and DNA SSBs containing modified 3′-ends (Dianov and Parsons, 2007). Altogether, these damages interfere with DNA replication and results in telomere shortening and loss in cells undergoing oxidative stress (Tchirkov and Lansdorp, 2003).

It was long believed that the biological effects of IR exposure were solely the consequence of DNA damage that occurs in cells during or shortly after *direct* traversal of an IR particle through a cell nucleus. However, this classical "target theory," which used to be the central paradigm of radiation biology, has since been challenged by accumulating evidence over the last three decades that demonstrate that non-irradiated, "bystander" cells in the vicinity of irradiated cells as well as the progeny of irradiated and bystander cells present molecular, biochemical, and genetic abnormalities. These effects, coined "non-targeted effects," include IR-induced bystander effects, genomic instability, and adaptive response.

The IR-induced bystander effect is the phenomenon where IR-induced stresses are transmitted from irradiated cells to their neighboring non-irradiated bystander cells (Little, 2003). Indeed, bystander effects are well known to induce a spectrum of detrimental cellular responses in non-irradiated bystander cells that are similar to those observed in directly irradiated cells, such as DNA damage, chromosomal rearrangements, micronuclei, gene amplifications, gene mutations and neoplastic transformation, reduced cell survival (lethal mutations or delayed reproductive cell death), apoptosis, and mitochondrial alterations with increased ROS production (Morgan, 2003b;a;Shao et al., 2004;Belyakov et al., 2005;Azzam et al., 2012). *In vivo* occurrence of IR-induced bystander effects are demonstrated in situations where humans are partially exposed to low doses/low dose-rates of IR, such as during deep space exploration, mining, or residential radon exposure, where a small fraction of cells is exposed to IR at any one time. Particularly, in the case of radiotherapy, IR-induced damage, especially in tissues irradiated with high doses, may induce systemic effects that affect the whole body during, or a short time after, exposure. Indeed, significant biological changes have been observed in tissues that are widely separated from the irradiated area, and treatment directed at a tumor at one site may profoundly affect tumors and/or normal tissues located elsewhere in the body; these systemic effects may be either detrimental or beneficial (if they lead to shrinkage of distant tumors), and have been termed "abscopal effects" (Morgan, 2003b;Prise and O'Sullivan, 2009;Newhauser and Durante, 2011).

Memory of the initial stressful IR injury has been shown to be maintained in the progeny of both directly irradiated and bystander cells in the form of genetic instability (Terzaghi and Little, 1976;Seymour and Mothersill, 1997;Watson et al., 2000;Morgan et al., 2002;Little, 2003), which induces increased rates of mutations and CAs in these progeny cells (Ilnytskyy and Kovalchuk, 2011). Propagation of IR-induced CAs through cell generations will be discussed in detail in Section 1.2.4, and the role of telomeres in the propagation of chromosomal instability has been discussed in Section 1.1.2. These long-term effects of IR exposure may be due to prolonged oxidative stress that lead to continuous accumulation of DNA damage in the progeny of both irradiated and bystander cells; strong evidence indicates that these effects are dependent on factors such as radiation quality, dose, dose-rate, genetic susceptibility, and age (Azzam et al., 2012). Delayed health effects can be observed many years after IR exposure, illustrated by a higher incidence of secondary malignancies and a variety of degenerative conditions in long-term cancer survivors (Newhauser and Durante, 2011). Delayed effects are also observed following occupational IR exposure in miners, nuclear workers, and astronauts. As exposure to IR is an inevitable part of modern life, an understanding of the mediating biochemical events may have profound implications for long-term human health risks, and may lead to refinement of radiation protection guidelines (Mosse, 2012;Morgan and Bair, 2013) and therapeutic protocols (Mothersill et al., 2004;Hei et al., 2011;Mancuso et al., 2012;Schmid and Multhoff, 2012). Conversely, knowledge of the mediating mechanisms of IR exposure may help in devising approaches to alleviate its detrimental effects.

Apart from these detrimental damages, non-targeted effects can also induce protective mechanisms, called adaptive responses, where exposure to a small priming dose of IR protects cells from stress induced by a subsequent challenge from IR or other environmental agents; adaptive responses, mainly observed following *in vitro* or *in vivo* exposures to low doses of low-LET IR (X- or γ-rays) delivered at low dose-rates, can include secretion of inhibitory factors (Komarova et al., 1998), enhanced cell differentiation (Belyakov et al., 2002), and radio-adaptation (Iyer and Lehnert, 2002). Ultimately, these targeted and non-targeted biological effects of IR that could manifest in seconds to even decades after irradiation could have important short-term and long-term consequences on the health of the organism/being.

1.2.3 DNA damage response pathways and DNA damage repair mechanisms

As mentioned in Section 1.1.1, DNA is continuously exposed to damaging agents throughout the cell lifespan via endogeneous DNA damaging factors, external environmental stress, and lifestyle factors. This constant assault on DNA yields tens of thousands of DNA

lesions per day in every human cell. These DNA lesions must be repaired to prevent loss or incorrect transmission of genetic material, which can lead to tumorigenesis and other pathologies (Jackson and Bartek, 2009;Lin et al., 2012;Price et al., 2013).

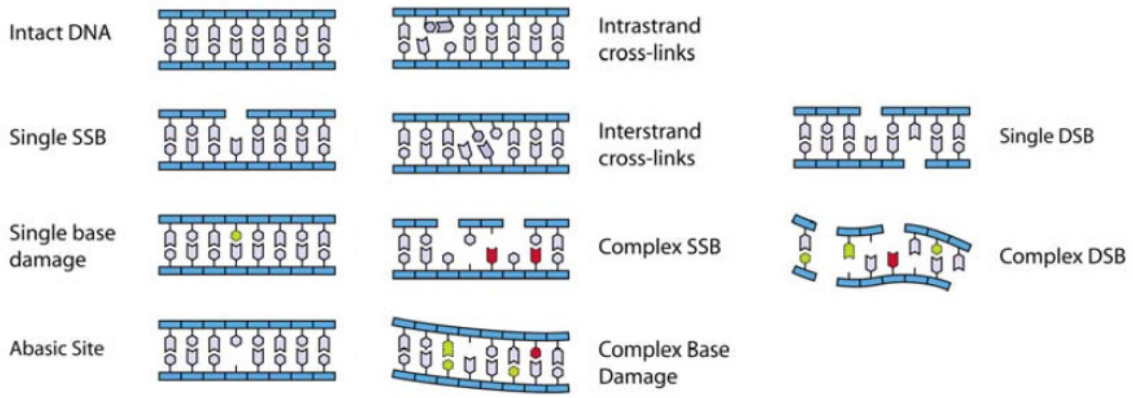

Figure 7. IR-induced DNA lesions. IR induces a wide range of damage in DNA including single strand breaks (SSB), base damage, abasic sites, DNA-protein cross-links, and double strand breaks (DSB) (Adapted from IAEA, 2011).

As illustrated in Figure 7, targeted and non-targeted effects of IR exposure and IR-induced ROS induce a wide range of DNA damage of varying levels of complexity, such as base damage, SSBs, abasic sites, DNA-protein cross-links, and DSBs (IAEA, 2011). As summarized in Figure 8, the choice of the repair system depends on the type of DNA lesion. SSBs or single-base damage (i.e. DNA lesions on a single strand that do not significantly disrupt the helical structure) are generally repaired by base excision repair (BER) (Chou et al., 2015), whereas DNA damage that significantly distorts the DNA helix (e.g. bulky lesions and crosslinks) is repaired by nucleotide excision repair (NER) (Petruseva et al., 2014). Small chemical changes affecting a single base are repaired via direct repair (DR) (Yi and He, 2013), and mismatches in base pairing caused by DNA replication errors are repaired by mismatch repair (MMR) (Larrea et al., 2010). Finally, as mentioned in Section 1.1.2 and will be discussed further in this section, DSBs are repaired via HR and/or NHEJ; the choice of repair system for DSB repair depends on the phase of the cell cycle, and the expression, availability, and activation of DNA repair proteins (Lieber, 2008;Shah and Mahmoudi, 2015).

Upon induction of DSBs, DDR pathways are activated, which trigger a complex signaling cascade that includes activation of DNA repair pathways, cell cycle arrest to allow time for repair of DNA damage, and in certain cases, initiation of senescence or apoptosis. The central components of DDR activation are ATM, ATR, and DNA-PK, members of the phosphatidyl inositol 3-kinase-like kinase (PIKK) family. ATM and DNA-PK are predominantly activated by DNA DSBs, whereas other types of DNA damage (e.g.

replication-induced DSBs, base adducts, and cross-links) activate ATR (Branzei and Foiani, 2008;Nam and Cortez, 2011;Shiloh and Ziv, 2013).

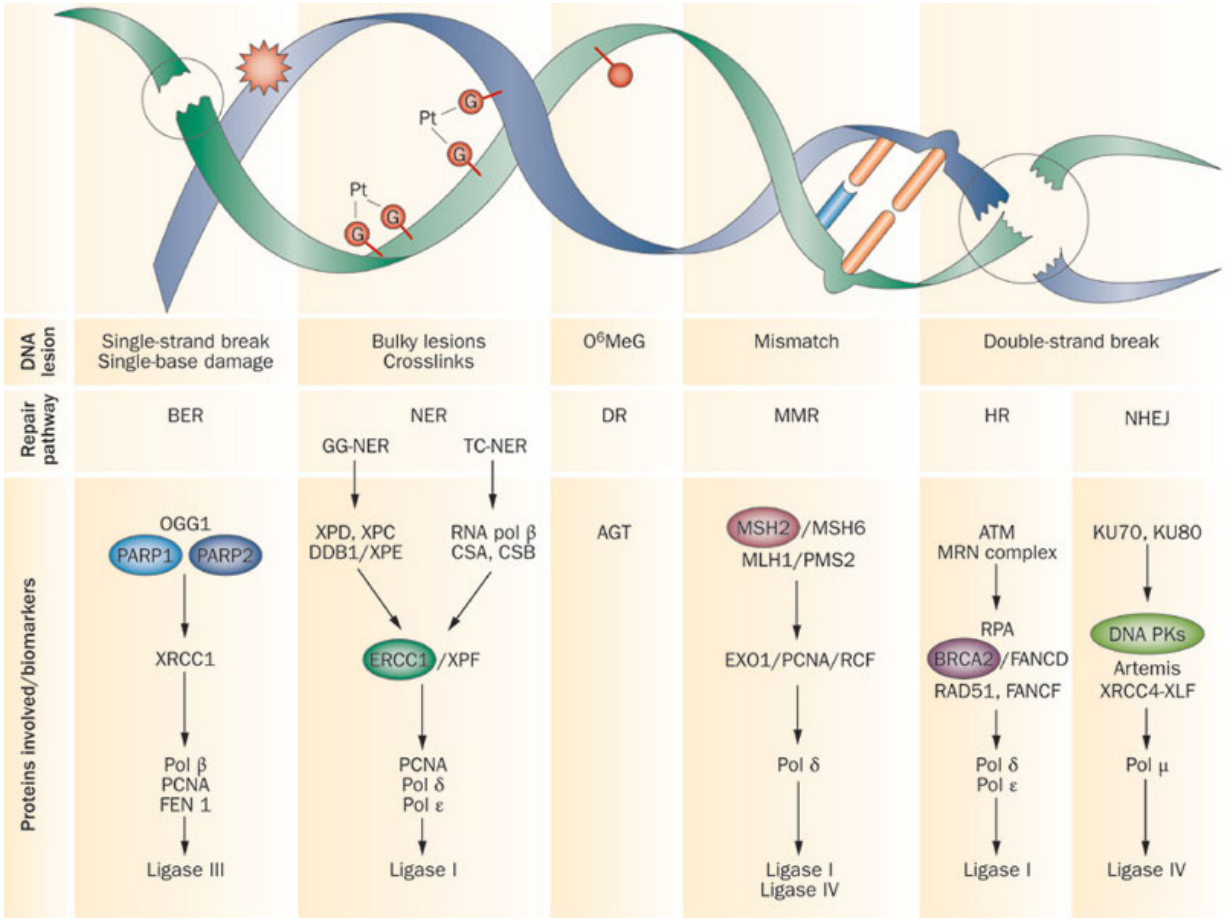

Figure 8. Types of DNA lesions and their corresponding DDR pathways. SSBs or single-base damage (i.e. DNA lesions on a single strand that do not significantly disrupt the helical structure) are generally repaired by base excision repair (BER), whereas DNA damage that significantly distorts the DNA helix (e.g. bulky lesions and crosslinks) is repaired by nucleotide excision repair (NER). Small chemical changes affecting a single base are repaired via direct repair (DR), and mismatches in base pairing caused by DNA replication errors are repaired by mismatch repair (MMR). Finally, DSBs are repaired via homologous recombination (HR) and non-homologous end joining (NHEJ). AGT=O6-alkylguanine-DNA alkyltransferase; GG-NER=global genome NER; 06MeG=O6-methylguanine; TC-NER=transcription-coupled NER (Adapted from Postel-Vinay et al., 2012).

As shown in Figure 8, DNA-PK and ATM are activated by the recruitment of KU70/KU80 and the MRN complex, respectively, to DSBs. KU70/KU80 and DNA-PK promote NHEJ repair of DSBs. As shown in detail in Figure 9, the DNA-PK catalytic subunit (DNA-PKcs) keeps the broken DNA ends in close proximity during NHEJ repair, and recruits end-processing factors (e.g. Artemis, PNKP, APE1, and TDP1), which prepare the DNA ends for re-ligation by the XRCC4–XLF– LIG4 complex (Postel-Vinay et al., 2012;Panier and Boulton, 2014). In recent years, alternative end-joining pathways have been described that

repair DSBs independently of one or more core components of this c-NHEJ machinery (Decottignies, 2013;Badie et al., 2015).

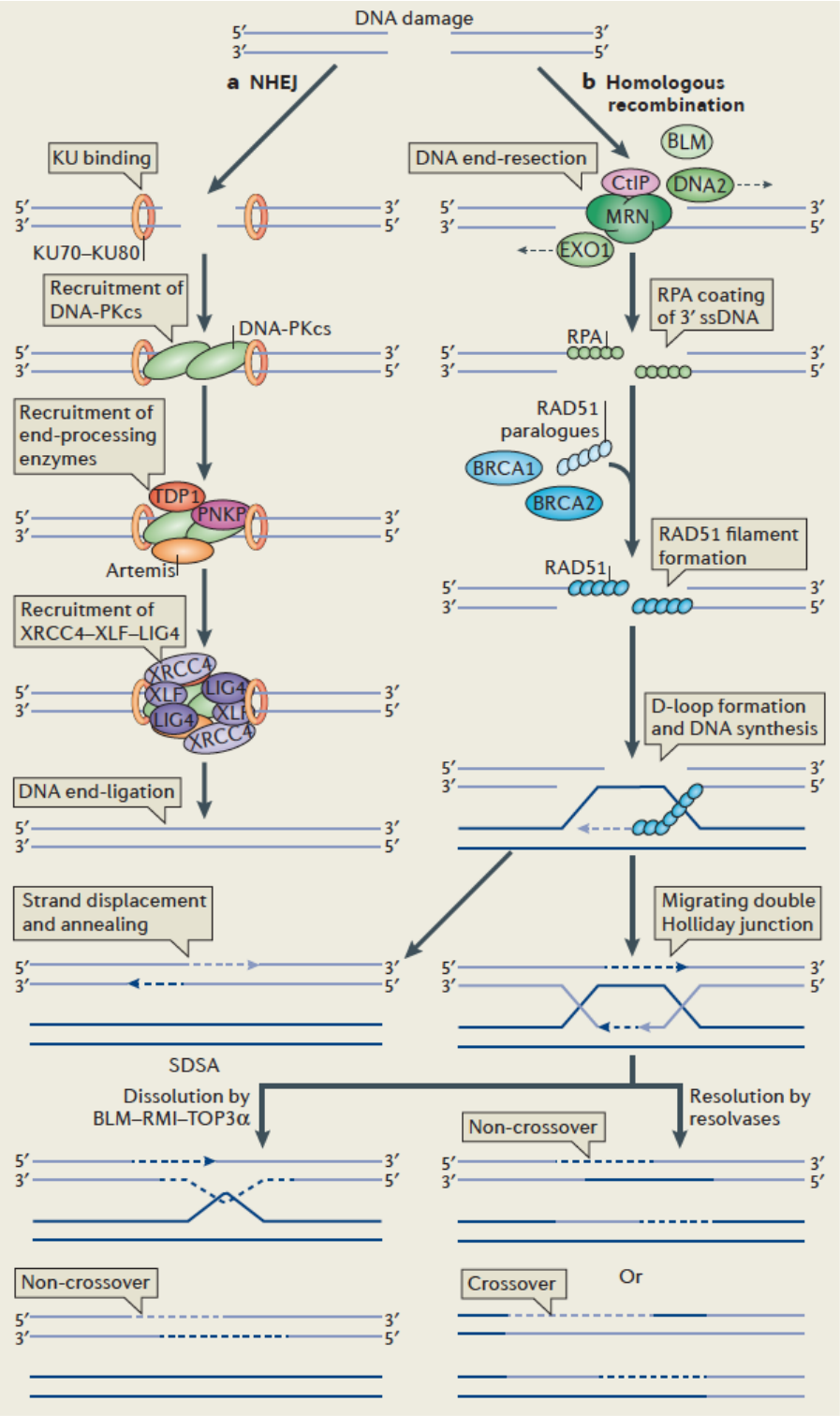

Figure 9. DNA DSB repair pathways. The two main DNA DSB repair pathways in eukaryotic cells: non-homologous end joining (NHEJ; part a) and homologous recombination (part b). BLM=Bloom's syndrome helicase; BRCA1/2=breast cancer 1/2; CtIP=CtBP-interacting protein; DNA2=DNA replication ATP-dependent helicase; DNA-PKcs=DNA-PK catalytic subunit; EXO1=exonuclease 1; LIG4=DNA ligase 4; MRN (MRE11–RAD50–NBS1) complex;

PNKP=polynucleotide kinase/phosphatase; RMI=RecQ-mediated genome instability protein 1; RPA= replication protein A; SDSA=synthesis-dependent strand annealing; ssDNA= single-stranded DNA; TDP1=tyrosyl–DNA phosphodiesterase 1; TOP3α=topoisomerase 3α; XLF=XRCC4-like factor; XRCC4=X-ray repair cross complementing protein 4 (Adapted from Panier and Boulton, 2014).

As a consequence of DSB induction, ATM is activated and phosphorylates the histone H2AX (to form γH2AX), which leads to both structural alterations to the chromatin around the damaged site to allow repair proteins access to the damaged regions of the DNA, as well as the recruitment and retention of key DDR factors; accumulating evidence indicates that γH2AX may also be involved in functions that are not directly related to its function as a DNA DSB marker[**] (reviewed in detail in Turinetto and Giachino, 2015). γH2AX foci are formed within minutes after IR exposure in a dose-dependent manner, peak at <1 hour post-irradiation, and then rapidly decay to baseline levels within one to several days, depending on the dose received. H2AX phosphorylation leads to recruitment of many checkpoint and repair factors, such as MDC1, MRN, and the ubiquitin ligases RNF8 and UBC13 (Postel-Vinay et al., 2012;Panier and Boulton, 2014). These factors promote the recruitment of 53BP1, BRCA1, and more ATM to facilitate the spreading of the DDR signal through the nucleus. These proteins go on to initiate the phosphorylation and dimerization of checkpoint kinases CHK2/CHK1, which targets effectors including p53, CDC25A, and CDC25C that in turn activates cell cycle checkpoints or induce apoptosis (Raynaud et al., 2008b;Thompson, 2012).

While NHEJ is active in all phases of the cell cycle, HR is restricted to the S and G2 phases when sister chromatids are available in close proximity as repair templates (Branzei and Foiani, 2008;Symington and Gautier, 2011). As shown in Figure 9, HR is initiated by the generation of long stretches of 3' single-stranded DNA (ssDNA), which activates ATR (Nam and Cortez, 2011). The 3' ssDNA are created via DNA end resection, a complex and highly regulated process that requires several nucleases including BLM, CtIP, the MRN complex, EXO1, and DNA2. The 3' ssDNA is then coated by RPA. Thereafter, RAD51, the key facilitator of HR, displaces RPA on the ssDNA with the help of mediator proteins such as BRCA1, BRCA2, and several RAD51 paralogues. The RAD51–ssDNA nucleofilament then forms a D-loop with a homologous sequence elsewhere in the genome, and DNA synthesis is initiated to replace the DNA around the former DSB site. Finally, depending on the type of

[**] These 'non-canonical' H2AX roles include sex chromosome inactivation in male germ cells, X inactivation in female somatic cells, chromatin regulation in mitosis, embryonic and neural stem cell development, asymmetric sister chromosome segregation in stem cells, and cellular senescence maintenance (Turinetto and Giachino, 2015).

HR, the D-loop is resolved either by dissociation of one of the invading strands via synthesis-dependent strand annealing (SDSA), or through migrating double Holliday junction intermediates that are either cleaved by resolvases or dissolved by the BLM–RMI–TOP3α complex (Panier and Boulton, 2014).

As HR requires sequence homology of undamaged DNA for DSB repairs (thereby being active during S and G2 phases when homologous sister strands are available in close proximity), HR provides 'error free' repair. However, NHEJ could join any two DSB ends in a homology-independent manner (two ends may not necessarily be the original partners generated by a break), thus leading to 'error-prone' repair of DSBs DNA. Most chromosome aberrations in mammalian cells are formed via chromosomal fusions via NHEJ (Sasaki, 2009).

As will be discussed further in Section 1.4.1, defects in genes/proteins involved in the NHEJ and HR pathways confer dramatically increased radiosensitivity and/or immunodeficiency. Radiosensitivity disorders can also be caused from defects in proteins involved in DDR signaling and/or activation of cell cycle checkpoints (e.g. ATM, 53BP1, the MRN complex, RFN168) and/or in carrying out histone modifications around the DSB (e.g. H2AX to form γH2AX), or due to mutations in cohesins (proteins involved in holding chromosomes together during DNA replication/repair). Currently, there are 15 known genetic disorders that are associated with increased cellular radiosensitivity, which in some cases could also be related to increased susceptibility to IR-induced cancer (Advisory Group on Ionising Radiation, 2013).

1.2.4 Radiation-induced chromosomal aberrations and chromosomal instability

As described in Section 1.2.2, IR exposure can produce DNA DSBs, with high-LET IR inducing more *clustered* damage at a given dose compared to low-LET IR, and could result in the formation of CAs if improperly repaired (Goodhead, 1994). IR-induced telomeric damage, post-irradiation telomere uncapping, and/or IR-induced alterations in telomere maintenance mechanisms could result in chromosome fusion (Murnane, 2012). CAs are of particular interest in the monitoring of IR-induced DNA damage as they can have significant cellular consequences, including cell death at short-term, or the initiation and propagation of human pathologies such as cancer at long-term if CAs are of the transmissible type that causes chromosomal instability (Sabatier et al., 1995;Raynaud et al., 2008b). CAs are also of special interest in the field of biodosimetry as their IR-induced frequency can provide sensitive dose estimates (IAEA, 2011).

IR-induced CAs can be of the chromatid- or chromosome-type. Chromatid-type aberrations may be induced by irradiation during the G2 or S phases of the cell cycle;

ultraviolet light and chemicals can induce chromatid-type aberrations at any phase of the cell cycle, so these aberrations may also be of interest in the context of background frequency of chromosomal damage and delayed chromosomal instability. Chromosome-type aberrations may be induced by irradiation during the G0 or G1 phases of the cell cycle. As PBL that have been irradiated in G0 phase are generally used for various biodosimetry assays, chromosome-type aberrations are of particular interest in this context. Chromosome-type aberrations can be unstable (i.e. non-transmissible to progeny cells) or stable (i.e. transmissible to progeny cells). Various types of chromosome-type aberrations are outlined below (IAEA, 2011):

Unstable IR-induced chromosome-type aberrations (non-transmissible):

- Dicentric chromosomes, the main aberration used for biodosimetry (discussed in Section 1.3.1), are formed from an exchange between the centromeric pieces of two broken chromosomes; in its complete form, it is accompanied by an acentric fragment, formed from the fusion of the two acentric pieces of these broken chromosomes.
- Centric rings are formed from an exchange between two breaks on separate arms of the same chromosome; they are much rarer than dicentrics, and they are also accompanied by an acentric fragment.
- Acentric fragments, or excess acentrics, can be formed independently of dicentrics and rings; they can be formed from either interstitial or terminal deletions.
- Complex chromosomal aberrations (CCAs) involve three or more DSBs.

Stable IR-induced chromosome-type aberrations (transmissible):

- Reciprocal translocations (also called two-way translocations) are formed from the exchange of terminal portions of two chromosomes.
- Non-reciprocal translocations (also called terminal, incomplete, or one-way translocations) are formed from an exchange of the terminal portion of just one chromosome; this type is less frequent and more unstable than reciprocal translocations.
- Interstitial translocations (also called insertions) are formed when an acentric piece of one chromosome is inserted within an arm of another chromosome.

Immediately following IR exposure of normal human cells, a selective process commences that selects against highly damaged cells; highly damaged cells harboring multiple CCAs either die or do not give rise to viable progeny cells. Interestingly, hypothermia during *in vitro* irradiation has been shown to have a sparing effect, inducing

decreased levels of chromosomal damage, which could be related to temperature-related effects on the indirect effects of IR (Lisowska et al., 2013). Irradiated cells that are viable undergo a delay in the cell cycle to allow for repair of IR-induced DNA damage (Azzam et al., 2000). The length of the cell cycle delay is dependent on the extent and complexity of IR-induced damage, and most DNA repair is completed within the first few hours after irradiation (Houtgraaf et al., 2006). These surviving cells undergoing their first cell division post-irradiation were shown to harbor both stable/balanced transmissible (translocations, inversions) and unstable/unbalanced non-transmissible rearrangements (dicentrics, rings, CCAs) (Martins et al., 1993), with high-LET IR causing more clustered DNA DSBs and higher frequencies of CCAs that may be less likely to be repaired correctly compared to equivalent doses of low-LET IR (Sabatier et al., 1987;Testard et al., 1997;Anderson et al., 2000;Testard and Sabatier, 2000).

Transmissible mutations that can be propagated to progeny cells are believed to be fixed during DNA synthesis and cell proliferation, and unstable aberrations and those chromosomal lesions not compatible with cell survival are eliminated at subsequent cell divisions post-irradiation; dicentrics and CCAs decrease by 50% and 30%, respectively, at each cell generation (Al-Achkar et al., 1988). Consequently, a few passages after irradiation, most karyotypes are apparently normal, with few remaining balanced/transmissible anomalies, and these cells may harbor IR-induced recessive gene mutations that accumulate with each successive generation. At later passages, unstable chromosomal rearrangements reappear, mostly non- or poorly transmissible dicentrics that recurrently involve specific chromosomes in telomeric end-to-end associations. The occurrence of IR-induced instability was shown to be further delayed in late passages after irradiation with higher LET IR (Sabatier et al., 1992;Martins et al., 1993); therefore, it can be concluded that high-LET IR has a higher capacity to induce delayed genomic instability compared to low-LET IR (Kadhim et al., 2006). Eventually, these IR-induced or pre-existing recessive mutations may be unmasked and amplified, and upon loss of tumor suppressor function, those cells that harbor genetic alterations that give them a proliferative advantage invade the cell population. Continuing chromosomal instability and cell proliferation may be key elements of the initiation and progression of multi-stage carcinogenesis (Sabatier et al., 1995;Raynaud et al., 2008b).

Interestingly, several new types of CCAs have very recently been described. These CCAs, proposed to be named ‘chromoanagenesis’ (meaning ‘chromosome rebirth’), are formed as a result of multiple DNA DSB breaks that gets stitched back together in random order (most likely via NHEJ), leading to the generation of a highly rearranged chromosome(s) (Holland and Cleveland, 2012). Though the direct link between these new

types of CCAs and IR exposure has not yet been evaluated, chromoanagenesis has been identified in cancer cells and is linked to congenital diseases. However, its overall frequency in germline cells, healthy tissue, and cancer types, and its causative link with human diseases are unknown (Hatch and Hetzer, 2015). Three types of chromoanagenesis that have been described are as follows:

- Chromothripsis (literally meaning 'chromosome shattering') involves the shattering of one (or a few) chromosome(s) typically into tens to hundreds of pieces from a single catastrophic event (during a single cell cycle) followed by repair by which the pieces are stitched back together in random order. Chromothripsis has been identified in at least 2%–3% of all cancers across many subtypes (and in ~25% of bone cancers) (Meyerson and Pellman, 2011;Stephens et al., 2011) and germline cells (Kloosterman et al., 2011), and may be important in the early stages of carcinogenesis (Kloosterman et al., 2014) and the development of congenital diseases (de Pagter et al., 2015), respectively. A mechanism of chromothripsis has recently been demonstrated to explain how these massive chromosomal rearrangements are restricted to one chromosome, namely micronucleation, which involves chromosomal fragmentation and rejoining within a single micronucleus (Zhang et al., 2015). Other mechanisms of chromothripsis have been proposed, including telomere dysfunction and B/F/B cycles limited to one chromosome (Sorzano et al., 2013), abortive apoptosis (Tubio and Estivill, 2011), mitotic errors (Jones and Jallepalli, 2012), and p53 inactivation (Rausch et al., 2012).
- Chromoanasynthesis affects a single chromosome or chromosome arm much like chromothripsis, but is characterized by the amplification of numerous chromosomal segments and has signatures of replication-mediated repair. This type of aberration has been linked to developmental delay and cognitive anomalies (Liu et al., 2011;Plaisancie et al., 2014).
- Chromoplexy involves the rejoining of multiple DNA breaks (tens of breakpoints) on multiple chromosomes, resulting in the joining of many distant loci and chromosomes together. This event has been shown to be a common occurrence in prostate cancer (Baca et al., 2013;Shen, 2013).

1.2.5 Low dose biological and health effects

As mentioned briefly in Section 1.2.1, the biological effects and health risks of high doses of IR (> 1 Gy) have been well characterized through extensive experimental studies and epidemiological surveys of survivors of atomic bombings and radiation accidents

(Brenner et al., 2003;National Research Council, 2006). It is well known that the extent and complexity of biological damage induced by direct IR exposure to high doses is directly proportional to the radiation dose and LET, and cancer risk at these doses is established to increase linearly with dose. However, the health risks of low levels of IR exposure (< 0.2 Gy) remain ambiguous and controversial. Epidemiological studies to evaluate the long-term health effects of exposure to low doses of IR are difficult to conduct and interpret, as humans are constantly exposed to many confounding factors that can also contribute to adverse health effects (e.g. diet, smoking, exposure to diagnostic radiology, stress, etc.). Therefore, mechanistic *in vitro* and *in vivo* studies are necessary to expand knowledge of cellular and molecular processes underlying low dose IR-induced biological effects (de Toledo et al., 2011;Il'yasova et al., 2014). Coupled with epidemiology, these mechanistic studies should further refine estimates of radiation risks at low doses and help formulate adequate radiation protection guidelines.

Due to the absence of reliable epidemiological estimates of health risks at low doses, the International Commission on Radiation Protection (ICRP) recommends a linear relationship between IR dose and cancer risk, termed the *linear no-threshold (LNT) model*, extrapolated from data obtained at high doses. This model states that exposure to any dose of IR, however small or large, causes a linear increase in risk of detrimental health effects that is directly proportional to the dose; furthermore, this model states that the effects of sequential doses are additive (curve ***a*** in Figure 10) (Preston, 2003;National Research Council, 2006). However, the validity of this LNT model is controversial and has been the subject of intense debate.

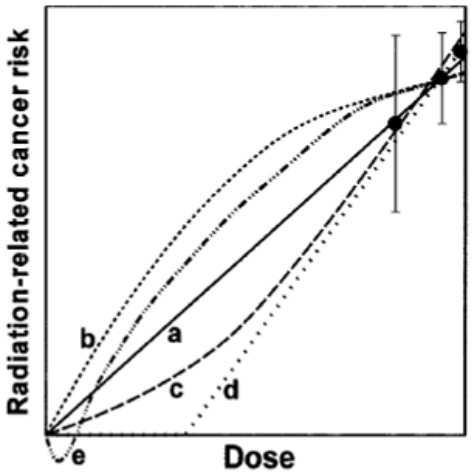

Figure 10. Proposed models for predicting the cancer risks from exposure to low doses of IR. The current linear no-threshold (LNT) model (curve *a*) extrapolates from data obtained at high doses, and assumes a linear relationship between IR dose and cancer risk, at all dose levels. Other proposed models of the relationships between radiation dose and cancer risk: the LNT model underestimates risk (curve *b*); the LNT model over-estimates risk (curve *c*); a threshold

exists below which harmful effects are unlikely to arise (curve *d*); a J-shaped curve (curve *e*) where exposure to very low dose radiation may be beneficial (hormesis) (Adapted from Brenner et al., 2003).

Different models have been proposed to represent cancer risk at low doses (Figure 10). Some postulate that the LNT model underestimates risk (curve ***b*** in Figure 10), while others postulate that the LNT model over-estimates risk (curve ***c*** in Figure 10). Some propose that there is a threshold below which harmful effects are unlikely to arise (curve ***d*** in Figure 10) (Tubiana and Aurengo, 2005), and others suggest a J-shaped curve (curve ***e*** in Figure 10) where exposure to very low dose radiation may be beneficial (hormesis). These extrapolations that challenge the LNT model are based on the observations of several complex biological phenomena that are not readily predictable by dose: growing evidence has emerged that the non-targeted IR effects discussed above in Section 1.2.2 (namely the adaptive response, bystander effects, and genomic instability) may be particularly important in modulating the biological responses to low doses of IR. These phenomena may or may not be harmful to the cell/being. Furthermore, the influence of LET in the induction of these low dose effects is also controversial.

In our original paper, (de Toledo et al., 2011) found in Appendix A.3.1 of this thesis, we discuss in detail evidence from mechanistic studies of the influence of radiation LET on the induction of the adaptive response and non-targeted effects following exposure to low doses of IR. In summary, normal human or rodent cells exposed to low chronic doses of *low-LET* IR were able to adapt to be better able to correctly repair DNA lesions resulting from endogenous metabolism or a subsequent challenge exposure to IR, and were less likely to be transformed to the neoplastic phenotype. In contrast, cells exposed to low-doses of *high-LET* IR (e.g. alpha and heavy ions) did not induce adaptive responses, but instead showed persistent stressful effects such as oxidative stress, mitochondrial dysfunction, and genomic DNA damage in the directly targeted cell, as well as their neighboring bystander cells and their progeny. This data strongly support a role for IR dose and quality (i.e. LET) in determining the nature of the induced IR effects at low doses.

1.2.6 Biomarkers of IR exposure

The wide range of biological effects following direct or indirect IR exposure, some of which are described in the preceding sections, can be quantified by measurements of a variety of biomarkers of IR exposure. Biomarkers are reviewed in detail in (Pernot et al., 2012;Manning and Rothkamm, 2013), and are illustrated in Figure 11.

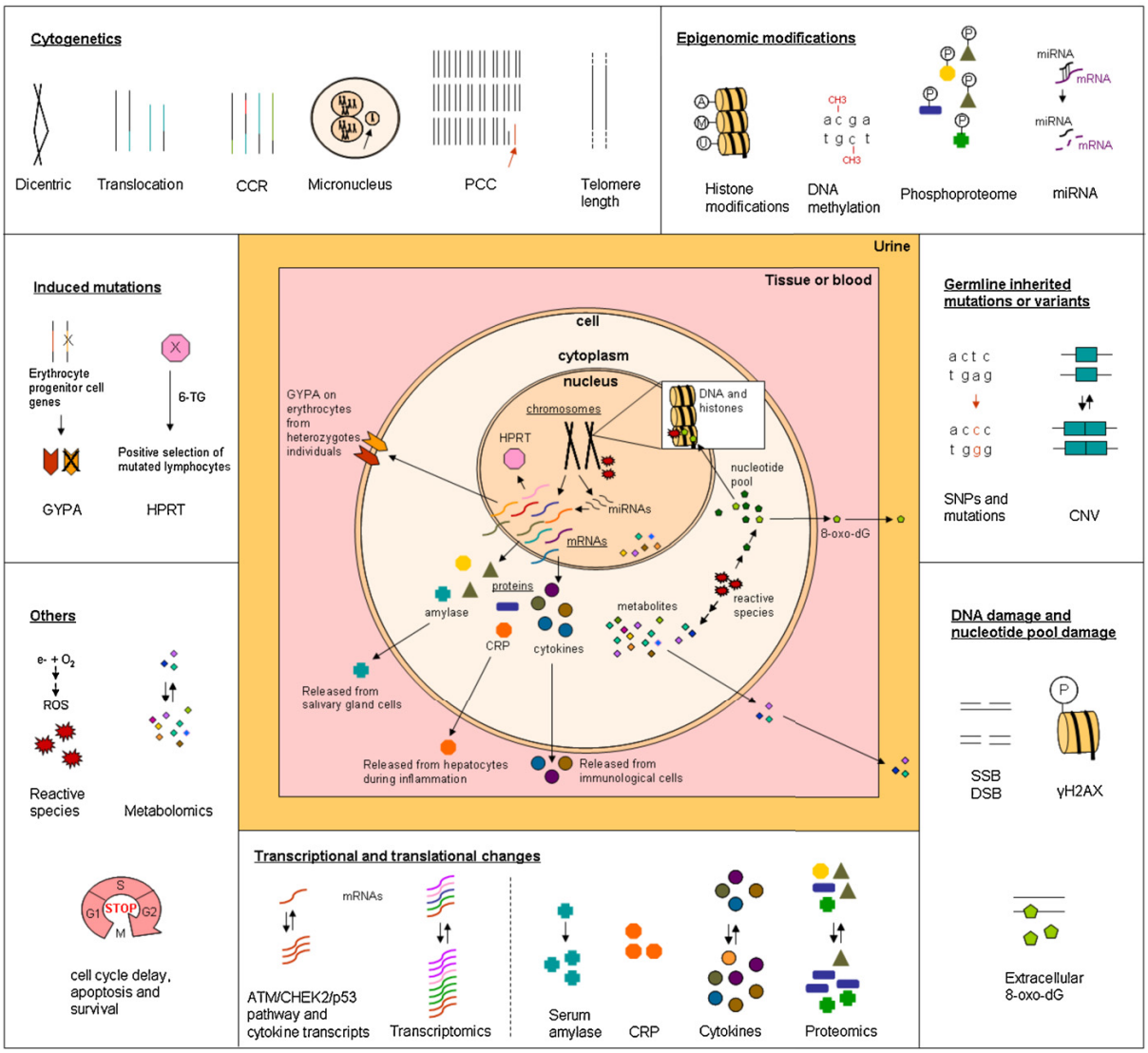

Figure 11. A non-exhaustive list of biomarkers of IR exposure. Vertical double lines represent pairs of chromosomes and horizontal double lines represent double strands of DNA. A=acetyl group; CCR=complex chromosomal rearrangement; CNV=copy number variant; CRP=C-reactive protein; GYPA=glycophorin A; HPRT=hypoxanthine-guanine phosphoribosyl transferase; M=methyl group; miRNA=microRNA; P=phosphate group; SNP=single nucleotide polymorphism; U=ubiquitin; 6-TG=6-Thioguanine; 8-oxo-DG=8-Oxo-deoxyguanosine (Adapted from Pernot et al., 2012).

As illustrated in Figure 11, biomarkers of IR exposure can be classified into seven categories (Pernot et al., 2012):

- *Cytogenetic biomarkers*: e.g. dicentrics, translocations, CCAs, prematurely condensed chromosomes (PCC), micronuclei, telomere length
- *Biomarkers related to nucleotide pool damage and DNA damage*: e.g. DNA SSBs and DSBs, γH2AX, extracellular 8-oxo-dG

- *Biomarkers related to germline inherited mutations and variants*: e.g. single nucleotide polymorphisms (SNP) and inherited gene mutations, copy number variants (CNV) and alterations (CNA)
- *Biomarkers related to induced mutations*: e.g. glycophorin A (GYPA) in MN blood group heterozygotes, hypoxanthine-guanine phosphoribosyl transferase (HPRT) gene
- *Biomarkers related to transcriptional and translational changes*: e.g. changes in RNA levels identified by transcriptomics, proteins identified by proteomics, ATM/CHK2/p53 pathway, serum amylase, Flt3-ligand, C-reactive protein (CRP), cytokines
- *Biomarkers related to epigenomic modifications*: e.g. histone modifications, DNA methylation, micro-RNA (miRNA), phosphoproteome
- *Other biomarkers*: e.g. ROS, metabolites and metabolomics, biomarkers associated with cell cycle delay, apoptosis and cell survival, biophysical markers of exposure (e.g. electron paramagnetic resonance, EPR)

As these biomarkers can detect IR-induced biological effects at various time points post-irradiation (ranging from seconds to years to decades), these biomarkers can be further classified based on their persistence post-irradiation into four categories (Pernot et al., 2012):

- *Biomarkers of exposure*, which can be used to assess IR-induced biological responses either shortly after exposure (seconds to hours to weeks) or long after exposure (months to years to decades)
- *Biomarkers of susceptibility*, which can be used to predict an increased risk of IR-induced health effects based on gene or protein profiles that remain constant throughout the lifetime of an individual
- *Biomarkers of late effects*, which can be used to assess health effects that are present a long time after IR exposure
- *Biomarkers of persistent effects*, which can be used to assess radiation effects present a long period of time after IR exposure

Table 2. Summary of the classifications of different types of biomarkers (Adapted from Pernot et al., 2012).

Biological classification of IR biomarkers		Temporal classification of IR biomarkers			
		Exposure	Susceptibility	Late effects	Persistent effects
Cytogenetics	Dicentrics	√	P	P[a]	P
	Translocations	√	P	P[a]	√
	CCR	√ (high LET IR)	P	P[a]	√
	PCC rings and fragments	√			
	Telomere length	P	P	P[a]	P
	Micronuclei	√	P	P[a]	
Nucleotide pool damage and DNA damage	SSB/DSB	√	P		
	γ-H2AX	√	P	P	P
	Extracellular 8-oxo-dG	(oxidative stress)	P		
Germline inherited mutations/variants and induced mutations	SNP, CNV and inherited gene mutations		√	P (minisatellites in offspring)	P
	CNA	P			P
	GYPA	√			√
	HPRT	√			√
Transcriptional and translational changes	Changes in the mRNA levels of the ATM/CHK2/p53 pathway	√	P		
	Changes in RNAs identified by transcriptomics	√	P	P	P
	Serum amylase	√			
	CRP	√			√
	Proteins identified by proteomics	P	P	P	P
	Cytokines	P	P	P	P
Epigenomic modifications	Histone modifications	P	P	P	P
	DNA methylation	P	P	P	P
	miRNA	√	P	P	P
	Phosphoproteomics	P	P		
Other biomarkers	ROS	√	P	P	P
	Metabolites and metabolomic	√	P	P	P
	Cell cycle delay, apoptosis and survival	P	P		
Direct dosimetry on samples	EPR/ESR	√			√
	Internal emitters	√			

√: direct evidence that this biomarker could be used as such; P: potential or theoretical use; CCR: complex chromosomal rearrangement; CNA: copy number alteration; CNV: copy number variant; CRP: c-reactive protein; DSB: double strand break; EPR/ESR: electron paramagnetic resonance/electron spin resonance; GYPA: glycophorin A; *HPRT*: hypoxanthine-guanine-phosphoribosyl transferase; IR: ionizing radiation; miRNA: microRNA; PCC: premature chromosome condensation; SNP: single nucleotide polymorphism; SSB: single strand break; ROS: reactive oxygen species.

[a] Chromosomal aberrations due to genomic instability.

These categories consider not only the immediate and short-term effects of IR exposure, but also the delayed effects of IR exposure, which can have profound implications for long-term human health risks (e.g. emergence of secondary cancers and other pathobiological conditions after radiotherapy and following occupational IR exposure in miners, nuclear workers, and astronauts) (Newhauser and Durante, 2011;Mosse, 2012;Morgan and Bair, 2013). As summarized in Table 2, there may be overlap between the types of biomarkers, and biomarkers can belong to multiple categories. Currently, the most well-established and validated biomarkers are the ones measured shortly after irradiation at moderate to high doses. Potential biomarkers of exposure, susceptibility, and late/persistent effects at low doses remain to be validated (Pernot et al., 2012).

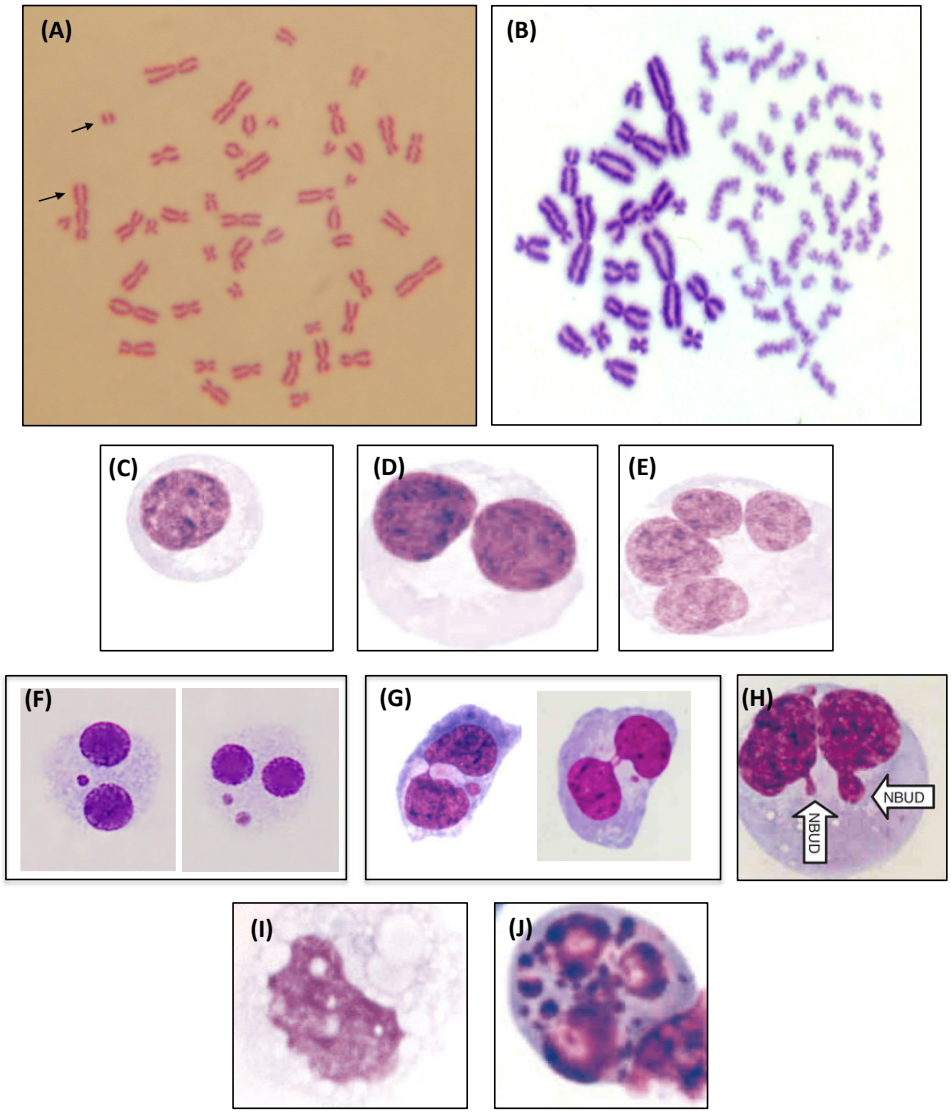

Figure 12. Examples of cytogenetic assays used for biodosimetry (Giemsa stained). (A) The DC assay, considered as the "gold standard" of biodosimetry. (B) The PCC assay. (C-J) Examples of the CBMN cytome assay: (C) mono-nucleate cell; (D) binucleate cell; (E) multi-nucleate cell; (F) binucleate cell containing one (left) or two (right) micronuclei; (G) binucleate cell containing nucleoplasmic bridges (and micronucleus); (H) binucleate cell containing nuclear buds (NBUD); (I) early necrotic cell; (J) late apoptotic cell (Adapted from Fenech, 2007;IAEA, 2011).

1.3 Biological dosimetry

In the event of accidental exposure to IR (e.g. radiation/nuclear accidents or mass casualty events), timely dose estimation and medical triage of exposed individuals (e.g. exposed workers or the general population) based on individual levels of exposure is essential. Some victims, for whom physical signs of IR exposure are not immediately observable but were exposed to significant amounts of IR (> 1 Gy), may be at risk of developing acute radiation syndrome (ARS)[††], which can be fatal (depending on the dose) even with proper medical attention (Lopez and Martin, 2011;Macia et al., 2011). Individuals exposed to smaller doses of IR may be at risk of eventually developing long-term IR-induced health effects (e.g. cataracts, cardiovascular diseases, cancer), and thus, may require medical follow-up. Biological dosimetry, which utilizes the measurement of IR-induced biological responses or consequences in an individual to estimate dose, can be used to properly triage and prioritize victims based on level of urgent medical care and/or need for medical follow-up following a large-scale accident.

Biodosimetry relies on the measurement of biomarkers, discussed above in Section 1.2.6 (Pernot et al., 2012). Listed below are the established and emerging dosimetry methods that are currently employed following accidental IR exposure (Sullivan et al., 2013):

- *Cytogenetic techniques*: dicentric chromosome (DC) assay, chromosomal translocations analysis, PCC assay, cytokinesis block micronuclei (CBMN) assay (Figure 12), and fluorescent *in situ* hybridization (FISH) which can be applied to each of these cytogenetic techniques (Figure 13) (Terzoudi and Pantelias, 2006;Pinto et al., 2010;IAEA, 2011;Wong et al., 2013)
- *Genetic techniques*: somatic mutation assays of GYPA or HPRT, and gene expression assays (Brzoska and Kruszewski, 2015)

[††] Acute radiation syndrome (ARS), also known as radiation toxicity or radiation sickness, is an acute illness following acute, high dose (> 1 Gy delivered within minutes) whole-body (or significant partial-body) irradiation with penetrating IR (i.e. able to reach internal organs, e.g. high energy X-rays, γ-rays, neutrons) that classically involves the cutaneous, hematopoietic, gastrointestinal (GI), and neurovascular systems, either individually or in combination. The onset, manifestation, and severity of ARS symptoms depend on the received dose: generally, doses of < 0.5 Gy are not expected to cause ARS, doses of 4.5 Gy are lethal for 50% of exposed persons, and doses of > 10–12 Gy are 100% fatal. ARS can occur within hours or up to several months after exposure, depending on the received dose ARS progresses in three phases, namely the prodromal phase (early symptoms of ARS, e.g. anorexia, apathy, nausea, vomiting, diarrhea), the latent phase (when the patient looks and feels generally healthy, but stem cells in bone marrow and/or cells lining GI tract are dying), and the manifest illness phase. Hematopoietic, GI, and neurovascular syndrome onsets occur at doses of > 2–3 Gy, 5–12 Gy, and 10–20 Gy, respectively (Lopez and Martin, 2011).

- *Haematological techniques*: differential blood cell count, and lymphocyte depletion rate (LDR) (Hu et al., 2015)
- *Protein expression techniques*: γH2AX, CRP, and serum amylase (Ainsbury et al., 2011;Sproull et al., 2015)
- *Physical techniques*: EPR with tooth enamel and bones (Wieser and Darroudi, 2014;Khvostunov et al., 2015), thermoluminescence or optically stimulated luminescence (OSL) in building materials or consumer products, and nuclear activation of biological tissues or metallic consumer products (Swartz et al., 2014b)
- *Computational techniques*: analytical dose reconstruction ('time and motion' calculations) using the state-of-the-art realistic analytical dose reconstruction with uncertainty estimation (RADRUE), and dose reconstruction by numerical approaches based on Monte Carlo radiation transport codes (Ainsbury et al., 2011)

The method of biodosimetry deployed would need to be adjusted depending on the scale of the emergency/accident and the urgency with which dosimetric results are needed (Swartz et al., 2014a;Swartz et al., 2014b); balancing accuracy, speed, and the ability to perform high-throughput analyses is important particularly in the case of a large-scale radiation incident. Several of these manual and automated systems (especially the DC, CBMN, and γH2AX assays) have been harmonized and validated as triage tools in the case of a large-scale radiological emergency within several national/regional/international networks, including:

- The European Multibiodose project (www.multibiodose.eu), a network of 11 European laboratories that recently adapted and harmonized seven biodosimetric tools, including the DC assay (Romm et al., 2013a;Romm et al., 2014a;Romm et al., 2014b), the CBMN assay (Thierens et al., 2014), the γH2AX assay (Ainsbury et al., 2014a), the skin speckle assay, serum protein assay, and EPR and OSL in portable electronic devices (Jaworska et al., 2013;Jaworska et al., 2015), to mass-casualty scenarios using common software to integrate and report dose estimates (Ainsbury et al., 2014b)
- The RENEB project (Realising the European Network of Biodosimetry, www.reneb.eu), a network of 23 laboratories from 16 European Union countries (Kulka et al., 2012;Kulka et al., 2015) that recently harmonized the γH2AX assay (Barnard et al., 2015)
- Other European platforms include some biodosimetry topics, e.g. EURADOS (European Radiation Dosimetry Group, www.eurados.org) (Ruhm et al., 2015) and NERIS

(European platform on preparedness for nuclear and radiological emergency response and recovery, www.eu-neris.net)

- Other national/regional networks in the USA (Blumenthal et al., 2014), Canada (Wilkins et al., 2015), Japan (Yoshida et al., 2007), and Latin America (Garcia et al., 1995;Di Giorgio et al., 2011;Garcia et al., 2013)
- International networks that include many of the members of national/regional networks, e.g. WHO BioDoseNet network (Blakely et al., 2009;Christie et al., 2010;Livingston et al., 2011;Maznyk et al., 2012), WHO REMPAN network (Radiation Emergency Medical Preparedness and Assistance Network, www.who.int/ionizing_radiation/a_e/rempan/en), and the International Atomic Energy Agency (IAEA) EPR-RANET network (Emergency Preparedness and Response-Response and Assistance Network, available at www-pub.iaea.org/MTCD/Publications/PDF/EPR-RANET_2013_web.pdf)
- The North Atlantic Treaty Organization (NATO) inter-comparison exercise organized by the NATO Research Task Group RTG-033 "Radiation Bioeffects and Countermeasures" of different biodosimetry assays (Rothkamm et al., 2013b), including the manual and automated DC assay (Beinke et al., 2013), CBMN assay (Romm et al., 2013b;De Sanctis et al., 2014), γH2AX assay (Rothkamm et al., 2013c), and the gene expression assay (Badie et al., 2013)

Historically, biodosimetric approaches have been focused on cytogenetic biodosimetry assays (illustrated in Figure 12), which estimate the absorbed dose in the exposed individual based on analysis of IR-induced chromosomal alterations. The DC assay (Figure 12A) remains the international "gold standard" of biodosimetry (Pinto et al., 2010;IAEA, 2011;Wong et al., 2013). In the following sections, we elaborate on the current status of each of the four cytogenetic assays (DC, translocations, PCC, CBMN; Figure 12), and the applications of FISH (Figure 13) as well as the widely used γH2AX assay (summarized in Table 3). As will be discussed in the following sections, each of these assays has potential advantages and challenges as biodosimeters, and many of these assays have been automated to allow for high-throughput analyses and faster acquisition of results.

Table 3. Summary of current status of cytogenetic assays used for biodosimetry (automated and manual).

	DC assay	PCC assay	CBMN assay	FISH assay	γH2AX assay
Types of aberrations scored for biodosimetry applications	• Dic • Rings	• Ac • Dic • Rings • Transloc	• MN • NPB • NBUD	• Dic • Rings • Ac • Transloc	• γH2AX foci • γH2AX fluorescence intensity
Typical IR scenario applications	• Acute / Chronic • Recent exposure	• Acute • Recent exposure	• Acute / Chronic • Recent exposure	• Acute / Chronic • Recent / Old exposure	• Acute • Recent exposure
Acute dose range limits	0.1 to 5 Gy	0.2 to 20 Gy	0.3 to 4 Gy	0.25 to 4 Gy	Depends on time point post-irradiation
Minimum time required to obtain results*	2.4-6 days	< 1 day	4-8 days	2-5 days, depending on assay	< 1 day – 2 days
Status of assay standardization	(ISO, 2008; 2014a)	NA	(ISO, 2014b)	NA	NA
Stability of aberration post-IR exposure	• Dic: weeks	• PCC fragments: immediately • PCC rings: weeks	• MN: weeks	• Transloc: years	• γH2AX: hours to 1 day

* Based on (IAEA, 2011;Beinke et al., 2013;Romm et al., 2013b;Rothkamm et al., 2013b;Rothkamm et al., 2013c). Ac=acentrics; Dic=dicentrics; Gy=Gray; MN=micronuclei; NA=not applicable; NBUD=nuclear buds; NPB=nucleoplasmic bridges; Transloc=translocations.

1.3.1 The dicentric chromosome (DC) assay

As mentioned above, the DC assay, considered the international "gold standard" method of biodosimetry, is the technique with which newer biodosimetric approaches are compared for validation. The dicentric chromosome is the biomarker of choice for biodosimetry (for recent IR exposure, as the frequency of this CA decreases with lymphocyte turnover) due to its relative specificity to IR exposure, low background levels, and high sensitivity. The technique and performance criteria in peripheral blood lymphocytes (PBL) are highly standardized by the IAEA and the International Organization for Standardization (ISO) to ensure reproducibility and accuracy for routine or triage use (ISO, 2008;IAEA, 2011;ISO, 2014a). The DC assay is considered the most precise and sensitive method of dose estimation; it is capable of detecting doses as low as 0.1 Gy, and can differentiate between partial and whole body exposures as well as chronic and acute exposures (IAEA, 2011).

However, the usefulness of this technique in a large-scale emergency setting is limited by the time-consuming and laborious nature of the assay, as this technique requires at least 4 to 5 days until results are available. This delay is due to several unavoidable

variables. To apply the DC assay, collected PBL need to be stimulated and cultured for a fixed, incompressible time of ~2 days until they reach first mitosis; a recent study investigating alternative methods of lymphocyte stimulation to determine whether this most time-consuming portion of the DC assay can be effectively reduced found that the conventional protocol using the lectin PHA-M (Phytohemagglutinin M) is superior to higher/lower concentrations of PHA-M and in comparison with seven other mitogens[‡‡] (Beinke et al., 2015). Additionally, low mitotic index of irradiated cells, especially at high doses (> 4 to 5 Gy of low-LET IR), as well as dose-dependent mitotic delay and/or cell death, may hinder acquisition of sufficient numbers of analyzable cells and may lead to underestimation of dose; a recent study demonstrated that treatment of lymphocyte cultures with caffeine can overcome the upper dose limit of 4 to 5 Gy and allows for DC analysis of doses of up to 25 Gy (Pujol et al., 2014). Furthermore, the classic DC assay utilizes uniform staining (i.e. Giemsa) of metaphases (Figure 12A), which requires a high level of trained expertise (as CAs are scored based solely on chromosomal morphology), and sufficient time is needed to individually analyze large numbers of cells to minimize large inter-cellular differences especially following low doses of IR exposure (IAEA, 2011).

Strategies to shorten analysis time and increase the throughput of the DC assay have been developed. Such strategies include modified methods of manual DC scoring following uniform metaphase staining, including scoring cells in a less restrictive manner (QuickScan Mode) (Flegal et al., 2010;Flegal et al., 2012;De Amicis et al., 2014), and scoring lower numbers of metaphases (Triage Mode) (Lloyd et al., 2000;Romm et al., 2011;De Amicis et al., 2014). The sharing of high resolution images via the internet and web-based manual scoring (tele-scoring) by trained scorers anywhere in the world (thereby eliminating the need to mail blood samples or slides) may be an immediate solution to increasing throughput of this labor-intensive analysis; this strategy has recently been recommended by the US Department of Homeland Security as an immediate solution to addressing the shortage of laboratory capacity in the US in the event of a nuclear detonation in an urban environment (along with providing biodosimetry and DC scoring training to the ~150 cytogenetics laboratories in the US to further improve capacity) (Blumenthal et al., 2014); scoring exercises and inter-comparisons have been performed within the networks of WHO BioDoseNet (Livingston et al., 2011;Maznyk et al., 2012), Latin America (Garcia et al., 2013), and Japan (Yoshida et al., 2007), and promising results have been reported in the

[‡‡] The seven mitogens investigated in this study included five lectins named CNA (concanavalin A), PW (pokeweed), LMA (lectin from *M. amurensis*), LTV (lectin from *T. vulgaris*), PHA-L (Phytohemagglutinin L), administered either alone or combined with LPS (*E. coli* lipopolysaccharide) and SLO (streptolysine O) (Beinke et al., 2015).

Multibiodose project with both conventional DC scoring and scoring in QuickScan Mode (Romm et al., 2014a).

Automation of at least some portions of the DC assay is recommended to further increase throughput analysis (Blumenthal et al., 2014). Several automated systems have been developed, including automated DC scoring via imaging flow cytometry (Beaton et al., 2013), and semi-automated DC scoring following uniform staining using commercial image analysis software DCScore (MetaSystems) (Vaurijoux et al., 2009;Vaurijoux et al., 2012;Gruel et al., 2013;Romm et al., 2013a;De Amicis et al., 2014). There have been joint efforts to harmonize these manual and automated scoring approaches in international networks (Wilkins et al., 2008;Di Giorgio et al., 2011;Wilkins et al., 2011;Beinke et al., 2013;Jaworska et al., 2013;Romm et al., 2013a;Rothkamm et al., 2013b;Ainsbury et al., 2014a;Romm et al., 2014b). However, existing software for automated DC scoring is able to detect only half of the dicentrics and rejects many of the metaphases. The difficulty in obtaining sufficient numbers of metaphases from irradiated samples due to the lack of sensitivity of the existing software, limits the capacity to perform sensitive and precise biological dosimetry at both low and high doses using existing automated DC scoring systems.

1.3.2 Fluorescence in situ *hybridization (FISH) and chromosomal translocations analysis*

The development of fluorescence *in situ* hybridization (FISH) techniques (Figure 13) have allowed for easy visualization and assessment of IR-induced structural CAs for routine biodosimetry applications that were not before possible with G banding and Giemsa staining (Edwards et al., 2005). As dicentric chromosomes and CCAs (a biomarker of high-LET IR exposure) are unstable, non-transmittable CAs, they decrease in frequency with PBL turnover and are thus reliable as biomarkers of recent IR exposure (weeks). Translocations, however, are stable, transmittable CAs and thus allow for biodosimetry for past IR exposure (years) (Anderson et al., 2000;Pernot et al., 2012;Cho et al., 2015). The FISH technique allows chromosomes to be “painted” by attaching specific DNA sequences (probes) to various fluorochromes. A large variety of probes are now available, so FISH can be employed to selectively visualize a wide spectrum of the genome: from a specific portion of chromosome (e.g. centromeres, telomeres; Figure 13A), to one or multiple specific chromosomes (chromosome painting), to painting of the entire genome (M-FISH and karyotype analyses; Figure 13B). Furthermore, by attaching fluorochromes in varying ratios to specific sites, different regions can be visualized simultaneous with a wide range of

colors. FISH can also be applied to other cytogenetic techniques like the PCC and CBMN (Figure 13C) assays to carry out various analyses (IAEA, 2011).

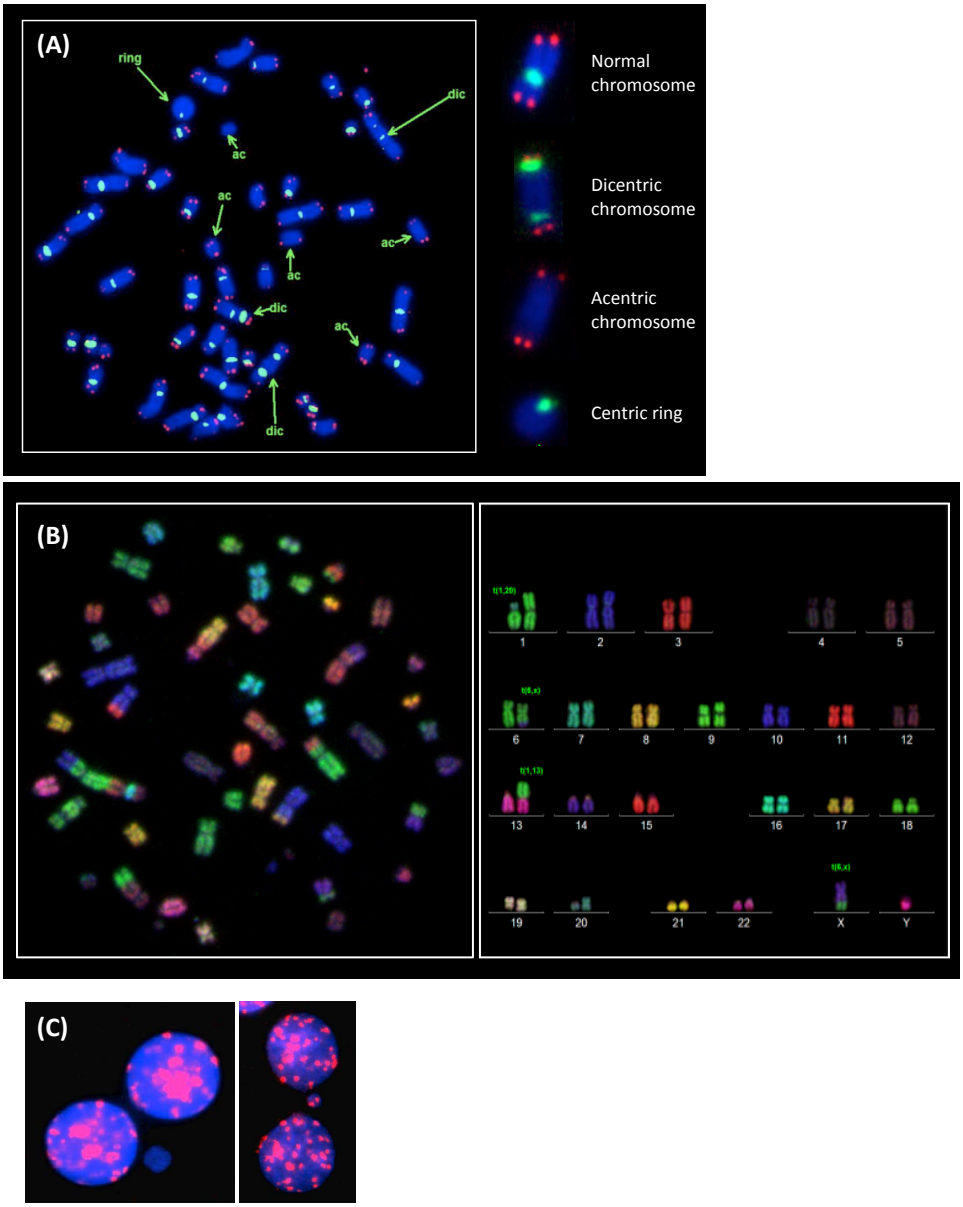

Figure 13. Examples of FISH assays. (A) Visualization of IR-induced dicentric chromosomes and other CAs using TC-FISH. (B) Visualization of IR-induced translocations using M-FISH and analysis of translocations using karyotyping (Images of CEA LRO). (C) Examples of a micronucleus that is centromere-negative and centromere-positive in binucleate cells stained with a pan-centromeric probe, and nuclei and micronuclei counterstained with DAPI (Adapted from IAEA, 2011).

As will be discussed in detail later in Section 3, the “gold standard” DC assay can be simplified and improved with the application of telomere/centromere-fluorescence *in situ*

hybridization (TC-FISH), which simultaneously stains telomeres and centromeres using peptide nucleic acid (PNA) probes[§§] (Shi et al., 2012;M'Kacher et al., 2014). The throughput of the TC-FISH technique can potentially be further enhanced by the use of a microwave oven to shorten the hybridization time of the PNA probes (Cartwright et al., 2013). In a recent study in our laboratory, TC-FISH staining was shown to be a cost-effective method that significantly simplifies the manual scoring of dicentric chromosomes (thereby eliminating the need for trained specialists to analyze samples). Furthermore, the automated scoring system (TCScore) developed in our laboratory is able to detect IR-induced CAs with the same efficacy as manual scoring in a fraction of the time. The TCScore software provides automated analysis of three-channel (RGB) images (red, green, and blue channels containing telomere, centromere, and DAPI DNA staining information, respectively) split into their individual channels by any image processing software (e.g. Image J) and generates an intuitive and interactive report of CA classes that can be reviewed and corrected in batches by an investigator (M'Kacher et al., 2014). Recent expansion of the robotically based ultra-high throughput biodosimetry workstation (RABiT, Rapid Automated Biodosimetry Technology), which was originally designed to implement the CBMN and γH2AX assays from a single drop of blood from a fingerstick, allows automated sample processing, image capture, and DC scoring using PNA or FISH probes (Garty et al., 2015). These improved, automated approaches will open up new horizons for the use of this assay for rapid biodosimetry.

The M-FISH technique is a powerful tool for detailed analyses of translocations and CCAs in the whole genome at very low to high doses of IR exposure, as it allows all chromosomal homolog pairs to be differentiated (Speicher et al., 1996;Loucas and Cornforth, 2001). It was shown to be sensitive enough to detect translocations and other CAs at doses as low as 0.1 Gy of low-LET IR (Nieri et al., 2013). Though the long-term stability of translocations and the usefulness of this technique was recently validated (Cho et al., 2015), M-FISH analysis is laborious, time-consuming (~ 5 days to obtain results), and expensive; standardization and automation will be key to improving the significance of FISH-based translocation assays. Furthermore, the frequencies of translocations at baseline and their persistence post-irradiation at various doses, as well as potential inter-individual

[§§] Peptide nucleic acid (PNA) probes have synthetic (unnatural) pseudo-peptide polymer backbones to which nucleobases are linked. Due to their unnatural backbones, PNA probes can hybridize faster and with higher affinity and specificity to complementary sequences of DNA and RNA compared to DNA or RNA probes (1 hour vs. ~12 hour hybridization times for PNA vs. DNA/RNA probes, respectively). PNA probes are also advantageous over DNA or RNA probes as they are resistant to nuclease and proteinase degradation and to polymerase amplification (Paulasova and Pellestor, 2004;Shi et al., 2012).

variability in their levels, need to be further characterized, especially in the low dose range (Tucker, 2008). Such data would be valuable for studying the long-term health risk of IR exposure, and may generally contribute to understanding the link between CAs and human diseases and cancer (Beinke and Meineke, 2012).

Recently, a new FISH approach called directional genomic hybridization (DGH) has been developed that combines DNA sequence information and the strand-specific Chromosome Orientation-FISH (CO-FISH) technique to hybridize genomic targets that share the same 5'→3' orientation. Based on this concept, painting of a single chromatid of human chromosome 3 was developed to analyze chromosomal inversions, a stable, transmissible CA like translocations. A recent study illustrated that DGH-detectable IR-induced inversions can be useful as a biodosimetric tool, as the frequency of IR-induced inversions increased with dose in human lymphocytes and fibroblasts following γ-irradiation (0 to 4 Gy) and high-LET iron and oxygen irradiations (0 to 0.4 Gy). Though more work needs to be done to establish chromosomal inversions as a reliable biomarker of past IR exposure, this technique provides a promising biodosimetry approach of measuring another stable, transmissible IR-induced CA with the added benefit of less labor-intensive analysis (Ray et al., 2013;Ray et al., 2014).

1.3.3 The premature chromosome condensation (PCC) assay

Premature chromosome condensation (PCC) enables the visualization of CAs in non-stimulated interphasic PBL (Figure 12B), thereby removing the delay due to the incompressible time needed to stimulate and culture the PBL until they reach first mitosis for the DC assay; IR-induced CA can be observed within 3 hours after blood sampling using PCC (compared to 49 hours using the DC assay). PCC can be induced by either mitotic cell fusion or by chemical means. Cell fusion-mediated PCC can be induced by fusing interphasic human PBL to mitotic Chinese hamster ovary (CHO) using polyethylene glycol (PEG) as the fusing agent; this fusion process takes only 4 minutes, and is followed by 1 hour of additional cell culture incubation with Colcemid. This technique enables the scoring of IR-induced human chromosomal fragments using Giemsa staining, and dicentric chromosomes using C banding or chromosome painting with or without a pan-centromere probe in other phases of the cell cycle than the conventional M (mitosis) phase, thus allowing these CAs to be tracked as cells cycle through each cell cycle phase (IAEA, 2011). PCC can also be induced by chemical means using inhibitors of DNA phosphorylation such as okadaic acid or calyculin A, adenosine triphosphate, and $p34^{cdc2}$/cyclin B kinase following cell culture of just 3 hours, i.e. the rapid interphase chromosome assay (RICA); IR-induced chromosomal exchanges between different chromosome domains can be visualized using

chromosome painting or FISH (Prasanna et al., 2000). Chemically-induced PCC can also be used to score ring chromosomes following Giemsa staining in other phases of the cell cycle (PCC-Rch), a useful technique to reduce scoring time particularly following very high doses (up to 20 Gy of low-LET IR vs. up to ~4 to 5 Gy for the conventional DC assay). However, this technique does not significantly reduce cell culture time compared to the DC assay (48 hours vs. 49 hours to obtain metaphases for the DC assay) (Kanda et al., 1999;IAEA, 2011), though the use of an automated metaphase finding system (MetaSystems) significantly increases the speed of scoring these chemically-induced PCC spreads (Balakrishnan et al., 2010); a recent study demonstrated that the culture time for this technique could be reduced to 40-42 hours (PCC-R assay) with adequate precision in dose estimation for doses between 5 and 10 Gy of low-LET IR (Romero et al., 2015).

The PCC assay (with the exception of the chemically-induced PCC-ring assays) is advantageous over the conventional DC assay because of the reduced cell culture time from blood sampling to analysis. The scoring of dicentric chromosomes using the PCC method is particularly interesting for biodosimetry, as it allows these CAs to be observed in cells that would otherwise not be observed with the conventional DC assay (irradiated cells may undergo cell death or never enter mitosis, especially at high doses when mitotic index decreases). Additionally, the PCC assay can accurately discriminate between whole and partial body exposures since the number of normal cells more accurately reflects the proportion of non-irradiated PBL (IAEA, 2011). However, despite the advantages of the PCC assay, it is not yet routinely used.

The major drawback of this approach, which utilizes Giemsa staining, is the difficulty of scoring the IR-induced CAs in the PCC spreads. Chromosomal fragments, rings, and acentric chromosomes can be scored with Giemsa staining, but dicentric chromosomes cannot be visualized because of the morphology of the interphase-condensed chromosomes and the inability to detect centromeric regions with Giemsa staining. Conventional techniques such as C banding or centromeric/whole-chromosome FISH can be applied to PCC spreads to simplify the scoring of CAs. However, FISH probes are costly, and FISH techniques can take from 2 days (for centromeric or simple chromosome painting) to 5 days (for M-FISH).

A few strategies to shorten analysis time and increase the throughput of the PCC assay have been developed, including dose estimation based on the length ratio of the longest and the shortest chromosome pieces (Gotoh and Tanno, 2005;Wang et al., 2007;Gonzalez et al., 2014), or based on the scoring of ring chromosomes in cell fusion-mediated PCC (PCC-Rf assay) instead of the more time-consuming chemically-induced PCC (Lamadrid Boada et al., 2013). Dose estimations for doses of up to 10 Gy may also be

made based on the proportion of condensed chromosomes in each cell cycle phase[***] (a novel biodosimetric parameter, the cell-cycle progression index) using the calyculin A-induced PCC assay (Miura et al., 2014); previously, G2-PCC chromosomes have been shown to be a simple and rapid method of biodosimetry following low-LET IR exposure (Gotoh et al., 2005) and after high-LET exposure with carbon ions (Wang et al., 2007).

The scoring of IR-induced CAs using the PCC assay has been improved with the application of TC-FISH, which shortens hybridization times, increases specificity and signal intensity, and lowers cost. Suto *et al* recently employed an improved rapid protocol that enabled dose estimation results to be obtained in as short as 6 hours after blood sampling; however, the detection of the much shorter, weakly staining telomere sequences (and analysis of IR-induced CAs) in human cells was impeded by the long, brightly staining, interstitial telomere sequences of CHO cells (Suto et al., 2013;Suto et al., 2015). By the same time, this TC-FISH technique on PCC spreads was further enhanced in our laboratory by optimizing hybridization conditions and image capture parameters, to increase the sensitivity and effectiveness of CA scoring. Furthermore, we have automated CA scoring using PCC-TCScore software, developed in our laboratory. This new approach will open up new horizons for biodosimetry, particularly following low and high doses, as well as partial-body irradiation, as it allows for the scoring of unstable CAs when conventional techniques are inadequate and when speed of obtaining results matters (M'Kacher et al., 2015a).

1.3.4 The cytokinesis block micronuclei (CBMN) assay

The cytokinesis block micronuclei (CBMN) assay in PBL (Figure 12F) is a well-established and standardized technique that is considered as a main biodosimetry tool for IR exposure along with the “gold standard” DC assay. This method has been proposed as an alternative to the DC assay, as it requires less time and cytogenetic expertise (IAEA, 2011;Vral et al., 2011;ISO, 2014b). Micronuclei are formed from acentric fragments or whole chromosomes that are unable to interact with the mitotic spindle during anaphase and are thus not included in the nuclei of daughter cells; they are small distinct spherical objects within the cytoplasm of the cell that have the same morphology and staining properties as the main nuclei. For the CBMN assay, cytokinesis is blocked in dividing lymphocytes by adding cytochalasin B to the medium; since division of the nuclei is not inhibited, cytokinesis block produces binucleate cells since the two daughter cells are not permitted to separate.

[***] Calyculin A induces chromosome condensation in various phases of the cell cycle and since IR exposure predominantly induces G2/M checkpoint in the cell cycle (Miura et al., 2014).

This protocol allows for distinction between proliferating and non-proliferating cells, and MN can be scored specifically in proliferating cells, i.e. binucleate cells (IAEA, 2011).

Micronuclei are not IR-specific (they can arise from exposure to various genotoxic agents), and inter-individual variability in baseline frequency of micronuclei exists based on age, gender, and life-style factors[†††] (Fenech and Bonassi, 2011); thus, the lower dose limit for the CBMN assay is ~0.2 to 0.3 Gy of low-LET IR (Vral et al., 2011;Tucker et al., 2013). Indeed, women are known to have higher baseline micronucleus frequencies than men (Bonassi et al., 2001;Fenech et al., 2011a), and the frequency of micronuclei has been shown to increase with age (Bolognesi et al., 1997;Bonassi et al., 2001). Micronuclei formation due to chromosome loss has been shown to increase with age, and the X-chromosome appears to be almost always involved in this chromosome loss, which may explain the gender difference observed in spontaneous micronuclei frequencies (Vral et al., 2011).

The number of IR-induced micronuclei is strongly correlated with IR dose. Generally, a linear-quadratic dose-response relationship ($y = c + \alpha D + \beta D^2$)[‡‡‡] has been reported for low-LET IR, while a linear dependence ($y = c + \alpha D$)[‡‡‡] has been observed for high-LET IR, with high-LET IR being more effective in generating micronuclei compared to equivalent doses of low-LET IR. These curve fittings follow the same shape as described for the standard DC assay (Vral et al., 2011). A recent study showed a linear-quadratic dose-response relationship following irradiation (1 to 5 Gy) with high-LET protons (30 MeV) (Litvinchuk et al., 2015). However, due to inter-laboratory differences caused by the use of different protocols, scoring criteria, etc, it is necessary that each laboratory intending to use this assay for biodosimetry establishes its own dose-response calibration curves (Romm et al., 2013b). Micronuclei induction has been shown to level off at doses higher than 5 Gy, a phenomenon that is well observed for other cytogenetic end points (i.e. dicentrics) that is attributed to the selection against heavily damaged cells that cannot enter mitosis (Vral et al., 2011). At higher doses (> 3 Gy), a wide range of inter-individual variability may also be observed (Kacprzak et al., 2013;Antunes et al., 2014). Interestingly, a recent study employing M-FISH on IR-induced micronuclei revealed that at high doses (> 2 Gy of low-

---

[†††] To assess environmental effects on chromosomal damage in the human population based on micronuclei frequency, an international collaborative project called HUMN (HUman MicroNucleus, www.humn.org) was launched in 1997. With over 40 laboratories participating worldwide, they aim to provide a powerful tool for the evaluation of micronuclei frequencies for public health and epidemiological studies by combining available micronuclei data from a variety of human populations.

[‡‡‡] In the equations, *y* represents the yield of micronuclei per binucleate cells, *c* is the background frequency of micronuclei, *D* is the absorbed dose (Gy), and the α and β coefficients refer to micronuclei per binucleate cell per Gy and per Gy^2, respectively.

LET IR), micronuclei formation might be complex involving multiple chromosome fragments (Balajee et al., 2014).

The development of new scoring approaches to increase the speed and decrease inter-scorer variability is required in order for this assay to be applied as a biodosimetry tool in a large-scale emergency. Several methods have been proposed, including manual scoring of lower numbers of cells (Triage Mode) (McNamee et al., 2009;De Amicis et al., 2014). Several automated micronuclei scoring systems, which enable faster delivery of results and reduced inter-scorer variability, have been developed, including imaging flow cytometry (ImageStream^X) (Rodrigues et al., 2014b;a) and laser scanning cytometry (Francois et al., 2014). Additionally, sophisticated image analysis software (e.g. Metasystem Metafer MNScore, IMSTAR PathFinder Screentox Auto-MN, Compucyte iCyte) have been tested and validated as biodosimetry tools for IR exposure; the automated and semi-automated MetaSystems platforms were recently harmonized within the framework of the European Multibiodose project, with the semi-automated approach showing more added value compared to the automated approach (Ainsbury et al., 2014a;Thierens et al., 2014). These automated techniques can be further refined with the use of centromere and telomere probes, which allow the origin of the micronuclei to be determined (from acentric fragments vs. whole chromosomes) (Decordier et al., 2011;Rossnerova et al., 2011;Fenech et al., 2013). Recent improvements of the ultra-high throughput RABiT workstation allows automated sample processing, image capture, and CBMN scoring from a single drop of blood from a fingerstick (Garty et al., 2010;Garty et al., 2015).

The CBMN assay has recently been expanded to a more comprehensive version known as the cytokinesis block micronucleus cytome (CBMN Cyt) assay (Figure 12C-J) (Fenech, 2007), which can be used for measurements for DNA damage, cytostasis (measure of cell proliferation), and cytotoxicity (measure of cell death). DNA damage events can be scored in binucleate cells as *micronuclei* (a biomarker of acentric fragments and/or whole chromosome loss), *nucleoplasmic bridges* (a biomarker of dicentric chromosomes), or *nuclear buds* (a biomarker of gene amplification) (Fenech et al., 2011b). Cytostatic effects can be measured by calculating the proportion of mono-, bi-, and multinucleated cells. Finally, cytotoxicity can be measured by determining the ratios of necrotic and/or apoptotic cells. These measures can provide additional details of the biological effects of IR exposure that are informative for biodosimetry and environmental/chemical genotoxicity studies (Fenech, 2010;IAEA, 2011).

Micronucleus induction following IR exposure has been reported in cell types and tissues other than lymphocytes (e.g. erythrocytes, hair root cells, buccal cells), but these methods have not yet been adequately validated for biodosimetry (Fenech, 2010). Indeed, a

recent study intra- and inter-laboratory comparison study demonstrated that the buccal micronucleus cytome (BMCyt) assay is at an early stage of development and requires further standardization to produce reproducible results (Bolognesi and Fenech, 2013;Bolognesi et al., 2013;Bolognesi et al., 2015).

1.3.5 Quantification of γH2AX

γH2AX, the phosphorylated form of the H2AX histone, is a promising candidate as a biomarker that can be used for rapid emergency biodosimetry shortly after acute irradiation (Rothkamm et al., 2013b). γH2AX foci form at the site of DNA DSBs (Scully and Xie, 2013;Valdiglesias et al., 2013), and can be readily visualized by immunofluorescence microscopy or flow cytometry. Foci are formed within minutes after IR exposure in a dose-dependent manner, peak at <1 hour post-irradiation, and then rapidly decay to baseline levels within one to several days, depending on the dose received.

Manual γH2AX foci scoring via immunofluorescence microscopy is currently the most sensitive method of γH2AX analysis. The number of manually scored γH2AX foci is well established to be correlated one-to-one with the number of DSBs, which in turn, can easily be correlated to the received IR dose (Rothkamm and Lobrich, 2003;Joubert et al., 2008). However, manually scoring foci is time-consuming, fastidious, requires trained investigators, and produces inter-investigator and inter-laboratory variations in results; indeed, recent inter-comparison exercises of several laboratories that analyzed the same samples of irradiated whole blood (Rothkamm et al., 2013c) and lymphocytes (Rothkamm et al., 2013a;Barnard et al., 2015) revealed dramatic variations of manually scored foci yields. Additionally, for the γH2AX assay to be used as a biodosimetric triage tool, inter- or intra-individual variability in the basal levels of γH2AX as well as the time course of γH2AX induction and decay following irradiation (which depend on individual DSB repair capacity, which in turn may reflect individual radiosensitivity) is a crucial issue that must be addressed (Rothkamm and Horn, 2009;Roch-Lefèvre et al., 2012).

To reduce γH2AX quantification time and minimize scoring artifacts, several automated foci scoring systems have been developed (Bocker and Iliakis, 2006;Hou et al., 2009;Roch-Lefevre et al., 2010;Runge et al., 2012). Another less automated approach based on individual foci scoring following a rapid "lyse/fix" method on a 96 well plate, which allows a significant reduction of sample processing time, was well correlated with the classical γH2AX quantification in isolated lymphocytes (Moquet et al., 2014). γH2AX can also be quantified as global fluorescence intensity in the whole nucleus, instead of scoring individual foci. This approach may be a more rapid method to obtaining biodosimetric results

than by foci scoring. Flow cytometry and immunofluorescence microscopy have previously been used for global γH2AX fluorescence quantification (MacPhail et al., 2003;Hamasaki et al., 2007;Ismail et al., 2007;Garty et al., 2010;Horn et al., 2011;Roch-Lefèvre et al., 2012); in our recent paper, presented in Section 2, we have validated global fluorescence intensity measurements via flow cytometry and immunofluorescence microscopy as a reliable dosimetry tool in comparison to the now well-established γH2AX foci scoring method (Viau et al., 2015). The ultra-high throughput RABiT workstation (previously discussed for automated DC and CBMN analyses) allows automated sample processing, image capture, and γH2AX analysis based on foci scoring or global fluorescence from a single drop of blood from a fingerstick (Garty et al., 2010;Garty et al., 2015;Sharma et al., 2015). The optimization of miniaturization and the increase in the number of analyzed samples have recently been improved (Repin et al., 2014). However, inter-comparison exercises of several laboratories to compare automated and manual foci scoring showed vast inter-laboratory differences in results (Rothkamm et al., 2013a;Ainsbury et al., 2014a;Barnard et al., 2015). Though these studies confirm that γH2AX foci assays can be useful as a biodosimetric triage tool, they brought to light the complexity in the standardization of an automated γH2AX biodosimetry protocol between multiple laboratories. Additionally, these studies showed the importance of balancing the higher speed and convenience of automated foci scoring systems with their compromised accuracy and sensitivity of dose estimation (Rothkamm et al., 2013a;Barnard et al., 2015).

In light of these limitations of the γH2AX immunofluorescence techniques as a high throughput assay, a promising new assay using a high throughput electrochemiluminescent platform from Mesoscale Discovery Systems was developed to quantify γH2AX levels in a larger dose range (Avondoglio et al., 2009). A simplified enzyme-linked immunosorbent assay (ELISA) has also been recently developed that relies on direct antibody-based detection of cellular proteins from sample lysate immobilized on a solid substrate from a small volume of minimally prepared sample (Johnston et al., 2015).

1.4 Individual radiosensitivity

With increasing levels of IR exposure throughout our lifetime, there is growing concern of the long-term health effects of such exposures. To "review work on the biological and medical effects of [IR] relevant to human health in the occupational, public health, medical and environmental fields and advise on research priorities," the Advisory Group on Ionising Radiation (AGIR) was convened in 1995 by the Health Protection Agency in the United Kingdom. In their most recent report, published in March 2013, they extensively review evidence of inter-individual variability in radiosensitivity from epidemiological, clinical, and experimental studies, consider mechanisms of radiosensitivity and the impact of individual variability on long-term human health effects, and discuss ethical implications for radiation protection of current and potential future knowledge on radiosensitivity in the human population. Based on this evidence, they conclude that there is growing evidence of inter-individual differences in radiosensitivity that can influence risk of IR-induced cancers. However, knowledge of the mechanisms that determine radiosensitivity is accumulating, but remains incomplete (Advisory Group on Ionising Radiation, 2013)[§§§].

1.4.1 Mechanisms of radiosensitivity

The term "radiosensitivity" can be referring to either the extent of IR-induced biological responses or the susceptibility to IR-induced carcinogenesis from the standpoint of the cell, tissue, or individual/organism. Cellular radiosensitivity can be quantified by measurements of a variety of biomarkers of IR exposure, which were discussed in detail in Section 1.2.6 (Pernot et al., 2012;Manning and Rothkamm, 2013). Notably, depending on the underlying cause of radiosensitivity, cellular radiosensitivity may not be detectable using one assay, but may be detectable using another. Based on these measurements, cellular variations in radiosensitivity are well observed between individuals, as well as between different cell types and between cells of the same type within a single individual; variations in radiosensitivity also exist between normal and cancer cells. It is well established that intrinsic, genetically determined differences in cellular responses to IR-induced damage, particularly the repair of DNA DSBs[****], is associated with these intra- and inter-individual differences in cellular radiosensitivity. Genetic differences in the initiation and maintenance

[§§§] Articles in French: (Joubert and Foray, 2007;Granzotto et al., 2011;Joubert et al., 2011;Foray et al., 2013;Lacombe et al., 2013).

[****] DNA SSBs and base damages are redundantly and efficiently repaired, so deficiencies in repair pathways for these types of DNA lesions causes only minor radiosensitivity (Advisory Group on Ionising Radiation, 2013).

of cell cycle checkpoint arrest, as well as the cellular ability to activate apoptosis, could also be a source of individual radiosensitivity. Moreover, the accuracy of DSB repair is important to avoid genetic instability and ultimately IR-induced carcinogenesis (Advisory Group on Ionising Radiation, 2013).

As discussed in Section 1.2.3, mammals possess two principal mechanisms of DNA DSB repair: NHEJ and HR repair. The NHEJ pathway is the major DNA DSB repair pathway in mammalian cells; defects in proteins involved in this pathway (e.g. DNA-PKcs, DNA LIG4, Artemis, Cernunnos) confer dramatically increased radiosensitivity and immunodeficiency (e.g. severe combined immunodeficiency, SCID, or T- and B-cell lymphocytopenia). HR repair is active in DSB repair in the G2 and S phases of the cell cycle; radiosensitivity disorders associated with defects in HR repair can be caused by mutations in genes that cause Fanconi anemia (e.g. *FANCD1* or *BRCA2*, *FANCD2*, *FANCI*, *FANCJ*, *FANCN*), *Rad51* paralogues (e.g. *RAD51C*, *RAD51B*, *RAD51D*, *XRCC2*, *XRCC3*), and possibly Bloom's syndrome (*BLM*). Radiosensitivity can also be caused from defects in proteins involved in DDR signaling and/or activation of cell cycle checkpoints (e.g. ATM, 53BP1, Mre11/Rad50/Nbs1 or the MRN complex, RFN168) and/or in carrying out histone modifications around the DSB (e.g. H2AX to form γH2AX), though these signaling are not required for DSB repair by NHEJ. Finally, cellular radiosensitivity disorders may arise due to mutations in cohesins, which are proteins involved in holding chromosomes together during DNA replication/repair; such disorders include the Cornelia de Lange syndrome (mutations in *NIPBL*, or in cohesin subunits *SMC1A* or *SMC3*), Robert's syndrome (mutations in *ESCO2*), and Warsaw breakage syndrome (mutations in *DDX11*) (Advisory Group on Ionising Radiation, 2013).

Overall, there are currently 15 known genetic disorders involving mutations in genes mentioned above that are associated with increased cellular radiosensitivity; all are rare recessive disorders, with the exception of the Cornelia de Lange syndrome (which is a rare autosomal dominant disorder). Several of these disorders have shown unusual radiosensitivity at the clinical level, namely ataxia telangiectasia (*ATM* mutation), LIG4 syndrome (*LIG4* mutation), Nijmegen breakage syndrome (*NBS* mutation), and potentially Fanconi anemia (Advisory Group on Ionising Radiation, 2013). Homozygous carriers of *LIG4* and *ATM* mutations are severely radiosensitive (hyper-radiosensitive), with clonogenic survival fraction at 2 Gy (SF2) of only 1%–3%; radiotherapy may be fatal for patients with *LIG4* and *ATM* mutations. However, the occurrence of these syndromes in the population is very rare: there is only one known case of *LIG4* mutations in the world, and *ATM* mutations are found at a frequency of ~1 in 100,000. Heterozygotes of *ATM* and *NBS* mutations may exhibit radiosensitivity that is intermediate (SF2 of 40%–60%) between individuals with

homozygous mutations and normal genotypes. Other homozygous recessive syndromes that are more frequent than homozygous *LIG4* and *ATM* mutations are less dramatically radiosensitive (intermediate or moderate radiosensitivity), with SF2 between 10% and 50%. Interestingly, *ATM* heterozygotes may be at two-fold greater risk of IR-induced breast cancer. Heterozygotes of *BRCA1*, *BRCA2*, and *P53* (Li-Fraumeni syndrome) are also predisposed to IR-induced cancers. *BRCA1*/*BRCA2* mutations are somewhat more common in the population, with an incidence of ~1 out of 1000; Li-Fraumeni syndrome occurs at an incidence of 1 out of 200,000 (Foray et al., 2012). Overall, hyper-radiosensitive individuals (homozygotes) comprise of ~1%–5% of the population, whereas moderately radiosensitive (heterozygotes) and radioresistant individual comprise of 5%–20% and 75%–85% of the population, respectively (Foray et al., 2013). All of the genetic mutations conferring increased radiosensitivity or susceptibility to IR-induced cancer may represent a significant proportion of the whole population (5%–15%) (Foray et al., 2012).

Besides inherent genetic factors related to DSB repair, radiosensitivity can also be influenced by confounding variables (e.g. co-morbid conditions such as diabetes and collagen vascular disease) and non-genetic exogenous factors (e.g. age, smoking). A range of stress responses, including cytokine signaling and activation of inflammatory responses, can also influence radiosensitivity by impacting the microenvironment around the irradiated/damaged cell/tissue; these responses can enhance tissue damage, prevent wound healing, and may exacerbate IR-induced oxidative stress. Furthermore, these IR-induced damages may be propagated to non-irradiated neighboring cells via bystander signaling (discussed in Section 1.2.2). Notably, there may be important distinctions between the mechanisms of radiosensitivity following exposure to high and low doses of IR due to differences in the triggering of mechanisms of DNA damage repair following these doses (which depend on the frequency of IR-induced cellular damages). Furthermore, as the type and extent of cellular damage (and mechanism of repair) differs between IR of high- and low-LET, individual radiosensitivity to different types of IR may not be equivalent (Advisory Group on Ionising Radiation, 2013).

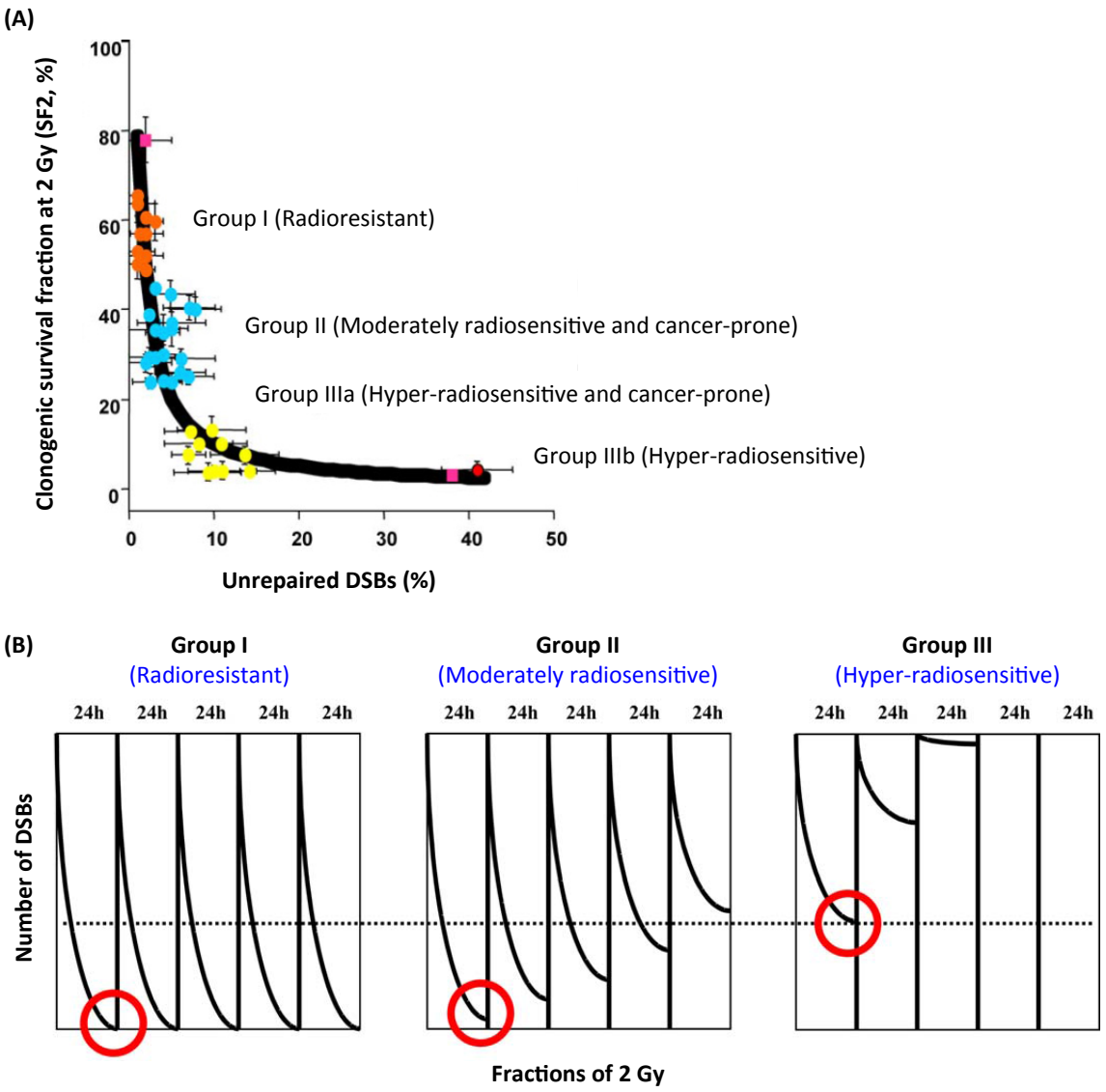

Figure 14. (A) Classification of 40 human fibroblast cell lines representing at least 8 different genetic syndromes into 3 radiosensitivity groups based on the surviving fraction of cells at 2 Gy (SF2) and the evaluation of unrepaired DSB using a variety of molecular markers (e.g. MRE11, MDC1, 53BP1, and phosphorylated forms of H2AX and DNA-PK). The radioresistant Group I (comprising of normal, healthy control cells) showed SF2 of 45–65%. The hyper-radiosensitive Group III (SF2 of < 7%) is comprised of the classical homozygous *ATM*-mutated (Group IIIa) and *LIG4*-mutated (Group IIIb) cell lines. The moderately radiosensitive Group II (SF2 of 7–45%) is comprised of fibroblasts derived from individuals with other genetic disorders that confer radiosensitivity. (B) Based on these radiosensitivity categories, the radioresistant Group I (which is capable of properly repairing IR-induced DSBs during the 24 hours between each fraction of radiotherapy with their intact DDR pathways) never accumulate the hypothetical level of unrepaired DNA damage (dotted line) to trigger toxic tissue overreactions. The moderately radiosensitive Group II, however, may reach this level of unrepaired DNA damage after several sessions, whereas the hyper-radiosensitive Group III may reach it following the first session (Adapted from Joubert et al., 2008;Granzotto et al., 2011).

In one of the largest studies of the spectrum of intrinsic radiosensitivity in human fibroblasts, Joubert *et al* (Joubert et al., 2008) characterized 40 human fibroblast cell lines

representing at least 8 different genetic syndromes. Based on SF2 and the evaluation of unrepaired DSB using a variety of molecular markers (e.g. MRE11, MDC1, 53BP1, and phosphorylated forms of H2AX and DNA-PK) at several time points post-irradiation, the authors categorized fibroblasts into three groups of radiosensitivity: Group I (radioresistant), Group II (moderately radiosensitive), and Group III (hyper-radiosensitive). As shown in Figure 14A, the radioresistant Group I (comprising of normal, healthy control cells) showed SF2 ranging from 45–65%, and is characterized by an intact NHEJ repair pathway. The hyper-radiosensitive Group III (SF2 of < 7%) is comprised of the classical homozygous *ATM*-mutated and *LIG4*-mutated cell lines. This hyper-radiosensitive group can be subdivided into two groups based on activation of MRE11: Group IIIa (*ATM*-mutated cells) are characterized by absent or rare MRE11 activation, and Group IIIb (*LIG4*-mutated cells) are characterized by deficiency in the DNA-PK-dependent NHEJ pathway but over-activation of MRE11 (thus making this group markedly less radiosensitive than Group IIIa, as some DSB repair is activated unlike Group IIIa). The moderately radiosensitive Group II was comprised of fibroblasts derived from individuals with other genetic disorders that confer radiosensitivity such as heterozygous *ATM* mutations, Nijmegen Breakage syndrome (*NBS* mutations), Fanconi anemia (*FANC* mutations), Bloom's syndrome (*BLM* mutations), Xeroderma Pigmentosum (*XP* mutations), Cockayne syndrome (*CS* mutations), and mutations of ligase I (*LIG1*). Group II showed SF2 of 7–45%, and is characterized by intact NHEJ repair pathway but abnormal MRE11 signaling, which may increase predisposition to cancer. Importantly, this study confirmed that no single assay is capable of discriminating all of the various causes of human radiosensitivity, and highlights that the choice of molecular assay depends on the characteristics of the underlying causes of radiosensitivity (Granzotto et al., 2011;Joubert et al., 2011).

1.4.2 Individual radiosensitivity and radiotherapy

Radiotherapy elicits a wide range of biological effects in not only the targeted (cancer) tissue/cells, but also in normal tissue/cells within or near the targeted region. IR-induced effects can also be observed in tumors and/or normal tissues that are widely separated from the irradiated area, a detrimental or beneficial (if they lead to shrinkage of distant tumors) phenomenon termed "abscopal effects" that is an illustration of the *in vivo* occurrence of IR-induced bystander responses (Mothersill et al., 2004;Hei et al., 2011;Mancuso et al., 2012;Schmid and Multhoff, 2012). Acute radiotherapy toxicity induces systemic effects that affects the whole body during, or a short time after, exposure, whereas late radiotherapy toxicity can be observed many years after the end of treatment, as illustrated by a higher incidence of secondary malignancies and a variety of degenerative

conditions in long-term cancer survivors (Morgan, 2003b;Prise and O'Sullivan, 2009;Newhauser and Durante, 2011).

Individual radiosensitivity is well established to significantly influence clinical outcomes of radiotherapy, termed “clinical radiosensitivity,” including normal tissue toxicity (in non-targeted tissue) as well as differences in responses to radiotherapy in targeted (cancer) tissues. For example, highly radiosensitive patients may develop early and/or late side effects due to radiation toxicity, while radioresistant patients may receive an insufficient dose of radiation due to dose limitations in current general radiotherapy protocols. Factors that can potentially influence radiotherapy toxicity and the prediction of clinical radiotherapy was reviewed by the AGIR (Advisory Group on Ionising Radiation, 2013). In their report, they concluded that the influence of sex, ethnicity, body mass index, diet, or alcohol consumption on clinical radiosensitivity is inconclusive. However, increased clinical radiosensitivity is associated with increasing age in adults, smoking, diabetes, and collagen vascular disease in radiotherapy patients. Genetic syndromes (e.g. *ATM*, *LIG4*, *NBS* mutations) also influence radiosensitivity, as discussed in Section 1.4.1. Importantly, cellular radiosensitivity may not necessarily be linked to clinical radiosensitivity, and vice versa.

Radiotherapy is often administered in fractionated doses, i.e. large total doses are delivered in small amounts over a period of time; conventional fractionated radiotherapy involves doses of 2 Gy administered every 24 hours over a period of several weeks. Administration of fractionated doses allows normal, healthy cells to recover between treatments, thereby decreasing side effects and the risk of induction of ARS (in the case of whole-body irradiation) compared to administering a single large dose. As the extent of IR-induced cellular damages and the speed of DNA damage repair differ based on individual radiosensitivity, individuals of differing radiosensitivity could react differently to each fraction of radiotherapy. As illustrated in Figure 14B, adapted from (Granzotto et al., 2011;Joubert et al., 2011) based on their radiosensitivity classification groups of human fibroblasts, the radioresistant Group I (with their intact DDR pathways) is capable of properly repairing IR-induced DSBs during the 24 hours between each fraction of radiotherapy, and therefore never accumulate the hypothetical level of unrepaired DNA damage (dotted line in Figure 14B) to trigger toxic tissue overreactions. The moderately radiosensitive Group II, however, may reach this level of unrepaired DNA damage after several sessions, whereas the hyper-radiosensitive Group III may reach it following the first session. A fast and reliable clinical method to measure radiosensitivity of cancer patients and/or predict radiotherapy toxicity (especially to identify hyper-radiosensitive individuals) would permit personalized radiotherapy treatment; however, such a method still remains to be established (Fernet and Hall, 2004;Andreassen et al., 2012).

1.4.3 Prediction of radiosensitivity

The ability to rank and predict individual radiosensitivity has a wide range of real-world applications as it directly impacts the formulation of cancer treatment strategies and the establishment of everyday/environmental/occupational radiation protection guidelines. Current radiotherapy and radiation protection protocols do not take into account the individual variations in radiosensitivity, but rather rely on population averages of radiation responses. Refining these protocols to consider individual radiosensitivity, especially the more radiosensitive and cancer-prone, may help to alleviate the detrimental delayed effects of IR. As mentioned above, knowledge of each patient's individual radiosensitivity would allow for personalization of radiotherapy regimens, including not only the customization of radiation dose, but potentially the prediction and prevention of acute and late radiation toxicity and secondary cancers (Fernet and Hall, 2004;Andreassen et al., 2012;Mirjolet et al., 2015). Additionally, knowing individual radiosensitivity can help to make an informed decision on the risk-benefit ratio in the use of diagnostic radiology or radiation treatment of those who are highly sensitive to IR. This logic can also be applied to other medical or non-medical situations, including the identification of highly sensitive individuals following environmental or occupational IR exposure, radiologic accidents, or nuclear catastrophe, and for the selection of candidates for spacecraft missions or atomic submarine crews (Il'yasova et al., 2014).

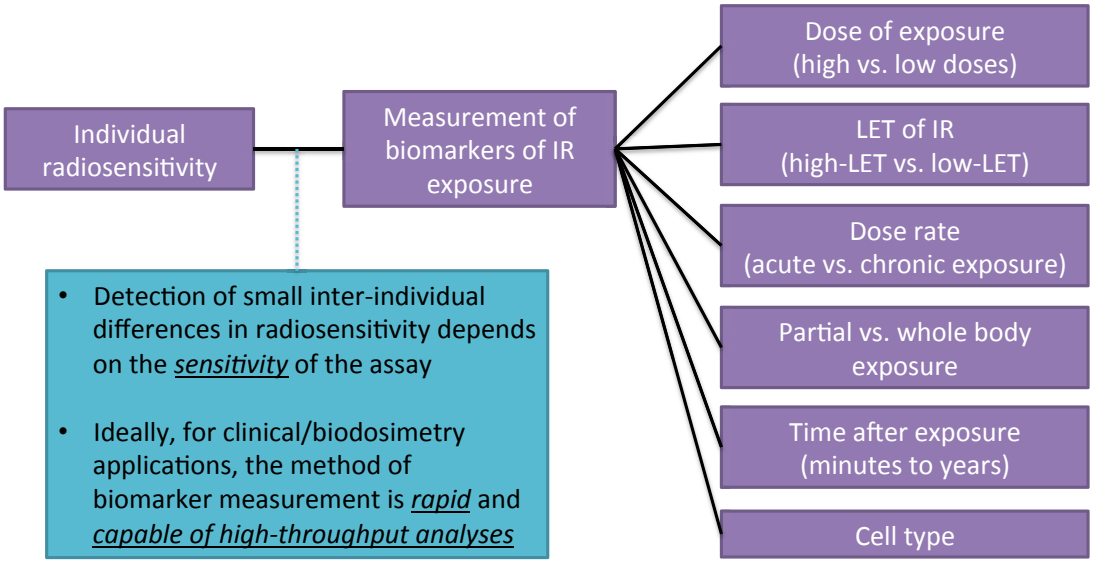

Figure 15. Confounding factors that influence the measurement of biomarkers, which in turn influence the study and measurement of individual radiosensitivity. Conversely, individual radiosensitivity for each of these confounding factors needs to be characterized.

The study and quantification of inter-individual variability in radiosensitivity directly depend on the measurement of biomarkers of IR exposure, which were discussed in detail in Section 1.2.6. Though these biomarkers allow for the detection and measurement of radiosensitivity, their measurements are difficult to translate into routine clinical or biodosimetric practice to rank and predict individual radiosensitivity. The ideal assay/technique for this purpose would be fast and easy, capable of high throughput applications, and would be able to distinguish between partial and whole body exposure; thus far, such an assay has not yet been established. The characterization and quantification of individual radiosensitivity has been challenging due to confounding factors that conversely also affect the induction of the biomarkers that are used to measure individual radiosensitivity (summarized in Figure 15). That is, the induction and kinetics of the biomarkers (i.e. dose-response curves) may vary depending on the dose of exposure (high vs. low doses), the LET of the IR (high-LET vs. low-LET), and dose rate (acute vs. chronic exposure). Dose response curves may also vary depending on the time point after exposure at which the biomarker is measured (seconds to years to decades), as well as the cell type chosen for these analyses. Additionally, the quantification of inter-individual variability in radiosensitivity depends on the ability of the assay/technique to detect the minute inter-individual differences of the biomarker, which is dependent on the sensitivity of the assay/technique. Notably, as discussed in previous sections, depending on the characteristics of the underlying cause of radiosensitivity, radiosensitivity may be detectable using one specific molecular assay but not with another; to date, no single assay is capable of discriminating all of the various causes of human radiosensitivity (Chua and Rothkamm, 2013). Furthermore, cellular radiosensitivity may not necessarily translate to manifestation of clinical radiosensitivity.

In addition to optimizing the ability to measure biomarkers to predict individual radiosensitivity, the effect of individual radiosensitivity on the individual induction of these biomarkers must also be contemplated. Evidently, in the context of biodosimetry, which estimates an unknown dose based on the measurement of IR-induced biological responses or consequences, the existence of individual variations in radiosensitivity confounds the development of protocols that can be applied to the general population. For use in the event of mass accidental exposure to IR, the ultimate goal is to develop a biodosimetric test that can accurately estimate dose with non-invasively obtained biological samples using a fast and easy technique that can handle high-throughput analysis. For medical triage purposes in this scenario, triage categories based on these results must be able to account for the existence of individual variations in radiosensitivity in the general population. This, again, relates back to the ability to measure and rank individuals based on their radiosensitivity.

The development of such an approach is yet to be accomplished. With accumulating knowledge, the AGIR advised that progress in the development of such an assay would require better standardization of assay protocols, development of guidelines and larger multi-center collaborative studies, and the identification of better predictive biomarkers (Advisory Group on Ionising Radiation, 2013).

Recently, the field of radiogenomics has evolved to accomplish the dual purposes of (1) developing an assay that can predict individual radiotherapy and normal tissue toxicity to radiotherapy, and (2) learning more about the molecular pathways responsible for IR-induced normal tissue toxicities. Radiogenomics is an upgrade from the traditional (thus far unsuccessful) approach of identifying single candidate genetic variants, mainly single-nucleotide polymorphisms (SNP) based on their known link to radiosensitivity (e.g. genes related to DDR, oxidative stress, apoptosis, cell proliferation), and takes advantage of recent advancements in genotyping technology. Radiogenomics employs the genome-wide association study (GWAS), which provides a comprehensive and unbiased assessment of the association between SNPs (the independent variable) and a phenotype of interest (the dependent variable, which in the case of radiogenomics is adverse effects of radiotherapy); this technique has successfully identified ~2000 new human trait/disease susceptibility loci, including those for prostate cancer and Hodgkin lymphoma. GWASs survey nearly all *common* genetic variants (rather than rare mutations such as those found in radiosensitivity syndrome genes, like those discussed in Section 1.4.1) in a cost-effectiveness manner using genotyping arrays to identify associations with adverse effects to radiotherapy. “Common” in the context of GWASs refers to SNPs that are present in the population with a prevalence of at least 1%. In order for the GWAS approach to be successful in the development of a reliable clinical assay, it requires large cohorts and rigorous testing of associations found using this method, both of which can be accomplished by large-scale multisite and multinational collaborative research (Kerns et al., 2014b;Rosenstein et al., 2014;Guo et al., 2015). Several national and international collaborative studies have been initiated, including Gene-PARE (Ho et al., 2006), RadGenomics (Iwakawa et al., 2002), RAPPER (Burnet et al., 2013), and the REQUITE project (West et al., 2014). Furthermore, the International Radiogenomics Consortium (RGC) has been established in 2009 to foster large-scale collaborative projects (West et al., 2010). To improve reproducibility of results and to improve the quality of research in this rapidly changing and advancing field, the RGC has recently provided the STROGAR guidelines to increase the transparency and completeness of reporting radiogenomics studies (Kerns et al., 2014a). The field of radiogenomics provides a promising approach to the personalization of radiotherapy protocols based on individual radiosensitivity (Kerns et al., 2014b;Rosenstein et al., 2014;Guo et al., 2015).

1.5 Aims and Hypothesis

In this thesis, we aim to paint a picture of the range of inter-individual variability in radiosensitivity in normal tissue of healthy individuals in the contexts of emergency dosimetry (Section 2) and radiotherapy (Section 3), and we explore the roles of telomeres in the prediction of these variations in radiosensitivity (Section 4) and long-term human health risks following IR exposure (specifically, cardiovascular diseases and/or cancer; Section 5). We study two biomarker assays for the measurement of individual radiosensitivity: global quantification of γH2AX via flow cytometry (Section 2) and chromosomal aberrations via TC-FISH (Section 3). We hypothesize that, in the context of emergency biodosimetry (when rapid dose estimates of each individual in an irradiated population are needed, and when the existence of individual radiosensitivity confounds the creation of effective triage categories), the measurement of global quantification of γH2AX can aid in the medical triage of irradiated individuals, independent of individual radiosensitivity, if a time point of few hours post-irradiation is used (Section 2). In the context of radiotherapy, we hypothesize that significant inter-individual differences in radiosensitivity exist in normal human tissue, measured in terms of IR-induced chromosomal aberrations, and we aim to determine whether individuals have different sensitivities to different types of IR (Section 3). Then, we investigate the potential link between telomeres and individual radiosensitivity, and we hypothesize that individual radiosensitivity can be predicted using a combination of telomere-related biomarkers, such as telomere length and IR-induced telomere dysfunctions (Section 4). Finally, as radiosensitivity can also have significant impact on long-term health following IR exposure, we postulate a role of telomeres and IR-induced telomere dysfunction in the development of cardiovascular diseases and/or cancer long after IR exposure (Section 5). Ultimately, these results can provide insight for the assessment of individual radiosensitivity and overall long-term human health that can have important implications in biodosimetry, radiation protection, and cancer radiotherapy.

1.5.1 Description of thesis contents

In the following chapters presenting the results of this thesis (Sections 2 to 5), previously published articles are included if available, along with a short introduction and a summary of the key results.

This thesis is structured as follows:

- In Section 2, we characterize the impact of individual radiosensitivity in the context of emergency biodosimetry. Results and discussion are presented in our published article: Viau M[¤], Testard I[¤], **Shim G[¤]**, et al. *Mutat Res Genet Toxicol Environ Mutagen*. 2015;

793: 123-131. ¤ co-first authors. The article is provided in this chapter, along with a short introduction and a summary of the key results.

- In Section 3, we study the extent and influence of individual radiosensitivity on the induction of chromosomal aberrations in lymphocytes of healthy individuals following irradiation with γ-rays, carbon ions (75 MeV/u), or proton beams (73 MeV and 200 MeV) using telomere/centromere-fluorescence in situ hybridization (TC-FISH). We also determine the relative biological effectiveness (RBE) of carbon ions and proton beams (ion species currently being used in charged particle radiotherapy) in comparison to γ-irradiation.
  - An article presenting these results is currently under preparation for submission: **Shim G**, et al. *Int J Radiat Oncol Biol Phys*. manuscript in preparation.

- In Section 4, we evaluate the roles of telomeres and IR-induced telomere dysfunction in the prediction of individual radiosensitivity. We find that inherent mean telomere length in combination with the IR-induced change in mean telomere length may be a strong predictor of individual radiosensitivity.
  - These results are not yet published, and so they are presented in full (in Section 4) with discussion and conclusions (in Section 6.2).

- In Section 5, we explore the roles of telomeres in long-term human health risks following IR exposure, specifically focusing on the development of cardiovascular diseases and/or the process of carcinogenesis. In Section 5.1, we show that telomere shortening could be a new prognostic factor for cardiovascular disease following radiotherapy. Results and discussion are presented in our published article (M'Kacher et al., 2015b); the article is provided, along with a short introduction and a summary of the key results. In Section 5.2, we provide our review article (Shim et al., 2014) that discusses the relationships between telomere maintenance and radiation effects, and propose a model of how telomeres could be key players in the process of IR-induced carcinogenesis.

- Finally, in Section 6, we integrate our findings on individual radiosensitivity and the novel link between telomere shortening and cardiovascular disease into our previously proposed model for IR-induced carcinogenesis (Shim et al., 2014); we postulate how telomeres could play important roles in the development of cardiovascular disease and the process of IR-induced carcinogenesis, we propose how these processes can be accelerated particularly in highly radiosensitive individuals (Section 6.1). We also argue how telomeres could predict individual radiosensitivity (Section 6.2).

2 - INDIVIDUAL RADIOSENSITIVITY AND ROUGH DOSE ESTIMATION FOR EMERGENCY BIODOSIMETRY

In the case of large-scale accidental exposure to radiation, a method of biodosimetry that is rapid, accurate, and can accommodate high throughput analysis is needed to efficiently triage victims of a mass accident based on individual levels of exposure. γH2AX, the phosphorylated form of the H2AX histone, is a promising candidate as a biomarker that can be used for this purpose shortly after acute irradiation. Manual and automated methods to quantify γH2AX are discussed in detail in Section 1.3.5 of this thesis. However, for the γH2AX assay to be used as a biodosimetric triage tool, inter- or intra-individual variability in the basal levels of γH2AX as well as the time course of γH2AX induction and decay following irradiation (which depend on individual DSB repair capacity, which in turn may reflect individual radiosensitivity) is a crucial issue that must be addressed. These inter-individual variations in the basal levels and kinetics of γH2AX induction and decay after irradiation are not yet well characterized at a range of time points post-irradiation (Rothkamm and Horn, 2009;Roch-Lefèvre et al., 2012).

Indeed, vast inter-individual differences in the basal levels of γH2AX and the kinetics of γH2AX induction and decay post-irradiation have been observed using γH2AX foci scoring methods (manual and automated) (Roch-Lefevre et al., 2010) as well as global quantification methods (Hamasaki et al., 2007;Ismail et al., 2007;Andrievski and Wilkins, 2009;Roch-Lefèvre et al., 2012). Basal levels of γH2AX may vary depending on a variety of physical, chemical, and biological factors (Takahashi and Ohnishi, 2005) as well as lifestyle factors (Roch-Lefevre et al., 2010). Basal levels of γH2AX measured by manual foci scoring have been shown to yield inter-individual differences of as much as 15 fold (Roch-Lefevre et al., 2010); we have also observed this large variability in basal levels both via manual scoring (shown in Figure A-1 in the Appendix) and global fluorescence quantification (shown in Figure 4 in **our recent paper** (Viau et al., 2015)). The induction and decay of γH2AX after irradiation may depend on inherent genetic factors (i.e. DNA repair capacity), which may in turn be linked to individual radiosensitivity; indeed, acute IR responses and reduced DSB repair kinetics are seen in individuals with well-known genetic disorders that directly impact the cellular DNA repair machinery, such as mutations in ATM, NBS1, MRE11, FANC, BLM or LIG1 (Nussenzweig and Nussenzweig, 2007;Joubert et al., 2008). A high individual variability leads to a decreased sensitivity of the γH2AX assay. Therefore, characterizing these inter-individual differences at various time points post-irradiation remains a crucial issue that needs to be addressed to establish dose response curves for biodosimetric purposes that can be applied to the general population.

In this study, presented in **our recent paper** (Viau et al., 2015), we assess the usefulness of global γH2AX quantification as a method for rapid biodosimetry in an emergency situation. For this purpose, we seek to better establish the correlation between global γH2AX fluorescence intensity (using flow cytometry and low-magnification immunofluorescence microscopy) and the foci scoring method (using high-magnification immunofluorescence microscopy) following exposure to a range of doses (0.25 Gy to 6 Gy) of either γ-rays from a Cesium-137 source or X-rays (200 kV). In the case of a large-scale accidental exposure, we estimate that biological samples cannot be obtained within less than 4 hours of IR exposure; therefore, we study this time point for γH2AX analyses. To evaluate the impact of inter-individual differences in the kinetics of IR-induced γH2AX induction and decay on dose-response curves at this time point, we studied human fibroblasts from 19 donors and lymphocytes from 11 donors of varying radiosensitivity.

2.1 Summary of key results

- The two approaches that we used to quantify global γH2AX fluorescence intensity (flow cytometry and low-magnification immunofluorescence microscopy) were well correlated with the now well-established γH2AX foci scoring method (R^2 = 0.81 to 0.89) in irradiated human fibroblasts (0.5 to 5 Gy of X- or γ-rays) at 4 hours after irradiation, indicating that global γH2AX fluorescence measurements are suitable for dose estimation at this time point post-irradiation.
- Based on these findings, we propose the use of flow cytometry for rapid triage purposes in an emergency situation, as it is more highly correlated with foci scoring and because of the speed and ease of the technique.
- Inter-individual variability in global γH2AX fluorescence using flow cytometry measurements is statistically insignificant at 4 hours post-irradiation in irradiated human fibroblasts (17 donors of varying radiosensitivity) and lymphocytes (11 healthy blood donors), based on their respectively plotted dose response curves (0.25 to 6 Gy of X- or γ-rays).
- In lymphocytes, there was a high level of inter-individual variability in the induction of global γH2AX fluorescence post-irradiation. The degree of inter-individual variations increased with dose and decreased with time. This was also observed following manual scoring of γH2AX foci (results shown in Figure A-1 in the Appendix). Inter-individual variability in the induction of global γH2AX fluorescence immediately after irradiation (30 min post-irradiation) may be moderately correlated (R^2 = 0.595) with cellular

radiosensitivity[††††] measured using cytogenetic approaches (correlation results are shown in Table A-1 and Figure A-2 in the Appendix). However, at later time points (> 3 hours) post-irradiation, no correlations with radiosensitivity[††††] were observed (results shown in Table A-1 in the Appendix), illustrating that at the time point studied in this paper (4 hours post-irradiation), inter-individual variability in global γH2AX fluorescence is independent from individual radiosensitivity.

- Based on these data, we propose calibration curves that can be applied to populations exposed to moderate radiation doses to estimate individual received doses, independent of individual radiosensitivity, at this specific time point post-irradiation using human fibroblasts and lymphocytes.
- We define three triage categories that could facilitate immediate and follow-up care in the case of a radiological accident. These triage categories were based on previously reported (IAEA, 2002;Rea et al., 2010) dose limits of 2 Gy and 3 Gy as the minimal values which result in moderate (variable care) and severe symptoms (urgent care), respectively.
- The usefulness and real-world applicability of this rapid and high-throughput technique using flow cytometry measurements of global γH2AX fluorescence may be limited by the time-sensitive nature of this radiosensitivity-independent measurement of γH2AX, which is heavily reliant on the specific time point of 4 hours post-irradiation. However, this method could potentially be developed into a commercialized kit that could be kept on site of radiation or nuclear facilities, and could offer new possibilities in the field of emergency biodosimetry.

[††††] Results of cellular radiosensitivity measured using cytogenetic approaches are presented in Section 3.1.1 of this thesis.

Mutation Research 793 (2015) 123–131

Contents lists available at ScienceDirect

Mutation Research/Genetic Toxicology and Environmental Mutagenesis

journal homepage: www.elsevier.com/locate/gentox
Community address: www.elsevier.com/locate/mutres

Global quantification of γH2AX as a triage tool for the rapid estimation of received dose in the event of accidental radiation exposure

Muriel Viau[a,1], Isabelle Testard[b,1], Grace Shim[a,1], Luc Morat[a], Marie D. Normil[a], William M. Hempel[a], Laure Sabatier[a,*]

[a] Commissariat à l'Energie Atomique (CEA), Laboratoire de Radiobiologie et Oncologie (LRO), 18 Route du Panorama – BP6, 92265 Fontenay-aux-Roses, France
[b] CEA Grenoble, Laboratoire de Chimie et Biologie des Métaux, DSV / iRTSV, 17 rue des Martyrs, 38054 Grenoble Cedex 5, France

ARTICLE INFO

Article history:
Received 24 May 2015
Accepted 26 May 2015
Available online 29 May 2015

Keywords:
Ionizing radiation
Biological dosimetry
H2AX phosphorylation
Flow cytometry
Accidental irradiation
Casualty triage

ABSTRACT

The phosphorylation of the H2AX histone to form γH2AX foci has been shown to be an accurate biomarker of ionizing radiation exposure. It is well established that there is a one-to-one correlation between the number of γH2AX foci and radiation-induced double strand breaks in cellular DNA, which can be translated to the received dose. However, manual counting of foci is time-consuming, and cannot accommodate high throughput analysis required to obtain rapid results for medical triage purposes in the case of large-scale accidental exposure. Furthermore, the accuracy of γH2AX measurements could potentially be compromised by delays between the time of exposure and analysis of results, as well as inter-cellular and inter-individual variability of this biological response. To evaluate more rapid approaches of quantifying γH2AX for use in an emergency situation, and to determine the impact of inter-individual variability, we compared two methods of global γH2AX fluorescence quantification (low magnification immunofluorescence microscopy and flow cytometry) to the well-established γH2AX foci scoring method in human primary fibroblasts. All three approaches were well correlated, indicating that global γH2AX fluorescence measurements are suitable for dose estimation. For rapid triage in an emergency situation, we propose the use of flow cytometry, as it is more highly correlated with foci scoring and because of the speed and ease of the method. Dose response curves (0.25–6 Gy) using flow cytometry measurements showed that inter-individual variability in global γH2AX fluorescence is statistically insignificant at 4 h post-irradiation. Based on these data, we propose calibration curves that can be applied to populations exposed to moderate radiation doses to estimate individual received doses, independent of individual radiosensitivity, at this specific time point post-irradiation using human fibroblasts and lymphocytes. Furthermore, we define three triage categories that could facilitate immediate and follow-up care in the case of a radiological accident.

1. Introduction

In the case of large-scale accidental exposure to radiation and following the estimation of direct physical injuries, the major difficulty faced by rescue responders is to rapidly determine the dose received by each victim to medically triage those who can return home, those who will require close follow-up, and those who should be hospitalized. This requires a method of biodosimetry that is rapid, accurate, and can accommodate high throughput analysis to efficiently triage victims of a mass accident based on individual levels of exposure.

Biodosimetry consists of the estimation of a received radiation dose based on the measurement of radiation-induced biological responses or consequences. Historically, biodosimetric approaches have been focused on cytogenetics, with the scoring of dicentric/ring chromosomes considered as the gold standard of biodosimetry [1]. These chromosomal aberrations are relatively specific to radiation exposure, are found at low background levels, and offer high sensitivity. Furthermore, validation standards have been developed for their detection [2]. These methods have recently been optimized and automated to increase their precision,

* Corresponding author. Tel.: +33 0 1 46 54 87 55; fax: +33 0 1 46 54 87 58.
E-mail addresses: muriel.viau@gmail.com (M. Viau), isabelle.testard@cea.fr (I. Testard), graceshim1@gmail.com (G. Shim), luc.morat@cea.fr (L. Morat), normil.mariedelna@yahoo.fr (M.D. Normil), william.hempel@cea.fr (W.M. Hempel), laure.sabatier@cea.fr (L. Sabatier).
[1] M. Viau, I. Testard and G. Shim contributed equally to the work.

http://dx.doi.org/10.1016/j.mrgentox.2015.05.009
1383-5718/

capacity, and reliability. However, the usefulness of this technique in a large-scale emergency setting is limited by the analysis delay due to the fixed, incompressible time needed to stimulate and culture the collected blood lymphocytes until they reach first mitosis [3]. Recent improvements of techniques based on premature condensation of chromosomes can remove the incompressible delay due to cell culture [4]. However, while this approach can provide accurate dose estimates, it cannot accommodate the high throughput analysis required in the case of a mass accident. Therefore, there is a need for the development of new and more rapid biodosimetry methods to be used in this emergency setting.

Among the cellular injuries induced by radiation are DNA double strand breaks (DSBs), which induce a rapid and coordinated series of cellular responses including the phosphorylation of the histone H2AX in large chromatin regions surrounding the break [5,6]. These regions are easily quantifiable shortly after irradiation as subnuclear foci of phosphorylated H2AX (γH2AX) using immunofluorescence microscopy. Indeed, there is a one-to-one correlation between the number of DSBs and γH2AX foci. DSB formation and repair after radiation exposure have been extensively studied (using pulsed-field gel electrophoresis or γH2AX foci scoring) and the number of DSBs can easily be correlated to the received dose [7,8]. A recent comparison between γH2AX foci scoring and the cytokinesis-block micronucleus assay, another established method for biodosimetry, demonstrated equivalent accuracy of dose estimation between the two methods early after radiation exposure [9]. However, manual counting of foci is time-consuming, fastidious, requires trained investigators, and produces inter-investigator and inter-laboratory variations in results; indeed, a recent inter-comparison of several laboratories that analyzed the same samples of irradiated lymphocytes revealed a dramatic variation of manually scored foci yields [10]. Several automated systems have been developed to minimize scoring artifacts and reduce quantification time [11–14]; interestingly, the recent comparative study cited above also brought to light the limitations of automation, and automated scoring of foci had to ultimately be rejected due to the lack of a standardized protocol and lack of reproducibility of results between the four participating laboratories [10]. γH2AX can also be quantified as total fluorescence intensity by fluorescence microscopy or flow cytometry [15–19]. These methods represent a robust approach to more rapidly obtaining results than by foci scoring. However, further investigation is required to translate global quantification into a reliable dosimetry system, notably to correlate total fluorescence intensity with the now well-established foci scoring method.

The accuracy of γH2AX foci or fluorescence intensity measurements can be confounded by several factors. First, delays between the time of exposure and analysis of the results could potentially compromise the accuracy of the measurements, as the number of foci and fluorescence intensity decline with time. Second, intercellular and inter-individual variability in γH2AX induction may also complicate these results. The variable responses observed following irradiation within the general population is primarily due to genetic background, and genetic defects represent the major cause of abnormal radiosensitivity. Mutations in proteins involved in cellular DNA repair, such as ATM, NBS1, MRE11, FANC, BLM or LIG1, have been associated with acute radiation responses, reduced DSB repair kinetics, and activation of more error-prone alternative DNA repair pathways [7,20].

However, genetic causes are not sufficient to explain all observed inter-individual differences in radiosensitivity, as individual responses to radiation are not the same even among the DNA repair deficient population. In 2008, the work of Joubert et al. [7] presented a model dividing individuals into three radiosensitivity groups based on the surviving fraction of cells after irradiation with a dose of 2 Gy and the percentage of γH2AX foci remaining at 24 h post-irradiation. The radiosensitivity groups were shown to be unevenly distributed within the general population, with a large proportion being radioresistant (Group I: 65–75%) and the hyper-radiosensitive Group III representing only 1–5% of the population. Notably, the proportion of the moderately radiosensitive Group II is not negligible, as it represents 10–20% of the population [21]. This inter-individual variability must be taken into account when determining the correlation between γH2AX flow cytometry and foci counting.

To evaluate the applicability of the γH2AX assay in an emergency situation, we have investigated the validity of two rapid methods for the global measurement of fluorescence that could be performed within a few hours after the exposure. In the case of large-scale accidental exposure, we estimate that biological samples cannot be obtained within less than 4 h after the accident; therefore, we have studied this time point for γH2AX analyses. We also assessed individual variability in γH2AX induction on the same fibroblasts as those described in the work of Joubert et al. [7]. Comparisons of flow cytometry and low-magnification (10× objective) microscopic quantifications to γH2AX foci scoring showed R^2 correlation coefficients that exceeded 0.8 for both, indicating that global quantification of fluorescence is suitable for dose estimation after irradiation. Using the calibration curves obtained for fibroblasts and lymphocytes, we propose triage categories based on flow cytometry measurements.

2. Materials and methods

2.1. Cell culture

Seventeen non-transformed human fibroblast lines of different origins [7] and normal human dermal fibroblasts (NHDF: CC-2511, Lonza) were used because of their genomic stability and to avoid any confounding effects of immortalization. Cells were frozen until use and routinely cultured as monolayers with Dulbecco's modified Eagle's minimum medium (DMEM), supplemented with 20% fetal calf serum (FCS) and 1% penicillin / streptomycin (all from Gibco® Life Technologies). All experiments were performed with cells in the plateau phase of growth (95–99% of cells in G0/G1).

Lymphocytes used in these studies were isolated from the whole blood of 11 healthy donors (with negative viral status) from the French Center of Blood Transfusions using the standard Ficoll isolation technique. After isolation, lymphocytes were frozen until use. At 24 h before irradiation, lymphocytes were thawed and cultured in RPMI 1640 medium supplemented with 10% FCS and 1% penicillin / streptomycin.

2.2. Irradiation

A clinical X-ray irradiator devoted to experimental research at the European Synchrotron Radiation Facility (ESRF, Grenoble, France) was used to perform a portion of the irradiations of fibroblasts as indicated. The X-ray beam was produced from a tungsten anode, applying a voltage setting of 200 kV, an intensity of 20 mA, and using a 0.1 mm copper filter (dose-rate of 1.324 Gy/min). Lymphocytes and NHDF cells were irradiated with γ-rays from a Cesium-137 source at the CEA, Fontenay aux Roses, France (dose-rate of 2 Gy/min).

2.3. Immunofluorescence

2.3.1. Lymphocytes

Cells were applied onto polylysine slides by Cytospin® and fixed for 15 min in 0.4% paraformaldehyde (PFA, Sigma–Aldrich) to arrest cell metabolism. Slides were then placed in a permeabilization buffer (HEPES, 50 mM sodium chloride, 3 mM magnesium chloride,

300 mM sucrose, and 0.5% Triton X-100, Sigma–Aldrich) for 30 min, followed by 1 h at 37 °C in blocking buffer (Blocking Reagent® and 0.5% Triton X-100). Slides were incubated with the primary antibody anti-γH2AX (Upstate Biotechnology) 1/800 in PBS-2% FCS for 1 h at 37 °C. Excess antibody was removed by three successive rinses in PBS-Triton X-100, and the slides were blocked once more for 10 min at room temperature (RT). Slides were then hybridized with the secondary antibody coupled to Cyanine 3 (1/100 in PBS-2% FCS, Sigma–Aldrich) for 1 h at 37 °C, and excess secondary antibody was removed with three rinses in PBS-Triton X-100. Slides were washed briefly in PBS, and mounted in *p*-phenylene diamine (PPD, Sigma–Aldrich) after counterstaining with 4,6-diamidino-2-phenylindole (DAPI, Sigma–Aldrich).

2.3.2. Fibroblasts

Cells were fixed in 3% PFA, 2% sucrose in PBS for 10 min at RT and permeabilized in 0.5% Triton X-100, 20 mM HEPES pH 7.4, 50 mM sodium chloride, 3 mM magnesium chloride, 300 mM sucrose solution (Sigma–Aldrich) for 3 min. Fixed fibroblasts were then incubated for 40 min at 37 °C in PBS-2% FCS with anti-γH2AX antibody (1/800). After washing in PBS, cells were incubated with an anti-mouse FITC secondary antibody (1/100 in PBS-2% FCS, Sigma–Aldrich) at 37 °C for 20 min. Slides were washed briefly in PBS, and mounted in PPD after counterstaining with DAPI.

2.3.3. Imaging and image analysis

Images of immunofluorescent stainings were captured with a charge-coupled device camera (Zeiss, Thornwood, NY) coupled to a Zeiss Axioplan microscope using MetaSystems® software that allows automatic image scanning. MetaCyte was used to photograph interphasic nuclei and quantify the fluorescence of γH2AX. Background staining intensity was used to normalize the obtained data so that the γH2AX signal at 0 Gy was equal to 0 for each experiment.

2.4. Flow cytometry staining

Cells were fixed with 70% ethanol for at least 10 min and stored at -20 °C until use. Prior to staining, cells were washed with PBS-2% FCS and incubated for 1 h at RT in PBS-2% FCS with anti-γH2AX antibody (1/800). After washing in PBS-2% FCS, cells were incubated with an anti-mouse FITC secondary antibody (1/100) at RT for 1 h. Cells were then washed and resuspended in PBS containing propidium iodide (20 μg/ml) and RNAse (10 μg/ml Sigma–Aldrich). At least 10^4 cells were analyzed using an LSR II flow cytometer (Becton Dickinson) and FSC Express 4 software (Denovosoftware®). Only cells in the G1 cell cycle phase were analyzed for γH2AX signal. Background staining intensity was used to normalize the obtained data so that the γH2AX signal at 0 Gy was equal to 0 for each experiment.

2.5. Statistical analysis

Statistical analyses of the results were performed using the Student *t*-test for two unpaired independent sample sets (different irradiation doses), and the standard error was calculated for the γH2AX signal between all the sample sets.

3. Results

3.1. Validation of global γH2AX quantification on fibroblasts

The first goal of this study was to compare different methods of γH2AX quantification following irradiation. To our knowledge, only foci counting has been quantitatively validated versus the well-established pulsed-field gel electrophoresis method, with one focus corresponding to one DSB [8]. Alternative methods for the quantification of γH2AX yields are based on the global quantification of fluorescence in the whole nucleus. Flow cytometry and total fluorescence quantification using immunofluorescence have recently been used by several groups [15–19]. However, we have not found any comparative studies that validate these methods in the literature. Most studies on global quantification were carried out on lymphocytes, where doses above 1–2 Gy are often underestimated by γH2AX foci scoring because of higher chromatin compaction [22] and focus overlapping [11,13,18]. Consequently, we started our investigation using human fibroblasts to compare the two methods of global fluorescence quantification of γH2AX (flow cytometry and immunofluorescence) to the foci scoring method.

For this purpose, we used two non-transformed fibroblast cell lines from radioresistant donors identified in our previous cytogenetic studies (personal communication). Fig. 1 presents the mean number of γH2AX foci scored 4 h after exposure to increasing doses of irradiation (0.5 to 4 Gy). The mean number of foci per cell increased in a linear dose-dependent manner (R^2 = 0.996). At 4 h after exposure to a dose of 2 Gy, 15.13 ± 2.78 foci per cell were observed, representing approximately 20 ± 3% of the number of foci observed immediately after irradiation and before any repair has taken place. This result is consistent with previous data obtained using fibroblasts from various origins [7,8].

The same fibroblast cell lines were then used to compare the three methods for γH2AX quantification. In these experiments, cells were irradiated at the same time under the same conditions (0.5 to 5 Gy) to reduce experimental variation. Half of the samples were used for flow cytometry, and the other half were used for immunofluorescent labeling on slides. Immunofluorescent images from the slides were then captured at 10× magnification for the global quantification of fluorescence and then at 63× magnification for foci scoring. Fig. 2A shows the correlation curves obtained between the three methods. Flow cytometry was better correlated with foci scoring (R^2 = 0.87) than global immunofluorescence measurement (R^2 = 0.81). Interestingly, flow cytometry and immunofluorescence, both global quantification methods, had the best correlation coefficient (R^2 = 0.89). These results indicate that flow cytometry and 10× quantification of fluorescence are suitable for dose estimation after irradiation.

For use in the rapid evaluation and triage of victims of large-scale accidental exposure to low or moderate doses, we estimate that flow cytometry is the more promising approach for rapid dosimetry because it is more highly correlated with foci scoring and because of the speed and ease of the method.

3.2. Individual radiosensitivity

As discussed above, inter-individual variability in radiosensitivity must be taken into account when determining the correlation between γH2AX flow cytometry and foci scoring. For this, we studied 17 non-transformed human fibroblast cell lines of different origins belonging to three previously described radiosensitivity groups [7]: 8 in Group I (radio-resistant), 7 in Group II (moderately radiosensitive), and 2 in Group III (hyper-radiosensitive).

Fig. 2B presents the correlations between the two methods conducted for each group (flow cytometry and foci scoring) at 4 h after radiation exposure. The good correlation coefficients for all groups (0.86, 0.97, and 0.94, respectively for Groups I to III) indicate that flow cytometry can be used to produce dose-response calibration curves after irradiation. As expected, the correlation coefficient and the curve equation for the radioresistant Group I was very similar to that depicted in Fig. 2A (radioresistant donors). These results demonstrate that individual radiosensitivity must be taken into account to guarantee a good estimation of the dose and the possible long-term health effects following accidental irradiation.

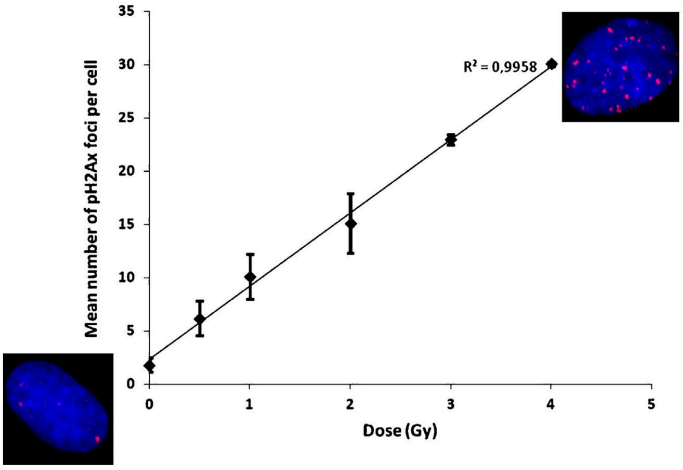

Fig. 1. Dose-dependent increase of γH2AX foci after irradiation.
Fibroblasts of two normal radioresistant donors (NHDF) were irradiated with γ-rays from a Cesium-137 source at the indicated doses and placed at 37 °C for repair. Cells were harvested at 4 h after irradiation. Immunofluorescent images were captured with a charge-coupled device camera (Zeiss, Thornwood, NY) coupled to a Zeiss Axioplan microscope using MetaSystems® software that allows automatic image scanning. Foci were then manually scored. Inserts show representative γH2AX signals observed after 0 and 4 Gy irradiation. Data points represent the mean ± standard error of two experiments.

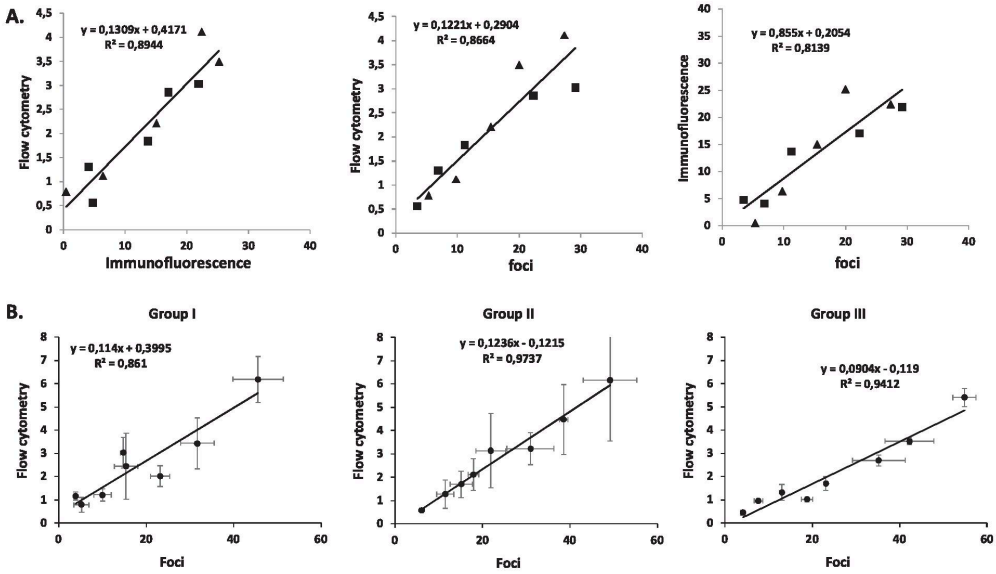

Fig. 2. Correlations between the three methods used for γH2AX quantification (flow cytometry, immunofluorescence, and foci scoring).
Human fibroblasts were irradiated (0.5 to 5 Gy) with X-rays (200 kV) or with γ-rays from a Cesium-137 source and placed at 37 °C for repair. Cells were harvested at 4 h after irradiation, divided into two parts, and then stained for flow cytometry or immunofluorescent imaging. MetaCyte® software (MetaSystems®) was used to quantify global γH2AX fluorescence, and foci were also scored manually. An LSRII flow cytometer (BD Biosciences®) was used to acquire cells, and data were analyzed using FCS Express 4 (Denovosoftware®). **A**. Correlations obtained with the two normal radioresistant donors (NHDF, triangles and squares). Data points represent normalized results obtained for one experiment with the two donors. **B**. Correlations obtained between flow cytometry and foci scoring for 17 fibroblast cell lines representing three radiosensitivity groups (Groups I < II < III). Each data point represents the mean ± standard error of experiments performed on at least 2 cell lines made in triplicate per group.

Upon plotting the dose-response curves of the three radiosensitivity groups evaluated by flow cytometry at 4 h after irradiation (Fig. 3A), all groups presented a high dose-dependent correlation (0.94 to 0.97). However, as inter-individual variability was relatively high for all groups, statistical analyses indicate that the three curves are indistinguishable from each other. Notably, of the three methods studied, only the scoring of individual γH2AX foci allowed for the discrimination of different radiosensitivity groups several hours after exposure; this inter-individual variability was not detectable using the global fluorescence techniques. Therefore, for triage purposes using global quantification of γH2AX fluorescence via flow cytometry, a calibration curve applicable for the

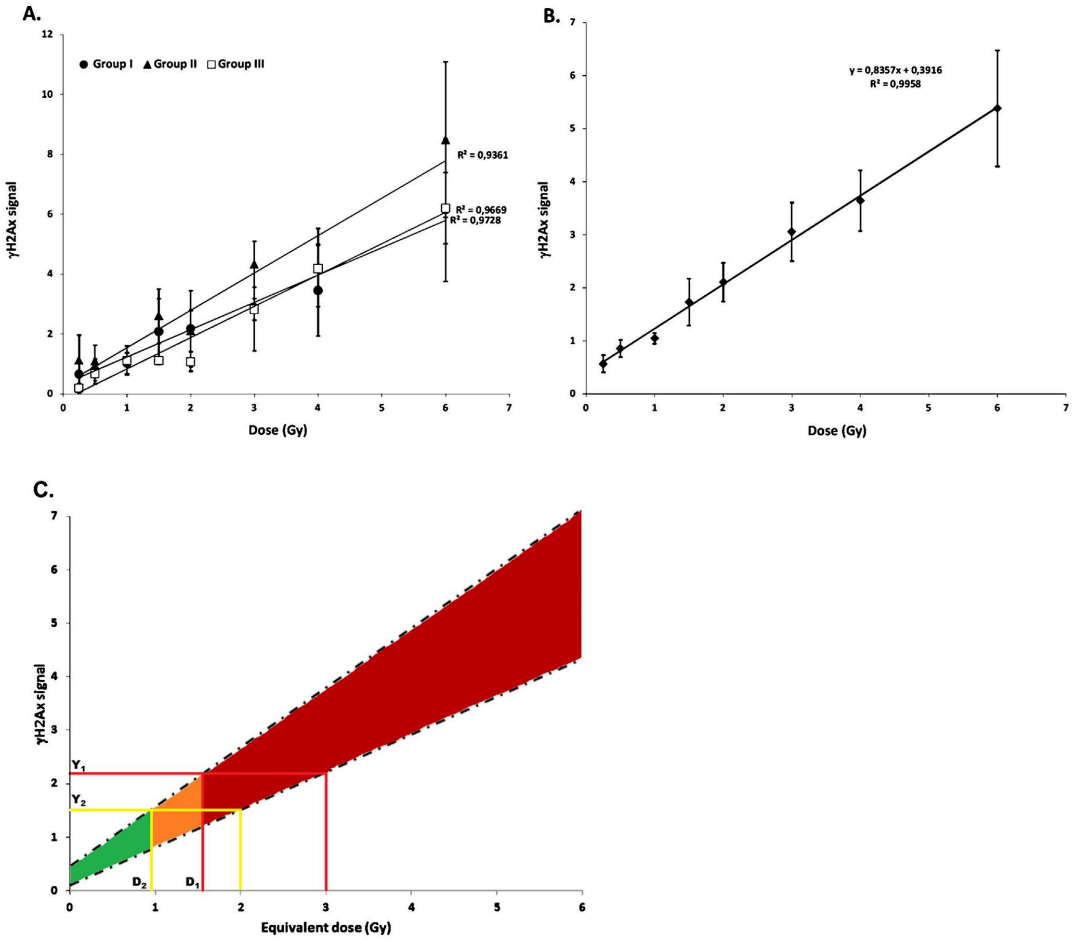

Fig. 3. Global fluorescence measurements using flow cytometry in fibroblasts for radiological triage.
Fibroblasts representing three radiosensitivity groups (Groups I < II < III) were irradiated with X-rays (200 kV) and placed at 37 °C for repair. Cells were harvested 4 h after irradiation and stained for flow cytometry. An LSRII flow cytometer (BD Biosciences®) was used to acquire cells, and data were analyzed using FCS Express 4 (Denovosoftware®). **A**. γH2AX signal observed for the indicated doses ranging from 0.25 to 6 Gy for each radiosensitivity group. Each data point represents the normalized mean ± standard error of experiments performed on at least 2 cell lines made in triplicate per group. **B**. Calibration curve obtained after pooling the γH2AX signal results from all groups. A weighting factor was applied to take into account the percentage of each group in the general population. **C**. Proposed triage categories based on the calibration curve in B: asymptomatic or unaffected population requiring minimal care (green section), population with moderate symptoms who will require no immediate medical attention (yellow section), and the population who should be hospitalized (red section).

general population can be generated that is independent of individual radiosensitivity.

3.3. Triage categories based on global γH2AX quantification on fibroblasts

Fig. 3B presents the calibration curve that can be used for the general population to estimate individual doses received in the event of accidental exposure. This curve was obtained after the application of a weighting index that considers the proportion of each radiosensitivity group within the general population. In the dose range studied (0.25 to 6 Gy), we obtained a linear dose dependence ($R^2 = 0.996$) with the following dose–effect relationship:

$$D = \frac{Y - (0.39 \pm 0.6)}{0.83 \pm 0.02}$$

where Y is the yield of γH2AX signal using flow cytometry, and D is the received dose (Gy). The error calculated on the linear coefficients of the regression curve reflects the observed inter-individual variability.

Based on this calibration curve (Fig. 3B) and the standard error, we propose the dose–response area plot and three triage categories presented in Fig. 3C. These triage categories are based on dose limits proposed by Rea et al., who defined doses of 2 Gy and 3 Gy as the minimal values which result in moderate (variable care) and severe symptoms (urgent care), respectively [23]. Moreover, 3 Gy was defined as the dose limit at the skin for medical intervention following skin exposure [24]. Using the minimal γH2AX signals measured at 2 Gy (yellow lines) and 3 Gy (red lines) in our dose-response area plot (labeled as Y_2 and Y_1, respectively), we extrapolated the minimum doses at which these same levels of

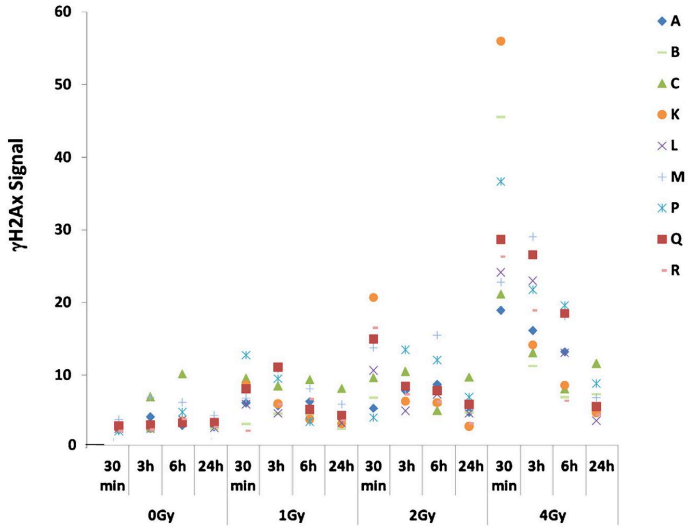

Fig. 4. Dispersion of γH2AX fluorescence intensity in lymphocytes.
Lymphocytes from 9 blood donors (increasing radiosensitivity measured using cytogenetic analysis associated with labels from A to R, Shim et al., in preparation) were irradiated with γ-rays from a Cesium-137 source at the indicated doses (0 to 4 Gy) and placed at 37 °C for repair. Cells were harvested at the indicated times (0.5–24 h post-irradiation) for staining. MetaCyte® software (MetaSystems®) was used to quantify global γH2AX fluorescence. Data points represent results obtained for one experiment with each donor.

γH2AX signal would be reached on our area plot (labeled as D_2 and D_1, respectively), which we designated as the dose limits for the three triage categories presented in Fig. 3C.

It is noteworthy that the relationships obtained between the foci and flow cytometry quantification for each group (Fig. 2B) are compatible with the area presented in Fig. 3C.

3.4. Inter-individual variability in lymphocytes

The work presented above validates the use of global quantification on irradiated fibroblasts to determine unknown doses of exposure. However, the most easily obtainable cells for triage are blood lymphocytes. Flow cytometry and global fluorescence quantification were recently used in lymphocytes to measure γH2AX yield following irradiation [15–19,25] and represent a good alternative to avoid the known underestimation of doses above 1–2 Gy obtained by γH2AX foci microscopy scoring in these cells. Furthermore, foci scoring in lymphocytes is not as straightforward as in fibroblasts because of their less defined nuclear area. Thus, we chose to reproduce the global measurement approach on human lymphocytes in order to validate our observations in a second cell type.

Fig. 4 shows the global γH2AX fluorescence quantified with microscopy at 10× magnification following *in vitro* irradiation of lymphocytes isolated from the blood of nine donors. As expected, γH2AX signals increased with increasing doses, and the signals decreased with repair time at each dose. Of note, γH2AX signals were not negligible in non-irradiated cells, probably due to the intrinsic fluorescence of lymphocytes. As observed in previous studies [15–17,25], our results demonstrate a high level of inter-individual variability that increases with dose. Interestingly, this inter-individual variability does not seem to be correlated with the relative radiosensitivity of each donor, estimated by cytogenetic approaches (increasing radiosensitivity associated with labels from A to R, Shim et al., in preparation). However, this variability tends to diminish with repair time in accordance with previously published observations [15–17,25]. This result was confirmed using the flow cytometry method (Fig. 5A).

3.5. Triage categories based on global γH2AX quantification in lymphocytes

Fig. 5 presents the results from the lymphocytes described above analyzed using the flow cytometry method. As for fibroblasts, we observed a linear dose-dependent increase in γH2AX signal at all tested time points ($R^2 = 0.99$) and a time-dependent decrease at each tested dose. These results are consistent with previous studies on lymphocytes displaying similar yields of fluorescence intensity [16,25].

Fig. 5B presents the calibration curve that can be used on lymphocytes to estimate individual doses received in the event of accidental exposure. The radiosensitivity status was not available for the donor lymphocytes, but we relied on the cytogenetic results mentioned in Section 3.4 and Fig. 4 to classify all of the donors into the radioresistant category; thus, no weighting factor was applied. The calibration curve obtained using lymphocytes at 4 h post-irradiation (Fig. 5B) is not comparable to that presented for fibroblasts (Fig. 3B) notably because of the intrinsic fluorescence of lymphocytes [26]. In the dose range studied (0.5 to 6 Gy), we measured a linear dose dependence ($R^2 = 0.99$) with the following dose–effect relationship:

$$D = \frac{Y + (0.58 \pm 0.55)}{2.77 \pm 0.17}$$

where Y is the yield of γH2AX signal using flow cytometry, and D is the received dose (Gy). The error calculated on the linear coefficients of the regression curve reflects the observed inter-individual variability.

As for fibroblasts, we used this calibration curve and the standard error to propose the dose-response area plot and triage

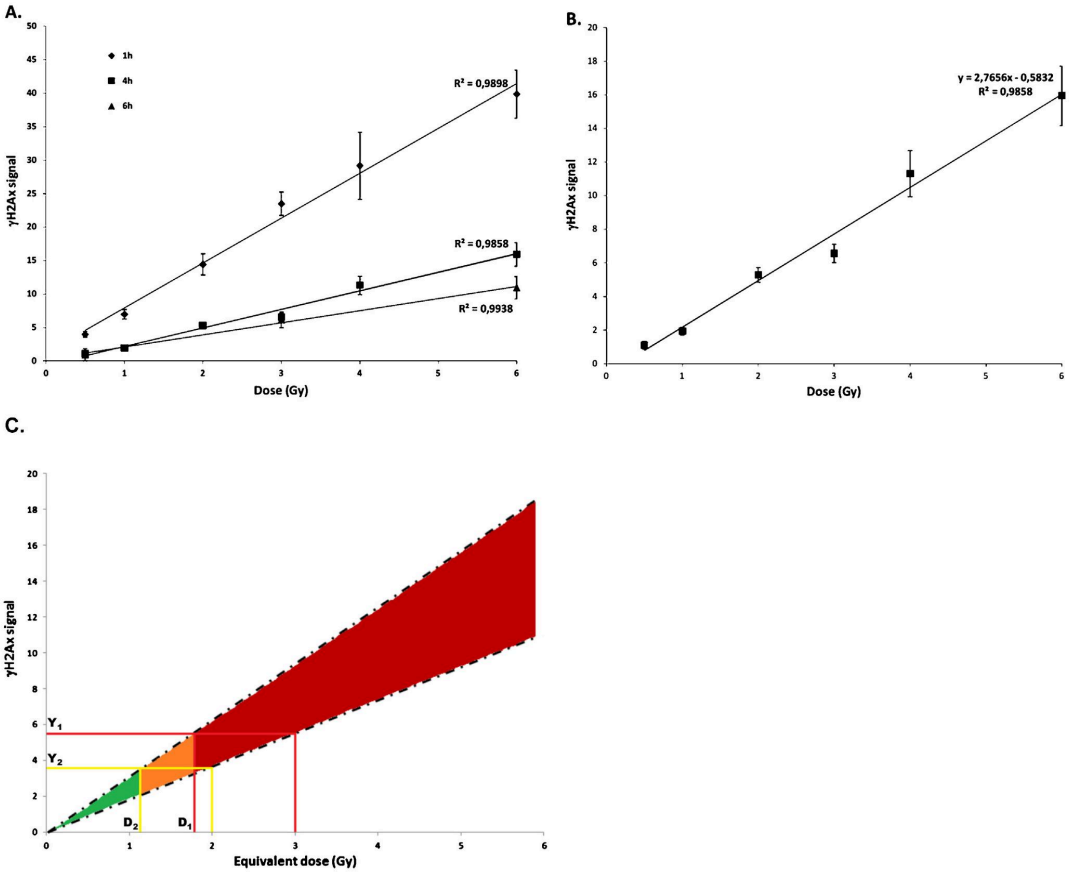

Fig. 5. Global fluorescence measurements using flow cytometry in lymphocytes for radiological triage.
Lymphocytes from 11 blood donors were irradiated with γ-rays from a Cesium-137 source and placed at 37 °C for repair. Cells were harvested at 1, 4, or 6 h post-irradiation as indicated and stained for flow cytometry. An LSRII flow cytometer (BD Biosciences®) was used to acquire cells, and data were analyzed using FCS Express 4 (Denovosoftware®). Each data point represents the normalized mean ± standard error of all donors. **A**. γH2AX signals observed for the indicated doses (0.5 to 6 Gy) after the indicated repair times. **B**. Calibration curve obtained for lymphocytes at 4 h after the indicated doses (0.5 to 6 Gy). **C**. Proposed triage categories based on the calibration curve in B: asymptomatic or unaffected population requiring minimal care (green section), population with moderate symptoms who will require no immediate medical attention (yellow section), and the population who should be hospitalized (red section).

categories presented in Fig. 5C. The same doses of 2 and 3 Gy were used to delineate the minimum doses (labeled as D_2 and D_1, respectively) at which these levels of γH2AX signal (labeled as Y_2 and Y_1, respectively) would be reached on our area plot. These minimum doses (D_1 and D_2) were used to designate the dose limits for the three triage categories presented in Fig. 5C.

4. Discussion

The aim of this work was to develop a method to carry out the rapid evaluation and triage of individuals following accidental irradiation at low to moderate doses. γH2AX foci scoring has been shown to be an accurate biomarker for ionizing radiation exposure. Here, by a direct comparison of the same samples, we demonstrate that global fluorescence quantification using flow cytometry and 10× magnification microscopy are suitable for dose estimation after irradiation. High correlations were obtained between γH2AX foci scoring and both methods of global γH2AX quantification (Fig. 2A). Although automated foci scoring reduces scoring time and laboratory variability [13,14], foci scoring is still significantly slower than flow cytometry; microscopy settings that are required to obtain images with high spatial resolution for foci scoring (e.g. fields of view, optical planes, fluorescence channels) are time consuming. Therefore, in the case of a large-scale nuclear event, we propose the use of flow cytometry for the triage of victims, as this method appears to be more readily applicable for the evaluation of individuals who have been exposed to radiation.

Calibration curves were obtained for fibroblasts (Fig. 3B) and lymphocytes (Fig. 5B) based on results obtained using flow cytometry, and triage categories were proposed for each cell type (Figs. 3 and 5C). The triage categories were designed from the calibration curves (and standard errors), and dose limits for each triage category were derived from the doses of 2 Gy and 3 Gy as advised in previous studies [23,24]. The γH2AX signal (Y) measured by flow cytometry should be placed on the calibration curve to match the highest triage category. As these triage categories are intended to aid medical responders, they are designed to overestimate the level of medical intervention needed for victims in the

radioresistant group (Group I), while taking into account the increased γH2AX signals in victims belonging to the non-negligible moderately radiosensitive population (Group II).

Biodosimetry on fibroblasts could be tempting in the case of heterogeneous irradiation and/or contamination. The results obtained with several fibroblast cell lines representing a large panel of radiosensitivities showed, however, that γH2AX levels are not indicative of individual radiosensitivity (Fig. 3A) as previously observed [27,28]. Notably, this observation is valid only for the doses and time points used for this study and does not presume that similar results can be obtained for other time points post-irradiation. For the appropriate triage of the different groups, clinical symptoms need to be taken into account and cytogenetic analysis must be performed following the emergency to precisely determine the received dose.

In lymphocytes, as previously reported [15–17,25], a high level of inter-individual variability in γH2AX signals was observed that did not correlate with the radiosensitivity of the donors measured using cytogenetic analysis. The sensitivity of γH2AX quantification using flow cytometry in lymphocytes, therefore, is lower than that using foci scoring. At low doses, automated foci scoring is easier than discriminating positive signals from the background by flow cytometry. As expected, flow cytometry yields a dose-dependent response curve ($R^2 > 0.98$) over a wider dose range than that obtained by foci scoring, which is limited by the overlapping of foci [13,14]. In this study, doses greater than 6 Gy were voluntarily not tested so as to focus on moderate doses that would likely be encountered in the context of an accident.

γH2AX signals observed in lymphocytes were higher than those seen in fibroblasts. This result was unexpected as lymphocytes are well known to present far fewer foci than fibroblasts for the same dose: in the literature, radioresistant cells show a maximal number of foci per Gy estimated to be between 10 and 12 for lymphocytes [13,16,29] and around 40 for fibroblasts [7]. In flow cytometry, intrinsic cellular fluorescence has an important impact on the results and auto-fluorescence has to be compensated for if several channels are used. In this study, we did not apply any compensation to quantify γH2AX signals, and thus higher intrinsic fluorescence of lymphocytes [26] has to be taken into account when comparing the measurements of lymphocytes and fibroblasts. Further investigation is required to better understand this cross relationship.

Radiation accidents or planned medical exposures are often characterized by acute partial-body or nonhomogeneous total-body radiation exposures. Studies have shown that the yield of γH2AX foci formation can allow the estimation of the applied integral body dose after local radiotherapy to different sites of the body [30]. Using flow cytometry, Horn et al. were able to distinguish the percentage of cells and their level of exposure from a mixture of irradiated and non-irradiated lymphocytes [16]. Estimations of the irradiation dose made only on cells containing foci were essentially accurate [16]. For lymphocytes, analytical methods need to be established as in the case for cytogenetic assays [9] to identify partial body exposures from blood samples, calculate the peak dose, and determine the irradiated fraction of the body. It should be noted that the dose estimation of localized exposure could also be performed following the analysis of biological samples distributed outside the body, such as fibroblasts or hair bulbs.

The possible delayed tissue damage could then be prevented or reduced by early clinical intervention. In order to perform the accurate triage of the different radiosensitivity groups, clinical symptoms have to first be taken into account and cytogenetic analyses have to be performed after the emergency to refine the dose estimation. Lymphocyte depletion kinetics would notably be useful to detect the moderately radiosensitive Group II that represents about 10–20% of the population: a patient presenting a mild decrease in the number of lymphocytes associated with a high γH2AX signal should be hospitalized, whereas a mild decrease in lymphocytes associated with a moderate γH2AX signal may require only close follow-up while awaiting more precise cytogenetic results. A software tool for prediction of clinical effects after irradiation using the database SEARCH (System for Evaluation and Archiving of Radiation Accident based on Case Histories) has been employed recently as part of a blind test. Blood cell counts measured at different times allowed the prediction of the severity of ARS (Acute Radiation Syndrome) with 80% accuracy [9]. We could speculate that at least a part of the 20% failure of the software could be due to the moderately radiosensitive Group II. This software could potentially be adapted to take into account this group and help first responders to make better-informed decisions.

Recent work has shown that radiation biodosimetry could be greatly enhanced by the automation of several steps of the process. For example, a robotically based biodosimetry workstation (RABIT) that can quantify total γH2AX fluorescence in nuclei has been developed [19]. This method is promising as it can automatically analyze small volumes of blood (<30 μl) and handle several samples at the same time, leading to the analysis of up to 6000 samples per day. The optimization of miniaturization and the increase in the number of analyzed samples have recently been improved [31]. However, this system is less sensitive than flow cytometry as it was developed for doses exceeding 2 Gy. Another less automated approach based on the rapid lyse/fix method on a 96 well plate was recently described [32]; this method has the advantage of being more affordable while still allowing a significant reduction in processing time. The measurements using this lyse/fix method were well correlated with the classical γH2AX quantification in isolated lymphocytes, but still relied on individual foci scoring. Only a few studies have focused on the global estimation of phosphorylated H2AX. One such promising system described by Avondoglio et al. [33] allows for the high throughput evaluation of γH2AX, in a larger dose range, via the chemiluminescent detection of trapped proteins. Nevertheless, the drawback of such automated systems is their unavailability at the site of the accident, thereby requiring samples to be sent to a laboratory for analysis. Currently, small transportable cytometers are available and can easily be installed near the accident site to save time. Cytometers are also widespread and can easily be found in laboratories near the scene. Moreover, unlike the foci scoring technique, flow cytometry is routinely carried out, and existing techniques can rapidly be adapted for the measurement of γH2AX signals. Thus, the validation of global quantification of γH2AX using flow cytometry as a triage tool might offer new possibilities in the case of a large radiological accident.

Conflict of interest

The authors declare that there are no conflicts of interest.

Competing interests

None.

Acknowledgments

This work was funded in part by the European 7th Security framework grant BOOSTER: grant agreement no. 242361 (FP7-SEC-2009-1, topic SEC-2009-4.3.2.). This work was also supported in part by a CEA grant from the NRBC-C2. We are grateful to Géraldine Leduc and Alberto Bravin for providing laboratory and irradiation facilities at the ESRF. We thank Nicolas Foray and Radhia M'Kacher for stimulating discussions and valuable advice.

References

[1] International Atomic Energy Agency, Cytogenetic analysis for radiation dose assessment, a manual, *Technical Reports Series* No. 405, IAEA, Vienna, 2001.
[2] P. Voisin, F. Barquinero, B. Blakely, C. Lindholm, D. Lloyd, C. Luccioni, S. Miller, F. Palitti, P.G. Prasanna, G. Stephan, H. Thierens, I. Turai, D. Wilkinson, A. Wojcik, Towards a standardization of biological dosimetry by cytogenetics, Cell Mol. Biol. (Noisy-le-grand) 48 (2002) 501–504.
[3] R. M.'Kacher, E.E.L. Maalouf, M. Ricoul, L. Heidingsfelder, E. Laplagne, C. Cuceu, W.M. Hempel, B. Colicchio, A. Dieterlen, L. Sabatier, New tool for biological dosimetry: reevaluation and automation of the gold standard method following telomere and centromere staining, Mutat. Res./Fundam. Mol. Mech. Mutagen. 770 (2014) 45–53.
[4] R. M'Kacher, E.E. Maalouf, G. Terzoudi, M. Ricoul, L. Heidingsfelder, I. Karachristou, E. Laplagne, W.M. Hempel, B. Colicchio, A. Dieterlen, G. Pantelias, L. Sabatier, Detection and automated scoring of dicentric chromosomes in nonstimulated lymphocyte prematurely condensed chromosomes after telomere and centromere staining, Int. J. Radiat. Oncol. Biol. Phys. 91 (2015) 640–649.
[5] T.T. Paull, E.P. Rogakou, V. Yamazaki, C.U. Kirchgessner, M. Gellert, W.M. Bonner, A critical role for histone H2AX in recruitment of repair factors to nuclear foci after DNA damage, Curr. Biol. 10 (2000) 886–895.
[6] E.P. Rogakou, D.R. Pilch, A.H. Orr, V.S. Ivanova, W.M. Bonner, DNA double-stranded breaks induce histone H2AX phosphorylation on serine 139, J. Biol. Chem. 273 (1998) 5858–5868.
[7] A. Joubert, K.M. Zimmerman, Z. Bencokova, J. Gastaldo, N. Chavaudra, V. Favaudon, C.F. Arlett, N. Foray, DNA double-strand break repair defects in syndromes associated with acute radiation response: at least two different assays to predict intrinsic radiosensitivity, Int. J. Radiat. Biol. 84 (2008) 107–125.
[8] K. Rothkamm, M. Lobrich, Evidence for a lack of DNA double-strand break repair in human cells exposed to very low X-ray doses, Proc. Natl. Acad. Sci. U. S. A. 100 (2003) 5057–5062.
[9] E.A. Ainsbury, E. Bakhanova, J.F. Barquinero, M. Brai, V. Chumak, V. Correcher, F. Darroudi, P. Fattibene, G. Gruel, I. Guclu, S. Horn, A. Jaworska, U. Kulka, C. Lindholm, D. Lloyd, A. Longo, M. Marrale, Monteiro Gil, O.U. Oestreicher, J. Pajic, B. Rakic, H. Romm, F. Trompier, I. Veronese, P. Voisin, A. Vral, C.A. Whitehouse, A. Wieser, C. Woda, A. Wojcik, K. Rothkamm, Review of retrospective dosimetry techniques for external ionising radiation exposures, Radiat. Prot. Dosim. 147 (2011) 573–592.
[10] K. Rothkamm, S. Horn, H. Scherthan, U. Rossler, A. De Amicis, S. Barnard, U. Kulka, F. Lista, V. Meineke, H. Braselmann, C. Beinke, M. Abend, Laboratory intercomparison on the gamma-H2AX foci assay, Radiat. Res. 180 (2013) 149–155.
[11] W. Bocker, G. Iliakis, Computational methods for analysis of foci: validation for radiation-induced gamma-H2AX foci in human cells, Radiat. Res. 165 (2006) 113–124.
[12] Y.N. Hou, A. Lavaf, D. Huang, S. Peters, R. Huq, V. Friedrich, B.S. Rosenstein, J. Kao, Development of an automated gamma-H2AX immunocytochemistry assay, Radiat. Res. 171 (2009) 360–367.
[13] S. Roch-Lefevre, T. Mandina, P. Voisin, G. Gaetan, J.E. Mesa, M. Valente, P. Bonnesoeur, O. Garcia, P. Voisin, L. Roy, Quantification of gamma-H2AX foci in human lymphocytes: a method for biological dosimetry after ionizing radiation exposure, Radiat. Res. 174 (2010) 185–194.
[14] R. Runge, R. Hiemann, M. Wendisch, U. Kasten-Pisula, K. Storch, K. Zophel, C. Fritz, D. Roggenbuck, G. Wunderlich, K. Conrad, J. Kotzerke, Fully automated interpretation of ionizing radiation-induced gammaH2AX foci by the novel pattern recognition system AKLIDES(R), Int. J. Radiat. Biol. 88 (2012) 439–447.
[15] K. Hamasaki, K. Imai, K. Nakachi, N. Takahashi, Y. Kodama, Y. Kusunoki, Short-term culture and gammaH2AX flow cytometry determine differences in individual radiosensitivity in human peripheral T lymphocytes, Environ. Mol. Mutagen. 48 (2007) 38–47.
[16] S. Horn, S. Barnard, K. Rothkamm, Gamma-H2AX-based dose estimation for whole and partial body radiation exposure, PLoS One 6 (2011) e25113.
[17] I.H. Ismail, T.I. Wadhra, O. Hammarsten, An optimized method for detecting gamma-H2AX in blood cells reveals a significant interindividual variation in the gamma-H2AX response among humans, Nucleic Acids Res. 35 (2007) e36.
[18] S.H. MacPhail, J.P. Banath, T.Y. Yu, E.H. Chu, H. Lambur, P.L. Olive, Expression of phosphorylated histone H2AX in cultured cell lines following exposure to X-rays, Int. J. Radiat. Biol. 79 (2003) 351–358.
[19] G. Garty, Y. Chen, A. Salerno, H. Turner, J. Zhang, O. Lyulko, A. Bertucci, Y. Xu, H. Wang, N. Simaan, G. Randers-Pehrson, Y.L. Yao, S.A. Amundson, D.J. Brenner, The RABIT: a rapid automated biodosimetry tool for radiological triage, Health Phys. 98 (2010) 209–217.
[20] A. Nussenzweig, M.C. Nussenzweig, A backup DNA repair pathway moves to the forefront, Cell 131 (2007) 223–225.
[21] A. Joubert, G. Vogin, C. Devic, A. Granzotto, M. Viau, M. Maalouf, C. Thomas, C. Colin, N. Foray, [Radiation biology: major advances and perspectives for radiotherapy], Cancer Radiother. 15 (2011) 348–354.
[22] E. Markova, J. Torudd, I. Belyaev, Long time persistence of residual 53BP1/gamma-H2AX foci in human lymphocytes in relationship to apoptosis, chromatin condensation and biological dosimetry, Int. J. Radiat. Biol. 87 (2011) 736–745.
[23] M.E. Rea, R.M. Gougelet, R.J. Nicolalde, J.A. Geiling, H.M. Swartz, Proposed triage categories for large-scale radiation incidents using high-accuracy biodosimetry methods, Health Phys. 98 (2010) 136–144.
[24] IAEA, Preparedness and response for a nuclear or radiological emergency, International atomic energy agency, Vienna, 2002.
[25] A. Andrievski, R.C. Wilkins, The response of gamma-H2AX in human lymphocytes and lymphocytes subsets measured in whole blood cultures, Int. J. Radiat. Biol. 85 (2009) 369–376.
[26] K. Rothkamm, S. Horn, Gamma-H2AX as protein biomarker for radiation exposure, Ann. Ist. Super. Sanita 45 (2009) 265–271.
[27] J. Werbrouck, K. De Ruyck, L. Beels, A. Vral, M. Van Eijkeren, W. De Neve, H. Thierens, Prediction of late normal tissue complications in RT treated gynaecological cancer patients: potential of the gamma-H2AX foci assay and association with chromosomal radiosensitivity, Oncol. Rep. 23 (2010) 571–578.
[28] J. Werbrouck, F. Duprez, W. De Neve, H. Thierens, Lack of a correlation between gammaH2AX foci kinetics in lymphocytes and the severity of acute normal tissue reactions during IMRT treatment for head and neck cancer, Int. J. Radiat. Biol. 87 (2011) 46–56.
[29] L. Beels, J. Werbrouck, H. Thierens, Dose response and repair kinetics of gamma-H2AX foci induced by in vitro irradiation of whole blood and T-lymphocytes with X- and gamma-radiation, Int. J. Radiat. Biol. 86 (2010) 760–768.
[30] A. Sak, S. Grehl, P. Erichsen, M. Engelhard, A. Grannass, S. Levegrun, C. Pottgen, M. Groneberg, M. Stuschke, gamma-H2AX foci formation in peripheral blood lymphocytes of tumor patients after local radiotherapy to different sites of the body: dependence on the dose-distribution, irradiated site and time from start of treatment, Int. J. Radiat. Biol. 83 (2007) 639–652.
[31] M. Repin, H.C. Turner, G. Garty, D.J. Brenner, Next generation platforms for high-throughput biodosimetry, Radiat. Prot. Dosim. 159 (2014) 105–110.
[32] J. Moquet, S. Barnard, K. Rothkamm, Gamma-H2AX biodosimetry for use in large scale radiation incidents: comparison of a rapid '96 well lyse/fix' protocol with a routine method, PeerJ 2 (2014) e282.
[33] D. Avondoglio, T. Scott, W.J. Kil, M. Sproull, P.J. Tofilon, K. Camphausen, High throughput evaluation of gamma-H2AX, Radiat. Oncol. 4 (2009) 31.

3 - INDIVIDUAL RADIOSENSITIVITY AND NORMAL TISSUE REACTIONS IN HEALTHY INDIVIDUALS

3.1 Individual radiosensitivity to γ-irradiation

As discussed in Section 1.4.2, inter-individual differences in radiosensitivity can have significant impact on clinical outcomes of radiotherapy. Thus, to characterize the extent and influence of individual radiosensitivity on normal tissue reactions to 2 Gy of γ-rays, a routinely administered dose during fractionated radiotherapy (Denekamp et al., 1997;Hartel et al., 2010), we evaluate the frequency of IR-induced DNA DSBs based on the scoring of IR-induced CAs visualized with TC-FISH (Figure 16) in PBL isolated from the whole blood of healthy individuals. We also examine radiosensitivity at other doses of γ-irradiation and formulate dose response curves. Additionally, we expand upon the findings of a recent paper of our laboratory (M'Kacher et al., 2014) to assess the sensitivity of TC-FISH analyses in cells cultured in different ways; for this analysis, we compare these results obtained in the isolated PBL to cells cultured in whole blood (without the isolation of PBL) of a separate cohort of healthy individuals that was analyzed in the article (M'Kacher et al., 2014).

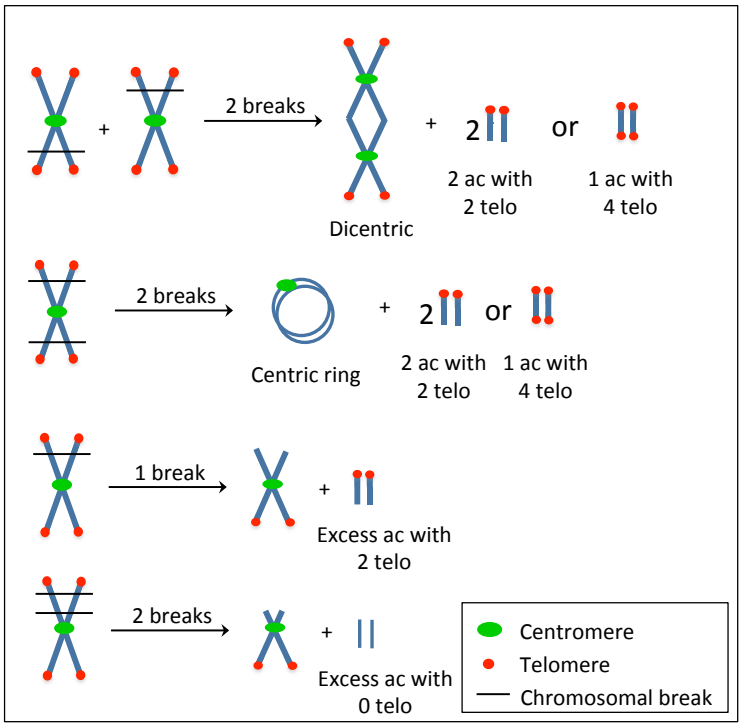

Figure 16. Method of estimating the number of IR-induced DSBs per cell that gave rise to each type of CA using TC-FISH. A dicentric or a centric ring with an acentric fragment (ac) containing 4 telomeres (telo) are considered as 2 DSBs. Excess acentric fragments with 2 telomeres are considered as resulting from 1 DSB (terminal deletion). Excess acentric fragments with 0 telomeres are considered as resulting from 2 DSBs (interstitial deletion).

For these analyses of individual radiosensitivity, we utilize TC-FISH, which as we briefly mentioned in Section 1.3.2, simultaneously stains telomeres and centromeres using PNA probes (Shi et al., 2012;M'Kacher et al., 2014). As demonstrated in a recent paper of our laboratory (M'Kacher et al., 2014), TC-FISH significantly simplifies the previously taxing DC analyses of Giemsa stained metaphases (discussed in Section 1.3.1), which required a trained cytogeneticist. It allows for a simple, rapid, and more accurate scoring of not only dicentrics, but also of all other types of IR-induced CA, such as centric and acentric rings and acentric fragments (with 0, 2, or 4 telomeres), without significantly increasing the cost. From this information, a precise estimate of the number of IR-induced DSBs that gave rise to the CA can be calculated (as illustrated in Figure 16). Generally, a dicentric or a centric ring with an acentric fragment containing 4 telomeres are considered as 2 DSBs; excess acentric fragments with 2 telomeres are considered as resulting from 1 DSB (terminal deletion); and excess acentric fragments with 0 telomeres are considered as resulting from 2 DSBs (interstitial deletion). This modified scoring technique was shown to provide improved sensitivity compared to the classical DC analyses. Additionally, in this same paper, the automated system that was developed in our laboratory for automated TC-FISH analysis (TCScore) is presented. This novel system allows for detection not only of 95% of dicentrics and centric rings, but also of different acentric fragments with the same efficacy as manual scoring, but in a fraction of the time. This improved, automated approach will open up new horizons for the assessment of genotoxic risk and for biological dosimetry, particularly for low doses (M'Kacher et al., 2014;M'Kacher et al., 2015a).

A summary of the key results of (M'Kacher et al., 2014) is as follows:

- Both the scoring of dicentrics and the frequency of DSBs per cell that was calculated using the TC-FISH technique at the low dose of 0.1 Gy allowed for statistically significant distinction from that of controls (0 Gy), a distinction that is less statistically significant with the traditional Giemsa staining.
- The calculated frequency of DSBs per cell was shown to be the more sensitive approach for detecting CAs at low doses compared to scoring of dicentrics alone.
- The scoring of CAs using the TC-FISH technique does not require a high level of trained expertise, as variability between results obtained from trained and untrained operators yielded no statistically significant differences.
- The improved sensitivity, ease, and replicability of analysis using TC-FISH demonstrate the robustness of this approach and the transferability of this technique to multiple cytogenetic laboratories.

Results

3.1.1 Individual radiosensitivity following exposure to 2 Gy of γ-rays

Here, we present the extent of individual radiosensitivity in PBL isolated from the whole blood of 18 healthy individuals, following *in vitro* exposure of PBL to 2 Gy of low-LET γ-rays, a routinely administered dose during fractionated radiotherapy (Denekamp et al., 1997;Hartel et al., 2010). Radiosensitivity was measured based on the mean number of IR-induced DSBs per cell, calculated based on the scoring of CAs following TC-FISH staining as described in Figure 16, in cells undergoing first mitosis at 60 hours post-irradiation.

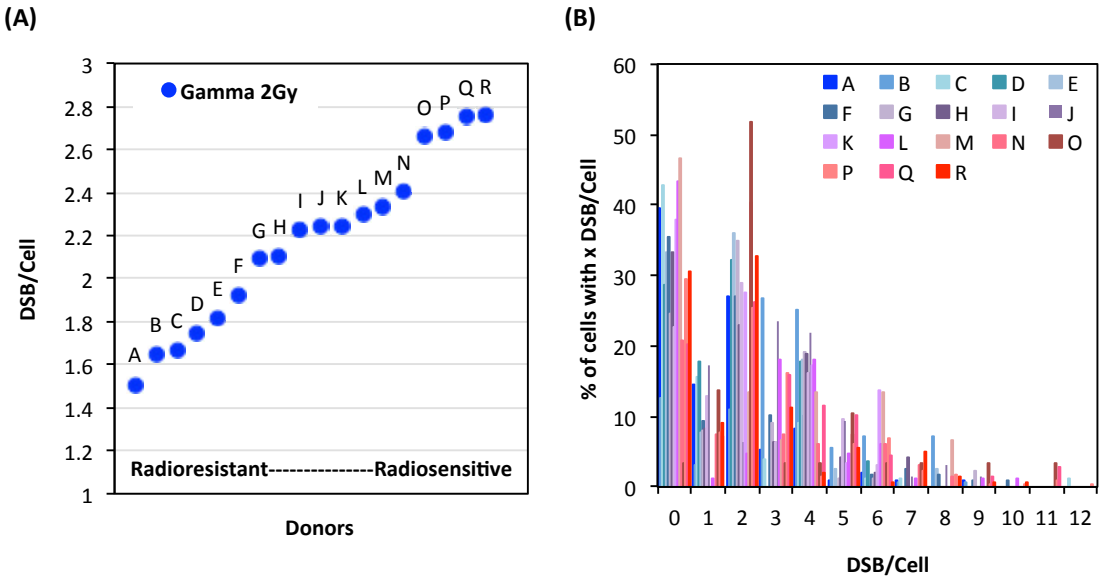

Figure 17. (A) Inter-individual differences in radiosensitivity following *in vitro* exposure to 2 Gy of γ-rays. Radiosensitivity was measured based on the mean number of DSBs per cell, calculated based on TC-FISH data as described in Figure 16, in PBL isolated from whole blood of 18 healthy individuals, in cells undergoing first mitosis at 60 hours post-irradiation. (B) Distribution of the number of DSBs per cell for each donor.

Radiosensitivity to 2 Gy of γ-irradiation is plotted in Figure 17A in the order of increasing sensitivity to radiation. Individuals were designated as Donors A through R in this order of 'radioresistant' to 'radiosensitive' donors. We use this ranking throughout the thesis as the definition of each of these donors' radiosensitivity. In other words, the ranking of the radiosensitivity of this cohort of donors was based on the mean number of DSBs per cell, calculated using TC-FISH analysis, following *in vitro* exposure of PBL to 2 Gy of γ-rays.

As shown in Figure 17A, following exposure to a dose of 2 Gy of γ-irradiation, there is a range of ~1.5 to 2.8 DSBs per cell. Comparison of data obtained from samples irradiated on different dates and analyzed by different individuals showed no significant differences in the measurement of the mean number of DSBs per donor ($p>0.05$). No correlations were

observed between this radiosensitivity and levels of spontaneous or IR-induced apoptosis (0 to 6 Gy; results shown in Figure A-3, Table A-2, and Table A-3 in the Appendix). As the *susceptibility* to IR-induced apoptosis in the T4-EM subpopulation was found to be correlated with radiosensitivity following γ-irradiation (Schmitz et al., 2007), we looked at whether the *slope* of IR-induced apoptosis in T4-EM lymphocytes between the doses of 0 and 6 Gy of γ-irradiation (blue data points in Figure A-3C) correlates to the individual radiosensitivity of these donors to 2 Gy of γ-irradiation (Figure 17A); as shown in Figure A-3D, no correlations were found (R^2 = 0.045). Radiosensitivity may be moderately correlated (R^2 = 0.595) with inter-individual variability in the induction of global γH2AX fluorescence immediately after irradiation (30 min post-irradiation) (results shown in Table A-1 and Figure A-2 in the Appendix); at later time points (3 to 24 hours) post-irradiation, no correlations with radiosensitivity were observed (results shown in Table A-1 in the Appendix). As shown in Figure 17B, donors classified as more radiosensitive harbor more DSBs per cell, with a wider range of distribution of DSBs per cell, compared to the more radioresistant donors. For example, the mean of the range of DSBs per cell in radioresistant donors (Donors A through F) is found to be 9.0 compared to 12.5 in radiosensitive donors (Donors M through R). This indicates the presence of more IR-induced damage in radiosensitive donors compared to radioresistant donors following exposure to a dose of 2 Gy of γ-rays.

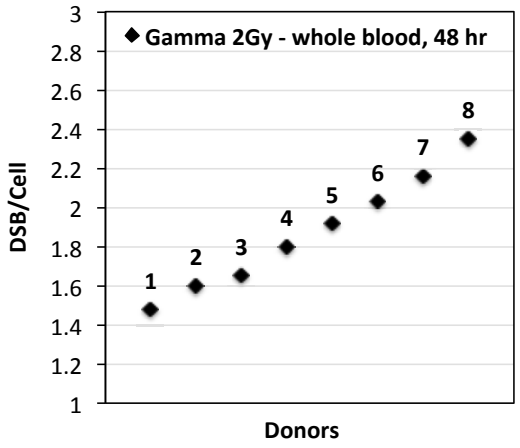

Figure 18. Inter-individual differences in radiosensitivity in a separate cohort of 8 healthy donors from (M'Kacher et al., 2014). Whole blood (without the isolation of PBL) was irradiated *in vitro* with 2 Gy of γ-rays, and radiosensitivity was measured based on the mean number of DSBs per cell, calculated based on TC-FISH data as described in Figure 16, in cells undergoing first mitosis at 48 hours post-irradiation.

These results were compared with the TC-FISH analysis of the whole blood (without the isolation of PBL) of a separate cohort of 8 healthy donors analyzed in (M'Kacher et al., 2014); whole blood was irradiated with a range of doses (0 to 6 Gy) of γ-rays, and cells were

analyzed at 48 hours post-irradiation. As shown in Figure 18, TC-FISH analysis in the whole blood of 8 donors (labeled as Donors 1 through 8) showed a range of ~1.4 to 2.4 DSBs per cell (1.7-fold difference) and a mean of 1.87 DSBs per cell, compared to the range of ~1.5 to 2.8 DSBs per cell (1.8-fold difference) and a mean of 2.17 DSBs per cell in the PBL samples (Figure 17A). Interestingly, the cohort in (M'Kacher et al., 2014), which comprised of a completely random group of healthy individuals that provided blood samples at the medical center at the CEA Fontenay-aux-Roses, France, yielded a range of IR-induced DSBs measured using TC-FISH that was similar to the cohort used for the analysis in Figure 17A, which comprises of individuals selected from a larger cohort of 63 individuals along the range of radiosensitivity measured previously based on the induction of IR-induced apoptosis (Schmitz et al., 2003); all TC-FISH analyses was, however, performed blindly. Though these analyses should be expanded to larger cohorts, the similarity in the range of these TC-FISH measurements between the randomly (M'Kacher et al., 2014) and non-randomly selected (Figure 17A) cohorts suggest that these measurements could represent the range of radiosensitivity of a significant portion of the population.

3.1.2 Individual radiosensitivity at other doses of γ-irradiation

To evaluate inter-individual differences in radiosensitivity at other doses, PBL of the same cohort of donors as in Figure 17 were irradiated *in vitro* with a range of doses (0 to 5 Gy) of γ-rays, and were analyzed using TC-FISH (Figure 16) at 60 hours post-irradiation. For the dose of 2 Gy, 18 donors (Donors A through R) were analyzed; to assess how dose-response curves may vary in different radiosensitivity groups, these donors were separated into 3 categories as follows: Donors A through F (‘radioresistant’), Donors G through L (‘medium radiosensitivity’), and Donors M through R (‘radiosensitive’). For all other doses, 6 of these donors were analyzed (Donors C, F, H, J, K, and O); these donors were separated into 3 radiosensitivity categories as follows: Donors C and F (‘radioresistant’), Donors H, J, and K (‘medium radiosensitivity’), and Donor O (‘radiosensitive’). Dose response curves for the doses of 0 to 5 Gy based on the mean number of dicentrics and DSBs per cell using TC-FISH analyses are shown in Figure 19A and Figure 19B, respectively, and zoom-ups of each of these curves at low doses (0 to 1 Gy) are shown in Figure 19C and Figure 19D. The dose response curves of the mean of all analyzed donors are plotted in Figure 20.

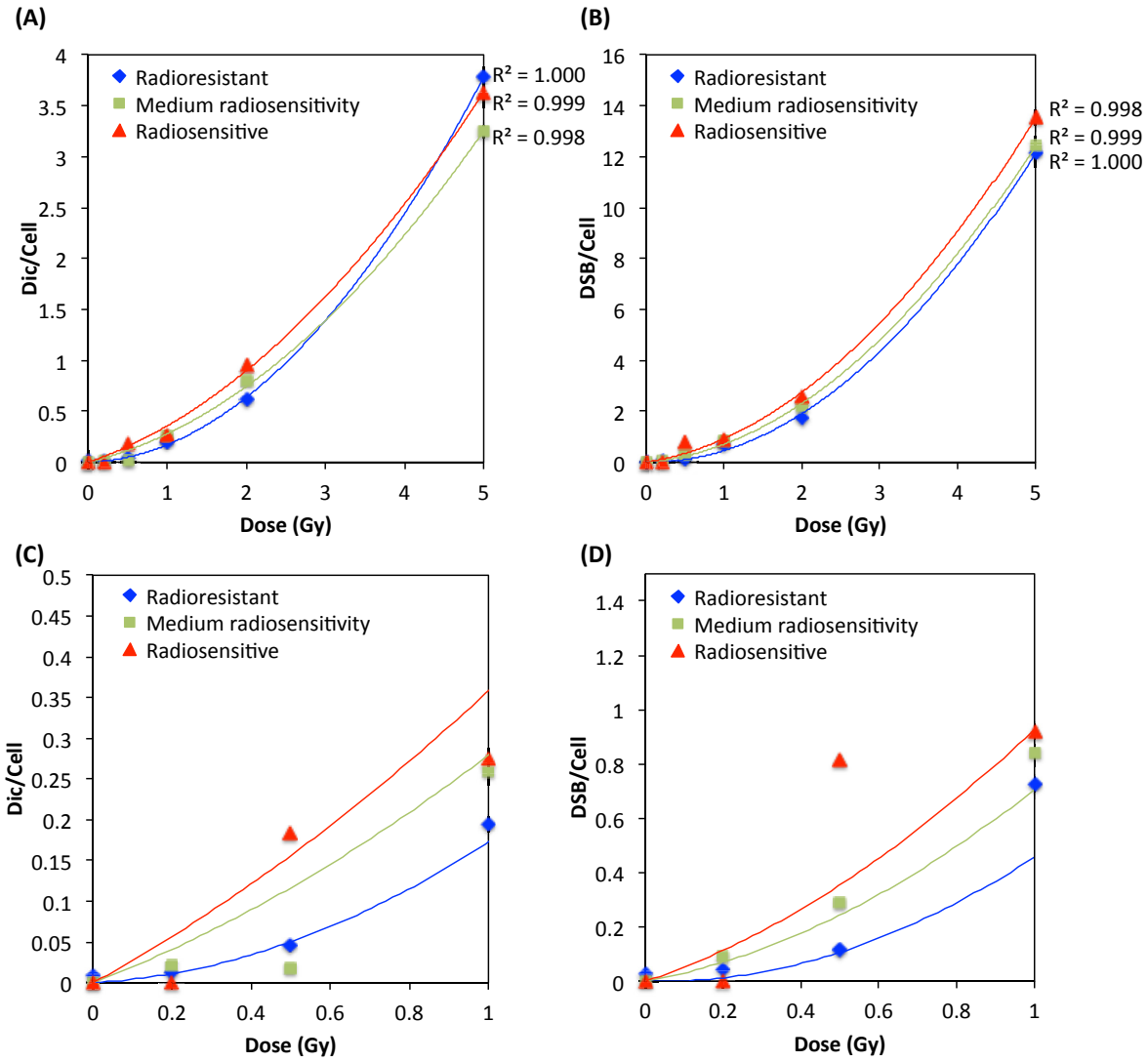

Figure 19. Dose response curves (0 to 5 Gy) based on individual radiosensitivity in PBL of healthy individuals following γ-irradiation. (A) Dose response curves based on mean dicentrics per cell, or (B) based on mean DSBs per cell. (C) and (D) Zoom-ups of each of these curves at low doses (0 to 1 Gy). For the dose of 2 Gy, 18 donors (Donors A through R) were analyzed at the dose of 2 Gy; these donors were separated into 3 categories as follows: Donors A through F ('radioresistant'), Donors G through L ('medium radiosensitivity'), and Donors M through R ('radiosensitive'). For all other doses, 6 of these donors were analyzed (Donors C, F, H, J, K, and O); these donors were separated into the 3 radiosensitivity categories as follows: Donors C and F ('radioresistant'), Donors H, J, and K ('medium radiosensitivity'), and Donor O ('radiosensitive').

As shown in Figure 19B, dose response curves for the doses of 0 to 5 Gy based on the mean number of DSBs show parallel dose response trends between the three groups of radiosensitivity at all studied doses (0 to 5 Gy). However, as shown in Figure 19A, measurements based on dicentrics alone may not provide as accurate an assessment compared to DSB measurements, as illustrated by the overlap between the trend lines between the three groups of radiosensitivity at the studied doses. The zoom-up for low doses (0 to 1 Gy) of the curve showing the mean number of DSBs per cell (Figure 19D)

suggests that the 'radiosensitive' group could exhibit a trend at low doses that does not conform as well to the overall trend over the wider dose range of 0 to 5 Gy; the trends at low doses for the moderately radiosensitive and radioresistant groups conform relatively well to the overall trend over the wider dose range. With dicentric measurements (Figure 19C), this deviation from the overall trend line (0 to 5 Gy) is also apparent in the moderately radiosensitive group; this may however be associated with the less sensitive measurement of scoring dicentrics compared to TC-FISH analyses, which considers all types of IR-induced CAs. These differences between radiosensitivity groups are especially apparent at the dose of ~0.5 Gy. Though these results must be verified in a larger cohort, they may demonstrate the drastically different response to low doses of IR exposure in individuals that are highly radiosensitive. These results may highlight the importance of identifying these highly radiosensitive individuals and adapting diagnostic radiology and radiation protection protocols based on individual radiosensitivity in order to better protect these individuals.

3.1.3 Dose response curves following exposure to γ-irradiation

Dose response curves based on the mean of all analyzed donors described above are shown in Figure 20. For the PBL samples, as described in Sections 3.1.1 and 3.1.2, 18 donors (Donors A through R) were analyzed at the dose of 2 Gy of γ-irradiation, and all other doses (0 to 5 Gy) include the analyses of 6 of these donors (Donors C, F, H, J, K, and O). Results were compared with the TC-FISH and uniform staining (Giemsa) analyses of the whole blood (without the isolation of PBL) of a cohort of 16 donors from (M'Kacher et al., 2014), irradiated with a range of doses (0 to 6 Gy) of γ-rays and analyzed at 48 hours post-irradiation.

Figure 20 shows the results of the comparisons of frequencies of dicentrics (Figure 20A, and a zoom-up of 0 to 1 Gy in Figure 20C) and DSBs (Figure 20B, and a zoom-up of 0 to 1 Gy in Figure 20D) per cell between these cohorts and techniques. The plots, which show the dose response curves based on the mean of all donors analyzed, indicate a second order polynomial trend between the doses of 0 Gy and 5 Gy (or 6 Gy for the cohort from M'Kacher *et al*). Notably, Giemsa-stained whole blood analysis of dicentrics per cell in the cohort from M'Kacher *et al* corresponds to the dose-response curves obtained after uniform staining by the CEA and published by the IAEA (IAEA, 2011), and obtained in a recent study of 14 healthy donors (Pajic et al., 2015).

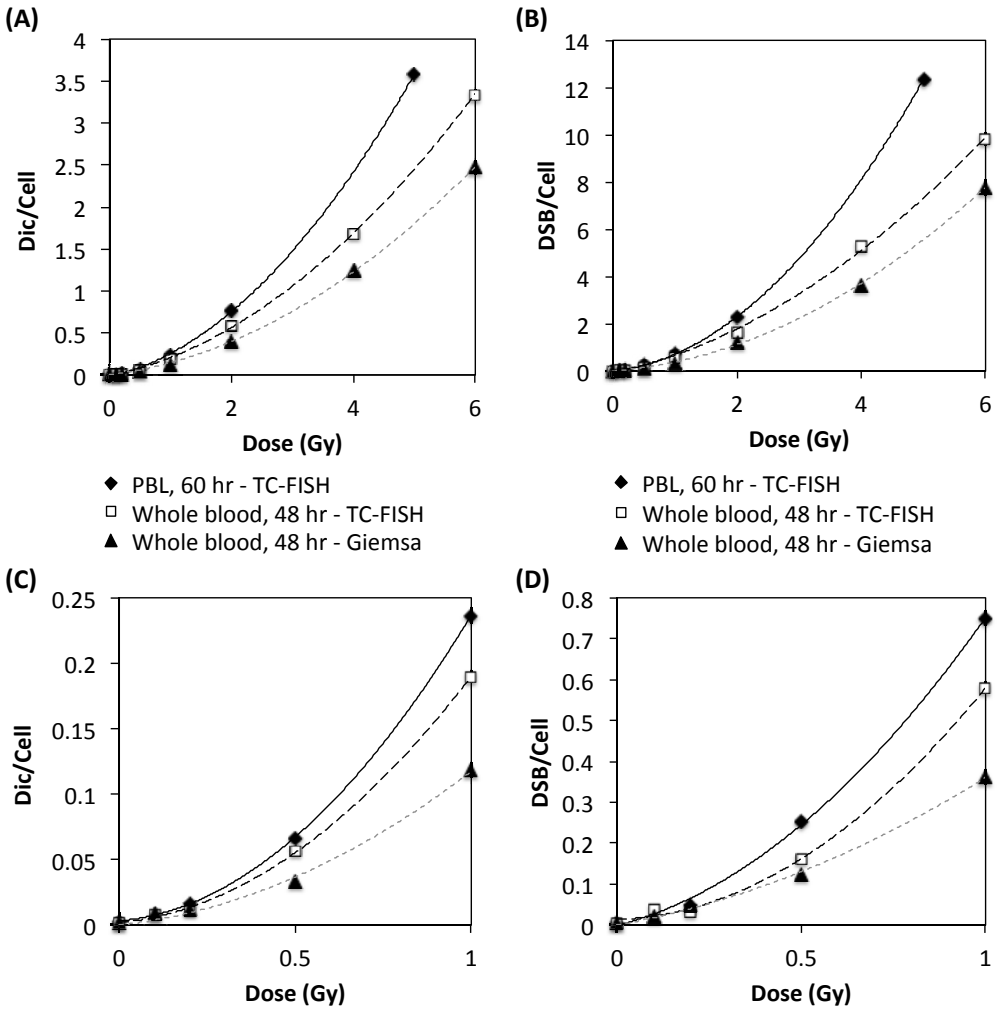

Figure 20. Dose-response curves of TC-FISH analysis of PBL isolated from whole blood (using the standard Ficoll isolation technique) of the cohort of 18 healthy blood donors following irradiation with 0 to 5 Gy of γ-rays, and analyzed at 60 hours post-irradiation. Results were compared to those of TC-FISH and uniform staining (Giemsa) analyses of the whole blood of the cohort of 16 donors from (M'Kacher et al., 2014), irradiated with a range of doses (0 to 6 Gy) of γ-rays and analyzed at 48 hours post-irradiation. (A) Dose-response curves (0 to 6 Gy) for dicentrics and (B) estimated DSBs per cell. (C) Zoom below 1 Gy of the dose-response curves for dicentrics and (D) estimated DSBs per cell.

As shown in Figure 20, at all studied doses, TC-FISH using PBL was able to detect approximately double the number of DSBs and dicentrics per cell compared to analysis using uniform staining in whole blood. The analysis of dicentrics and DSBs using isolated PBL is more sensitive than the use of whole blood (cohort from M'Kacher *et al*), as more dicentrics and DSBs were scored at any given dose in isolated PBL compared to whole blood. A larger difference between TC-FISH analyses in PBL versus whole blood is observed using DSB measurements (Figure 20B and D) compared to dicentric measurements (Figure 20A and C) at all studied doses, illustrating the improved sensitivity of DSB scoring over the traditional dicentric scoring; this increased sensitivity is also

apparent at low doses (<1 Gy; Figure 20C and D). As described in Section 3.1.1, at the dose of 2 Gy, TC-FISH analysis in whole blood showed a range of ~1.4 to 2.4 DSBs per cell, with a mean of 1.87 DSBs per cell (Figure 18) compared to the mean of 2.17 DSBs per cell in the PBL samples (Figure 17A). TC-FISH analysis in PBL therefore detected 35-40% more DSBs and dicentrics per cell compared to TC-FISH analysis in whole blood. These data illustrate that using TC-FISH analyses in isolated PBL offers an even more precise estimation of dose than using the same analyses on whole blood. This improved approach may have important implications in the assessment of genotoxic risk and for biological dosimetry, especially at low doses. Whether the automated DCScore technique can confirm these results is yet to be determined.

Notably, whole blood samples were harvested at 48 hours post-irradiation compared to the 60-hour incubation time for PBL. This shorter incubation time for whole blood samples allows less time for DNA damage repair to take place; therefore, more heavily damaged cells (especially after irradiation at higher doses) may not enter mitosis by this time and thus will not be included in analysis. The longer post-irradiation incubation time in PBLs allows additional time for heavily damaged cells to enter mitosis, and these cells are thereby included in analysis. This may explain the higher levels of DSBs found in PBLs in this analysis. Therefore, to verify the sensitivity of the TC-FISH analysis in whole blood samples versus PBL samples, it will be important to perform analysis in cells harvested at the same time point post-irradiation. However, as TC-FISH analysis in whole blood at 48 hours (Figure 18) yielded DSBs per cell that were in the same general range as in PBL at 60 hours (Figure 17A) at the dose of 2 Gy, it may be plausible to perform analysis in PBL at 48 hours to reduce the time to obtain results at this dose.

3.2 Comparison of individual radiosensitivity to γ-rays and carbon ions

Current radiotherapy regimens use photons (either X- or γ-rays) or protons for the treatment of a plethora of malignancies. However, radiotherapy for the treatment of cancer is now shifting to the use of heavier ion species (Schlaff et al., 2014), which may potentially offer radiobiological advantages over low-LET IR due to their inherent characteristics that are useful especially for the precisely targeted treatment of deep-seated tumors in the human body. Among various types of heavy ion species considered for radiotherapy, carbon ions are considered to have the most balanced and optimal properties in terms of physical dose distribution and RBE along its Bragg peak curve (Kamada et al., 2015). However, carbon ion radiotherapy is not yet widely used, with only a few centers worldwide (6 in Asia and 2 in Europe) that have treated ~13,000 patients (as of December 2013), compared to

~50 active proton therapy centers worldwide that have treated over 105,000 patients (Jermann, 2014). Though preliminary clinical data from the existing carbon ion therapy centers suggest favorable results for many of the malignancies that do poorly with conventional radiotherapy (Kamada et al., 2015), further clinical research and development of more carbon ion (and other charged particles heavier than protons) therapy centers in the US and worldwide are hindered by the lack of sufficient clinical evidence of the benefit of carbon ion therapy over conventional radiotherapy that would cost-effectively justify the establishment of such expensive facilities (Schlaff et al., 2014). Further investigation is necessary to characterize and understand how carbon ion therapy works in comparison to conventional radiotherapy.

As mentioned above, one of the potential biological advantages of heavier ions like carbon ions is their significantly increased RBE, particularly in the Bragg peak region. Current experimental treatment planning with photon, proton, and carbon ion regimens assumes that the same biological effective dose is administered with a standardized fractionation dose. However, increased RBE with heavy ion therapy has to be taken into account in treatment planning, and additional knowledge is needed to better establish the RBE of heavy ions compared to conventional photon and proton therapies at the traditional fractionation dose of ~2 Gy per fraction to determine the appropriate prescribed dose for heavy ion treatments. Additionally, as RBE depends in a complex manner on physical and biological parameters, such as the particle species, ion beam energy, LET, dose, and the cell/tissue type under consideration, the effect of each of these parameters on RBE need to be determined. The accurate description and understanding of RBE at various doses is of particular interest for treatment planning since hypofractionated treatment schedules have become increasingly important in ion beam therapy (Friedrich et al., 2014). Furthermore, whether inter-individual differences in radiosensitivity exists following high-LET IR exposure and whether it plays a role in determining RBE of heavy ions remains to be established.

In this study, we characterize inter-individual differences in radiosensitivity using the TC-FISH technique following a dose of 2 Gy of carbon-13 ions in PBL of healthy blood donors. We also examine radiosensitivity at other doses of carbon ions and formulate dose response curves. We compare these results with those obtained following γ-irradiation and provide RBE estimates for carbon ions at a range of doses in irradiated normal human lymphocytes. Furthermore, we compare a second cytogenetic technique, M-FISH, to the TC-FISH technique to estimate RBE.

Results

3.2.1 *Individual radiosensitivity following exposure to 2 Gy of carbon ions*

As with γ-irradiation, inter-individual differences in radiosensitivity following *in vitro* exposure to 2 Gy of high-LET carbon-13 ions (75 MeV/u; LET ~36.5 keV/µm at the plateau region of the Bragg peak curve) was measured in PBL of 13 of the healthy blood donors analyzed for γ-irradiation above in cells undergoing first mitosis at 60 hours post-irradiation. Radiosensitivity was measured based on the mean number of IR-induced DSBs per cell, calculated based on TC-FISH data as described in Figure 16. Radiosensitivity to 2 Gy of carbon ions is plotted in Figure 21A in order of increasing sensitivity to radiation.

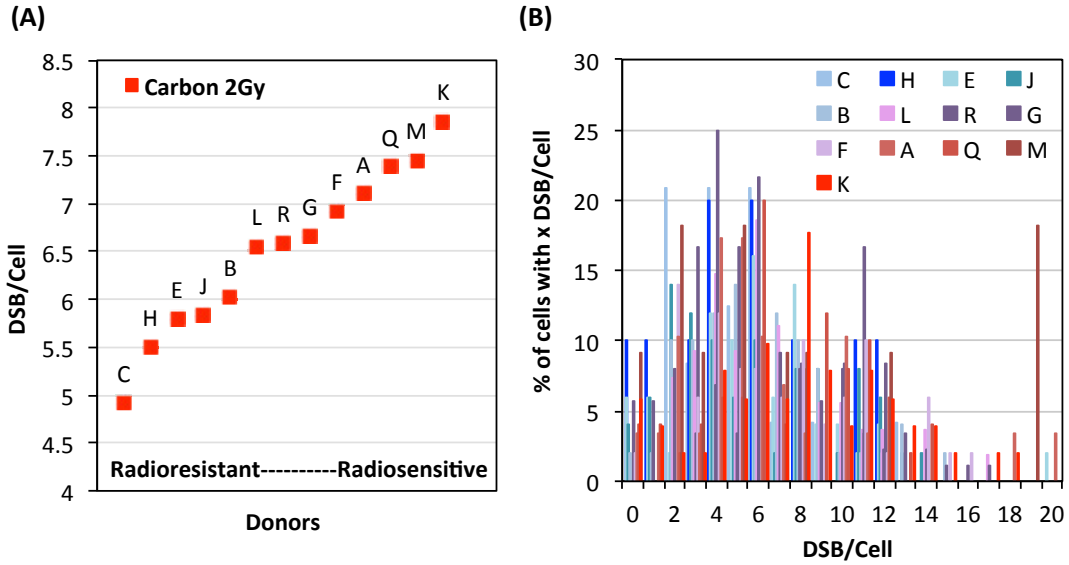

Figure 21. (A) Inter-individual differences in radiosensitivity following *in vitro* exposure to 2 Gy of high-LET carbon-13 ions (75 MeV/u; LET ~36.5 keV/µm at the plateau region of the Bragg peak curve). Radiosensitivity was measured based on the mean number of DSBs per cell, calculated based on TC-FISH data as described in Figure 16, in PBL isolated from whole blood of 13 healthy individuals, in cells undergoing first mitosis at 60 hours post-irradiation. (B) Distribution of the number of DSBs per cell for each donor.

As shown in Figure 21A, within the same cohort of blood donors studied for γ-irradiation, inter-individual radiosensitivity was also observed following carbon irradiation; a range of ~5 to 8 DSB per cell was measured. Furthermore, within this cohort, the order of radiosensitivity to carbon irradiation was different from that for γ-irradiation (to be discussed further in Section 3.2.2). Based on this ranking of radiosensitivity, we find that the more radiosensitive donors to carbon irradiation harbored more DSBs per cell compared to the more radioresistant donors, as shown in Figure 21B; for example, the mean of the range of DSBs per cell in radioresistant donors (Donors C, H, E, J) was found to be 14.8 compared to

19.8 in radiosensitive donors (Donors F, A, Q, M, K). Upon analysis of the relationship between the susceptibility to IR-induced apoptosis in the T4-EM subpopulation and radiosensitivity (Schmitz et al., 2007), as we did for γ-irradiation in Section 3.1.1, no correlations were found (R^2 = 0.004; Figure A-4D) between the slope of IR-induced apoptosis between the doses of 0 and 6 Gy of carbon irradiation (the blue data points in Figure A-4C) in the T4-EM subpopulation and radiosensitivity following 2 Gy carbon irradiation (Figure 21A).

3.2.2 No correlations between radiosensitivity to 2 Gy of γ-rays and carbon ions

To determine individual radiosensitivity in normal tissue of healthy individuals to IR of different LET, we compare radiosensitivity measurements using TC-FISH following exposure to 2 Gy of carbon ions (data from Section 3.2.1) and γ-rays (data from Section 3.1.1) in PBL of healthy blood donors.

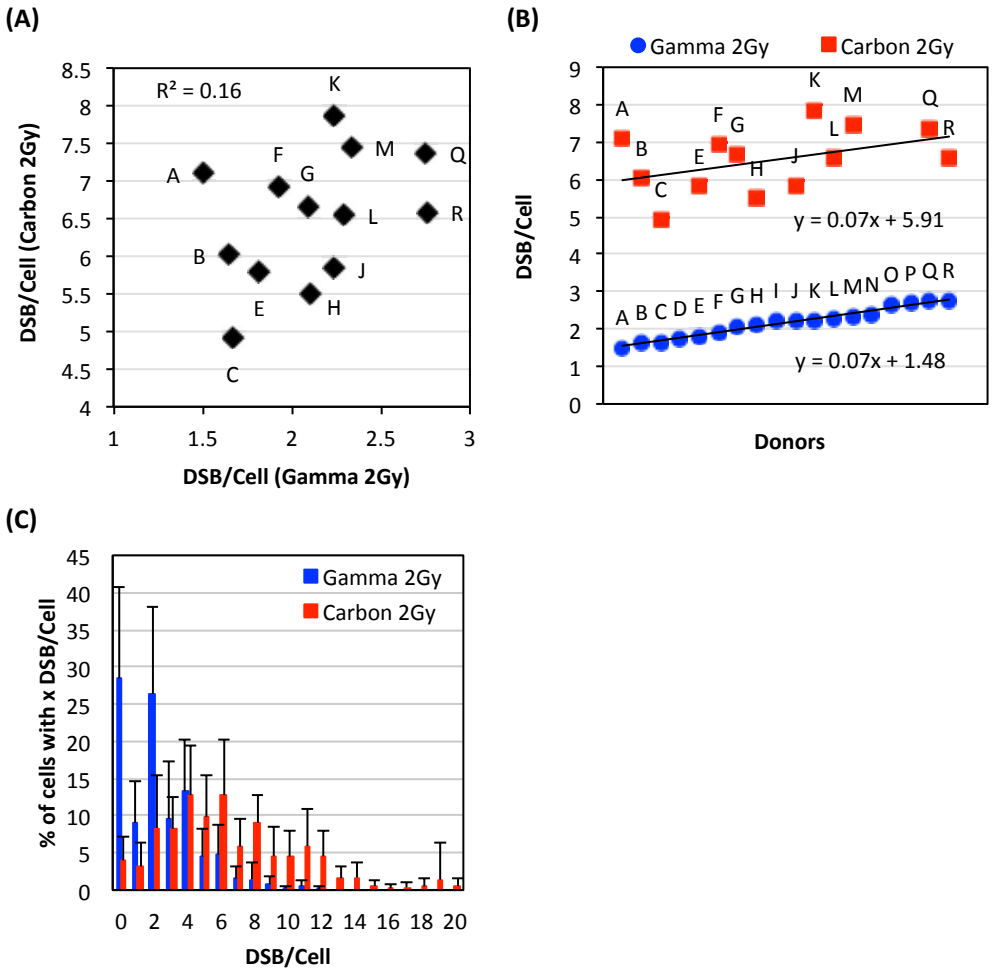

Figure 22. (A) No correlations between individual radiosensitivity following *in vitro* exposure to 2 Gy of carbon ions and γ-rays. (B) Ranking of individual radiosensitivity to 2 Gy of carbon

ions and γ-rays. (C) Distribution of the number of DSBs per cell for each type of IR for all donors analyzed.

As shown in Figure 22A, we find that there are no correlations between radiosensitivity to carbon ions and γ-rays at the dose of 2 Gy (R^2 = 0.16). Indeed, the order of low to high radiosensitivity as classified according to 2 Gy of γ-irradiation did not hold for carbon irradiation following exposure to the same dose (Figure 22B, a compilation of plots Figure 17A and Figure 21A). This indicates that donors are not equally sensitive to different types of IR. Interestingly, though the ranking of radiosensitivity to carbon ions and γ-rays was different within this cohort, the trend lines for radiosensitivity to each type of IR (plotted in the order of increasing radiosensitivity to γ-rays) were parallel, both with a slope of 0.07. Notably, a high intra-cellular variability of IR-induced DSB among cells of the same donor was observed, illustrated by large error bars representing the 95% confidence interval for each data point. Intra-cellular variations following carbon irradiation were generally found to be larger than those following γ-irradiation. This may be expected due to the non-uniform spatial distribution of IR-induced DNA damage following heavy ion irradiation. Interestingly, a modest correlation was found between the dispersion of DSBs per donor (95% confidence interval) following γ- and carbon irradiation (R^2 = 0.51). Finally, as expected, carbon irradiation cause more dispersion in the number of DSBs induced per cell compared to γ-irradiation, with carbon ranging to up to 20 DSBs per cell and γ-rays ranging up to 12 DSBs (Figure 22C). This indicates that carbon irradiation cause a larger range of DSBs per cell and more IR damage that is less repaired compared to γ-rays.

3.2.3 RBE factor of 3 after 2 Gy irradiation using both TC-FISH and M-FISH techniques

We calculate RBE by dividing the mean DSBs per cell determined using TC-FISH following exposure to carbon ions by that following exposure to the same dose of γ-rays. At the dose of 2 Gy, the mean number of DSBs per cell was found to be 2.17 DSB per cell after γ-irradiation (18 donors), and 6.45 DSB after carbon irradiation (13 donors). Therefore, the RBE of carbon ions was determined to be approximately 3 times that of γ-rays at the dose of 2 Gy using TC-FISH. These results were confirmed using M-FISH analysis of chromosomal rearrangements, visualized as illustrated in Figure 13B. The number of DSBs per cell using M-FISH analysis was calculated as illustrated in Figure 23; in general, dicentrics and translocations often involve 2 DSBs, whereas CCAs involve at least 3 DSBs of at least 2 chromosomes (Loucas et al., 2013).

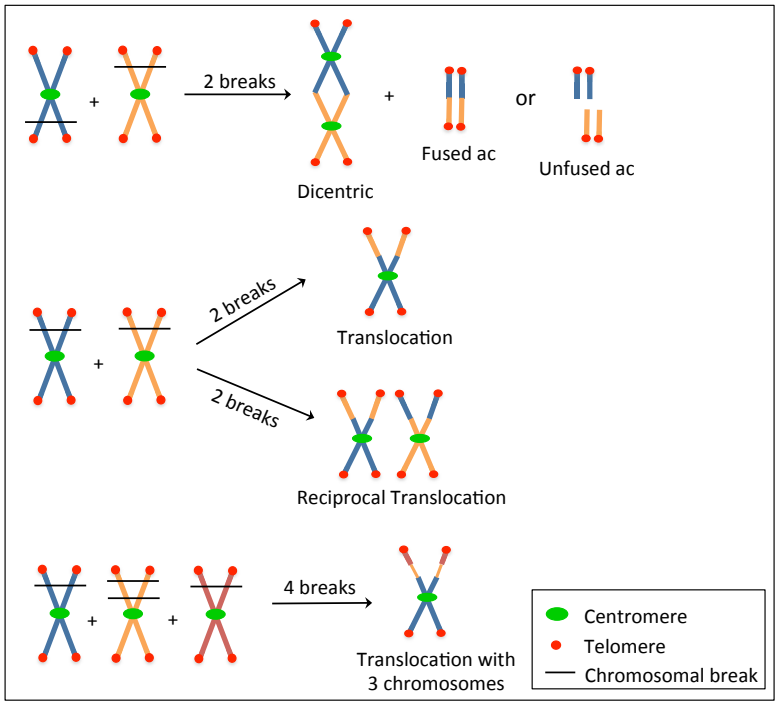

Figure 23. Method of estimating the number of IR-induced DSBs that gave rise to each type of chromosomal aberration using M-FISH. Dicentrics or translocations often involve 2 DSBs. CCAs (e.g. translocations with 3 chromosomes) involve at least 3 DSBs of at least 2 chromosomes.

M-FISH analyses in 4 donors (Donors A, C, L, R) indicated 3.26 DSBs per cell after γ-irradiation and 9.81 DSBs per cell following carbon irradiation. As M-FISH is a more detailed analysis of chromosomal damage compared to TC-FISH (since M-FISH allows analysis of translocations which are not visible with TC-FISH), it is expected that more DSBs per cell be calculated using M-FISH than using TC-FISH. However, as both techniques give an RBE factor of 3 at the dose of 2 Gy, the determination of RBE factor of carbon compared to γ-rays is independent of the method of scoring chromosomal damage. TC-FISH and M-FISH can thus be considered to be two alternative approaches for scoring chromosomal damage. Based on these results, we propose that the TC-FISH technique is more practical for use in radiation dosimetry, as M-FISH is both expensive and time consuming in terms of hybridization technique and analysis compared to TC-FISH.

3.2.4 RBE at various doses: high RBE factors at low doses

To determine RBE at various doses, we compare mean DSBs per cell determined using TC-FISH following exposure to a range of doses (0.2 to 15 Gy) of high-LET carbon ions (75 MeV/u; LET ~36.5 keV/μm at the plateau region of the Bragg peak curve) and low-LET γ-rays in PBL of healthy blood donors. For γ-irradiation at all doses except for 2 Gy

(which is the average of 18 donors; data in Figure 17A), the mean DSBs per cell represent the average of 6 donors (Donors C, F, H, J, K, and O; data in Figure 20B). For carbon irradiation at all doses except for 2 Gy (which is the average of 13 donors; data in Figure 21A), the mean frequencies represent the average of 4 donors (Donors G, H, K, and M).

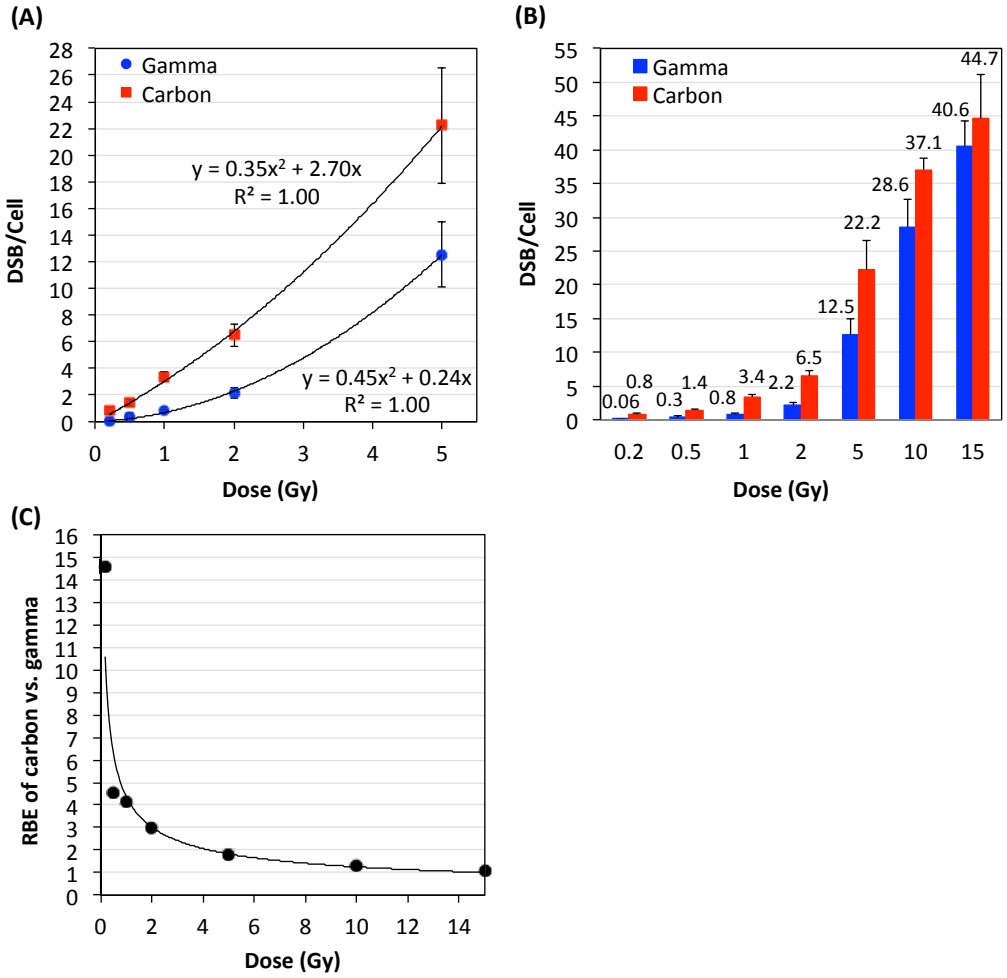

Figure 24. RBE of carbon ions versus γ-rays at different doses. The mean number of DSBs per cell was determined using TC-FISH and plotted versus doses of up to (A) 5 Gy and (B) 15 Gy. The mean DSBs per cell for all donors analyzed are indicated above each bar in (B). Error bars represent the standard deviation of the frequencies of DSBs per cell among the donors. (C) RBE factor of carbon ion versus γ-rays as a function of dose.

Figure 24A shows a plot of the dose (0 to 5 Gy) of γ or carbon irradiation and the mean number of DSBs per cell averaged for all donors analyzed calculated using TC-FISH. This plot indicated second order polynomial trends between the doses of 0 and 5 Gy for both IR types. This plot was expanded to doses of up to 15 Gy in Figure 24B, which shows data for the frequency of DSBs per cell (averaged for all donors analyzed) at each dose with the exact mean indicated above each bar. Error bars in Figure 24A and Figure 24B represent the standard deviation of the frequencies of DSBs per cell among the averaged donors,

illustrating inter-individual variations in radiosensitivity at various doses. As for the RBE calculated at the dose of 2 Gy in Section 3.2.3, RBE factors shown in Figure 24C were calculated by dividing the mean DSBs per cell following a dose of carbon irradiation by the mean DSBs per cell following the same dose of γ-irradiation (values shown in Figure 24B). As shown previously (Friedrich et al., 2014), the RBE factor is dose dependent, with high RBE factors at low doses (0.2 and 0.5 Gy), and an RBE factor approaching 1 at high doses (10 and 15 Gy). It would be interesting to confirm these results using the automated DCScore technique that we discussed above, especially within the low dose range.

3.3 Evaluation of the RBE of protons, and the effect of IR energy on radiosensitivity

As mentioned above, current radiotherapy regimens use photons (either X- or γ-rays) or protons for the treatment of a plethora of malignancies. Proton therapy has been used at ~50 active centers worldwide to treat over 105,000 patients (as of December 2013) (Jermann, 2014). Proton beams, like other charged particles, are characterized by a higher LET than photons, and provide a more localized energy deposition at their Bragg peak, which allows precise targeting of the tumor while limiting IR-induced damages in the surrounding normal tissue. During radiotherapy with proton beams, to treat the entire depth of the tumor, several individual proton beams of different energies (with Bragg peaks at different depths) are applied; the therapeutic radiation distribution of these proton beams optimized for radiotherapy, illustrated in Figure 25A below, is called the spread-out Bragg peak (SOBP).

Despite the comparably large experience in the therapeutic use of protons compared to heavier ions, the differences in biological responses elicited in cells and tissues by protons compared to photons is not yet well established, and large uncertainties can be found in the literature concerning the definition of a RBE–LET relationship for protons. Currently, high-energy protons are considered as a photon-like low-LET IR, and a fixed RBE of 1.1 compared to therapeutic photons is being used in photon therapy for the whole radiation field. While some studies support the idea that this fixed RBE is a reasonable approximation, it remains to be discussed whether the use of a fixed RBE in proton is still appropriate, or whether current knowledge justifies a switch toward a variable RBE, taking into account the dependency on LET, tissue properties, dose, and dose fractionation. Recent studies suggest that the biological response is differentially modulated by protons compared to photons, and thus favors a new approach where high-energy protons should no longer be considered as a photon-like low-LET IR. Additionally, research in the field of medical physics highlights how variations in RBE that are currently neglected might actually

result in deposition of significant doses in healthy organs, particularly for normal tissues in the entrance region and for organs at risk close behind the tumor (Tommasino and Durante, 2015).

In this study, we evaluate the RBE of proton beams of two different energies (73 MeV and 200 MeV) at 3 different positions along the SOBP (Figure 25A) at the dose of 2 Gy. We then compare the effect of IR energy on radiosensitivity by comparing these results with those of γ-rays and carbon-13 ions (75 MeV/u; LET ~36.5 keV/μm at the plateau region of the Bragg peak curve) discussed above (Sections 3.1.1 and 3.2.1).

Results

3.3.1 RBE of 2 Gy of proton irradiation at different locations of the Bragg peak

To evaluate RBE of protons optimized for radiotherapy (SOBP), samples were irradiated with 2 Gy of protons of two different energies (73 MeV and 200 MeV) at 3 different positions along the SOBP (illustrated in Figure 25A): at the entrance of the SOBP (Position A), in the middle of the SOBP (Position B), and at the end of the SOBP (Position C). The PBL of two healthy blood donors of moderate radiosensitivity to γ-rays (Donors H, K) were analyzed using TC-FISH.

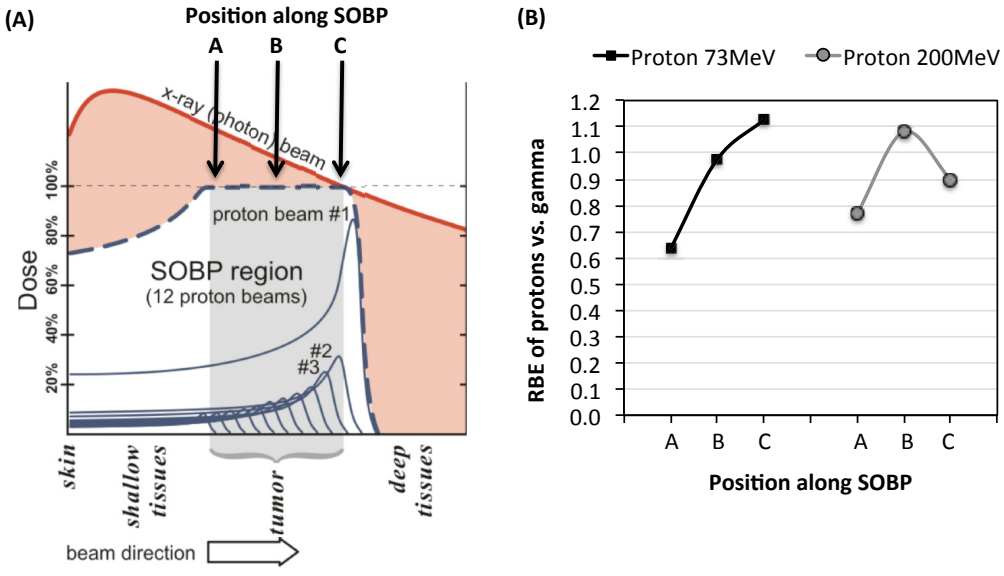

Figure 25. (A) Example of a spread-out Bragg peak (SOBP) used in proton radiotherapy. PBL samples were irradiated with 2 Gy of protons of two different energies (73 MeV and 200 MeV) at 3 different positions along the SOBP: at the entrance of the SOBP (Position A), in the middle of the SOBP (Position B), and at the end of the SOBP (Position C). (B) RBE at the dose of 2 Gy of protons at different locations along the SOBP relative to γ-rays in PBL of two healthy blood donors of moderate radiosensitivity to γ-rays (Donors H, K) analyzed using TC-FISH.

Mean DSBs per cell of these two donors following 2 Gy of proton (73 MeV) irradiation at each position were as follows: 1.39 at Position A, 2.12 at Position B, and 2.45 at Position C. Mean DSBs per cell of these two donors following 2 Gy of proton (200 MeV) irradiation at each position were as follows: 1.68 at Position A, 2.35 at Position B, and 1.95 at Position C. Figure 25B shows the RBE at each position compared to the mean DSBs per cell of these same two donors following 2 Gy of γ-irradiation (2.17 DSBs per cell). As shown in Figure 25B, the RBE is lower at the entrance of the SOBP (Position A) compared to the mid- to end of the SOBP (Positions B and C, respectively) for both proton energy beams, and RBE ranges from 1.0 to 1.1 at the mid-region of the SOBP (Position B). Our data at the mid-region of the SOBP (Position B) of RBE ranging from 1.0 to 1.1 for both proton energy beams are in general agreement of previous studies that find that high-energy protons can be considered as a photon-like low-LET IR in terms of biological effectiveness (Tommasino and Durante, 2015).

3.3.2 Effect of IR energy on radiosensitivity at the dose of 2 Gy

To study the effect of IR energy on radiosensitivity, we compare the effects of γ-rays (0.0013 MeV), carbon-13 ions (75 MeV/u), and protons of two different energies (73 MeV and 200 MeV) in PBL of healthy blood donors using TC-FISH.

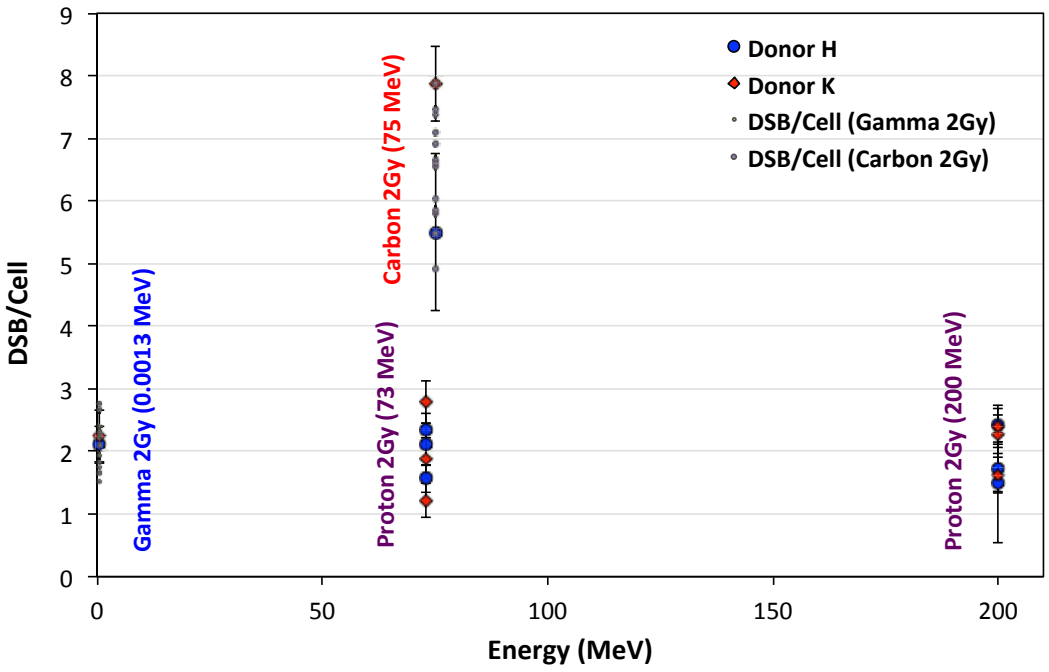

Figure 26. Effect of IR energy on radiosensitivity. The effects of 2 Gy irradiations of γ-rays (0.0013 MeV), carbon-13 ions (75 MeV/u), and protons of two different energies (73 MeV and 200 MeV) were compared in PBL of healthy blood donors using TC-FISH. The three data points shown for each of the donors (Donor H in blue, and Donor K in red) for proton irradiations

represent the DSB per cell at the three positions along the SOBP (data shown in Figure 25B) to illustrate the possible range along the SOBP of proton beams. The relative radiosensitivity of Donors H and K are also highlighted, among the other donors (represented by each of the small gray data points), for γ- and carbon irradiations; each of these points are of the results shown in Figure 17A for γ-irradiation and Figure 21A for carbon irradiation. Error bars represent standard errors.

Figure 26 shows the compiled results shown in previous sections of all analyzed donors for each type of irradiation at the dose of 2 Gy (Figure 17A for γ-irradiation, Figure 21A for carbon irradiation, and Figure 25B for proton irradiations); error bars represent standard errors. Donors H and K are highlighted separately for comparative reference, and results of irradiations at the 3 points along the SOBP of proton beams (Positions A, B, and C; data shown in Figure 25B) are shown for each of the donors to illustrate the possible range along the SOBP. As shown in Figure 26, the two energies of protons (73 MeV and 200 MeV) induce comparable ranges of DSBs per cell as γ-rays (0.0013 MeV) despite the drastic increase in IR energy from that of γ-rays (~1 to 3 DSBs per cell). Carbon ions (75 MeV/u), however, induced an RBE of ~3.00 ± 0.15 compared to γ-rays and the two proton energy beams. These results, though it remains to be confirmed in a larger cohort, suggest that high-energy protons can be considered as a photon-like low-LET IR in terms of biological effectiveness, as previously described (Tommasino and Durante, 2015).

4 - TELOMERES AND THE PREDICTION OF INDIVIDUAL RADIOSENSITIVITY

4.1 Inherent individual variations in telomere length and telomere instability

As discussed in Section 1.1.1, telomere length (TL) varies between individuals and on individual chromosome arms (Pommier and Sabatier, 2002). This inherent heterogeneity of TL is conserved during life as TL in somatic proliferative tissues naturally declines with each cell replication cycle (Graakjaer et al., 2003), and telomere abnormalities and genomic instability may eventually arise. To better characterize the inherent levels of variability in TL and telomere dysfunction in healthy individuals before we study IR-induced effects on these variables, we measure TL and analyze basal levels of telomere dysfunction in metaphasic chromosomes of PBL of healthy individuals following TC-FISH staining.

Results

4.1.1 Inherent individual variations in telomere length

We characterized the inherent differences in TL in PBL of 12 healthy individuals (5 females and 7 males), ranging from age 32 to 57 (mean age of 47).

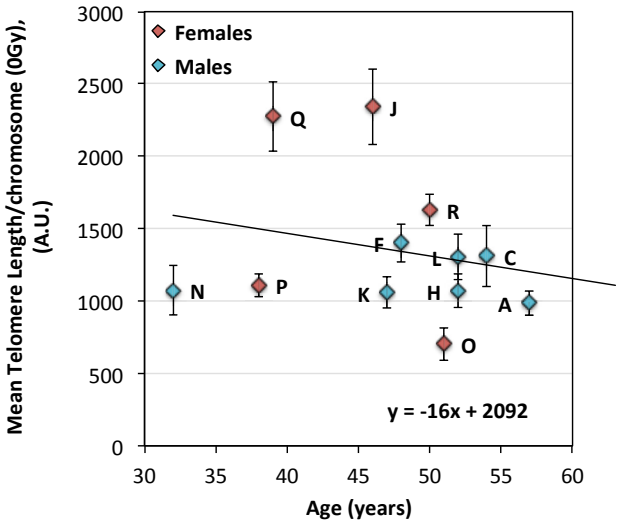

Figure 27. Mean inherent telomere lengths of PBL of 12 healthy individuals in correlation to each individual's age. Telomere lengths were measured as total fluorescence intensity (arbitrary units, A.U.) of telomeres per metaphase following TC-FISH staining, normalized to the number of chromosomes per metaphase. Error bars represent standard error of measurements per donor.

Following TC-FISH staining, metaphases were photographed under 63X objective using the AutoCapt software (MetaSystems), and TL was manually measured as total fluorescence intensity of the telomere probe in each metaphase using the ISIS analysis software (MetaSystems). As TL was measured in terms of fluorescence intensity, results here are given in terms of arbitrary (fluorescence) units (A.U.) instead of the conventional kb measurement. TL per metaphase was normalized to the number of chromosomes per metaphase.

In this cohort of 12 healthy individuals, a wide range in TL was observed, ranging from 703 A.U. to 2343 A.U. and a mean TL of 1356 A.U. ± 502 (standard deviation). The correlation of inherent TL with age is shown in Figure 27. A general trend of decreasing TL with increasing age is observed (with a decrease by 16 A.U. per year), as would be expected since TL in somatic cells naturally declines with each cell replication cycle (Harley et al., 1990) due to the incomplete replication of telomere ends by conventional DNA polymerases, a situation known as the 'end replication problem' (de Lange, 2009). For the 5 females analyzed (age range of 38 to 51, mean age of 45), the mean TL was 1612 A.U. ± 717 (standard deviation), whereas mean TL was found to be 1173 A.U. ± 162 (standard deviation) for the 7 males analyzed (age range of 32 to 57, mean age of 49). Despite the higher mean age of the males, females showed longer TL than males, which is in agreement with recent findings of TL analyses of a large cohort of 110,266 individuals (Lapham et al., 2015). Furthermore, the variability in TL within the male group was significantly less than in the female group, as illustrated by the standard deviation values (162 for males vs. 717 for females). Though the size of this cohort limits the power of this study on the effect of gender on TL, we speculate that the more homogenous TL in the male group can be attributed to the steady decrease in TL observed in males from young adulthood to approximately the age of 75, as found in (Lapham et al., 2015). Females, however, were shown to exhibit a change in TL patterns around the age of 50 (Lapham et al., 2015); though we measured TL in only 5 females in this study, as the mean age of these 5 females was 45, we can speculate that the large heterogeneity in TL observed can be attributed to the age-related changes in TL that are taking place around this age.

4.1.2 Basal individual variations in telomere instability

To assess variations in basal levels of telomere abnormalities, we also quantified levels of telomere loss of 1 telomere or of 2 telomeres (from both sister chromatids) and doublets using TC-FISH (as shown in Figure 28A) in a separate cohort of 35 healthy individuals (age range of 23 to 58, mean age of 39.5); this study was an expansion of the data included in **our original paper**, (Pottier et al., 2013) found in Appendix A.3.4 of this thesis, which included this analysis for 20 healthy individuals. To evaluate inter-scorer variability in the scoring of each type of telomere abnormality via TC-FISH analysis, the same images were scored by 3 independent scorers in the laboratory.

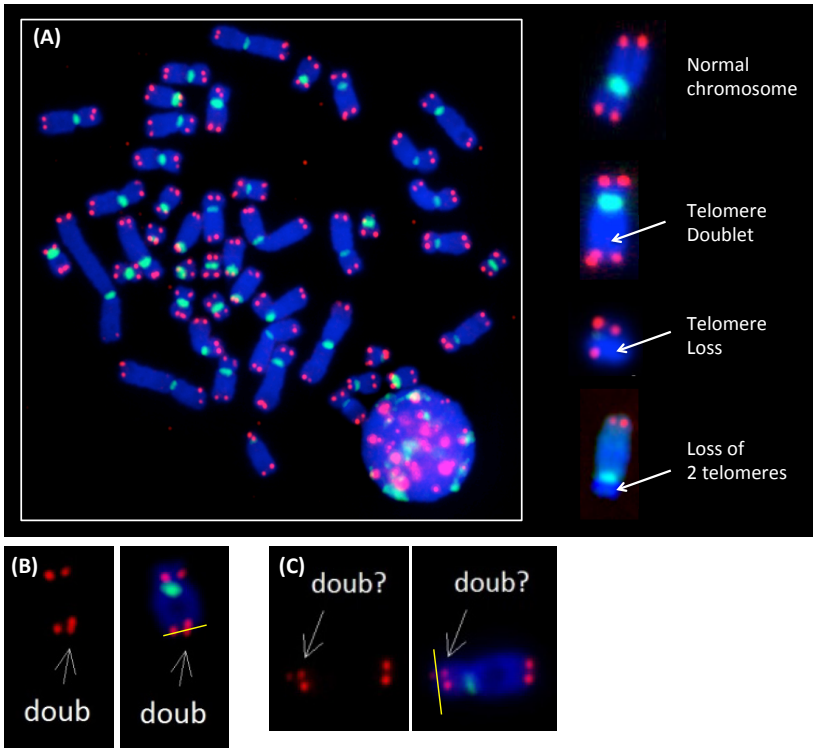

Figure 28. (A) Types of telomere abnormalities (telomere doublets, or loss of 1 or 2 telomeres) visualized with TC-FISH staining. Two examples of difficulties that may arise in interpreting fluorescence signals in the image as duplicated (doublet) are shown in (B) and (C). (B) The doublet signal is on the border of the end of the chromosome (marked by the yellow line), as seen with DAPI counterstaining of the DNA. (C) The doublet signal is slightly separated from the other telomere signal, and placed slightly away from the end of the chromosome (yellow line). Whether the scorer counts these as doublets or not is left to the scorer's discretion; this is a source of inter-scorer variability in the frequency of these telomere abnormalities.

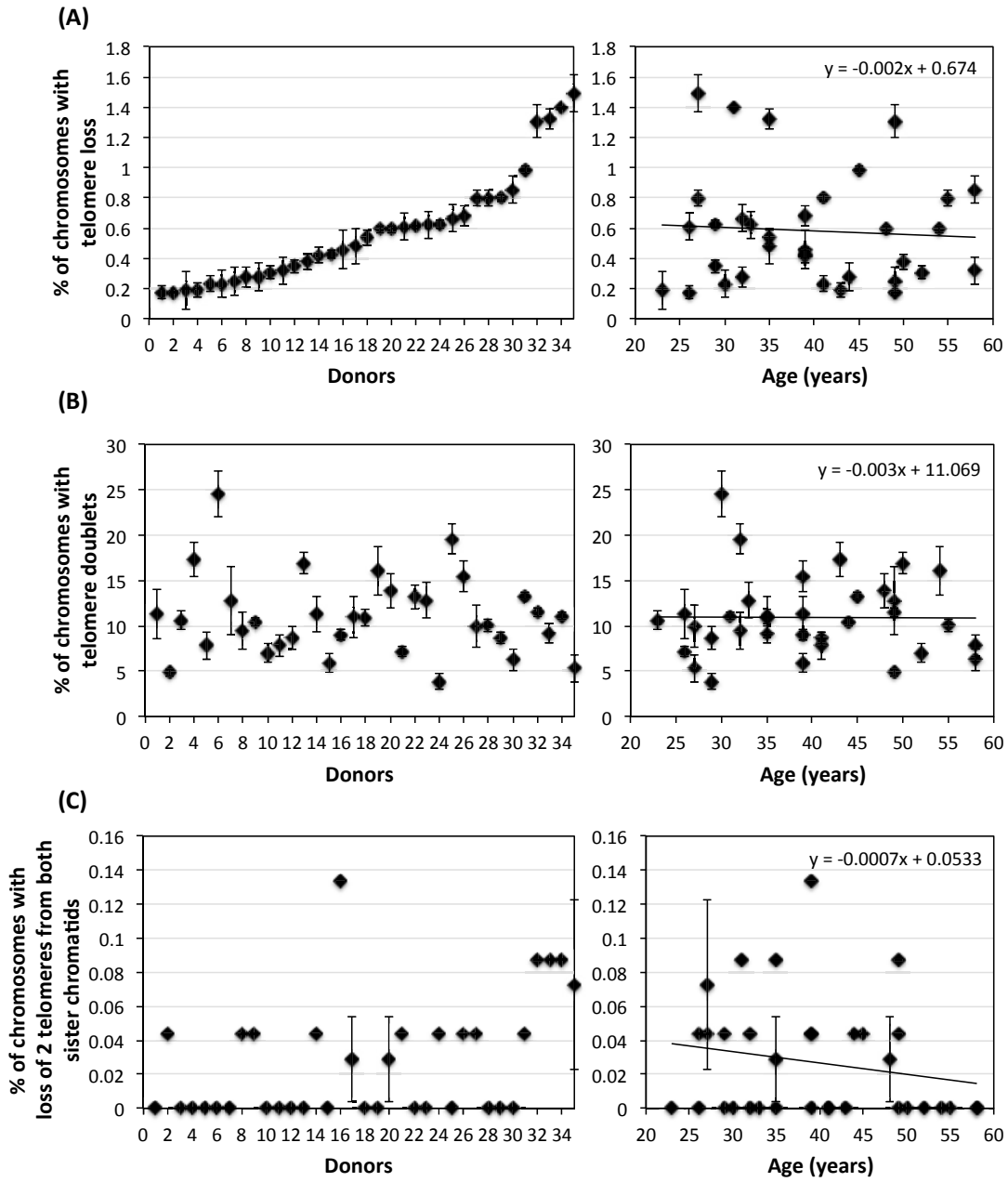

Figure 29. Basal levels of telomere abnormalities in PBL of 35 healthy individuals, analyzed by 3 independent scorers using TC-FISH staining as shown in Figure 28A. Basal levels of (A) telomere loss, (B) telomere doublets, and (C) loss of 2 telomeres from both sister chromatids in increasing order of telomere loss, and their respective correlations with age. Error bars indicate inter-scorer variability in scoring each type of telomere abnormality.

As shown in Figure 29, there is a large range of variation in basal levels of telomere abnormalities in human PBL. Within this cohort of 35 healthy individuals, a ~8 fold difference in basal levels of telomere loss (Figure 29A) and a ~5 fold difference in basal levels of telomere doublets (Figure 29B) is observed. Despite this large inter-individual variability, telomere doublets are, on average, the most frequently observed type of telomere abnormality, found in ~11% of chromosomes; telomere loss occurs at ~0.6% of

chromosomes, and loss of 2 telomeres from both sister chromatids occur at only ~0.03% of chromosomes. These basal levels of telomere abnormalities do not appear to be correlated with age, as illustrated by the lack of any trend in the respective plots in Figure 29. We hypothesize that though inherent telomere length is strongly influenced by age (Figure 27), basal levels of telomere instability are related to confounding factors such as lifestyle (Lin et al., 2012;Price et al., 2013).

In our original paper, (Pottier et al., 2013) found in Appendix A.3.4 of this thesis, we found that in B3 cells (isolated from the human EJ30 bladder cell carcinoma cell line), telomere abnormalities following *in vitro* exposure to lead (Pb) in the form of lead nitrate ($Pb(NO_3)_2$) arose due to Pb-induced TIFs, which are formed when DNA repair machinery (e.g. γH2AX) recognize short or dysfunctional telomeres (uncapped or damaged telomeres) as DSBs, thus leading to γH2AX localization at these (intact) telomeres. The formation of TIFs at these intact telomeres likely leads to their loss due to perturbations of telomere replication (Pottier et al., 2013). Whether this same mechanism is true in normal lymphocytes remains to be determined. It would be interesting to investigate further the inter-individual variations in the basal levels of TIFs in lymphocytes of healthy individuals to determine whether correlations exist with levels of telomere abnormalities, as seen following Pb exposure in (Pottier et al., 2013).

In addition to the above analysis, we also evaluated the reproducibility of scoring telomere abnormalities using TC-FISH. To assess inter-scorer variability, the gallery of TC-FISH images (comprised of 50 metaphases for each of the 35 donors, for which results are shown in Figure 29) were scored by 3 independent scorers in the laboratory. As shown by the error bars in Figure 29, the scoring of telomere abnormalities using TC-FISH may produce inter-scorer variability. This is especially evident in the scoring of the loss of 2 telomeres from both sister chromatids (Figure 29C) and, to a lesser extent, the scoring of telomere doublets (Figure 29B). As the manual scoring of telomere abnormalities of TC-FISH stained metaphases requires visualization of every telomere on every chromosome in the metaphase, this inter-scorer variability can be attributed to either incomplete visualization of all the abnormalities in the metaphase, or the difficulties of interpreting fluorescence signals in the image as either missing (for the case of telomere loss) or duplicated (for the case of telomere doublets). Two examples of such are illustrated in Figure 28B and Figure 28C; whether the scorer counts these as doublets or not is left to the scorer's discretion, thus becoming a source of inter-scorer variability in the frequency of these telomere abnormalities. Consequently, it may be required for multiple scorers to verify the analysis of telomere abnormalities using TC-FISH. This complication may be resolved with the development of automated software for TC-FISH analysis of telomere abnormalities.

4.2 Telomere length as a predictor of short-term radiosensitivity to γ-irradiation

In this study, we evaluate whether individual radiosensitivity to the therapeutic dose of 2 Gy of low-LET γ-rays (described previously in Section 3.1.1 and presented in Figure 17A of this thesis) can be predicted by a single or combination of variables, such as age, gender, inherent and IR-induced changes in telomere length (TL). For this discussion, we consider 'radiosensitivity' solely in terms of the mean number of IR-induced DSBs per cell, as described in Section 3.1.1. As plotted in Figure 17A, radiosensitivity to 2 Gy of *in vitro* γ-irradiation of PBL isolated from whole blood samples of 18 healthy individuals was plotted in order of increasing DSBs per cell using TC-FISH analysis, as illustrated in Figure 16, and individuals were designated as Donors A through R in this order of 'radioresistant' to 'radiosensitive' donors.

In this section, using the Stata software, we estimate linear regression equations of various combinations of variables with the ordinary least squares (OLS) method to estimate whether radiosensitivity can be predicted by these variables. Linear regression equations are of the following general format:

$$y = \alpha + \beta_1 x_1 + \beta_2 x_2 + \ldots$$

Equation 1. General linear regression equation.

In this general equation (Equation 1), y is the dependent variable that is being predicted or explained, and the x variables are the independent variables that are being used to predict the y variable. α is the constant or y-intercept, or the expected effect if all independent variables equal zero, and each β coefficient is the slope (or the expected *extent* of effect on the y variable) for each corresponding x variable.

For our study, the y variable is the radiosensitivity to 2 Gy of γ-rays (simplified to the variable $RS2g$). To simply discussion of each x variable in the following sections, we define each of the variables of interest below:

- Age (in years)
- Sex_{Male} (gender of the individual is denoted as either 'male' or 'not male' in the regression)
- $TL0$: inherent telomere length (0 Gy), shown in Figure 27 to be correlated with age
- $TL2g$: telomere length following 2 Gy γ-irradiation
- ΔTLg, or the change in telomere length after 2 Gy γ-irradiation, was calculated from $TL0$ and $TL2g$ as follows: $\Delta TLg = TL2g - TL0$

Results

4.2.1 Age and gender significantly predict radiosensitivity

To determine whether age and gender can be used to predict $RS2g$ in this cohort of blood donors, we estimate Equation 2 with the ordinary least squares (OLS) method. The results of the regression in Equation 2 are reported in Table 4.

$$RS2g = \alpha + \beta_1(Age) + \beta_2(Sex_{Male})$$

Equation 2. Linear regression equation to determine effects of age and gender on the prediction of radiosensitivity to 2 Gy γ-irradiation. Results are reported in Table 4.

Table 4. Results of the linear regression in Equation 2: effects of age and gender on the prediction of radiosensitivity to 2 Gy γ-irradiation‡‡‡‡.

Explanatory Variable		(1)	(2)	(3)
Age	β_1 :	-0.026** (-2.184)	---	-0.029**** (-3.121)
Sex_{Male}	β_2 :	---	-0.425*** (-2.431)	-0.465**** (-3.332)
Constant	α :	3.413 (5.921)	2.419 (18.055)	3.822 (8.270)
Adjusted R^2		0.191	0.235	0.516
N		17	17	17

β coefficients are given for each variable, and the t-statistics are reported in parentheses under each β coefficient. *, **, ***, **** correspond to p-values < 10%, 5%, 1%, 0.1%, respectively. Each column corresponds to a separate regression.

‡‡‡‡ In these regression tables, each column corresponds to a separate regression. For example, Column (1) presents the prediction of $RS2g$ in Equation 2 using age alone as the independent variable. Column (2), in turn, presents the prediction of $RS2g$ using gender alone, while Column (3) takes into account both age and gender to predict $RS2g$. β coefficients are given for each variable, and the t-statistics are reported in parentheses under each β coefficient. The sign on the β coefficient (positive or negative) indicates the direction of the effect: a positive coefficient indicates how much the $RS2g$ is expected to increase when that independent variable increases by one, holding all the other independent variables constant. Adjusted R^2 values indicate R^2 values adjusted to reflect the number of variables in the equation, and N is the number of donors analyzed.

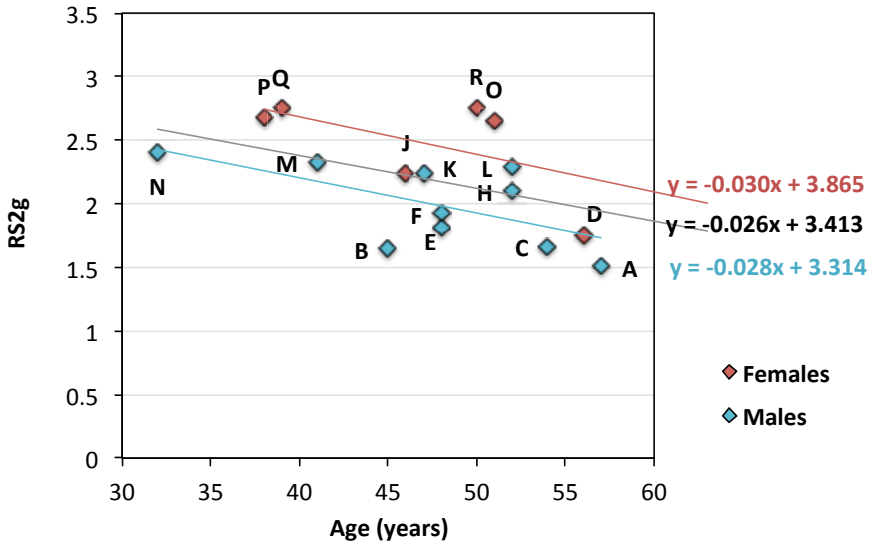

Figure 30. Correlations between *Age* and *RS2g*. The gender of each individual is also indicated.

As shown in Column (1), age alone is a significant predictor of $RS2g$ ($p<0.05$). The correlation between age and $RS2g$ per donor is also illustrated in Figure 30; it is notable that the equation to predict $RS2g$ in terms of age alone (both genders) in Figure 30, $y = -0.026x+3.413$, corresponds to the results of the regression in Column (1) of Table 4, with the constant (α variable) of 3.413 and a β coefficient (or slope) of -0.026. As shown in Figure 30, females in this cohort are slightly more radiosensitive compared to males of the same age. However, age-related decline in radiosensitivity in males and females each exhibit almost parallel slopes to the mean of this cohort, with β coefficients of -0.028 (in males) and -0.030 (in females).

As shown in Column (2) of Table 4, gender alone is also a significant predictor of $RS2g$ ($p<0.01$). It is notable that though age is a significant predictor of $RS2g$, gender alone is a significantly stronger predictor of $RS2g$ than age alone, as illustrated by the β coefficients of -0.425 for gender alone vs. -0.026 for age alone; thus, we can say that in comparison to the effect of gender on $RS2g$, the effect of age on $RS2g$ is almost negligible. This is also illustrated the β coefficients in the regression of age and gender together (-0.029 and -0.465, respectively), as shown in Column (3) of Table 4, which was the strongest predictor of $RS2g$ ($p<0.001$). Overall, age and gender are significant predictors of radiosensitivity to 2 Gy of γ-irradiation.

4.2.2 *Inherent telomere length in conjunction with change in telomere length following γ-irradiation significantly predicts radiosensitivity*

As discussed in Section 4.1.1 and presented in Figure 27 of this thesis, TL was measured following TC-FISH staining as total fluorescence intensity of telomeres (arbitrary units, A.U.) per metaphase, which was normalized to the number of chromosomes per metaphase. A wide range in TL was observed in this cohort of 12 healthy individuals (5 females and 7 males), ranging from age 32 to 57 (mean age of 47), and inherent TL ($TL0$) in this cohort of blood donors decreased (by 16 A.U. per year) with increasing age, as expected (Figure 27).

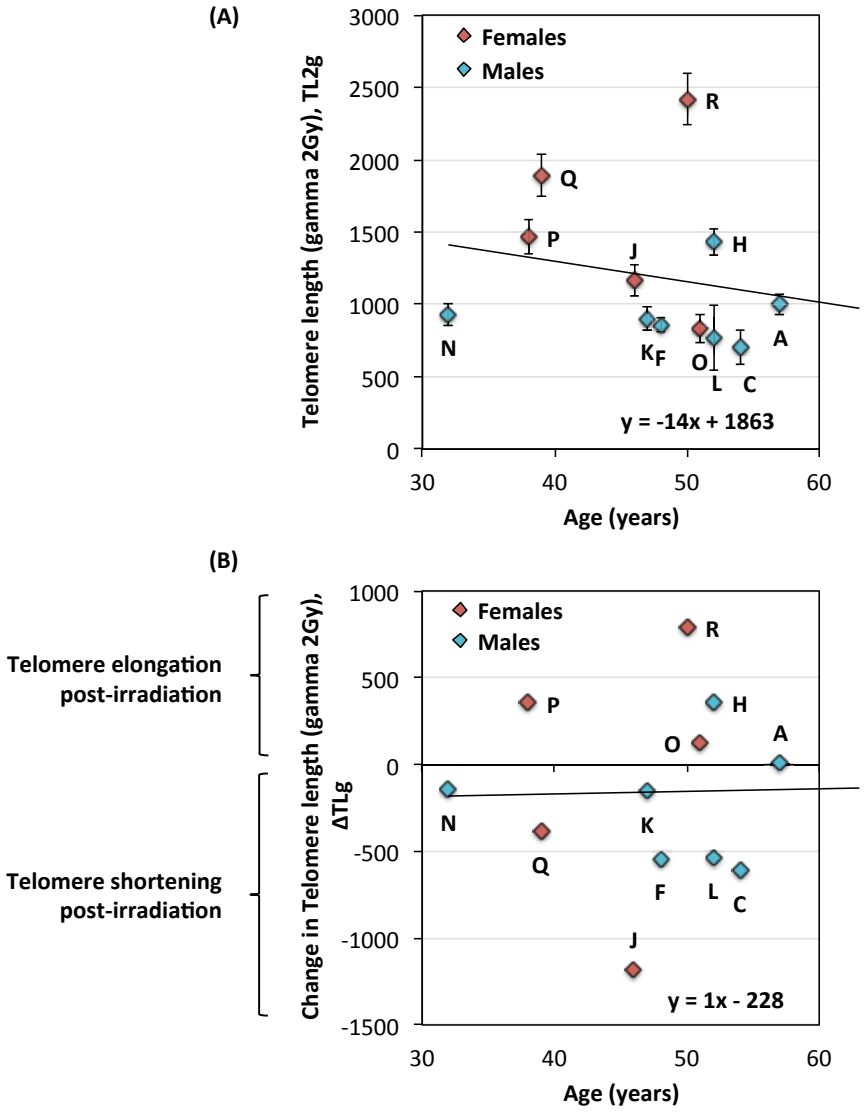

Figure 31. Mean TL after exposure to 2 Gy of γ-irradiation in PBL of 12 healthy individuals in correlation to each individual's age. TL was measured as total fluorescence intensity of telomeres per metaphase following TC-FISH staining, normalized to the number of chromosomes per metaphase. Error bars represent standard error of measurements per donor. (A) TL measured after exposure to 2 Gy of γ-irradiation ($TL2g$) shows an age-dependent

decrease, decreasing at a rate of 14 A.U. per year. (B) Though there is no age-related trend in the change in TL following exposure to 2 Gy of γ-irradiation (ΔTLg), there is an overall shortening of TL post-irradiation.

As shown in Figure 31A, TL measured after exposure to 2 Gy of γ-irradiation ($TL2g$) also shows an age-dependent decrease at a rate of 14 A.U. per year. Though there is no age-related trend in the change in TL following exposure to 2 Gy of γ-irradiation (ΔTLg) (as shown by the horizontal slope of 1 in Figure 31B), there is an overall shortening of TL post-irradiation in this cohort.

To determine whether inherent and post-irradiation TL ($TL0$ and $TL2g$, respectively) and IR-induced changes in TL after 2 Gy γ-irradiation (ΔTLg) can be used to predict $RS2g$ in this cohort of blood donors, we estimate Equation 3 with the ordinary least squares (OLS) method. The results of the regression in Equation 3 are reported in Table 5.

$$RS2g = \alpha + \beta_1(\Delta TLg) + \beta_2(TL0) + \beta_3(TL2g)$$

Equation 3. Linear regression equation to determine effects of telomere length on the prediction of radiosensitivity to 2 Gy γ-irradiation. Results are reported in Table 5.

Table 5. Results of the linear regression in Equation 3: effects of telomere length on the prediction of radiosensitivity to 2 Gy γ-irradiation.

Explanatory Variable		(1)	(2)	(3)	(4)
ΔTLg	β_1 :	0.284 (1.235)	---	0.489** (2.017)	---
$TL0$	β_2 :	---	0.181 (0.707)	0.439* (1.704)	---
$TL2g$	β_3 :	---	---	---	0.467** (2.276)
Constant	α :	2.315 (18.840)	2.024 (5.502)	1.751 (5.015)	1.710 (6.421)
Adjusted R^2		0.046	-0.048	0.198	0.275
N		12	12	12	12

β coefficients are given for each variable, and the t-statistics are reported in parentheses under each β coefficient. *, **, ***, **** correspond to p-values < 10%, 5%, 1%, 0.1%, respectively. Each column corresponds to a separate regression. β coefficients for ΔTLg and $TL0$ were scaled by a factor of 1000 to account for differences in magnitude within the data. Actual β coefficients are the above given number $\times 10^{-3}$.

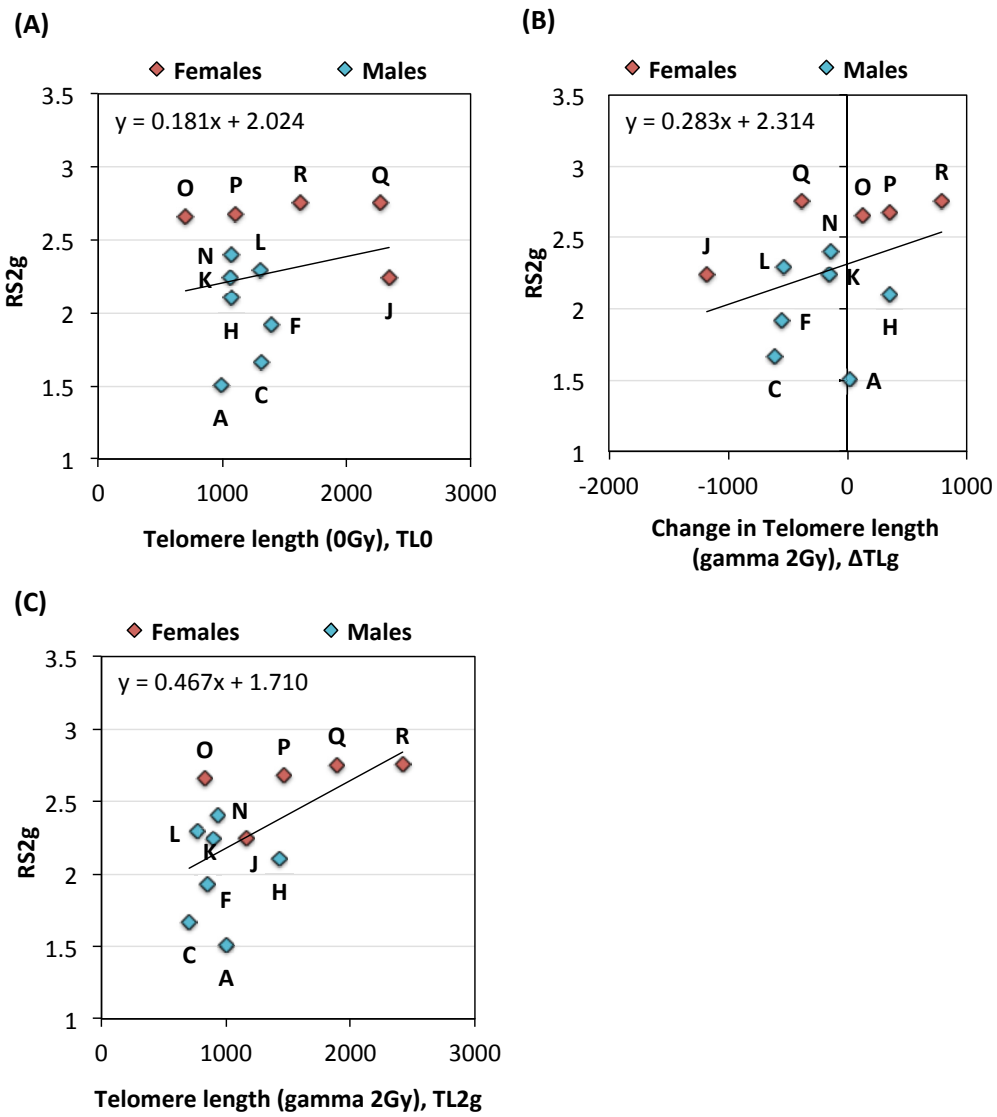

Figure 32. (A) $TL0$ and (B) ΔTLg alone do not predict $RS2g$. However, the regression (shown in Table 5 Column (3)) shows that ΔTLg and $TL0$ *together* is a strong predictor of $RS2g$. (C) $TL2g$ alone was shown to be a strong predictor of $RS2g$.

As shown in Column (1) and (2) respectively, ΔTLg and $TL0$ alone do not predict $RS2g$; this is also illustrated in Figure 32A and B. However, as shown in Column (3), ΔTLg and $TL0$ ***together*** was shown to be a strong predictor of $RS2g$, with β coefficients of 0.489 ($p<0.05$) and 0.439 ($p<0.10$), respectively. Additionally, $TL2g$ alone was shown to be a strong predictor of $RS2g$ ($p<0.05$) as shown in Column (4) in Table 5 and in Figure 32C. These preliminary results require further validation in a larger cohort of individuals characterized with extreme telomere lengths using other standard techniques of measuring TL (e.g. terminal restriction fragment [TRF] or Q-FISH).

4.2.3 *Radiosensitivity differentially affects IR-induced changes in telomere lengths in cells with the shortest mean telomere lengths*

Interestingly, though ΔTLg, or the changes in *mean* TL following γ-irradiation, did not correlate with $RS2g$ (Column (1) in Table 5 or Figure 32B), slight correlations between $RS2g$ and changes in TL in cells with the *shortest* mean TL is suggested, as shown in Figure 33.

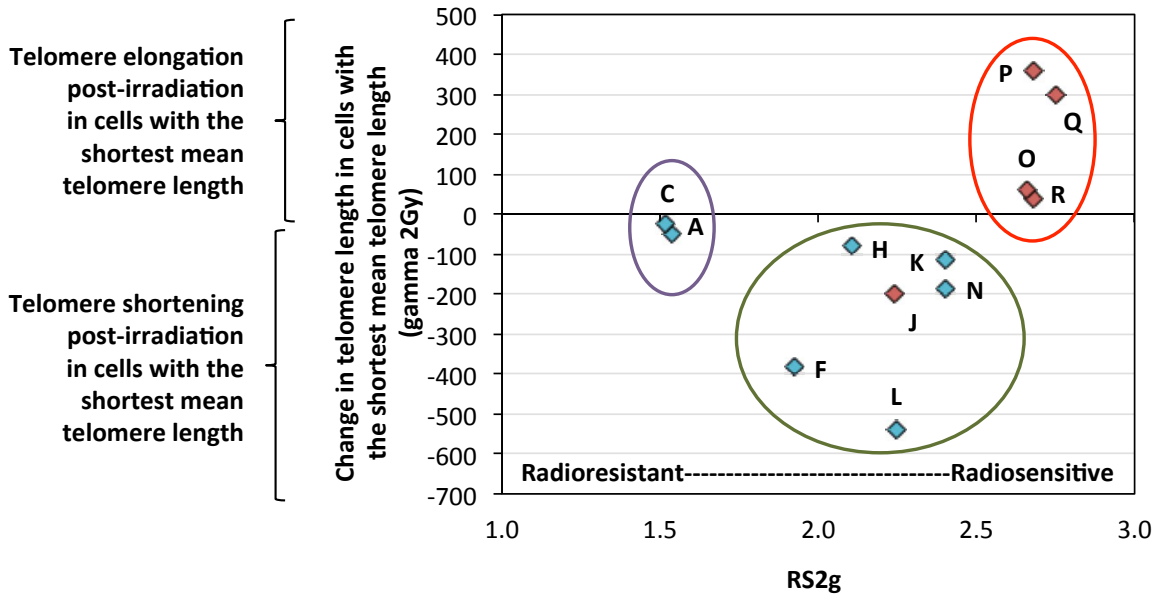

Figure 33. Slight correlations between $RS2g$ and IR-induced changes in TL in cells with the *shortest* mean TL. Radioresistant donors (Donors A and C) show little changes in TL following irradiation, whereas radiosensitive donors (Donors O, P, Q, R) exhibit elongation in these cells. Donors of medium radiosensitivity exhibit telomere shortening in the cells with the shortest mean TL.

Radioresistant donors (Donors A and C) show little changes in TL in cells with the shortest mean TL following irradiation, while radiosensitive donors (Donors O, P, Q, R) exhibit elongation in these cells. Donors of medium radiosensitivity, on the other hand, exhibit telomere shortening in cells with the shortest mean TL. Indeed, a recent clinical study found that while mean TL was not affected in peripheral leukocytes from patients after *in vivo* radiation treatment with a mean dose of 52 Gy, there was a significant decrease in the proportion of cells with short telomeres (Maeda et al., 2013). An *in vitro* study of changes in TL (assessed using the traditional TRF analyses) over the course of 4 days after X-ray irradiation (0.5 Gy) in normal human umbilical vein endothelial cells also found changes in TL distribution post-irradiation; in the irradiated cells, in the first 3 days post-irradiation, no significant telomere shortening of mean TRF length was found, but a decrease in the percentage of longer telomeres along with an increased percentage of the shortest

telomeres was demonstrated. These results suggest that the shortest telomeres are more sensitive to IR than longer telomeres (Guan et al., 2014).

Though further studies are needed to verify our observations in this cohort, we speculate that our findings could be related to excessive IR-induced oxidative stress and the differential sensitivity of telomeres of different lengths to oxidative stress, as hypothesized by the authors of Guan *et al* (Guan et al., 2014). Less oxidative stress may be induced in radioresistant individuals compared to radiosensitive individuals, which may correlate with the decreased frequency of DNA damage (DSBs) found in radioresistant individuals (Figure 17A). The increased levels of oxidative stress in radiosensitive individuals may cause excessive genomic damages that leads to senescence or apoptosis, which inflicts cells with the shortest mean telomeres first, and thereby leads to their loss from the cell population; we speculate that the apparent telomere elongation post-irradiation in radiosensitive individuals (Figure 33) could be due to the lack of the inclusion of these cells that underwent senescence or apoptosis. Another explanation for these findings could be related to varying levels of activation of telomerase activity in individuals of different radiosensitivity. Inherent telomerase activity in radioresistant donors (which may protect against IR-induced changes in TL) may in fact explain their radioresistance, as ectopic over-expression of telomerase in a human fibroblast cell line was previously shown to be associated with unusual spontaneous and IR-induced chromosome stability (Pirzio et al., 2004). Meanwhile, we hypothesize that activation of telomerase (thereby resulting in telomere elongation) infers increased radiosensitivity, whereas the lack thereof explains the telomere shortening observed in moderately radiosensitive individuals.

5 - ROLE OF TELOMERES IN LONG-TERM HUMAN HEALTH RISKS AFTER RADIATION EXPOSURE

5.1 Telomere length as a predictor of cardiovascular disease

Cardiovascular disease is well observed following IR exposure to the chest or heart (such as during radiotherapy for breast cancer, Hodgkin's lymphoma, or head and neck cancer). Indeed, excess risk of cardiovascular and cerebrovascular diseases is proven following an acute dose of as low as 0.5 Gy (500 mSv) (Schultz-Hector and Trott, 2007;Bhatti et al., 2008;Little et al., 2008;Baker et al., 2011). Most of the risk of developing cardiovascular disease could be accounted for by classical risk factors such as hypertension, smoking, dyslipidemia, age, and family history. However, wide variations are seen in both the occurrence of cardiovascular disease and the age of manifestation, even in individuals with the same classical risk factors. Though the reasons for this variability are unclear, it has been proposed that it is due to differences in the rate of biological aging. Aging is indeed a major risk factor of atherosclerosis, which is a common underlying cause of cardiovascular diseases, and aging-related endothelial dysfunction has been proposed to be the link between these variables. Endothelial dysfunction can arise due to constant bombardment of endothelial cells by atherogenic stimuli (e.g. elevated plasma cholesterol level, hypertension, diabetes, smoking). Endothelial dysfunction has been shown to be of central importance in the development and progression of atherosclerosis. Continuous mechanical, hemodynamic, and/or immunological damage (probably involving oxidative stress) to vascular endothelial cells during the progression of atherosclerosis may cause increased localized cellular turnover, leading to cellular senescence, myocardial cell death, or fibrosis (Schultz-Hector and Trott, 2007;Little et al., 2008;Sabatino et al., 2012;Shah and Mahmoudi, 2015).

Telomere shortening has been shown to occur in human vascular tissue, which may be related to age-associated vascular disease. Telomeres have also been linked to several factors that influence cardiovascular risk (e.g. hypertension, diabetes, estrogens, oxidative stress, psychological stress), neovascularization, atherosclerosis, and heart disease. Furthermore, genomic instability may play a crucial role in the onset of atherosclerotic events (Balasubramanyam et al., 2007;Lin et al., 2012;Sabatino et al., 2012); a recent study showed that accelerated vascular aging and early atherosclerosis can be associated with telomere shortening, genomic instability, and deficient DNA repair capacity following chronic exposure to low doses of IR in catheterization laboratory personnel (Andreassi et al., 2015). However, additional studies are needed to clarify the link between IR-induced telomere

shortening and the development/progression of cardiovascular and other vascular effects (Sabatino et al., 2012).

Hodgkin lymphoma is a malignant hematological disease that predominantly affects young patients. Despite the very high cure rate of this cancer using radiotherapy and chemotherapy (Specht et al., 2014), it is associated with low long-term survival rates due to non-cancer related secondary complications (such as cardiovascular diseases), as well as secondary cancers, long after being cured of their initial disease (Castellino et al., 2011). In this study, presented in **our recent paper** (M'Kacher et al., 2015b), we evaluate telomere length (TL) in PBL of 179 Hodgkin lymphoma patients that were treated with radiotherapy (and chemotherapy) and cured of their cancer, and investigate if TL can be correlated with the development of cardiovascular disease in this subset of patients long after their treatment. Other conventional prognostic factors investigated are described in detail in (Girinsky et al., 2014). Our study is the first to demonstrate the major role of telomeres in the occurrence of cardiovascular disease in a population exposed to IR for medical purposes.

5.1.1 Summary of key results

- This study included 179 Hodgkin lymphoma patients that were treated with radiotherapy (and chemotherapy in 173 of these patients) at a median age of 29 (range of 9 to 75) and cured of their cancer. Evidence of cardiovascular disease was evaluated with coronary computed tomography angiography (CCTA). CCTA was performed in these patients at a median age of 42 (range of 19 to 79), which is a median of 13 years after the treatment that cured their Hodgkin lymphoma.
- TL was measured following quantitative fluorescent *in situ* hybridization (Q-FISH) of metaphases of PBL with a telomere-specific Cyanine3-labeled PNA probe, and quantitative image acquisition and analysis using MetaCyte software (MetaSystems); blood samples for TL analysis were obtained from patients before their CCTA procedure. I aided in the cell culture, sample processing and hybridization, and image acquisition of this analysis.
- Comparisons of TL in Hodgkin lymphoma patients with cardiovascular disease (abnormal CCTA) vs. patients with no evident cardiovascular disease indicated that patients with cardiovascular disease have significant telomere shortening: mean TL of 7.1 kb in patients with cardiovascular disease (mean age 48.5; 41 patients) vs. 7.9 kb in patients with no evident cardiovascular disease (mean age of 40.9; 125 patients).

- Patients with no evident cardiovascular disease had higher heterogeneity in mean TL (range of TL of 4.7 to 11.1 kb) compared to patients with cardiovascular disease (range of TL of 4.8 to 8.7 kb); this may be explained by short period of follow-up of some patients or possibly the occurrence of another complication (e.g. secondary cancer).
- Univariate and multivariate analysis of conventional risk factors confirmed the significance of well-known prognostic factors of cardiovascular disease (e.g. hypertension, hypercholesterolemia, age at treatment, radiation dose to coronary artery origins).
- Univariate analysis of *less conventional* risk factors, e.g. telomere length, showed that TL was a highly significant risk factor (p=0.006).
- A multivariate analysis of *all* risk factors, including TL, found that only hypertension (p=0.007) and TL (p=0.03) were significant prognostic factors.
- This study provides additional evidence that TL could be linked to inter-individual sensitivity to IR and other genotoxic agents.
- These findings support the hypothesis that telomere shortening may represent an important mediator between IR exposure and vascular damage, and could be used to define new radiation protection strategies. As this study supports the quantification of telomeres as a prognostic factor of cardiovascular risk of population exposed to IR, this will require the development of a clinical method to measure telomere length.

Radiation Protection Dosimetry (2015), Vol. 164, No. 1–2, pp. 134–137 doi:10.1093/rpd/ncu296
Advance Access publication 1 October 2014

TELOMERE SHORTENING: A NEW PROGNOSTIC FACTOR FOR CARDIOVASCULAR DISEASE POST-RADIATION EXPOSURE

R. M'kacher[1,2,*], T. Girinsky[3], B. Colicchio[4], M. Ricoul[1], A. Dieterlen[4], E. Jeandidier[5], L. Heidingsfelder[6], C. Cuceu[1], G. Shim[1], M. Frenzel, A. Lenain[1], L. Morat[1], J. Bourhis[2,3,4,5], W. M. Hempel[1], S. Koscielny[7], J. F. Paul[8], P. Carde[9] and L. Sabatier[1]
[1]Laboratory of Radiobiology and Oncology, CEA, DSV/iRCM, Fontenay-aux-Roses 92265, France
[2]Laboratory of Radiation Sensitivity and Radio-carcinogenesis INSERM 1030, Institut Gustave Roussy, Villejuif 94 804, France
[3]Department of Radiation Oncology, Institut Gustave Roussy, Villejuif 94 804, France
[4]Laboratoire MIPS – Groupe TIIM3D, Université de Haute-Alsace, Mulhouse Cedex F-68093, France
[5]Department of genetics, CHU, Mulhouse Cedex 68093, France
[6]MetaSystems GmbH, Robert-Bosch-Str. 6, Altlussheim D-68804, Germany
[7]Biostatistics and Epidemiology Unit, Institut Gustave Roussy, Villejuif 94 804, France
[8]Department of Radiology, Marie Lannelongue, Chatenay-Malabry 92019, France
[9]Department of hematology, Institut Gustave Roussy, Villejuif 94 804, France

*Corresponding author: radhia.mkacher@cea.fr and Radhia.mkacher@gmail.com

Telomere length has been proposed as a marker of mitotic cell age and as a general index of human organism aging. Telomere shortening in peripheral blood lymphocytes has been linked to cardiovascular-related morbidity and mortality. The authors investigated the potential correlation of conventional risk factors, radiation dose and telomere shortening with the development of coronary artery disease (CAD) following radiation therapy in a large cohort of Hodgkin lymphoma (HL) patients. Multivariate analysis demonstrated that hypertension and telomere length were the only independent risk factors. This is the first study in a large cohort of patients that demonstrates significant telomere shortening in patients treated by radiation therapy who developed cardiovascular disease. Telomere length appears to be an independent prognostic factor that could help determine patients at high risk of developing CAD after exposure in order to implement early detection and prevention.

INTRODUCTION

Recent epidemiological studies have documented vascular and cardiovascular effects following exposure to radiation at doses much lower than those normally associated with cardiac injury when the irradiation is localised to the mediastinal field[1, 2]. According to the International Commission on Radiological Protection[3], excess cardiovascular risk has been proven with a threshold acute dose of ~0.5 Gy for both cardiovascular and cerebrovascular diseases[4]. In addition, several cardiovascular risk factors that could potentially account for most of the risk for coronary heart disease in a population[5] were proposed. At the individual level, there is wide variation in both the occurrence of coronary heart disease and the age of manifestation, even in individuals with the same classical risk factors. The reasons for this wide inter-individual variation in susceptibility are poorly understood. The hypothesis has emerged that inter-individual variation for the risk of coronary heart disease might result from variations in the rate of biological ageing[6, 7].

Telomeres are found at the very ends of chromosomal DNA and are involved in the maintenance of genome stability[6, 8]. Mean telomere length is considered to be a marker for biological age with shorter telomeres indicative of greater biological age[9]. Telomere shortening in peripheral blood lymphocytes has been linked to cardiovascular-related morbidity and mortality in the general population[10, 11]. However, a link between telomere shortening and the vascular effects of ionising radiation is still lacking[12].

The aim of the present study was to investigate conventional risk factors as well as radiation dose and telomere shortening in a large cohort of HL patients who developed coronary artery disease (CAD) post-treatment as biological age could affect susceptibility to coronary heart disease.

Hodgkin lymphoma is a malignant haematologic disease for which current treatment provides a very high cure rate. Because of this successes, the first amongst the best examples in oncology, and because this disease affects young patients, it is the object of intense interest amongst oncologists and radiobiologists, insofar as lessons learned from the study of this disease and its treatment can serve as a basis for the therapeutics and the follow-up of other cancers. Nevertheless, the cohort study of Hodgkin's disease patients shows that the survival of these patients who are essentially cured is much lower than that which would be expected[13]. The risk of these former patients of dying from a complication of treatment,

given in the distant past, is greater than the risk of dying from a recurrence of the disease itself. The extent and nature of these morbidities and late mortalities has been the subject of numerous and detailed studies. For these reasons, the authors decided to investigate conventional and non-conventional prognostic factors, such as telomere length, for the occurrence of CADs in HL patients.

The authors demonstrate, in this study, that following multivariate analysis, hypertension and telomere length were the only significant prognostic factors for the occurrence of secondary cardiovascular diseases.

STUDY DESIGN

Patients

A prospective cohort of 179 HL patients treated and followed up at the Gustave Roussy Institute from 2007 to 2012 without a prior history of CAD was entered into the study (Table 1). Treatment was standard: all patients underwent mediastinal radiation therapy, and chemotherapy was given to 173 of 179 HL patients. All radiation treatment charts or computerised records were reviewed, and the radiation doses were estimated according to isodose curves encompassing the area of the coronary artery origins (CAOs)[14].

Blood samples were obtained before Coronary CT angiography (CCTA). The study was approved by the local ethics committee (approval no. 97-56). All subjects signed an informed consent form.

Table 1. Clinical characteristics, modalities of treatment and CCTA findings of HL patients.

Characteristics	Patients ($N = 179$)
Age at treatment (median and range)	29 (9–75)
Age at CCTA (median and range)	42 (19–79)
Male/female ratio	82/97 (0.85)
Stage	
Early stage	151 (84 %)
Advanced stage	28 (16 %)
Treatment	
Chemotherapy	173 (97 %)
Radiation therapy	179 (100 %)
Total radiation dose (Gy)	36 (35,4–36,8)
Radiation dose to the origin of coronary arteries (Gy)	33.4 (32,4–34,6)
Patients with abnormal CCTA	46 (26 %)
Treatments	
Surgery	10 (22 %)
Angioplasty with stent placement	8
Bypass grafting	2
Medical treatment	24 (52 %)
Follow-up alone	10 (22 %)
Outcome	
Alive	43
Deceased	3

Coronary artery status

Coronary CT angiography was performed on patients using a dual-source CT scanner (Somatom Definition Flash, Siemens AG, Forchheim, Germany). The mean radiation dose delivered during the CCTA procedure was 4.5 mSv with a standard deviation of ± 2. All imaging data were reviewed by two experienced radiologists

Telomere quantification

Blood lymphocytes were cultured for 48 h, and metaphase preparations were performed using standard procedures[15]. Slides were spread and stored at -20°C until use. Telomeres were stained using the Q-FISH technique with a Cy-3-labelled PNA probe specific for TTAGGG for telomere sequences (from Panagene, Daejeon, South Korea). Quantification image acquisition and analysis were performed using Metacyte software (version 3.9.1, MetaSystems, Newton, MA, USA).

Statistical analysis

All the parameters including radiation dose and telomere length were first tested for their association with CCTA abnormalities by univariate analysis. Cox Proportional Hazard regression analyses assessed the association of all parameters and CCTA abnormalities. Multivariate analysis included all the parameters whose p-values were <0.10 in the univariate analysis (all tests were two-sided; p-values of <0.05 were considered significant).

RESULTS AND DISCUSSION

The incidence of CCTA abnormalities is given in Table 1. In the total cohort of 178 patients, 3 patients died due to myocardial infarction and 46 patients had abnormalities of their CCTA. Univariate analysis of risk factors was performed and showed the presence of significant conventional risk factors for cardiovascular disease such as hypertension ($p < 2 \times 10^{-5}$), hypercholesterolaemia ($p = 0.001$), age at treatment ($p < 0.04$) and at CCTA ($p = 0.004$). The radiation dose to CAO was also a significant risk factor ($p = 0.015$). A less conventional risk factor, telomere length, was highly significant ($p = 0.006$). Multivariate analysis of conventional risk factors demonstrates that radiation dose to CAO is the most significant factor ($p = 0.005$). Age at treatment ($p < 0.02$), hypertension ($p = 0.006$) and hypercholesterolaemia ($p = 0.01$) were independent prognostic factors. The second multivariate analysis was performed with all risk factors including telomere length. Only hypertension ($p = 0.007$) and telomere length ($p = 0.03$) were found to be significant prognostic factors.

The multivariate analysis of conventional risk factors corroborated the significance of well-known

prognostic factors. The details for the conventional risk factors are given in Girinsky *et al.*[16] Figure 1 shows the mean and the range of telomere lengths of circulating lymphocytes from HL patients with CCTA abnormalities compared with patients with no evident disease. The mean age and the number of patients are represented. There was a significant association between telomere length and age in HL patients.

In this study, the authors compared only cardiovascular disease versus no cardiovascular disease. Some patients exhibit drastic telomere shortening (<5 kb). The principle finding of this investigation is the prognostic factor of telomere length for cardiovascular disease in HL patients, post-treatment. This study is the first to demonstrate the major role of telomeres in the occurrence of cardiovascular disease in a population exposed to ionising radiation for medical purposes. It is very well documented that individuals with short telomeres of their peripheral blood lymphocytes carry a higher risk for dying of cardiovascular disease in the general population[6]. Cardiovascular complications are the second most frequent fatal post-radiation therapy complication, and epidemiological studies have linked this to exposure to ionising radiation. However, the link between telomere shortening and the higher risk of cardiovascular disease post-exposure was lack.

These findings demonstrate, using multivariate analysis, on the one hand, that the dose to CAO plays a major role in the incidence of CCTA abnormalities, whereas on the other hand, the implication of telomere shortening in the occurrence of these abnormalities.

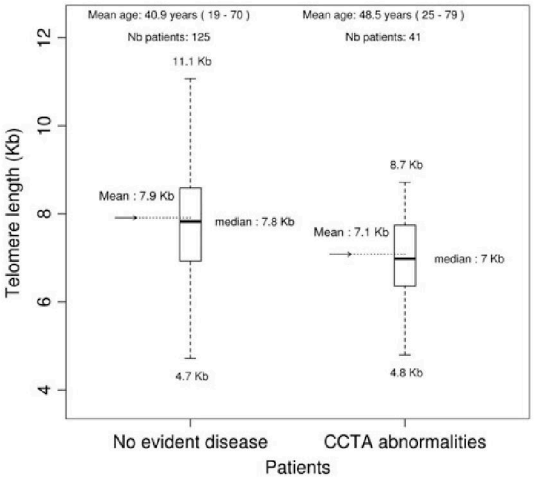

Figure 1. Telomere length in peripheral blood lymphocytes of HL patients with CCTA abnormalities compared with those with no evident cardiovascular disease. Higher heterogeneity in the mean telomere length was observed in patients with no evident cardiovascular disease, which can be explained by the short follow-up of some patients as well as the possible occurrence of another complication such as secondary cancer.

The link between telomeres and the DNA damage response has been strengthened by several studies, both at the cellular and organismal levels, demonstrating that telomere shortening is a determinant of radiation sensitivity[15, 17–19]. Interestingly, in a previous study, the authors have demonstrated that a subset of newly diagnosed, untreated patients with HL demonstrated pre-treatment telomere shortening associated with increased *in vitro* radiation sensitivity and higher frequency of chromosomal aberrations[15]. These findings suggest that HL patients exhibiting short telomeres prior to treatment who received mediastinal radiation might be at higher risk of developing CCTA abnormalities. This plausible hypothesis that telomere shortening may represent an important mediator between radiation exposure and vascular damage could be used to define new radiation protection strategies and supports the quantification of telomere as a prognostic factor of cardiovascular risk of population exposed to ionising radiation.

Two possible hypotheses, oxidative stress and viral infections, could be investigated to elucidate the mechanisms of this telomere shortening. Hodgkin lymphoma patients offer a specific profile from the double point of view of oxidative stress (immunosuppression) and viral infection (role of EBV)[20]. These hypotheses can be used in the monitoring of telomere length in populations before they are exposed to genotoxic agents in order to define new radiation protection strategies on an individual basis (Figure 2).

This study is the first to link telomere length in peripheral blood lymphocytes to cardiovascular disease in a population medically exposed to ionising radiation and provides additional evidence that telomere

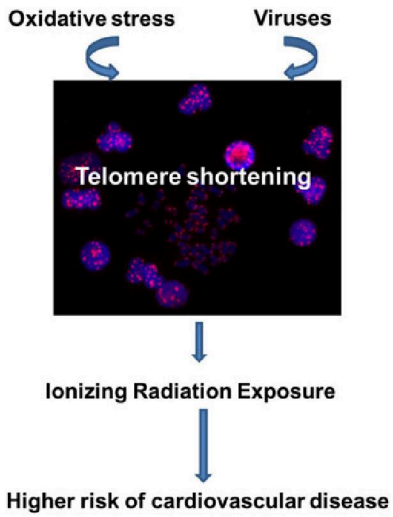

Figure 2. Schematic representation of telomere shortening and higher risk of cardiovascular disease hypothesis in HL patients.

length may be a proxy for underlying inter-individual sensitivity.

These findings need to be confirmed in larger exposed cohorts (accidentally exposed populations, professionally exposed personnel, breast cancer patients, etc.). The introduction of telomere length as a prognostic factor for cardiovascular diseases will require the development of a reliable, easy and automated method to quantify telomere length.

ACKNOWLEDGMENTS

The authors are grateful to the nurses, technologists and secretaries in the department of Medicine and Radiation Oncology of the Institut Gustave Roussy (Villejuif) and Marie Lannelongue (Chatenay-Malabry).

FUNDING

This work was supported by a grant from the European Community's Seventh Framework Program (EURATOM) contracts Fission-2011-249689 (DoReMi), Fission-2011-295513 (RENEB).

REFERENCES

1. Rugbjerg, K., Mellemkjaer, L., Boice, J. D., Kober, L., Ewertz, M. and Olsen, J. H. *Cardiovascular disease in survivors of adolescent and young adult cancer: a Danish cohort study, 1943–2009*. J. Natl Cancer Inst. **106**(6), dju110 (2014).
2. Santoro, F., Tarantino, N., Pellegrino, P. L., Caivano, M., Lopizzo, A., Di Biase, M. *et al. Cardiovascular sequelae of radiation therapy*. Clin. Res. Cardiol. (2014) Epub 08 May 2014.
3. *United Nations Scientific Committee on the effects of Atomic Radiation (UNSCEAR). Report: sources and effects of ionizing radiation*. (2008) Volume I. Annex A. Available on http://www.unscear.org/docs/reports.2008/09-86753_Report_2008_Annex_A.pdf and Annex B. Available on http://www.unscear.org/docs/reports/2008/09-86753_Report_2008_Annex_B.pdf (25 October 2011, date last accessed).
4. (ICRP), *2012 ICRP Statement on Tissue Reactions/ Early and Late Effects of Radiation in Normal Tissues and Organs – Threshold Doses for Tissue Reactions in a Radiation Protection Context*. ICRP Publication 118. Ann. ICRP **41**(1/2).
5. Yusuf, S., Vaz, M. and Pais, P. *Tackling the challenge of cardiovascular disease burden in developing countries*. Am. Heart J. **148**(1),1–4 (2004).
6. Cawthon, R. M., Smith, K. R., O'Brien, E., Sivatchenko, A. and Kerber, R. A. *Association between telomere length in blood and mortality in people aged 60 years or older*. Lancet **361**(9355), 393–395 (2003).
7. Samani, N. J., Boultby, R., Butler, R., Thompson, J. R. and Goodall, A. H. *Telomere shortening in atherosclerosis*. Lancet **358**(9280), 472–473 (2001).
8. Sabatier, L., Ricoul, M., Pottier, G. and Murnane, J. P. *The loss of a single telomere can result in instability of multiple chromosomes in a human tumor cell line*. Mol. Cancer Res. **3**(3), 139–150 (2005).
9. Vera, E., Bernardes de Jesus, B., Foronda, M., Flores, J. M. and Blasco, M. A. *The rate of increase of short telomeres predicts longevity in mammals*. Cell Rep. **2**(4), 732–737 (2012).
10. Brouilette, S. W., Moore, J. S., McMahon, A. D., Thompson, J. R., Ford, I., Shepherd, J. *et al. Telomere length, risk of coronary heart disease, and statin treatment in the West of Scotland Primary Prevention Study: a nested case-control study*. Lancet **369**(9556), 107–114 (2007).
11. Maubaret, C. G., Salpea, K. D., Jain, A., Cooper, J. A., Hamsten, A., Sanders, J. *et al. Telomeres are shorter in myocardial infarction patients compared to healthy subjects: correlation with environmental risk factors*. J. Mol. Med. (Berl) **88**(8), 785–794 (2010).
12. Sabatino, L., Picano, E. and Andreassi, M. G. *Telomere shortening and ionizing radiation: a possible role in vascular dysfunction?* Int. J. Radiat. Biol. **88**(11), 830–839 (2012).
13. Castellino, S. M., Geiger, A. M., Mertens, A. C., Leisenring, W. M., Tooze, J. A., Goodman, P. *et al. Morbidity and mortality in long-term survivors of Hodgkin lymphoma: a report from the Childhood Cancer Survivor Study*. Blood **117**(6), 1806–1816 (2011).
14. Miller, J. M., Rochitte, C. E., Dewey, M., Arbab-Zadeh, A., Niinuma, H., Gottlieb, I. *et al. Diagnostic performance of coronary angiography by 64-row CT*. N. Engl. J. Med. **359**(22), 2324–2336 (2008).
15. M'Kacher, R., Bennaceur-Griscelli, A., Girinsky, T., Koscielny, S., Delhommeau, F., Dossou, J. *et al. Telomere shortening and associated chromosomal instability in peripheral blood lymphocytes of patients with Hodgkin's lymphoma prior to any treatment are predictive of second cancers*. Int. J. Radiat. Oncol. Biol. Phys. **68**(2), 465–471 (2007).
16. Girinsky, T., M'Kacher, R., Lessard, N., Koscielny, S., Elfassy, E., Raoux, F. *et al. Prospective coronary heart disease screening in asymptomatic Hodgkin lymphoma patients using coronary computed tomography angiography: results and risk factor analysis*. Int. J. Radiat. Oncol. Biol. Phys. **89**(1), 59–66 (2014).
17. Goytisolo, F. A., Samper, E., Martin-Caballero, J., Finnon, P., Herrera, E., Flores, J. M. *et al. Short telomeres result in organismal hypersensitivity to ionizing radiation in mammals*. J. Exp. Med. **192**(11), 1625–1636 (2000).
18. Sedelnikova, O. A., Horikawa, I., Redon, C., Nakamura, A., Zimonjic, D. B., Popescu, N. C. *et al. Delayed kinetics of DNA double-strand break processing in normal and pathological aging*. Aging Cell **7**(1), 89–100 (2008).
19. Wong, K. K., Chang, S., Weiler, S. R., Ganesan, S., Chaudhuri, J., Zhu, C. *et al. Telomere dysfunction impairs DNA repair and enhances sensitivity to ionizing radiation*. Nat. Genet. **26**(1), 85–88 (2000).
20. Kanakry, J. A., Li, H., Gellert, L. L., Lemas, M. V., Hsieh, W. S., Hong, F. *et al. Plasma Epstein-Barr virus DNA predicts outcome in advanced Hodgkin lymphoma: correlative analysis from a large North American cooperative group trial*. Blood **121**(18), 3547–3553 (2013).

5.2 Telomeres as a key player in the process of radiation-induced carcinogenesis

As discussed in previous chapters, telomeres are involved in aging (Section 1.1.1), age-related human (non-cancer) pathologies (Section 1.1.3), and the development of cardiovascular diseases (Section 5.1). Telomeres can also be associated with the process of carcinogenesis, as telomere dysfunction (Section 1.1.2) via deregulation of telomere length, shelterin proteins, and DNA damage repair proteins (each of which have also been linked to cancer progression) induces genomic instability, which in turn is an important enabling factor that aids in the acquisition of the hallmark traits of cancer that allow cancer cells to survive, proliferate, and disseminate. In **our review article** (Shim et al., 2014), we present what is currently known on these related topics.

5.2.1 Summary of key points

- We review the current knowledge and understanding of telomeres, mechanisms of telomere maintenance, and mechanisms of telomere damage and repair.
- We have compiled all the significant studies published in literature on telomeric shelterin proteins and DDR proteins and the consequences of their deficiency or dysfunction on telomere length and fusion in humans and mice. Upon combing through a plethora of conflicting data in literature, these novel tables (Tables 1 and 2 on page 4 of the article) highlight the complexity in studying these mechanisms *in vitro* and *in vivo*.
- We discuss what is currently known about telomeric and chromosomal damage induced by direct and indirect IR exposure, and mechanisms by which these IR-induced damages may lead to genetic instability during proliferation.
- Finally, we conclude the review paper with the proposal of a detailed model for how telomeres may be a key player in the process of IR-induced carcinogenesis. Briefly, telomeres and IR-induced dysfunction of telomere maintenance mechanisms play a central role in the emergence of delayed genetic instability and accelerated aging following irradiation (Figure 1 on page 10 of the article). As genomic instability can be induced by telomere dysfunction (due to deregulation of telomere length, shelterin proteins, and DDR proteins, factors that have all been linked to cancer progression), telomeres may facilitate the process of IR-induced carcinogenesis (Figures 2 and 3 on pages 11 and 12 of the article, respectively). These factors may have profound implications for long-term human health risks, and may be directly applicable to the efficacy and long-term consequences of cancer treatment with radiotherapy.

Mutation Research 760 (2014) 1–17

Contents lists available at ScienceDirect

Mutation Research/Reviews in Mutation Research

journal homepage: www.elsevier.com/locate/reviewsmr
Community address: www.elsevier.com/locate/mutres

Review

Crosstalk between telomere maintenance and radiation effects: A key player in the process of radiation-induced carcinogenesis☆

Grace Shim [a,b], Michelle Ricoul [a], William M. Hempel [a], Edouard I. Azzam [b], Laure Sabatier [a,*]

[a] Commissariat à l'Energie Atomique (CEA), DSV/IRCM/SRO – Laboratory of Radiobiology and Oncology, 18 route du Panorama, 92265 Fontenay-aux-Roses, France
[b] Department of Radiology, Rutgers New Jersey Medical School Cancer Center, 205 South Orange Avenue, Newark, NJ 07103, USA

ARTICLE INFO

Article history:
Received 6 August 2013
Received in revised form 14 January 2014
Accepted 22 January 2014
Available online 31 January 2014

Keywords:
Telomeres
Ionizing radiation
Bystander effect
Radiosensitivity
Chromosomal instability

ABSTRACT

It is well established that ionizing radiation induces chromosomal damage, both following direct radiation exposure and via non-targeted (bystander) effects, activating DNA damage repair pathways, of which the proteins are closely linked to telomeric proteins and telomere maintenance. Long-term propagation of this radiation-induced chromosomal damage during cell proliferation results in chromosomal instability. Many studies have shown the link between radiation exposure and radiation-induced changes in oxidative stress and DNA damage repair in both targeted and non-targeted cells. However, the effect of these factors on telomeres, long established as guardians of the genome, still remains to be clarified. In this review, we will focus on what is known about how telomeres are affected by exposure to low- and high-LET ionizing radiation and during proliferation, and will discuss how telomeres may be a key player in the process of radiation-induced carcinogenesis.

Contents

* Corresponding author. Tel.: +33 1 46 54 83 51; fax: +33 1 46 54 87 58.
E-mail addresses: graceshim1@gmail.com (G. Shim), michelle.ricoul@cea.fr (M. Ricoul), william.hempel@cea.fr (W.M. Hempel), azzamei@njms.rutgers.edu (E.I. Azzam), laure.sabatier@cea.fr (L. Sabatier).

1383-5742/$ – see front matter © 2014 The Authors. Published by Elsevier B.V. All rights reserved.
http://dx.doi.org/10.1016/j.mrrev.2014.01.001

1. Introduction

We are all constantly exposed to ionizing radiation (IR) from natural sources such as cosmic rays, radon decay products in the air, and various radionuclides found in food and water. We may also be exposed to low doses of IR released to the environment from man-made sources, including fallout from nuclear weapons testing, discharges of radioactive waste, and consumer products. In addition, individuals may be exposed to IR during occupational activities related to nuclear technology, mining, high altitude airline travel, and deep space exploration [1]. In particular, with the explosive growth in the use of diagnostic radiology, increasing numbers of individuals are being repeatedly exposed to IR. The use of different irradiation modalities remains an effective and widely used means to treat cancer and other pathological conditions [2]. Therefore, exposure to IR is an inevitable part of the environment, and increasingly of modern life.

During cancer radiotherapy, both malignant and normal cells are exposed to IR. Radiation-induced damage, particularly in tissues irradiated with high doses, induces systemic effects that affect the whole body during, or a short time after, exposure. Importantly, delayed effects are also sometimes observed many years after the end of treatment, as illustrated by a higher incidence of secondary malignancies and a variety of degenerative conditions in long-term cancer survivors. Strikingly, in patients receiving radiation treatment, significant biological changes have been observed in tissues that are widely separated from the irradiated area, and treatment directed at a tumor at one site may profoundly affect tumors and/or normal tissues located elsewhere in the body. These non-targeted effects can therefore be either detrimental or beneficial (if they lead to shrinkage of distant tumors), and have been termed "abscopal effects." These diverse physiological effects of IR illustrate the in vivo occurrence of radiation-induced "*bystander*" responses [3–5].

The spread of IR-induced effects among irradiated cells, between irradiated and non-irradiated cells, and their persistence in progeny of both targeted and non-targeted cells, can therefore have profound implications for long-term human health risks. The emergence of secondary cancers and other pathobiological conditions after radiotherapy [3] and the possibility of delayed effects following occupational radiation exposure in miners, nuclear workers, and astronauts directly impact the formulation of cancer treatment strategies and the establishment of occupational radiation protection guidelines [6,7]. Conversely, understanding the mediating mechanisms of IR exposure may help in devising approaches to alleviate its detrimental effects.

Over the last two decades, as will be discussed in the following chapters, increasing evidence has been gathered that shows that the long-term effects of IR exposure are due to oxidative changes leading to the continuous accumulation of DNA damage in the progeny of both irradiated and non-irradiated bystander cells. Strong evidence indicates that these effects are dependent on radiation quality, dose, dose-rate, genetic susceptibility, and age, for example. Based on previous studies in our laboratory, we postulate that the emergence of late radiation effects in directly irradiated or bystander cells may be due to delayed chromosomal instability caused by telomere dysfunction.

2. Telomeres

2.1. Background

The critical role of telomeres in maintaining chromosomal stability was first described in the 1930s by Barbara McClintock in maize [8] and Hermann Muller in fruit flies [9]. Telomeres are specialized nucleoprotein structures located at the ends of linear eukaryotic chromosomes [10]. They consist of tandem repeats of 5′-TTAGGG-3′ (T_2AG_3) DNA sequences and several associated proteins. Together, they form a protective cap called the shelterin complex, which protects chromosome ends from being recognized as DNA double strand breaks (DSBs), and prevent unwanted activation of DNA damage checkpoints and DSB repair pathways [11]. The complex is found in the form of a T-loop, which is formed when the double-stranded telomeric DNA regions fold back to interact with the 3′ single-stranded portion with the help of the shelterin proteins [12,13]. Because of the G-rich nature of the single-stranded telomeric DNA, this region may also form G-quadruplexes, which are formed from a series of G-quartets each containing four guanine bases arranged in a helical fashion [14,15].

The shelterin complex in humans includes six proteins that are associated with telomeric DNA, named TRF1, TRF2, TIN2, POT1 (POT1a/b in rodents [16]), TPP1, and RAP1. Each of these proteins has evolved specific functions for telomere maintenance, including the regulation of telomerase access and activity as well as the interaction with many DNA repair/recombination factors. In this way, telomeres play a critical role as the guardians of genomic stability and integrity. Generally, TRF1 and TRF2 bind to the double-stranded telomeric DNA, while POT1 binds the single-stranded overhang and interacts with the other shelterin proteins via the linker proteins TIN2 and TPP1 [17]. Multiple POT1–TPP1 molecules were shown to coat long stretches of telomeric single stranded DNA and form compact ordered structures that may serve to protect this region from telomerase access and/or DNA damage response (DDR) factors [18,19]. TIN2 stabilizes both TRF1 and TRF2 on the double stranded DNA region [20] and TPP1/POT1 on the single stranded portion [21]. Finally, RAP1, which interacts with TRF2, has been shown to be non-essential for the functions of TRF2, but is important for the repression of DDR factors at the telomeres [22].

2.2. Mechanisms of telomere maintenance in normal human cells

Telomere length (TL) varies between organisms; in humans, the length of the double-stranded end can be 2–20 kb, while the length of the single-stranded G-rich overhang can be 50–500 nucleotides. TL also varies on individual chromosome arms [23], and this inherent heterogeneity of TL is conserved during life [24]. TL in somatic proliferative tissues naturally declines with each cell replication cycle at a rate of approximately 20–300 base pairs per population doubling (varying with cell type) [25] due to the incomplete replication of telomere ends by conventional DNA polymerases, a situation known as the 'end replication problem' [26]. After many rounds of cell division, telomeres eventually become critically short and dysfunctional. In normal cells with intact p53 functions and cell cycle checkpoints, these dysfunctional/uncapped telomeres are sensed as DNA damage and trigger DDR pathways, forming telomere dysfunction-induced foci, termed TIFs [27]. Indeed, induction of DDR factors (such as ATM and gamma-H2AX) was inversely correlated with TL and shelterin protein levels [28–30]. An important recent study suggested that normal human cells are able to tolerate small numbers of dysfunctional telomeres, and cells can continue to proliferate without significant induction of telomere fusions and chromosomal instability until a threshold of five TIFs per cell is reached [31]. At this point, these DDR signals prevent the cell from further division [32], and cells enter a stage of permanent growth arrest called "replicative senescence" [33]. The lack of chromosomal fusions in pre-senescent cells may indicate that sufficient levels of shelterin proteins are present at the telomeres to retain their protective roles. However, in cells that are unable to senesce due to the loss of cell cycle checkpoint proteins such as p53 or p16, senescence is temporarily bypassed, and cells continue to proliferate with further telomere shortening, until "telomeric crisis" is reached

involving massive chromosome fusion and cell death [34–36]. In normal human cells undergoing crisis, more than 5 dysfunctional telomeres were found, along with fused telomeres, perhaps due to extreme telomere shortening and loss of shelterin proteins [31].

Progressive telomere shortening therefore acts as a 'molecular clock' that limits the number of cell divisions, thereby regulating cellular lifespan and aging [37]. The persistent shortening of telomeres can be offset in different cell types (i.e. normal somatic cells, germ cells, cancer cells) via two mechanisms of telomere elongation: (1) telomerase, a specialized reverse transcriptase [38], and (2) homologous recombination of telomeres via "alternative lengthening of telomeres" (ALT), a pathway independent of telomerase activity [39]. Furthermore, growing evidence suggests that telomere maintenance is influenced by the transcription and localization of TERRA (TElomeric Repeats-containing RNA) (discussed in detail in [40–42]). Indeed, telomeres were found to be actively transcribed into TERRA, which localize to telomeres, and the presence of these molecules at the telomeres was suggested to cause delayed entry into senescence in yeast cells by promoting recombination-mediated telomere elongation at critically short telomeres [42]. Interestingly, however, a recent study showed no correlation between TL, TERRA levels, and radiosensitivity in several human cancer cell lines [43]. Shelterin proteins, in conjunction with DDR mechanisms, have also been shown to be involved in telomere protection and maintenance [11,17].

2.2.1. Telomere maintenance by telomerase

Telomerase is a specialized reverse transcriptase that elongates telomeres by adding TTAGGG DNA sequence repeats to the 3′ G-strand overhang at chromosome ends. It is a ribonucleic protein complex composed of two core components: the rate-limiting catalytic human *telomerase reverse transcriptase* (*hTERT*), which reverse transcribes the template region of the second component, the *RNA subunit* (*hTR or hTERC*), onto the 3′ end of the telomeric DNA [44]. Telomerase is primarily expressed in stem cells, germ cells, regenerating tissues, and cancer cells; it is silent in most differentiated cells, such as normal somatic cells [45], thereby resulting in telomere shortening after each round of cell division.

The access of telomerase to telomeres is regulated by the G-quadruplex structure and shelterin proteins. The G-quadruplex structure has been shown to protect the single-stranded overhang from telomerase access [46]. Furthermore, the amount of shelterin proteins at the telomeres has been shown to be directly proportional to TL in mammalian cells and the degree of telomerase inhibition [11]. Despite this general negative regulation of telomerase by shelterin proteins, TPP1 was shown to recruit telomerase to the telomeres [47,48], and the presence of the POT1-TPP1 dimer has been shown to increase the processivity of the enzyme [49]. TIN2 has also been shown to promote telomerase activity, independent of its interaction with TPP1; indeed, mutations in TIN2 leads to dyskeratosis congenita, a disease characterized by telomere shortening due to interference of telomerase function [50]. In addition, telomerase has been shown to preferentially elongate the shortest telomeres [51].

Aside from its telomere elongation functions, telomerase also appears to be involved in many additional biological processes in the cytoplasm and mitochondria, including cellular proliferation, the regulation of gene expression, and the protection of mitochondrial functionality. Telomerase has been shown to influence DNA damage repair, which is also closely linked to shelterin interactions [52,53]. In addition, telomerase activity also exerts an anti-apoptotic effect where its inhibition may promote apoptosis in malignant cells [54]; the use of telomerase inhibitors during cancer therapy would thereby sensitize cancer cells to cancer treatments. These properties make telomerase an attractive target for anti-cancer therapies [55,56].

Abnormal telomerase activity and TL regulation have been linked to the pathology of several age-related human diseases. For instance, telomerase deficiency can lead to untimely telomere shortening. A variety of degenerative disorders, recently termed 'the telomere syndromes,' are all characterized by the presence of short telomeres due to telomere dysfunctions caused by heritable mutations in telomere and/or telomerase genes; such diseases include dyskeratosis congenita, pulmonary fibrosis, and bone marrow failure [57,58]. On the other hand, up-regulation of telomerase prevents telomere shortening and sustains cell growth and viability. Indeed, the enzyme is up-regulated in about 85% of human cancers, suggesting its important role in the process of cellular immortalization and tumorigenesis [59]. Its down-regulation or inhibition would therefore target and impair telomerase-positive malignant cancers while normal somatic cells, which do not express telomerase, are minimally affected [60]. In cancer cells or in cells with defective p53/Rb checkpoint pathways, telomerase may also have a role in protecting t-stumps, defined as extremely short telomeres still protected by the shelterin proteins [61].

Although telomerase reactivation is the most common telomere elongation mechanism in human cancers, a significant subset of human tumors (10–15%) employs the telomerase-independent ALT pathway [39,59]. Whether the cancer cell uses telomerase activation or the ALT pathway seems to depend on the origin of the tumor. ALT involves telomere elongation through homologous recombination (HR). This pathway can co-exist with telomerase activity in some tumors [62], rendering these tumors resistant to treatment with telomerase inhibitors [63]. The ALT-positive phenotype in human tumor cells may render cells more resistant to IR compared to telomerase-positive cells, which may be due to the interference of the ALT pathway with DDR mechanisms [64].

2.2.2. Telomere maintenance by shelterin proteins and DNA damage repair mechanisms

Shelterin protein levels are generally inversely correlated with TL in humans and mice, as summarized in Table 1. Additionally, the shelterin proteins were shown to repress the activation of six independent DDR mechanisms at telomeres, indicating that many mechanisms are used to protect chromosomal ends from DNA damage surveillance proteins [65]. Whether DDR proteins, with or without interactions with the shelterin proteins, play a role in the maintenance of TL is still debatable, as noted in Table 2. However, it is clear that telomeres and the DDR mechanisms exhibit a co-dependent, bi-directional relationship, as dysfunctional telomeres are recognized as DSBs and trigger the DDR pathways, whose proteins are also involved in the normal maintenance and protection of telomeres. Hence, understanding the mechanisms and consequences of dysfunctional telomeres requires knowledge of the DSB repair pathways.

Mammals possess two principle mechanisms of DNA DSB repair: non-homologous end joining (NHEJ) and homologous recombination (HR) repair. Both pathways have similar initial steps in commencing DNA repair, involving the binding of the MRE11/RAD50/NBS1 (MRN) complex to the site of the DSB, followed by activation of ATM. ATM then goes on to phosphorylate various proteins to recruit repair complexes to the site of the DSB, modify chromatin structure at the DSB to allow repair protein access, and activate cell cycle checkpoints to delay progression through the cell cycle until repair is complete [66]. Whether the cell undergoes repair via NHEJ or HR appears to depend on four proteins: RIF1 (Rap1-interacting factor 1), 53BP1 (p53 binding protein 1), BRCA1 (breast cancer type 1 susceptibility protein), and CtIP (C terminus-binding protein-interacting protein). 53BP1 and RIF1 may stimulate NHEJ, while BRCA1 and CtIP together promote HR [67]. NHEJ repairs DSBs in all cell-cycle phases (especially in G1), and HR functions in S/G2 phase [68].

Table 1
Telomeric shelterin proteins and consequences of their deficiency or dysfunction on telomere length and fusions in humans and mice. Negative regulation of telomere length is defined as ↑ protein levels causing ↓ telomere length, or vice versa. Positive regulation of telomere length is defined as ↑ protein levels causing ↑ telomere length, or ↓ protein levels causing ↓ telomere length.

Protein	Negative/ positive regulator of telomere length	Fusions			
		Sister/chromatid/ chromosome – type fusions	Via	Involving leading/ lagging strand	With/without telomere signal at junction
TRF1					
Human	Negative [216–226]	Sister-type [226]	C/A-NHEJ [227]	Both [226]	With [226]
Mouse	Negative [228] No effect [229,230]	Sister/chromosome-type [227,229,231,232]		Both [229]	Both [229,233]
TRF2					
Human	Negative [218–220,224,225]	Chromatid-type [234]	C-NHEJ [235]	Leading [234]	With [216,234]
Mouse	Negative [228]	Massive chromatid/ chromosome-type [236]	C-NHEJ [70]	Leading [236]	With [236]
POT1					
Human	Negative [221,237,238]	Minor sister/chromosome-type [239,240]	A-NHEJ [69,70,241]	Both [239]	With [239]
Mouse	Negative [242]	Minor sister/chromatid/ chromosome-type [16,21]		Both [21]	Both [16]
TIN2					
Human	Negative [219,220,222,223]	Chromosome-type [243]	C-NHEJ [21]	Both [243]	Both [243]
Mouse	Negative [244]	Sister/Chromatid/ Chromosome-type [21]		Both [21]	With [21]
TPP1					
Human	Negative [238]	Sister/chromosome-type [21,245,246]	A-NHEJ [69,70,241]	Both [247]	Both [245,247]
Mouse	Positive [231,246] Negative [246]				
RAP1					
Human	Positive [248,249] Negative [250,251]	No fusions [252]	C-NHEJ (with TRF2) [70,235]	N/A [252]	N/A [252]
Mouse	Positive [253]	No fusions [22,253,254]		N/A [22,253,254]	N/A [22,253,254]

NHEJ, non-homologous end joining; C-NHEJ, classical-NHEJ; A-NHEJ, alternative-NHEJ; N/A, not applicable; ↑, up-regulation; ↓, down-regulation.

Table 2
DNA damage repair proteins and consequences of their deficiency on telomere length and fusions in humans and mice. Negative regulation of telomere length is defined as ↑ protein levels causing ↓ telomere length, or vice versa. Positive regulation of telomere length is defined as ↑ protein levels causing ↑ telomere length, or ↓ protein levels causing ↓ telomere length.

Protein	Negative/positive regulator of telomere length	Via	Fusions		
			Sister/chromatid/ chromosome – type fusions	Involving leading/ lagging strand	With/without telomere signal at junction
DNA-PKcs	No effect via gene deletion [255,256] Different results in SCID mice, or via IC86621 inhibition in mice and human cells [255–257]	TRF2	Chromatid-type (via IC86621 inhibition) [257,258]	Leading (via IC86621 inhibition) [258]	With [255]
Ku70	Conflicting data [219,259]	TRF2	Chromatid/chromosome-type [259]	Both [259]	With [259]
Ku86	Conflicting data [260,261]	TRF1 [262]	Chromatid/chromosome-type [260,262]	Leading/both [260,262]	With [260,262]
Lig4	N/A [263]	TRF2 [264]	Chromatid/chromosome-type [264]	Both [264]	Both [264]
PARP1/PARP2	No effect [265]	TRF2 [265,266]	Minor chromosome-type [265,266]	Both [265,266]	Without [265,266]
53BP1	No effect	TRF2	Sister-type [227]	Leading	With [227]
MRN (MRE11/ Rad50/NBS1)	No effect [267,268]	TRF2 [267]	Chromatid-type [236,268]	Leading [236,268]	With [236,268]
Tankyrase	Positive [223,249,266,269,270] No effect [271]	TRF1 [270]	Major sister-type [270] Minor chromatid/chromosome-type [270]	Both [270]	With [270]

N/A, not-applicable; ↑, up-regulation; ↓, down-regulation.

As summarized in Tables 1 and 2, dysfunctional telomeres, due to loss or dysfunction of shelterin or DDR proteins, often lead to chromosomal instability, including the formation of telomeric end-to-end fusions. As denoted in these tables, fusions can be formed between two different chromosomes ('chromosome-type'), sister chromatids ('sister-type'), or leading/lagging chromatids of different chromosomes ('chromatid-type'). The presence of telomeric signals at the junction of these fusions can illustrate whether the fusion occurred with or without telomere loss. Dicentric chromosomes that are formed from these fusions cause cell cycle arrest in

normal cells with intact cell cycle checkpoints; however, cells lacking normal checkpoints continue to divide, and the unstable dicentric chromosomes break during cell division, leading to the propagation of chromosomal instability via the breakage-fusion-bridge (B/F/B) cycle [69].

Chromosome fusions due to loss or dysfunction of shelterin or DDR proteins have thus far been shown to occur via two pathways, as shown in Tables 1 and 2: the classical-NHEJ (C-NHEJ) pathway, or the alternative-NHEJ (A-NHEJ) pathway. However, it should be noted that many conflicting data exists, and the consequences of the dysfunction of these proteins also appear to differ among species. Most chromosome fusions in mammalian cells occur via the C-NHEJ pathway. This pathway involves direct joining of DNA ends utilizing several well-characterized proteins such as KU70, KU86, DNA-PKcs, LIG4, XRCC4, XLF, and Artemis. These proteins are also essential for telomere function and protection, and deregulation of these NHEJ components can alter telomere stability and lead to genomic instability. Recently, alternative repair pathways were identified in cells deficient in NHEJ, though it is still unclear whether only one or several backup pathways exist. However, it is currently proposed that there are two "alternative end joining" pathways: (1) the microhomology-mediated end-joining (MMEJ) pathway, which relies on pre-existing micro-homologies around the DSB and appears to rely on Ligase III (LIG3) for sealing, and (2) the A-NHEJ pathway, which does not require the presence of pre-existing microhomologies, and may rely on Ligase I (LIG1) [67]. A-NHEJ is associated with large deletions and chromosome rearrangements, and may also lead to fusions of dysfunctional telomeres [70]. However, these alternative pathways remain to be better characterized [67,68].

2.3. Telomere damage and mechanisms of repair

DNA is continuously exposed to damaging agents, many of which may cause the acceleration of the natural shortening of telomeres and can lead to premature replicative senescence. Some of these endogeneous factors include point mutations or deletions in genes encoding proteins involved in telomere protection, as well as recombination and epigenetic regulation. Telomere shortening can also be accelerated by external environmental stress and lifestyle factors that cause DNA DSBs or mis-replication of telomeres such as IR and other oxidizing agents, oxidative stress, inflammation, hyperoxia, oncogenes, toxins, chronic viral infections, smoking, alcohol consumption, obesity, stress, and even psychiatric conditions [71–73]. Indeed, reduced TL has been associated with numerous chronic diseases that are generally considered to be diseases of aging, such as diabetes, cancer, and heart disease. Furthermore, abnormal and persistent loss of telomeres may contribute to the increased frequency of secondary complications seen in long-term cancer survivors [57,58].

Telomeric regions (and sub-telomeric regions, extending at least 100 kb from the telomere) have been shown to be particularly sensitive to DSBs, perhaps due to their inappropriate processing. The presence of DNA damage within telomeric repeat sequences hinders telomere replication, leading to telomere shortening or loss, and the deficiency of DSB repair near telomeres has been suggested to play a role in chromosomal instability associated with human cancers [74]. Additionally, telomeric sequences can also be found at internal sites of chromosomes and may colocalize with fragile chromosomal sites that are more prone to breakage; these interstitial telomeric sequences have been associated with genomic instability, human disease, and cancers [75,76]. Large deletions and gross chromosomal rearrangements (inversions, translocations, dicentric chromosomes) have been observed when DSBs occur near telomeres [74] or at interstitial telomeric sequences [76], while small deletions have been found to be the most common chromosomal aberrations when DSBs were induced at interstitial DNA sites. DSBs near telomeres are repaired predominantly by A-NHEJ due to repression of C-NHEJ repair by TRF2, while DSB repair at interstitial sites occurs primarily through C-NHEJ [74].

Additionally, chromosome healing, or the de novo addition of telomeric repeat sequences at DSB sites may serve as an alternate mechanism of repair to compensate for the increased sensitivity to DSBs near telomeres. Chromosomal healing in human cells may or may not involve telomerase, and does not occur at interstitial DSBs in somatic cells [69,74,77]. However, interestingly, strong evidence suggests that telomerase was involved in the insertion of interstitial telomeric sequences during the repair of DSBs in rodents and primates during evolution [78]). Chromosome healing results in terminal deletions, which are less detrimental than gross chromosome rearrangements, and thereby prevents chromosomal instability resulting from DSBs near telomeres. Chromosome healing may be deficient in human cancer cells, and may be responsible for the chromosomal instability observed in these cells [69,74].

3. Telomere maintenance and the effects of ionizing radiation

3.1. Background

It was long believed that the biological effects of IR exposure were solely the consequence of DNA damage that occurs in cells during or shortly after *direct* traversal of an IR particle through a cell nucleus. However, this classical "target theory," which used to be the central paradigm of radiation biology, was challenged by two important discoveries: (1) genomic instability following cytoplasmic irradiation without direct nuclear traversal [79], and (2) the phenomenon termed "non-targeted radiation-induced bystander effects" [80]. Furthermore, delayed genomic instability was found to occur in progeny cells of directly irradiated cells [81], as well as in progeny of non-irradiated bystander cells [82]. These findings illustrated that cells that were not directly exposed to IR can exhibit cellular responses similar to those of directly irradiated cells. Overall, these findings suggest that radiation-induced stresses from directly irradiated cells are transmissible both to their progeny and to their neighboring cells, and can facilitate the appearance of delayed genetic effects long after direct or indirect IR exposure.

This section discusses what is currently known about telomeric and chromosomal damage induced by direct and indirect IR exposure, and how this may lead to genetic instability during proliferation. As it is well established that the chromosomal damage induced by IR triggers DDR pathways, and DDR proteins are closely linked with telomeric proteins and telomere maintenance, we ask how/if telomeres are affected after direct or indirect IR exposure and during subsequent proliferation. These factors may have profound implications for long-term human health risks, and may be directly applicable to the efficacy and long-term consequences of cancer treatment with radiotherapy.

3.2. Radiation-induced damage

It is well known that the extent and complexity of biological damage induced by direct IR exposure is directly proportional to the radiation energy deposition patterns and linear energy transfer (LET), which is defined as the amount of energy lost per unit length along the path traveled by the radiation (expressed in keV μm^{-1}). As will be discussed in this section, immediately following direct IR exposure, chromosomal damage is known to be induced in a dose- and LET-dependent manner due to differences in both the severity and the spatial distribution of the DNA damage induced by IR of varying LET. Low-LET IR such as high energy X-rays and ^{137}Cs and

^{60}Co γ-rays deposit exponentially decreasing amounts of energy as a function of penetration depth in the target material (e.g. cell, tissue, animal). Doses of low-LET radiation produce a uniform pattern of distribution throughout the target. When X- and γ-rays are absorbed by cells or tissues, they interact with atoms or molecules, especially water which makes up 80% of the cell, to produce free radicals (e.g. hydroxyl, superoxide radicals) and other reactive oxygen species (ROS), which then go on to damage critical targets in the vicinity, such as DNA [83]. In contrast, high-LET IR, such as protons, neutrons, α particles, and heavy charged particles, deposit energy that is concentrated along the radiation track; thus, the local dose at the center of a track may be thousands of gray, but a few microns away (i.e. a neighboring cell), the dose may be close to zero [84]. Therefore, when high-LET IR traverses living matter, it induces direct, clustered damage along the radiation track to critical cellular targets such as DNA that result in DNA DSBs, gene mutations, and other complex chromosomal lesions, with the extent of damage depending on the specific physical characteristics of the radiation such as energy and mass [83]. The ability of high-LET IR to cause more cellular damage per unit dose than low-LET IR, along with the ability to localize a great amount of energy at the Bragg peak, are advantageous for use in cancer radiotherapy. Indeed, proton and carbon ions are increasingly being used, with very promising clinical results [85]. However, further characterizations are needed with respect to defining the relative biological effectiveness (RBE) of heavy ions and the risks of late effects following IR exposure [86].

The notion that DNA damage induced by direct IR (low- or high-LET) exposure can be transmitted to the progeny of directly irradiated cells to cause delayed genomic instability was first realized by Terzaghi and Little in 1976 [81], when they observed in vitro malignant transformation in progeny of X-irradiated mouse embryo fibroblasts. Later in 1990, Little et al. [87] hypothesized that IR caused increased rates of mutations that persist through many cell generations, suggesting that these DNA lesions are transmissible and facilitate the appearance of delayed genetic effects in the progeny of irradiated cells. Importantly, two key models were developed around this time to study the rate and mechanism of transmission of mutations in progeny cells, namely the measurement of the frequency of spontaneous mutations at the hprt locus on the X chromosome among the progeny of irradiated CHO and BALB/3T3 cells [87,88], and the measurement of the rate of unmasking of recessive alleles via loss of heterozygosity (LOH) using a human lymphoblastoid cell line (TK6) that contains one mutant thymidine kinase (tk) allele on chromosome 17 [89]; as IR predominantly causes recessive, loss of function mutations in the genome, these tools allow the study of the mechanisms of induction of delayed mutagenic effects of IR that can ultimately lead to the development of cancer. Furthermore, in 1992, Kadhim et al. [90] observed non-clonal chromosomal instability in the clonal descendants of alpha-particle irradiated mouse hematopoietic stem cells; that is, progeny cells harbored genetic lesions that were different in nature from those that occurred in the irradiated parental cells. At the same time, Sabatier et al. [91,92] found that this type of instability was also observed in the progeny of normal human cells irradiated with heavy ions over a large range of LETs; this delayed chromosomal instability was found to be non-random, as aberrations recurrently involved specific chromosomes and telomeric regions. Delayed chromosomal instability has since been demonstrated in a number of other cellular systems and it is clear that it can be induced by both high-LET and low-LET IR in most, but not all, cell types [5,93].

Immediately following IR exposure of normal human cells, a selective process commences that selects against highly damaged cells; highly damaged cells harboring multiple complex chromosome aberrations either die or do not give rise to viable progeny cells. Irradiated cells that are viable undergo a delay in the cell cycle to allow for repair of IR-induced DNA damage [94]. The length of the cell cycle delay is dependent on the extent and complexity of IR-induced damage, and most DNA repair is completed within the first few hours after irradiation [95]. These surviving cells undergoing their first cell division post-irradiation were shown to harbor both stable/balanced transmissible (translocations, inversions) and unstable/unbalanced non-transmissible rearrangements (dicentrics, rings, complex rearrangements) [92], with high-LET IR causing more DNA DSBs and complex chromosomal aberrations (defined as involving three or more breaks) that are clustered and may be less likely to be repaired correctly compared to equivalent doses of low-LET IR [96–99]. A recent study proposed that an increasing frequency of incomplete exchanges would be observed, irrespective of LET, with increasing numbers of chromosomal breaks and increasing complexity of chromosomal rearrangements that is not caused by the number of initial breaks, but is dependent on the spatial proximity between the breaks [100].

Transmissible mutations that can be propagated to progeny cells are believed to be fixed during DNA synthesis and cell proliferation, and unstable aberrations and those chromosomal lesions not compatible with cell survival are eliminated at subsequent cell divisions post-irradiation, decreasing by half at each cell generation [101]. Consequently, a few passages after irradiation, most karyotypes are apparently normal, with few remaining balanced/transmissible anomalies, and these cells may harbor radiation-induced recessive gene mutations that accumulate with each successive generation. At later passages, unstable chromosomal rearrangements reappear, mostly non- or poorly transmissible dicentrics that recurrently involve specific chromosomes in telomeric end-to-end associations. The occurrence of IR-induced instability was shown to be further delayed in late passages after irradiation with higher LET IR [91,92]; therefore, it can be concluded that high-LET IR has a higher capacity to induce delayed genomic instability compared to low-LET IR [102]. Furthermore, long-term instability can even be induced by a single alpha-particle [103] or carbon ion [104] from a focused microbeam, as well as following cytoplasmic irradiation with alpha particles [105,106]. Eventually, these IR-induced or pre-existing recessive mutations may be unmasked and amplified, and upon loss of tumor suppressor function, those cells that harbor genetic alterations that give them a proliferative advantage invade the cell population. Continuing chromosomal instability and cell proliferation may be key elements of the initiation and progression of multi-stage carcinogenesis [107,108].

Meanwhile, the discovery of "non-targeted radiation-induced bystander effects" by Nagasawa and Little in 1992 [80] brought about a new model of interaction between an irradiated cell and IR. In these early studies of the bystander effect, alpha-particle irradiation of only 1% of Chinese hamster ovary nuclei in a cell population induced sister chromatid exchanges in more than 30% of the cells, which is significantly more than would be expected under the target theory. These findings suggested that communication of stress signals exists between directly irradiated and neighboring non-irradiated bystander cells. Over the last two decades, further data have emerged that support the validity of this new non-targeted theory in a variety of cell and animal models [5,93,109–111]. Bystander effects have a wide array of important implications on human health, as it is pertinent to situations where humans are partially exposed to low doses/low dose-rates of IR under bystander conditions, such as during cancer radiotherapy, deep space exploration, mining, or residential radon exposure, in which case a small fraction of cells is exposed to IR at any one time. An understanding of the mediating biochemical events may have profound implications for long-term human health risks, and may

lead to refinement of therapeutic protocols and increase the efficacy of radiotherapy [112–115].

Indeed, manifestations of non-targeted bystander effects (some harmful, others beneficial) are well described. It is well established that IR-induced bystander effects induce a spectrum of detrimental radiation damage in non-irradiated neighboring cells that are similar to those observed in directly irradiated cells [116,117]. These effects include chromosomal rearrangements, chromosomal aberrations, micronuclei, gene amplifications, gene mutations and neoplastic transformation, reduced cell survival (lethal mutations or delayed reproductive cell death), apoptosis, DNA damage, and mitochondrial alterations with increased ROS production [5,93,118]. The characterization of the induction of bystander effects by IR of different LET has proven to be challenging. While the induction of bystander effects following high-LET α-particle irradiation is well established [119–122], the effects following low-LET IR remains debatable [123], and knowledge of the induction of bystander effects following other types of high-LET IR is only beginning to emerge [124–129]. Delayed IR-induced chromosomal instability was also shown to occur in progeny of bystander cells in both in vitro and in vivo studies [5,93,130–132]. Indeed, progeny of bystander cells were shown to exhibit similar types of cellular stresses as cells that were directly exposed to IR, such as mitochondrial dysfunction and excess ROS production [118]. A recent study demonstrated that progeny of bystander cells exhibited similar types of chromosomal rearrangements and aberrations as those found in progeny of cells following direct cytoplasmic or nuclear IR exposure [105]. However, much conflicting data exists, as bystander effects are not universally observed, are highly variable even after high-LET IR exposure, and dependent on the individual donors or cell lines [123,127,133]. Furthermore, the mechanisms of how IR induces delayed chromosomal instability following both direct and indirect IR exposure is not yet well understood. However, based on previous studies in our laboratory, we postulate that this delayed chromosomal instability is due to telomere dysfunction following telomeric DNA damage.

3.3. Radiation-induced telomeric DNA damage

As discussed in the preceding section, direct exposure to IR of high- or low-LET is well known to cause DNA damage, both from the direct traversal of the radiation particle itself or from radiation-induced physiological changes in the cell or tissue; these physiological changes are also seen in their progeny cells, as well as in their bystander cells and their progeny. Similarly, radiation damage of telomeres can also occur directly (via ionization events via direct traversal of IR within telomere sequences) or indirectly (via post-irradiation telomere uncapping and alterations in telomere maintenance mechanisms) [134]. Since telomeres make up only a tiny portion (0.02%) of the total human genome [135], the probability that a radiation particle will directly traverse a telomeric sequence is very small. Therefore, IR-induced damage of telomeres more likely occurs through perturbations of telomere maintenance post-irradiation. These perturbations may continue in the progeny of directly irradiated cells, and similar telomere dysfunction may occur in non-irradiated bystander cells and their progeny.

Telomeres have been shown to be particularly sensitive to damage from oxygen species [136], which have been well established to be formed in excess following direct and indirect IR exposure due to mitochondrial dysfunction and oxidative stress that can persist long after the initial exposure in progeny cells [118]. As mentioned in Section 3.1, IR traversing through cells or tissues inevitably interacts with atoms or molecules, especially water which makes up 80% of the cell, to produce free radicals (e.g. hydroxyl, superoxide radicals) and other ROS. These excess oxygen species can go on to damage critical targets in the vicinity, such as DNA. As discussed in Section 2.3, telomeres and sub-telomeres, as well as interstitial telomeric sequences, have been shown to be particularly sensitive to DNA damage. The guanine-triplet repeats in telomeric sequences (5′-GGG-3′) were shown to be preferential targets for oxidative damage [136]. The presence of oxidized guanine bases in telomeric nucleotides has been shown to disrupt telomerase activity [137] as well as inhibit the binding of TRF1 and TRF2 [138]. Excess ROS has also been shown to generate other oxidative DNA lesions including oxidized bases and single-strand breaks (SSBs) containing modified 3′-ends, which are modified mainly by the base excision repair (BER) pathway [139]. Altogether, this damage interferes with DNA replication and results in telomere shortening and loss in cells undergoing oxidative stress [140]. Antioxidant treatment, such as over-expression of antioxidant enzymes such as manganese superoxide dismutase (MnSOD), has been shown to slow down IR-induced acceleration of telomere shortening in directly irradiated cells [141,142] as well as bystander cells [143], illustrating that antioxidant defense capacity is important in TL control.

Additionally, telomeres have been shown to be hypersensitive to damage following ultraviolet (UV) irradiation, a type of non-ionizing radiation. As UV-induced DNA damage is a preeminent risk factor in the development of skin cancer, its effects on telomeres, along with the contribution of UV-induced bystander effects, may have important implications for human health. UV radiation causes the formation of cyclobutane pyrimidine dimers (CPD) between two adjacent pyrimidine bases (cytosine and thymine), and the pyrimidine-rich telomeric sequences (5′-TTAGGG/CCCTAA-3′) make telomeres hotspots for UV-induced damage. Indeed, one important study showed that there was a seven-fold higher induction of CPDs at the telomeres than in the rest of the genome. TT-CPDs on the G-strand were the most frequent dimer formed, and CC-CPDs and CT-CPDs were formed to a lesser extent on the C-strand [144]. The repair of UV-induced damage via the nucleotide excision repair (NER) pathway is well characterized, and repair of this damage was demonstrated to be independent of telomerase status in human cells [145]. Furthermore, it has been suggested that cells may be able to tolerate unrepaired CPDs at telomeres and continue to proliferate without acceleration of telomere shortening, indicating that cells can somehow tolerate chronic UV exposure in order to avoid genetic catastrophe [144].

3.4. Mechanisms for the transmission of radiation-induced damage

Studies to determine the mechanisms for the transmission of IR-induced genomic damage during cell proliferation have highlighted its complexity. The fact that IR-induced genomic instability is transmitted through many generations after irradiation suggests that there may be a mechanism by which the effects of radiation exposure are preserved. Little is known about the mechanisms involved in the maintenance of genomic instability across multiple cell divisions in affected clonal populations; however, existing data strongly implicate heritable epigenetic deregulation [146–148] paralleled by persistent changes in oxidative metabolism [149,150]. Since radiation-induced genomic instability induces increased rates of mutations and chromosomal aberrations, characteristic of the beginning stages of cancer, it has been suggested to be one of the driving forces behind radiation-induced carcinogenesis [108].

Several different mechanisms for the propagation of IR-induced genomic instability have been proposed, including the transmission of nonlethal, potentially unstable chromosome regions (PUCR). As DSBs are not likely inherited during cellular proliferation, memory of

the initial radiation damage is likely not transmitted via direct inheritance of the DNA damage itself to progeny. It has been proposed that PUCRs are created via DDR mechanisms that convert the initial IR-induced DSBs to other types of structures in the genome, such as gross chromosomal rearrangements and large chromosome deletions. These changes in the genome may be transmitted to progeny of surviving cells for many generations following irradiation, and may be responsible for the initiation of delayed genomic instability in long-term progeny of irradiated cells. Indeed, though these PUCRs are unstable, they are able to persist for prolonged periods [151]. Alternatively, they may be transmitted through the B/F/B cycle [152]. PUCRs can be reactivated by chance to cause delayed, unscheduled DNA DSBs in the progeny of surviving cells, leading to delayed p53 activation and delayed manifestations of genomic instability [153].

PUCRs can occur either near the telomeres or in interstitial regions (knowing that interstitial telomeric sequences are potentially more unstable than non-telomeric sequences), and would lead to different consequences in the long-term progeny. PUCRs near the telomere region could cause telomere instability, and may explain how chromosome aberrations involving telomere sequences lead to genomic instability across many generations [154]. PUCRs near telomeres might be less detrimental to the cell, as it would result in loss of less genetic material compared to PUCRs at interstitial regions, which may lead to chromosome fragments or large deletions. As telomeric PUCRs would not be lethal, these abnormal structures would be transmissible for many generations and may be reactivated by natural processes such as DNA replication. However, the global existence of PUCRs in the genome remains to be confirmed [151,155].

Nonetheless, telomeres themselves can be considered as PUCRs. Indeed, the role of telomeres in delayed chromosomal instability was first suggested from the observation that telomeric end-to-end associations recurrently involving specific chromosomes were observed at the time that unstable chromosomal rearrangements reappeared at late passages in the progeny of irradiated cells. No drastic changes in mean TL were observed along with these chromosome fusions and no interstitial telomeric sequences were detected at the junctions of these end-to-end associations. This suggested that chromosomal instability in late passage progeny of irradiated cells was correlated with telomere shortening associated with either cell divisions or telomere loss due to a DNA DSB occurring near the end of a chromosome [91,92,156,157]. In addition, the loss of a single telomere in cancer cells was shown to lead to instability in multiple chromosomes [158]. Other mechanisms responsible for delayed instability have been suggested, including telomere loss and sister chromatid fusion events, as well as chromosome fusions involving interstitial telomere repeat-like sequences and amplification via B/F/B cycles in both rodent and human cells [69,75,159]. It has also been suggested that terminal deletions and transmission of telomere-free chromosomes may be key events in the emergence of late effects after exposure to high-LET IR [160]. Overall, despite recent efforts, the detailed mechanisms for the transmission of genomic instability following direct IR exposure still remain obscure.

Meanwhile, though manifestations of the bystander effect are well described, as discussed in Section 3.2, the mechanisms of propagation of the IR-induced stress signals from directly irradiated to bystander cells are not yet well characterized. Studies of the bystander effect focus on one or a combination of two mechanisms: intercellular communication via physical cell-to-cell channels called gap junctions [121,161,162], or via secretion of soluble stress factors by irradiated cells that can be shared with non-irradiated cells within a certain proximity [163]. These two mechanisms may be relevant to radiotherapy, as the effects of IR can be observed in neighboring, non-irradiated cells, and may, at least partially, explain phenomena such as the abscopal effect [4]. The exact nature of the bystander signals communicated via gap junctions and soluble factors in culture media are not yet well characterized, but may involve up-regulation of stress-induced cytokines, including TGFα, TGFβ, nitric oxide, interleukin-8, and the pro-inflammatory cytokine Tnfα (involved in the generation of ROS and apoptosis) [115,164,165]. Excess long-lived ROS in culture media following irradiation have been documented to be important mediators of bystander signaling [161,166], and the induction of bystander events was shown to be inhibited by manipulation at the mitochondrial level [167] and by using free radical scavengers [122].

Furthermore, the mechanisms of the transmission of bystander-induced damage to cause long-term genomic instability in the progeny of bystander cells, and whether telomeres play a role in the propagation of long-term bystander effects, remain relatively unstudied. However, bystander cells and their progeny were shown to exhibit similar cellular stresses as in directly irradiated cells and their progeny such as persistent oxidative stress [118], dysfunctional cell cycle checkpoints [125] and DDR pathways [168–170], and perturbations in gene expression [171,172]. Therefore, the propagation of bystander-induced genomic instability in bystander cells and their progeny may involve similar mechanisms as the transmission of instability following direct IR exposure. Heritable epigenetic changes that change cellular signaling processes without changing the primary structure of the DNA, such as DNA methylation, histone modification, and small RNA mediated silencing, may also be involved [148,173]. Characterization of the mechanisms of transmission of chromosomal instability and telomere dysfunction induced by IR and the bystander effects may have important implications in human health, especially in terms of the long-term effects of radiotherapy and radiation-induced secondary cancers [111].

3.5. Radiation-induced changes in telomere length and telomerase activity

As discussed above, the presence of DNA damage at telomeres may lead to acceleration of telomere shortening, as these lesions may interfere with proper DNA replication of telomeres during cell proliferation. Whether or not IR induces accelerated telomere shortening in normal human cells is important to consider, as it is associated with accelerated aging and telomere dysfunction. This dysfunction, as discussed in previous sections, is intimately linked to chromosomal instability, can lead to apoptosis or replicative senescence, and can contribute to the multi-step carcinogenesis process. However, much conflicting data exist concerning the effect of IR on TL in normal human cells, especially with respect to the contributions of LET and bystander effects.

A few studies suggest that the immediate effects of IR on TL in normal human cells are dose- and LET-dependent. At 24 and 48 h after in vitro irradiation with low doses in the range of 0.1–1 Gy, no changes in TL in normal human AG1522 fibroblasts were observed after either low- or high-LET irradiation [174]. However, following a higher dose of 4 Gy in normal human HFFF2 fibroblasts, no changes in TL were observed after low-LET X-ray exposure, whereas telomere elongation was detected after high-LET proton irradiation [175,176]. Furthermore, in vitro gamma-irradiation at clinical doses (18 to >40 Gy) were shown to induce telomere shortening in normal human lymphocytes and fibroblasts at 24 h post-irradiation [177]. One recent clinical study found that while mean TL was not affected in peripheral leukocytes from patients after in vivo radiation treatment with a mean dose of 52 Gy, there was a significant decrease in the proportion of cells with short telomeres [178], which may have been subjected to elongation by IR-induced telomerase activation [179]. Overall, these results

suggest that measurable changes in TL in human cells are seen only after high doses of IR exposure. However, it remains unclear whether this is truly radiation-induced telomere shortening or cell selection in the population based on survival following irradiation, as discussed in Section 3.2.

A few studies of the long-term effects of IR on TL indicate that while normal human fibroblasts irradiated with 4 Gy of low-LET X-rays showed no changes in TL at 24 h post-irradiation, they exhibited significant telomere shortening at 4 days, followed by delayed telomere elongation at 15 days after irradiation. On the other hand, the equivalent dose of high-LET protons caused telomere lengthening shortly after irradiation as well as at longer harvesting times [175,176]. This has also been previously shown in interphase nuclei [180]. These results suggest that modulation of TL occurs in different ways following lesions of differing complexity, such as those expected after low-LET vs. high-LET IR exposure. The induction of telomere elongation after 4 Gy of high-LET irradiation in human primary cells, which are telomerase-negative, may suggest an activation of the ALT pathway via recombination between telomere sequences following severe DNA damage [181]. The equivalent dose of low-LET X-ray irradiation, on the other hand, may elicit delayed telomere shortening due to indirect effects, such as oxidative stress [175]. As mentioned previously, there is accumulating evidence that IR-induced oxidative stress may continue for a long time following irradiation due to persistent effects on oxidative metabolism [118]. Additionally, the selective process against highly damaged cells as discussed in Section 3.2 may contribute to the telomere elongation seen in these later progeny. These IR-induced effects on TL may contribute to the rise of delayed chromosome instability observed in long-term progeny of irradiated cells. However, the long-term effects of low doses of IR on TL are largely unknown, and more studies are needed (e.g. effect of excess ROS on DDR proteins) to better understand the mechanisms involved in the long-term effects of IR on telomeres and to determine whether the effect of IR on TL conserves individual TL heterogeneity or renders the distribution of TL more homogeneous.

Concerning indirect IR exposure, not much is known of the short and long-term radiation-induced bystander effects on TL, despite the fact that manifestations of bystander-induced genetic instability are very well documented. Several studies suggest that bystander effects via media transfer may induce telomere shortening, coupled with mitochondrial dysfunction, excess ROS production, and apoptosis. Indeed, bystander lymphocytes with shorter telomeres displayed depolarized mitochondrial membranes and significantly higher levels of ROS. Telomere shortening in bystander cells appears to be independent of radiation dose (i.e. higher doses do not induce more telomere shortening or stronger bystander effects), and there seems to be a dose threshold at which the bystander signal is not induced [143,182]. However, further work is needed to verify these observations and to determine the molecular mechanisms behind these bystander effects at telomeres.

As the shelterin proteins are directly involved in maintaining TL, as discussed in previous sections, changes in TL after irradiation can be due to IR-induced changes in the shelterin proteins. However, little is known if and how IR affects shelterin protein levels. One study suggested that in vitro irradiation of normal human cells at clinical doses (18 to >40 Gy) induced a significant decrease in TPP1 and POT1, a slight decrease in TRF1 and TRF2, and no evident alterations in TIN2 and RAP1 [177]. This general decrease in shelterin protein levels after irradiation may correlate with the IR-induced telomere shortening observed in normal human cells. However, other mechanisms may be involved, and further work is needed to verify and explain these observations.

Additionally, as TL is maintained by telomerase activity, whether IR itself induces up-regulation of telomerase activity is important to consider, especially in terms of radiotherapy. Indeed, IR-induced up-regulation of telomerase activity in cancer cells would enhance radioresistance in these cells during treatment, and would require the use of telomerase inhibitors during radiotherapy. Inhibition of telomerase in cancer cells has been shown to impair tumor growth and sensitize cancer cells to radiation treatment, as discussed in Section 2.2.1. IR exposure was shown to up-regulate telomerase in human hematopoietic and cancer cells [183–188]. However, this is still a matter of debate, as much conflicting data exists. These discrepancies may be due to different methodologies such as different cell lines, varying radiation doses, and different time points after irradiation. Deciphering the mechanisms of IR-induced regulation of telomerase is important for the development of future cancer therapy methods.

3.6. Radiation sensitivity

In addition to the differences in biological effects as a function of radiation dose and quality in cancer radiotherapy, it is also important to consider inherent differences in sensitivity to IR. Indeed, it is well established that there is considerable variation in sensitivity to IR among both cancer patients and healthy individuals, and that radiation sensitivity can contribute significantly to the clinical outcomes of radiotherapy. For example, highly radiosensitive patients may develop early and/or late side effects due to radiation toxicity, while radioresistant patients may receive an insufficient dose of radiation due to dose limitations in current general radiotherapy protocols. A fast and reliable clinical method to determine both radioresistance in tumor cells and radiosensitivity in normal cells of cancer patients (to better personalize treatment) still remains to be established [189,190].

One of the biomarkers for radiosensitivity under consideration [191] is telomere length (TL) [192]. TL varies among healthy individuals (lengths strongly depending on both genetic and environmental factors) [193], and individuals with short telomeres have been shown to have higher frequencies of IR-induced micronuclei, a commonly used marker of cell damage and DSBs, than individuals with longer telomeres [194]. TL has indeed been well correlated with radiosensitivity in many in vivo and in vitro studies in telomerase-deficient mouse and human cells [134,195]. These studies established that there is an inverse correlation between radiation sensitivity and mean TL; that is, telomere shortening was shown to enhance radiosensitivity, though long telomeres did not necessarily render cells radioresistant. Late-passage normal human fibroblasts with short telomeres are more sensitive to IR than their younger counterparts with longer telomeres [196]. Whether this holds true in telomerase-positive cells is still debatable, as a recent study demonstrated no correlation between TL and radiosensitivity in this setting [43]. It has also been suggested that radiosensitivity is correlated with telomere loss, not mean TL, with no observable IR-induced changes in levels of telomerase expression [197]. The enhanced radiosensitivity observed in telomerase-deficient cells with short telomeres may be due to chromosome fusions that occur between the short telomeres and the radiation-induced DSBs, which interfere with the proper repair of the DSB, leading to the formation of chromosomal rearrangements [198,199].

Radiosensitivity is fairly well correlated with inhibition of telomerase activity in human cancer cells. Down-regulation or inhibition of telomerase activity, and the resulting telomere shortening, was shown to compromise the viability of cancer cells by causing senescence and impairing tumor growth; thus, as mentioned in Section 2.2.1, the use of telomerase inhibitors during cancer therapy may sensitize cancer cells to chemotherapy and radiotherapy [200–203]. Radioresistant carcinoma cells, on the

other hand, exhibited up-regulation of telomerase activity and longer telomeres [204,205]. The ability of telomerase to confer radioresistance may depend on its ability to preferentially elongate short, near-dysfunctional telomeres [179] and protect cells from IR-induced apoptosis and necrosis [206,207].

Radiosensitivity may also be closely linked with impairment of DDR processes. Telomere shortening may cause increased radiosensitivity by altering the kinetics of repair due to changes in chromatid structure that limits the access of DDR proteins; indeed, higher baseline levels of gamma-H2AX [208], considered to be a reliable marker for the detection of DSB even at very low doses [209], as well as delayed gamma-H2AX induction following irradiation (signifying delayed repair), were observed in older cells [208]. These delayed kinetics of DNA repair have been observed in both normal and pathologic aging [210]. Moreover, patients with genetic defects in DDR, including ataxia telangiectasia, Fanconi anemia, Nijmegen breakage syndrome, and xeroderma pigmentosum, have been shown to be highly sensitive to IR. These patients were also shown to have shorter telomeres compared to normal cells, indicating that these genetic defects also affect telomere maintenance [211]. Defects in NHEJ proteins (such as DNA-PKcs) and HR proteins (such as BRCA1 and BRCA2) are associated with increased sensitivity to IR and other DNA damaging agents, making inhibitors of proteins in these pathways potentially useful for cancer therapy [212].

Overall, the many examples of conflicting data highlight the complexity of the relationships between IR, radiosensitivity, TL, telomerase activity, and DDR. At the present time, the existing data remain inconclusive, and the direct effects of IR on telomeres and their maintenance remain unclear.

4. Telomeres: a key player in the process of radiation-induced carcinogenesis

Carcinogenesis is a complex, multi-step process that requires the acquisition of six biological capabilities that allow cancer cells to survive, proliferate, and disseminate. These hallmarks of cancer include the ability to sustain proliferative signaling, evade growth suppressors, resist cell death, enable replicative immortality, induce angiogenesis, and activate invasion and metastasis. Cells acquire each function at different times during the course of carcinogenesis via unique mechanisms depending on tumor type. Genomic instability is an important enabling factor that aids in the acquisition of these hallmark traits of cancer, as it generates mutations, chromosomal rearrangements, and other types of genetic alterations that may facilitate the unmasking of recessive mutations via LOH. As the process of carcinogenesis requires accumulation and unmasking of recessive mutations at a combination of oncogenes and tumor suppressor genes, genomic instability and LOH can thereby fuel tumor progression [213]. As discussed in this paper, genomic instability can be induced by deregulation of telomere length, shelterin proteins, and DNA damage repair proteins, factors that have all been linked to cancer progression. Furthermore, direct and indirect exposure to IR induces a variety of types of cellular and DNA damage and eventually leads to long-term IR-induced genomic instability. We propose, therefore, that modifications of telomere maintenance induced following direct or indirect IR exposure, and the resulting accelerated aging, play a central role in the emergence of delayed genetic instability following irradiation, and leads to higher frequencies of radiation-induced carcinogenesis, as illustrated in Figs. 1–3.

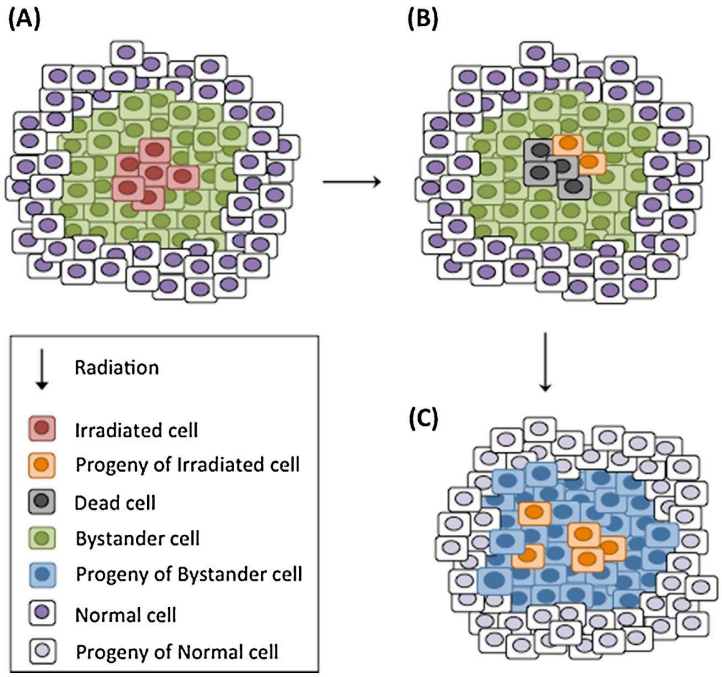

Fig. 1. Model for delayed radiation effects and accelerated aging following irradiation at the tissue level. (A) Cells are irradiated with a high dose of ionizing radiation. Bystander cells in the proximity of directly exposed cells would be subjected to stress signals propagated by the irradiated cells. (B) The majority of directly irradiated cells die, but the few surviving cells may harbor radiation-induced damages. (C) To replenish the tissue following death of directly irradiated cells and to compensate for the slower dividing progeny of directly irradiated cells, the surrounding bystander cells may divide more than they normally would without radiation exposure, leading to faster telomere shortening and localized, accelerated aging in the irradiated tissue.

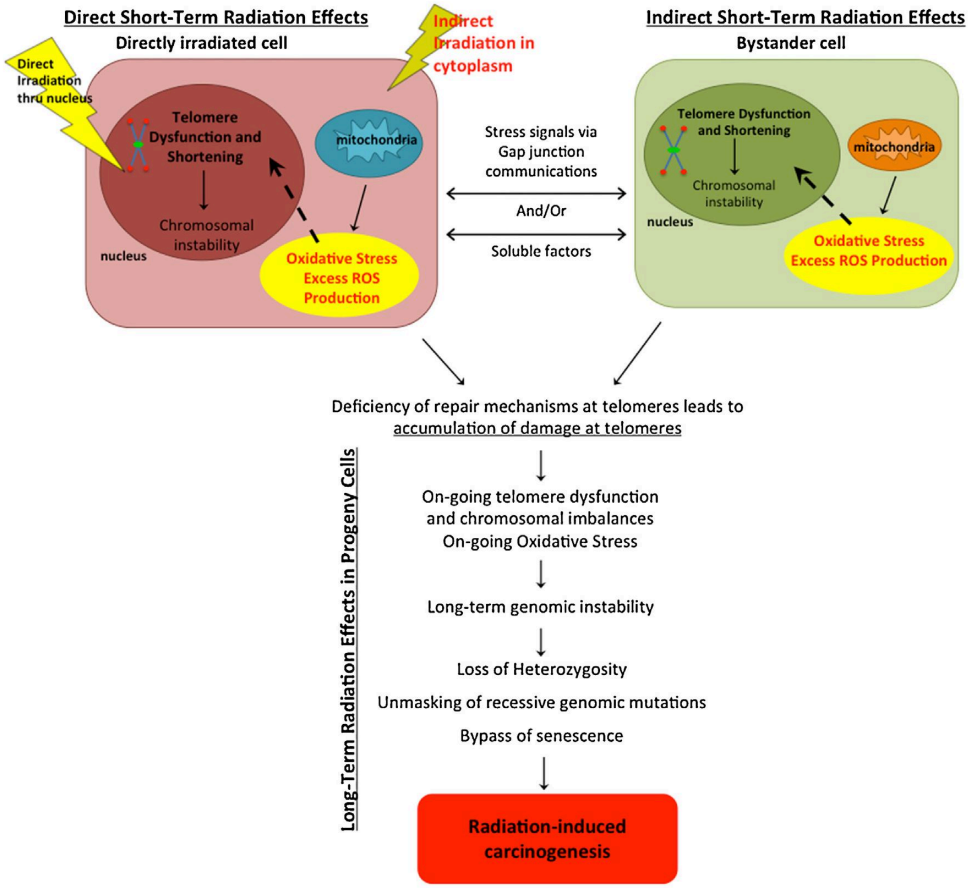

Fig. 2. Proposed hypothesis of short-term and long-term effects of exposure to ionizing radiation in directly irradiated and bystander cells at the cellular level.

The acceleration of aging *at the tissue level*, as shown in Fig. 1, would commence upon the induction of cell death following exposure to a high dose of radiation in the majority of directly irradiated cells (Fig. 1A). Bystander cells within the proximity of directly exposed cells would be subjected to stress signals propagated by the irradiated cells (Fig. 1B). Directly irradiated cells that survive may continue to divide, with the resulting progeny cells harboring long-term effects of radiation exposure and possibly dividing more slowly than the surrounding cells. In order to replenish the tissue with new cells following the death of irradiated cells and to compensate for the more slowly dividing progeny of directly irradiated cells, the unexposed bystander cells may divide more rapidly than they normally would without IR exposure. This would result in faster telomere shortening and localized, accelerated replicative aging in the irradiated tissue of both the directly irradiated and bystander cells (Fig. 1C).

More specifically, *at the cellular level*, as illustrated in Fig. 2, surviving cells of direct IR exposure, such as in Fig. 1, may harbor dysfunctional telomeres either via a direct hit at the telomere level, which is unlikely due to the infinitesimal length compared to the length of the whole genome, or via the more probable, indirect processes such as radiation-induced mitochondrial dysfunction and the resulting excess ROS production and oxidative stress. These stresses can be communicated to neighboring bystander cells via gap junctions and/or soluble factors, which may then create the same type of oxidative stress in bystander cells. Due to deficiencies in repair mechanisms at telomeres in addition to natural aging processes and continuous exposure to DNA damaging agents throughout life, recessive mutations may accumulate throughout the genome leading to long-term genomic instability due to on-going, long-term telomere dysfunction, chromosomal imbalances, and oxidative stress in progeny cells.

Furthermore, *at the telomeric level*, as illustrated in Fig. 3, continuous telomere shortening will eventually lead to dysfunctional telomeres that signal DDR pathways. Proper signaling of approximately 5 dysfunctional telomeres has been proposed [31] to trigger senescence and arrested proliferation. The *acceleration of telomere shortening* due to exposure to IR and/or other DNA damaging agents during life may lead to acceleration of this entire process. However, as long as replicative senescence is induced, as they say, "all will be well." We propose that it is what happens when there are 1–4 dysfunctional telomeres that is key to the fate of the cell/being. This low level of telomere loss, that does not induce signaling, would allow a low level of chromosomal instability that could lead to the emergence of cells with a proliferative advantage. If, for example, defects in DNA repair responses and cell cycle checkpoints induce increasing chromosomal instability and allow bypass of senescence, cells continue to divide, and telomeres continue to shorten until "telomeric crisis" is reached. Loss of whole chromosomes or partial chromosomal arms may be induced due to chromosomal instability caused by telomere loss, leading to loss of heterozygosity (LOH), a

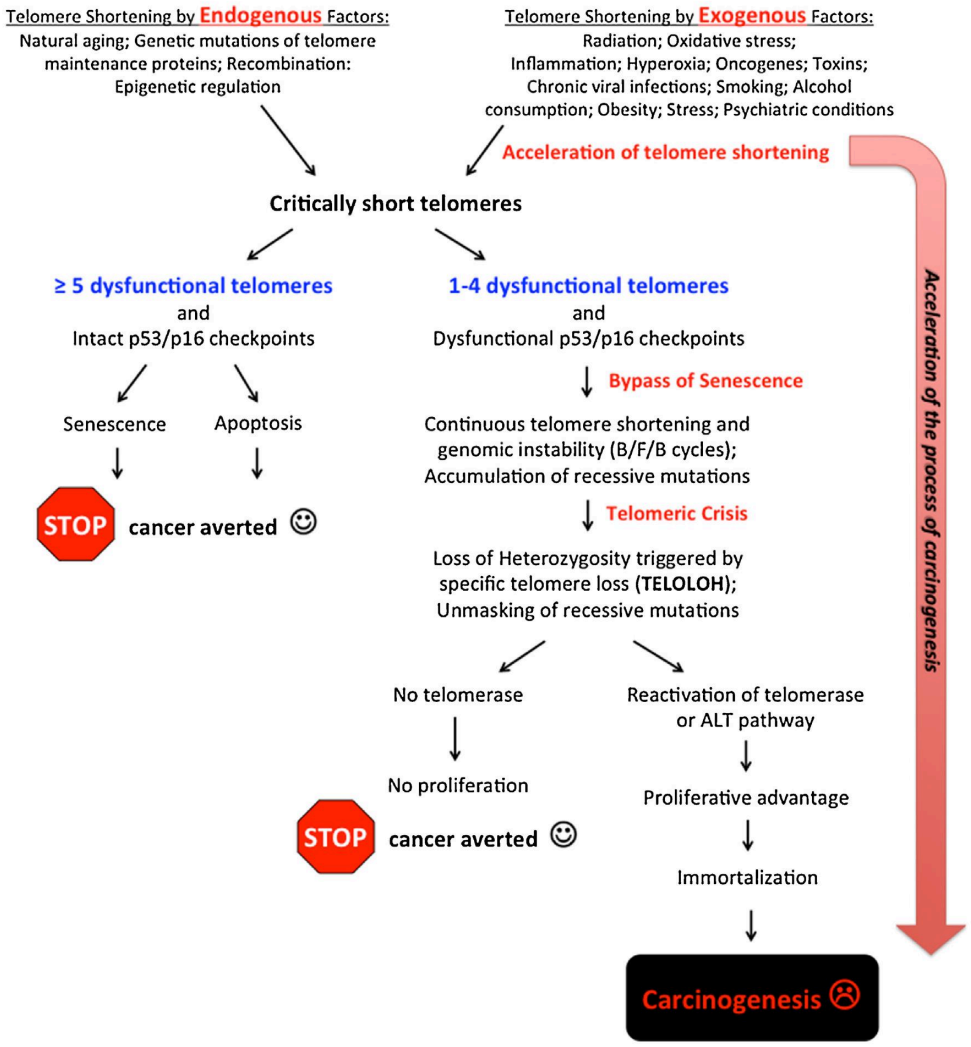

Fig. 3. Proposed impact of telomere length heterogeneity on the processes of cellular aging, senescence, crisis, and carcinogenesis. During the lifespan of the cell, telomere length decreases with each cell division and cells accumulate recessive mutations in the genome. Telomere shortening can be accelerated due to both endogeneous and exogeneous factors such as exposure to DNA damaging agents such as ionizing radiation. With intact cell cycle checkpoints and DNA damage repair responses, senescence will be induced when 5 dysfunctional telomeres are present in the cell. Even with the induction of premature senescence due to the acceleration of telomere shortening, as long as replicative senescence is induced, the cell would no longer have a risk of the initiation of carcinogenic processes. If, however, defects in cell cycle checkpoints and DNA damage repair responses occur before the threshold of five dysfunctional telomeres is reached, the cell would be able to initiate the carcinogenic process. Furthermore, the acceleration of telomere shortening may lead to acceleration of this entire process. The pace of the process of carcinogenesis is dependent on the intra-individual and inter-individual heterogeneity of telomere length.

phenomenon that we have coined "TELOLOH" which is triggered by the shortest telomere that will first reach the threshold of instability [214]. Thus, in a single step via telomere-induced chromosomal imbalances, the recessive mutations of hundreds of genes that have accumulated in the genome become unmasked; these recessive mutations would otherwise remain silent unless the other, normal allele becomes mutated, a highly unlikely event. Coupled with activation of telomerase and/or ALT pathways, these mutant cells may gain a proliferative advantage, leading to cell immortalization and eventually, carcinogenesis [107,214]. Therefore, as telomere dysfunction (natural and/or IR-induced) may cause and propagate genetic instability and LOH, *telomeres may be considered as a key player in the process of radiation-induced carcinogenesis*.

Importantly, the rate at which these processes occur will vary depending on the inherent TL of the given individual, which may be considered as the cornerstone of individual predisposition to carcinogenesis. Indeed, as previously mentioned, there are inter-individual and intra-individual differences in TL; that is, TL varies among healthy individuals [193], and it also varies on each chromosome arm in a cell of a given individual [23], with this inherent cellular heterogeneity of TL being conserved throughout the lifespan of the individual [24]. Therefore, the starting point (i.e. the inherent TL and TL heterogeneity both per individual and within the individual) on the road to senescence, crisis (premature or not), and/or carcinogenesis can determine whether that road is taken, and how long the journey will be. Furthermore, along the road to carcinogenesis, a careful level of genetic instability must be

Table 3
Well-established knowledge of the effects of direct ionizing radiation (IR) exposure and the bystander effect.

	Direct effects	Bystander effects
IR ⇒ Oxidative stress	WD [118]	WD [161]
IR ⇒ Long-term oxidative stress	WD [118]	WD [171]
IR ⇒ Long-term chromosomal instability	D [5,93,104]	PD [5,93]
IR ⇒ Shelterin protein levels	PD	PD
IR ⇒ Telomere dysfunction	PD	PD
IR ⇒ Long-term telomere dysfunction	PD	PD
LET of IR ⇒ Directly proportional to complexity of induced biological damage	WD [83]	CF [119,272]
Telomere dysfunction ⇒ Chromosomal instability	D [69]	PD
Telomere length ⇔ Radiation sensitivity	D [134]	PD

WD, well documented; D, documented; PD, poorly documented; CF, conflicting findings.

maintained, as 'too much' instability would be detrimental and would result in cell death or senescence, while 'too little' instability would slow the progression to tumorigenesis. Thus, just the right amount of instability would minimize the rate of cell death/senescence while maximizing the rate of progression to carcinogenesis [215].

As humans are constantly exposed to IR via natural and/or man-made sources, it is important to study the immediate and long-term consequences of IR exposure, and the contribution of the bystander effect, on telomeres and telomere maintenance. The understanding of these mechanisms may have important implications in human health, cancer radiotherapy regimens, and radiation protection protocols. Considering this wide range of important applications, it is of great importance to study the radiation-induced effects on telomeres and their maintenance, and the role of telomeres in the manifestation of radiation-induced effects. Much work is still needed to confirm not only the fundamental effects of various types of IR on telomeres and telomere maintenance in normal human cells, but to determine if/how telomeres play a role in the mechanisms of these direct and indirect radiation-induced effects (see Table 3). Understanding these mechanisms, and studying if/how telomeres play a role in the transmission of these radiation-induced effects during cell proliferation to progeny of both directly irradiated and bystander cells may explain the instabilities observed in these cells and enhance our understanding of how they arise. This knowledge can be critical to the determination of the long-term effects of IR on human health, and can contribute to our understanding of how radiation-induced cancers arise.

Conflict of interest statement

The authors declare that there are no conflicts of interest.

Acknowledgements

Work in the laboratory has been supported by the European Community Seventh Framework (Euratom) Grants EpiRadBio and DoReMi. WMH was supported by the European Community Seventh Framework (Euratom) Grant DoReMi and GS was supported by an MESR fellowship from the French Ministry of Education. EA was supported by the grant CA049062 from the National Institute of Health, USA.

References

[1] E.J. Hall, Radiation and Life, 2nd ed., Pergamon, New York, 1984.
[2] D.J. Brenner, E.J. Hall, Computed tomography – an increasing source of radiation exposure, N. Engl. J. Med. 357 (2007) 2277–2284.
[3] W.D. Newhauser, M. Durante, Assessing the risk of second malignancies after modern radiotherapy, Nat. Rev. Cancer 11 (2011) 438–448.
[4] K.M. Prise, J.M. O'Sullivan, Radiation-induced bystander signalling in cancer therapy, Nat. Rev. Cancer 9 (2009) 351–360.
[5] W.F. Morgan, Non-targeted and delayed effects of exposure to ionizing radiation: II. Radiation-induced genomic instability and bystander effects in vivo, clastogenic factors and transgenerational effects, Radiat. Res. 159 (2003) 581–596.
[6] I.B. Mosse, Genetic effects of ionizing radiation – some questions with no answers, J. Environ. Radioact. 112 (2012) 70–75.
[7] W.F. Morgan, W.J. Bair, Issues in low dose radiation biology: the controversy continues. A perspective, Radiat. Res. 179 (2013) 501–510.
[8] B. McClintock, The stability of broken ends of chromosomes in *Zea mays*, Genetics 26 (1941) 234–282.
[9] H. Muller, The remaking of chromosomes, Collect. Net 13 (1938) 181–198.
[10] E.H. Blackburn, C.W. Greider, J.W. Szostak, Telomeres and telomerase: the path from maize, *Tetrahymena* and yeast to human cancer and aging, Nat. Med. 12 (2006) 1133–1138.
[11] T. de Lange, Shelterin: the protein complex that shapes and safeguards human telomeres, Genes Dev. 19 (2005) 2100–2110.
[12] T. de Lange, T-loops and the origin of telomeres, Nat. Rev. Mol. Cell Biol. 5 (2004) 323–329.
[13] J.D. Griffith, L. Comeau, S. Rosenfield, R.M. Stansel, A. Bianchi, H. Moss, T. de Lange, Mammalian telomeres end in a large duplex loop, Cell 97 (1999) 503–514.
[14] J.L. Huppert, Hunting G-quadruplexes, Biochimie 90 (2008) 1140–1148.
[15] H.J. Lipps, D. Rhodes, G-quadruplex structures: in vivo evidence and function, Trends Cell Biol. 19 (2009) 414–422.
[16] D. Hockemeyer, J.P. Daniels, H. Takai, T. de Lange, Recent expansion of the telomeric complex in rodents: two distinct POT1 proteins protect mouse telomeres, Cell 126 (2006) 63–77.
[17] W. Palm, T. de Lange, How shelterin protects mammalian telomeres, Annu. Rev. Genet. 42 (2008) 301–334.
[18] D.J. Taylor, E.R. Podell, D.J. Taatjes, T.R. Cech, Multiple POT1-TPP1 proteins coat and compact long telomeric single-stranded DNA, J. Mol. Biol. 410 (2011) 10–17.
[19] D. Hockemeyer, W. Palm, T. Else, J.P. Daniels, K.K. Takai, J.Z. Ye, C.E. Keegan, T. de Lange, G.D. Hammer, Telomere protection by mammalian Pot1 requires interaction with Tpp1, Nat. Struct. Mol. Biol. 14 (2007) 754–761.
[20] J.Z. Ye, J.R. Donigian, M. van Overbeek, D. Loayza, Y. Luo, A.N. Krutchinsky, B.T. Chait, T. de Lange, TIN2 binds TRF1 and TRF2 simultaneously and stabilizes the TRF2 complex on telomeres, J. Biol. Chem. 279 (2004) 47264–47271.
[21] K.K. Takai, T. Kibe, J.R. Donigian, D. Frescas, T. de Lange, Telomere protection by TPP1/POT1 requires tethering to TIN2, Mol. Cell 44 (2011) 647–659.
[22] A. Sfeir, S. Kabir, M. van Overbeek, G.B. Celli, T. de Lange, Loss of Rap1 induces telomere recombination in the absence of NHEJ or a DNA damage signal, Science 327 (2010) 1657–1661.
[23] J.P. Pommier, L. Sabatier, Telomere length distribution. Digital image processing and statistical analysis, Methods Mol. Biol. 191 (2002) 33–63.
[24] J. Graakjaer, C. Bischoff, L. Korsholm, S. Holstebroe, W. Vach, V.A. Bohr, K. Christensen, S. Kolvraa, The pattern of chromosome-specific variations in telomere length in humans is determined by inherited, telomere-near factors and is maintained throughout life, Mech. Ageing Dev. 124 (2003) 629–640.
[25] C.B. Harley, A.B. Futcher, C.W. Greider, Telomeres shorten during ageing of human fibroblasts, Nature 345 (1990) 458–460.
[26] T. de Lange, How telomeres solve the end-protection problem, Science 326 (2009) 948–952.
[27] H. Takai, A. Smogorzewska, T. de Lange, DNA damage foci at dysfunctional telomeres, Curr. Biol. 13 (2003) 1549–1556.
[28] C.M. Raynaud, J. Hernandez, F.P. Llorca, P. Nuciforo, M.C. Mathieu, F. Commo, S. Delaloge, L. Sabatier, F. Andre, J.C. Soria, DNA damage repair and telomere length in normal breast, preneoplastic lesions, and invasive cancer, Am. J. Clin. Oncol. 33 (2010) 341–345.
[29] C.M. Raynaud, S.J. Jang, P. Nuciforo, S. Lantuejoul, E. Brambilla, N. Mounier, K.A. Olaussen, F. Andre, L. Morat, L. Sabatier, J.C. Soria, Telomere shortening is correlated with the DNA damage response and telomeric protein down-regulation in colorectal preneoplastic lesions, Ann. Oncol. 19 (2008) 1875–1881.
[30] C.M. Raynaud, O. Mercier, F. Commo, P. Dartevelle, C. Gomez-Roca, V. de Montpreville, L. Sabatier, J.C. Soria, Telomere length, telomeric proteins and DNA damage repair proteins are differentially expressed between primary lung tumors and their adrenal metastases, Lung Cancer 65 (2009) 144–149.
[31] Z. Kaul, A.J. Cesare, L.I. Huschtscha, A.A. Neumann, R.R. Reddel, Five dysfunctional telomeres predict onset of senescence in human cells, EMBO Rep. 13 (2012) 52–59.
[32] F. d'Adda di Fagagna, P.M. Reaper, L. Clay-Farrace, H. Fiegler, P. Carr, T. Von Zglinicki, G. Saretzki, N.P. Carter, S.P. Jackson, A DNA damage checkpoint response in telomere-initiated senescence, Nature 426 (2003) 194–198.
[33] L. Hayflick, P.S. Moorhead, The serial cultivation of human diploid cell strains, Exp. Cell Res. 25 (1961) 585–621.
[34] C.M. Counter, A.A. Avilion, C.E. LeFeuvre, N.G. Stewart, C.W. Greider, C.B. Harley, S. Bacchetti, Telomere shortening associated with chromosome instability is arrested in immortal cells which express telomerase activity, EMBO J. 11 (1992) 1921–1929.
[35] C.M. Counter, F.M. Botelho, P. Wang, C.B. Harley, S. Bacchetti, Stabilization of short telomeres and telomerase activity accompany immortalization of Epstein–Barr virus-transformed human B lymphocytes, J. Virol. 68 (1994) 3410–3414.
[36] C. Ducray, J.P. Pommier, L. Martins, F.D. Boussin, L. Sabatier, Telomere dynamics, end-to-end fusions and telomerase activation during the human fibroblast immortalization process, Oncogene 18 (1999) 4211–4223.

[37] C.B. Harley, Telomere loss: mitotic clock or genetic time bomb? Mutat. Res. 256 (1991) 271–282.
[38] C.W. Greider, E.H. Blackburn, Identification of a specific telomere terminal transferase activity in *Tetrahymena* extracts, Cell 43 (1985) 405–413.
[39] T.M. Bryan, A. Englezou, J. Gupta, S. Bacchetti, R.R. Reddel, Telomere elongation in immortal human cells without detectable telomerase activity, EMBO J. 14 (1995) 4240–4248.
[40] B. Luke, J. Lingner, TERRA: telomeric repeat-containing RNA, EMBO J. 28 (2009) 2503–2510.
[41] C.M. Azzalin, P. Reichenbach, L. Khoriauli, E. Giulotto, J. Lingner, Telomeric repeat containing RNA and RNA surveillance factors at mammalian chromosome ends, Science 318 (2007) 798–801.
[42] B. Balk, A. Maicher, M. Dees, J. Klermund, S. Luke-Glaser, K. Bender, B. Luke, Telomeric RNA–DNA hybrids affect telomere-length dynamics and senescence, Nat. Struct. Mol. Biol. 20 (2013) 1199–1205.
[43] A. Smirnova, R. Gamba, L. Khoriauli, V. Vitelli, S.G. Nergadze, E. Giulotto, TERRA expression levels do not correlate with telomere length and radiation sensitivity in human cancer cell lines, Front. Oncol. 3 (2013) 115.
[44] C.W. Greider, E.H. Blackburn, The telomere terminal transferase of *Tetrahymena* is a ribonucleoprotein enzyme with two kinds of primer specificity, Cell 51 (1987) 887–898.
[45] W.E. Wright, M.A. Piatyszek, W.E. Rainey, W. Byrd, J.W. Shay, Telomerase activity in human germline and embryonic tissues and cells, Dev. Genet. 18 (1996) 173–179.
[46] A.M. Zahler, J.R. Williamson, T.R. Cech, D.M. Prescott, Inhibition of telomerase by G-quartet DNA structures, Nature 350 (1991) 718–720.
[47] Y. Zhang, L.Y. Chen, X. Han, W. Xie, H. Kim, D. Yang, D. Liu, Z. Songyang, Phosphorylation of TPP1 regulates cell cycle-dependent telomerase recruitment, Proc. Natl. Acad. Sci. U. S. A. 110 (2013) 5457–5462.
[48] E. Abreu, E. Aritonovska, P. Reichenbach, G. Cristofari, B. Culp, R.M. Terns, J. Lingner, M.P. Terns, TIN2-tethered TPP1 recruits human telomerase to telomeres in vivo, Mol. Cell. Biol. 30 (2010) 2971–2982.
[49] F. Wang, E.R. Podell, A.J. Zaug, Y. Yang, P. Baciu, T.R. Cech, M. Lei, The POT1-TPP1 telomere complex is a telomerase processivity factor, Nature 445 (2007) 506–510.
[50] J. Nandakumar, T.R. Cech, Finding the end: recruitment of telomerase to telomeres, Nat. Rev. Mol. Cell Biol. 14 (2013) 69–82.
[51] B. Britt-Compton, R. Capper, J. Rowson, D.M. Baird, Short telomeres are preferentially elongated by telomerase in human cells, FEBS Lett. 583 (2009) 3076–3080.
[52] I. Chiodi, C. Mondello, Telomere-independent functions of telomerase in nuclei, cytoplasm, and mitochondria, Front. Oncol. 2 (2012) 133.
[53] P. Martinez, M.A. Blasco, Telomeric and extra-telomeric roles for telomerase and the telomere-binding proteins, Nat. Rev. Cancer 11 (2011) 161–176.
[54] C. Massard, Y. Zermati, A.L. Pauleau, N. Larochette, D. Metivier, L. Sabatier, G. Kroemer, J.C. Soria, hTERT: a novel endogenous inhibitor of the mitochondrial cell death pathway, Oncogene 25 (2006) 4505–4514.
[55] S. Mocellin, K.A. Pooley, D. Nitti, Telomerase and the search for the end of cancer, Trends Mol. Med. 19 (2013) 125–133.
[56] K.A. Olaussen, K. Dubrana, J. Domont, J.P. Spano, L. Sabatier, J.C. Soria, Telomeres and telomerase as targets for anticancer drug development, Crit. Rev. Oncol. Hematol. 57 (2006) 191–214.
[57] M. Armanios, E.H. Blackburn, The telomere syndromes, Nat. Rev. Genet. 13 (2012) 693–704.
[58] M.A. Blasco, Telomeres and human disease: ageing, cancer and beyond, Nature reviews, Genetics 6 (2005) 611–622.
[59] J.W. Shay, S. Bacchetti, A survey of telomerase activity in human cancer, Eur. J. Cancer 33 (1997) 787–791.
[60] C.M. Buseman, W.E. Wright, J.W. Shay, Is telomerase a viable target in cancer? Mutat. Res. 730 (2012) 90–97.
[61] L. Xu, E.H. Blackburn, Human cancer cells harbor T-stumps, a distinct class of extremely short telomeres, Mol. Cell 28 (2007) 315–327.
[62] M.A. Cerone, J.A. Londono-Vallejo, S. Bacchetti, Telomere maintenance by telomerase and by recombination can coexist in human cells, Hum. Mol. Genet. 10 (2001) 1945–1952.
[63] J.W. Shay, R.R. Reddel, W.E. Wright, Cancer. Cancer and telomeres – an ALTernative to telomerase, Science 336 (2012) 1388–1390.
[64] D.C. Silvestre, J.R. Pineda, F. Hoffschir, J.M. Studler, M.A. Mouthon, F. Pflumio, M.P. Junier, H. Chneiweiss, F.D. Boussin, Alternative lengthening of telomeres in human glioma stem cells, Stem Cells 29 (2011) 440–451.
[65] A. Sfeir, T. de Lange, Removal of shelterin reveals the telomere end-protection problem, Science 336 (2012) 593–597.
[66] K. Muraki, L. Han, D. Miller, J.P. Murnane, The role of ATM in the deficiency in nonhomologous end-joining near telomeres in a human cancer cell line, PLoS Genet 9 (2013) e1003386.
[67] A. Decottignies, Alternative end-joining mechanisms: a historical perspective, Front. Genet. 4 (2013) 48.
[68] L.S. Symington, J. Gautier, Double-strand break end resection and repair pathway choice, Annu. Rev. Genet. 45 (2011) 247–271.
[69] J.P. Murnane, Telomere dysfunction and chromosome instability, Mutat. Res. 730 (2012) 28–36.
[70] R. Rai, H. Zheng, H. He, Y. Luo, A. Multani, P.B. Carpenter, S. Chang, The function of classical and alternative non-homologous end-joining pathways in the fusion of dysfunctional telomeres, EMBO J. 29 (2010) 2598–2610.
[71] S.P. Jackson, J. Bartek, The DNA-damage response in human biology and disease, Nature 461 (2009) 1071–1078.
[72] J. Lin, E. Epel, E. Blackburn, Telomeres and lifestyle factors: roles in cellular aging, Mutat. Res. 730 (2012) 85–89.
[73] L.H. Price, H.T. Kao, D.E. Burgers, L.L. Carpenter, A.R. Tyrka, Telomeres and early-life stress: an overview, Biol. Psychiatry 73 (2013) 15–23.
[74] K. Muraki, K. Nyhan, L. Han, J.P. Murnane, Mechanisms of telomere loss and their consequences for chromosome instability, Front. Oncol. 2 (2012) 135.
[75] C. Desmaze, C. Alberti, L. Martins, G. Pottier, C.N. Sprung, J.P. Murnane, L. Sabatier, The influence of interstitial telomeric sequences on chromosome instability in human cells, Cytogenet. Cell Genet. 86 (1999) 288–295.
[76] A.Y. Aksenova, P.W. Greenwell, M. Dominska, A.A. Shishkin, J.C. Kim, T.D. Petes, S.M. Mirkin, Genome rearrangements caused by interstitial telomeric sequences in yeast, Proc. Natl. Acad. Sci. U. S. A. 110 (2013) 19866–19871.
[77] P. Rebuzzini, L. Khoriauli, C.M. Azzalin, E. Magnani, C. Mondello, E. Giulotto, New mammalian cellular systems to study mutations introduced at the break site by non-homologous end-joining, DNA Repair (Amst.) 4 (2005) 546–555.
[78] S.G. Nergadze, M.A. Santagostino, A. Salzano, C. Mondello, E. Giulotto, Contribution of telomerase RNA retrotranscription to DNA double-strand break repair during mammalian genome evolution, Genome Biol. 8 (2007) R260.
[79] L.J. Wu, G. Randers-Pehrson, A. Xu, C.A. Waldren, C.R. Geard, Z. Yu, T.K. Hei, Targeted cytoplasmic irradiation with alpha particles induces mutations in mammalian cells, Proc. Natl. Acad. Sci. U. S. A. 96 (1999) 4959–4964.
[80] H. Nagasawa, J.B. Little, Induction of sister chromatid exchanges by extremely low doses of alpha-particles, Cancer Res. 52 (1992) 6394–6396.
[81] M. Terzaghi, J.B. Little, X-radiation-induced transformation in a C3H mouse embryo-derived cell line, Cancer Res. 36 (1976) 1367–1374.
[82] J.B. Little, Genomic instability and bystander effects: a historical perspective, Oncogene 22 (2003) 6978–6987.
[83] E.J. Hall, Radiobiology for the Radiologist, 6th ed., Lippincott Williams & Wilkins, Philadelphia, 2006.
[84] F.A. Cucinotta, H. Nikjoo, D.T. Goodhead, Model for radial dependence of frequency distributions for energy imparted in nanometer volumes from HZE particles, Radiat. Res. 153 (2000) 459–468.
[85] J.S. Loeffler, M. Durante, Charged particle therapy-optimization, challenges and future directions, Nat. Rev. Clin. Oncol. 10 (2013) 411–424.
[86] S. Ritter, M. Durante, Heavy-ion induced chromosomal aberrations: a review, Mutat. Res. 701 (2010) 38–46.
[87] J.B. Little, L. Gorgojo, H. Vetrovs, Delayed appearance of lethal and specific gene mutations in irradiated mammalian cells, Int. J. Radiat. Oncol. Biol. Phys. 19 (1990) 1425–1429.
[88] J.M. Whaley, J.B. Little, Molecular characterization of hprt mutants induced by low- and high-LET radiations in human cells, Mutat. Res. 243 (1990) 35–45.
[89] J.B. Little, In vitro models of carcinogenesis: expression of recessive genes by chromosomal mutations, Environ. Health Perspect. 81 (1989) 63–66.
[90] M.A. Kadhim, D.A. Macdonald, D.T. Goodhead, S.A. Lorimore, S.J. Marsden, E.G. Wright, Transmission of chromosomal instability after plutonium alpha-particle irradiation, Nature 355 (1992) 738–740.
[91] L. Sabatier, B. Dutrillaux, M.B. Martin, Chromosomal instability, Nature 357 (1992) 548.
[92] M.B. Martins, L. Sabatier, M. Ricoul, A. Pinton, B. Dutrillaux, Specific chromosome instability induced by heavy ions: a step towards transformation of human fibroblasts? Mutat. Res. 285 (1993) 229–237.
[93] W.F. Morgan, Non-targeted and delayed effects of exposure to ionizing radiation: I. Radiation-induced genomic instability and bystander effects in vitro, Radiat. Res. 159 (2003) 567–580.
[94] E.I. Azzam, S.M. de Toledo, A.J. Waker, J.B. Little, High and low fluences of alpha-particles induce a G1 checkpoint in human diploid fibroblasts, Cancer Res. 60 (2000) 2623–2631.
[95] J.H. Houtgraaf, J. Versmissen, W.J. van der Giessen, A concise review of DNA damage checkpoints and repair in mammalian cells, Cardiovasc. Revasc. Med.: Includ. Mol. Intervent. 7 (2006) 165–172.
[96] L. Sabatier, W. Al Achkar, F. Hoffschir, C. Luccioni, B. Dutrillaux, Qualitative study of chromosomal lesions induced by neutrons and neon ions in human lymphocytes at G0 phase, Mutat. Res. 178 (1987) 91–97.
[97] I. Testard, B. Dutrillaux, L. Sabatier, Chromosomal aberrations induced in human lymphocytes by high-LET irradiation, Int. J. Radiat. Biol. 72 (1997) 423–433.
[98] I. Testard, L. Sabatier, Assessment of DNA damage induced by high-LET ions in human lymphocytes using the comet assay, Mutat. Res. 448 (2000) 105–115.
[99] R.M. Anderson, S.J. Marsden, E.G. Wright, M.A. Kadhim, D.T. Goodhead, C.S. Griffin, Complex chromosome aberrations in peripheral blood lymphocytes as a potential biomarker of exposure to high-LET alpha-particles, Int. J. Radiat. Biol. 76 (2000) 31–42.
[100] B.D. Loucas, M.N. Cornforth, The LET dependence of unrepaired chromosome damage in human cells: a break too far? Radiat. Res. 179 (2013) 393–405.
[101] W. Al-Achkar, L. Sabatier, B. Dutrillaux, Transmission of radiation-induced rearrangements through cell divisions, Mutat. Res. 198 (1988) 191–198.
[102] M.A. Kadhim, M.A. Hill, S.R. Moore, Genomic instability and the role of radiation quality, Radiat. Prot. Dosim. 122 (2006) 221–227.
[103] M.A. Kadhim, S.J. Marsden, D.T. Goodhead, A.M. Malcolmson, M. Folkard, K.M. Prise, B.D. Michael, Long-term genomic instability in human lymphocytes induced by single-particle irradiation, Radiat. Res. 155 (2001) 122–126.
[104] C. Fournier, S. Zahnreich, D. Kraft, T. Friedrich, K.O. Voss, M. Durante, S. Ritter, The fate of a normal human cell traversed by a single charged particle, Sci. Rep. 2 (2012) 643.
[105] B. Hu, P. Grabham, J. Nie, A.S. Balajee, H. Zhou, T.K. Hei, C.R. Geard, Intrachromosomal changes and genomic instability in site-specific microbeam-irradiated and bystander human-hamster hybrid cells, Radiat. Res. 177 (2012) 25–34.

[106] H. Zhou, M. Hong, Y. Chai, T.K. Hei, Consequences of cytoplasmic irradiation: studies from microbeam, J. Radiat. Res. 50 (Suppl. A) (2009) A59–A65.
[107] C.M. Raynaud, L. Sabatier, O. Philipot, K.A. Olaussen, J.C. Soria, Telomere length, telomeric proteins and genomic instability during the multistep carcinogenic process, Crit. Rev. Oncol. Hematol. 66 (2008) 99–117.
[108] L. Sabatier, J. Lebeau, B. Dutrillaux, Radiation-induced carcinogenesis: individual sensitivity and genomic instability, Radiat. Environ. Biophys. 34 (1995) 229–232.
[109] Y. Chai, T.K. Hei, Radiation induced bystander effect in vivo, Acta Med. Nagasaki. 53 (2008) S65–S69.
[110] H. Matsumoto, N. Hamada, A. Takahashi, Y. Kobayashi, T. Ohnishi, Vanguards of paradigm shift in radiation biology: radiation-induced adaptive and bystander responses, J. Radiat. Res. 48 (2007) 97–106.
[111] R. Baskar, Emerging role of radiation induced bystander effects: cell communications and carcinogenesis, Genome Integr. 1 (2010) 13.
[112] M. Mancuso, E. Pasquali, P. Giardullo, S. Leonardi, M. Tanori, V. Di Majo, S. Pazzaglia, A. Saran, The radiation bystander effect and its potential implications for human health, Curr. Mol. Med. 12 (2012) 613–624.
[113] C.E. Mothersill, M.J. Moriarty, C.B. Seymour, Radiotherapy and the potential exploitation of bystander effects, Int. J. Radiat. Oncol. Biol. Phys. 58 (2004) 575–579.
[114] T.E. Schmid, G. Multhoff, Non-targeted effects of photon and particle irradiation and the interaction with the immune system, Front. Oncol. 2 (2012) 80.
[115] T.K. Hei, H. Zhou, Y. Chai, B. Ponnaiya, V.N. Ivanov, Radiation induced non-targeted response: mechanism and potential clinical implications, Curr. Mol. Pharmacol. 4 (2011) 96–105.
[116] O.V. Belyakov, S.A. Mitchell, D. Parikh, G. Randers-Pehrson, S.A. Marino, S.A. Amundson, C.R. Geard, D.J. Brenner, Biological effects in unirradiated human tissue induced by radiation damage up to 1 mm away, Proc. Natl. Acad. Sci. U. S. A. 102 (2005) 14203–14208.
[117] C. Shao, M. Folkard, B.D. Michael, K.M. Prise, Targeted cytoplasmic irradiation induces bystander responses, Proc. Natl. Acad. Sci. U. S. A. 101 (2004) 13495–13500.
[118] E.I. Azzam, J.P. Jay-Gerin, D. Pain, Ionizing radiation-induced metabolic oxidative stress and prolonged cell injury, Cancer Lett. 327 (2012) 48–60.
[119] S.M. de Toledo, E.I. Azzam, Adaptive and bystander responses in human and rodent cell cultures exposed to low level ionizing radiation: the impact of linear energy transfer, Dose Response 4 (2006) 291–301.
[120] H. Zhou, G. Randers-Pehrson, C.A. Waldren, D. Vannais, E.J. Hall, T.K. Hei, Induction of a bystander mutagenic effect of alpha particles in mammalian cells, Proc. Natl. Acad. Sci. U. S. A. 97 (2000) 2099–2104.
[121] E.I. Azzam, S.M. de Toledo, J.B. Little, Direct evidence for the participation of gap junction-mediated intercellular communication in the transmission of damage signals from alpha-particle irradiated to nonirradiated cells, Proc. Natl. Acad. Sci. U. S. A. 98 (2001) 473–478.
[122] E.I. Azzam, S.M. De Toledo, D.R. Spitz, J.B. Little, Oxidative metabolism modulates signal transduction and micronucleus formation in bystander cells from alpha-particle-irradiated normal human fibroblast cultures, Cancer Res. 62 (2002) 5436–5442.
[123] M.B. Sowa, W. Goetz, J.E. Baulch, D.N. Pyles, J. Dziegielewski, S. Yovino, A.R. Snyder, S.M. de Toledo, E.I. Azzam, W.F. Morgan, Lack of evidence for low-LET radiation induced bystander response in normal human fibroblasts and colon carcinoma cells, Int. J. Radiat. Biol. 86 (2010) 102–113.
[124] G. Gonon, J.E. Groetz, S.M. de Toledo, R.W. Howell, M. Fromm, E.I. Azzam, Nontargeted stressful effects in normal human fibroblast cultures exposed to low fluences of high charge, high energy (HZE) particles: kinetics of biologic responses and significance of secondary radiations, Radiat. Res. 179 (2013) 444–457.
[125] C. Fournier, D. Becker, M. Winter, P. Barberet, M. Heiss, B. Fischer, J. Topsch, G. Taucher-Scholz, Cell cycle-related bystander responses are not increased with LET after heavy-ion irradiation, Radiat. Res. 167 (2007) 194–206.
[126] C. Fournier, P. Barberet, T. Pouthier, S. Ritter, B. Fischer, K.O. Voss, T. Funayama, N. Hamada, Y. Kobayashi, G. Taucher-Scholz, No evidence for DNA and early cytogenetic damage in bystander cells after heavy-ion microirradiation at two facilities, Radiat. Res. 171 (2009) 530–540.
[127] T. Groesser, B. Cooper, B. Rydberg, Lack of bystander effects from high-LET radiation for early cytogenetic end points, Radiat. Res. 170 (2008) 794–802.
[128] H. Yang, V. Anzenberg, K.D. Held, The time dependence of bystander responses induced by iron-ion radiation in normal human skin fibroblasts, Radiat. Res. 168 (2007) 292–298.
[129] B. Ponnaiya, M. Suzuki, C. Tsuruoka, Y. Uchihori, Y. Wei, T.K. Hei, Detection of chromosomal instability in bystander cells after Si490-ion irradiation, Radiat. Res. 176 (2011) 280–290.
[130] G.E. Watson, S.A. Lorimore, D.A. Macdonald, E.G. Wright, Chromosomal instability in unirradiated cells induced in vivo by a bystander effect of ionizing radiation, Cancer Res. 60 (2000) 5608–5611.
[131] S.A. Lorimore, J.M. McIlrath, P.J. Coates, E.G. Wright, Chromosomal instability in unirradiated hemopoietic cells resulting from a delayed in vivo bystander effect of gamma radiation, Cancer Res. 65 (2005) 5668–5673.
[132] N. Mukaida, S. Kodama, K. Suzuki, M. Oshimura, M. Watanabe, Transmission of genomic instability from a single irradiated human chromosome to the progeny of unirradiated cells, Radiat. Res. 167 (2007) 675–681.
[133] L. Huang, P.M. Kim, J.A. Nickoloff, W.F. Morgan, Targeted and nontargeted effects of low-dose ionizing radiation on delayed genomic instability in human cells, Cancer Res. 67 (2007) 1099–1104.
[134] A. Ayouaz, C. Raynaud, C. Heride, D. Revaud, L. Sabatier, Telomeres: hallmarks of radiosensitivity, Biochimie 90 (2008) 60–72.
[135] M. Fumagalli, F. Rossiello, M. Clerici, S. Barozzi, D. Cittaro, J.M. Kaplunov, G. Bucci, M. Dobreva, V. Matti, C.M. Beausejour, U. Herbig, M.P. Longhese, F. d'Adda di Fagagna, Telomeric DNA damage is irreparable and causes persistent DNA-damage-response activation, Nat. Cell Biol. 14 (2012) 355–365.
[136] E.S. Henle, Z. Han, N. Tang, P. Rai, Y. Luo, S. Linn, Sequence-specific DNA cleavage by Fe^{2+}-mediated Fenton reactions has possible biological implications, J. Biol. Chem. 274 (1999) 962–971.
[137] V.A. Szalai, M.J. Singer, H.H. Thorp, Site-specific probing of oxidative reactivity and telomerase function using 7,8-dihydro-8-oxoguanine in telomeric DNA, J. Am. Chem. Soc. 124 (2002) 1625–1631.
[138] P.L. Opresko, J. Fan, S. Danzy, D.M. Wilson 3rd, V.A. Bohr, Oxidative damage in telomeric DNA disrupts recognition by TRF1 and TRF2, Nucleic Acids Res. 33 (2005) 1230–1239.
[139] G.L. Dianov, J.L. Parsons, Co-ordination of DNA single strand break repair, DNA Repair (Amst.) 6 (2007) 454–460.
[140] A. Tchirkov, P.M. Lansdorp, Role of oxidative stress in telomere shortening in cultured fibroblasts from normal individuals and patients with ataxia-telangiectasia, Hum. Mol. Genet. 12 (2003) 227–232.
[141] T. von Zglinicki, Oxidative stress shortens telomeres, Trends Biochem. Sci. 27 (2002) 339–344.
[142] V. Serra, T. von Zglinicki, M. Lorenz, G. Saretzki, Extracellular superoxide dismutase is a major antioxidant in human fibroblasts and slows telomere shortening, J. Biol. Chem. 278 (2003) 6824–6830.
[143] S. Gorman, M. Tosetto, F. Lyng, O. Howe, K. Sheahan, D. O'Donoghue, J. Hyland, H. Mulcahy, J. O'Sullivan, Radiation and chemotherapy bystander effects induce early genomic instability events: telomere shortening and bridge formation coupled with mitochondrial dysfunction, Mutat. Res. 669 (2009) 131–138.
[144] P.J. Rochette, D.E. Brash, Human telomeres are hypersensitive to UV-induced DNA Damage and refractory to repair, PLoS Genet 6 (2010) e1000926.
[145] S.E. Bates, N.Y. Zhou, L.E. Federico, L. Xia, T.R. O'Connor, Repair of cyclobutane pyrimidine dimers or dimethylsulfate damage in DNA is identical in normal or telomerase-immortalized human skin fibroblasts, Nucleic Acids Res. 33 (2005) 2475–2485.
[146] M. Merrifield, O. Kovalchuk, Epigenetics in radiation biology: a new research frontier, Front. Genet. 4 (2013) 40.
[147] C. Mothersill, C. Seymour, Are epigenetic mechanisms involved in radiation-induced bystander effects? Front. Genet. 3 (2012) 74.
[148] Y. Ilnytskyy, O. Kovalchuk, Non-targeted radiation effects – an epigenetic connection, Mutat. Res. 714 (2011) 113–125.
[149] C.L. Limoli, E. Giedzinski, W.F. Morgan, S.G. Swarts, G.D. Jones, W. Hyun, Persistent oxidative stress in chromosomally unstable cells, Cancer Res. 63 (2003) 3107–3111.
[150] C.L. Limoli, E. Giedzinski, Induction of chromosomal instability by chronic oxidative stress, Neoplasia 5 (2003) 339–346.
[151] K. Suzuki, M. Ojima, S. Kodama, M. Watanabe, Radiation-induced DNA damage and delayed induced genomic instability, Oncogene 22 (2003) 6988–6993.
[152] B.A. Marder, W.F. Morgan, Delayed chromosomal instability induced by DNA damage, Mol. Cell. Biol. 13 (1993) 6667–6677.
[153] K. Suzuki, S. Yokoyama, S. Waseda, S. Kodama, M. Watanabe, Delayed reactivation of p53 in the progeny of cells surviving ionizing radiation, Cancer Res. 63 (2003) 936–941.
[154] A.W. Lo, C.N. Sprung, B. Fouladi, M. Pedram, L. Sabatier, M. Ricoul, G.E. Reynolds, J.P. Murnane, Chromosome instability as a result of double-strand breaks near telomeres in mouse embryonic stem cells, Mol. Cell. Biol. 22 (2002) 4836–4850.
[155] G. Obe, P. Pfeiffer, J.R. Savage, C. Johannes, W. Goedecke, P. Jeppesen, A.T. Natarajan, W. Martinez-Lopez, G.A. Folle, M.E. Drets, Chromosomal aberrations: formation, identification and distribution, Mutat. Res. 504 (2002) 17–36.
[156] L. Sabatier, J. Lebeau, B. Dutrillaux, Chromosomal instability and alterations of telomeric repeats in irradiated human fibroblasts, Int. J. Radiat. Biol. 66 (1994) 611–613.
[157] L. Chauveinc, A.M. Dutrillaux, P. Validire, E. Padoy, L. Sabatier, J. Couturier, B. Dutrillaux, Cytogenetic study of eight new cases of radiation-induced solid tumors, Cancer Genet. Cytogenet. 114 (1999) 1–8.
[158] L. Sabatier, M. Ricoul, G. Pottier, J.P. Murnane, The loss of a single telomere can result in instability of multiple chromosomes in a human tumor cell line, Mol. Cancer Res. 3 (2005) 139–150.
[159] J.P. Murnane, L. Sabatier, Chromosome rearrangements resulting from telomere dysfunction and their role in cancer, Bioessays 26 (2004) 1164–1174.
[160] M. Durante, K. George, F.A. Cucinotta, Chromosomes lacking telomeres are present in the progeny of human lymphocytes exposed to heavy ions, Radiat. Res. 165 (2006) 51–58.
[161] E.I. Azzam, S.M. de Toledo, J.B. Little, Oxidative metabolism, gap junctions and the ionizing radiation-induced bystander effect, Oncogene 22 (2003) 7050–7057.
[162] S. Gaillard, D. Pusset, S.M. de Toledo, M. Fromm, E.I. Azzam, Propagation distance of the alpha-particle-induced bystander effect: the role of nuclear traversal and gap junction communication, Radiat. Res. 171 (2009) 513–520.
[163] H. Yang, N. Asaad, K.D. Held, Medium-mediated intercellular communication is involved in bystander responses of X-ray-irradiated normal human fibroblasts, Oncogene 24 (2005) 2096–2103.
[164] K. Valerie, A. Yacoub, M.P. Hagan, D.T. Curiel, P.B. Fisher, S. Grant, P. Dent, Radiation-induced cell signaling: inside-out and outside-in, Mol. Cancer Ther. 6 (2007) 789–801.

[165] F.M. Lyng, C.B. Seymour, C. Mothersill, Production of a signal by irradiated cells which leads to a response in unirradiated cells characteristic of initiation of apoptosis, Br. J. Cancer 83 (2000) 1223–1230.
[166] N. Autsavapromporn, S.M. de Toledo, J.B. Little, J.P. Jay-Gerin, A.L. Harris, E.I. Azzam, The role of gap junction communication and oxidative stress in the propagation of toxic effects among high-dose alpha-particle-irradiated human cells, Radiat. Res. 175 (2011) 347–357.
[167] T.K. Hei, H. Zhou, V.N. Ivanov, M. Hong, H.B. Lieberman, D.J. Brenner, S.A. Amundson, C.R. Geard, Mechanism of radiation-induced bystander effects: a unifying model, J. Pharm. Pharmacol. 60 (2008) 943–950.
[168] R.T. Hagelstrom, K.F. Askin, A.J. Williams, L. Ramaiah, C. Desaintes, E.H. Goodwin, R.L. Ullrich, S.M. Bailey, DNA-PKcs and ATM influence generation of ionizing radiation-induced bystander signals, Oncogene 27 (2008) 6761–6769.
[169] S. Burdak-Rothkamm, K. Rothkamm, K.M. Prise, ATM acts downstream of ATR in the DNA damage response signaling of bystander cells, Cancer Res. 68 (2008) 7059–7065.
[170] M.V. Sokolov, L.B. Smilenov, E.J. Hall, I.G. Panyutin, W.M. Bonner, O.A. Sedelnikova, Ionizing radiation induces DNA double-strand breaks in bystander primary human fibroblasts, Oncogene 24 (2005) 7257–7265.
[171] M. Buonanno, S.M. de Toledo, D. Pain, E.I. Azzam, Long-term consequences of radiation-induced bystander effects depend on radiation quality and dose and correlate with oxidative stress, Radiat. Res. 175 (2011) 405–415.
[172] M. Buonanno, S.M. de Toledo, E.I. Azzam, Increased frequency of spontaneous neoplastic transformation in progeny of bystander cells from cultures exposed to densely ionizing radiation, PLoS ONE 6 (2011) e21540.
[173] I. Koturbash, R.E. Rugo, C.A. Hendricks, J. Loree, B. Thibault, K. Kutanzi, I. Pogribny, J.C. Yanch, B.P. Engelward, O. Kovalchuk, Irradiation induces DNA damage and modulates epigenetic effectors in distant bystander tissue in vivo, Oncogene 25 (2006) 4267–4275.
[174] D. Nieri, F. Berardinelli, A. Sgura, R. Cherubini, V. De Nadal, S. Gerardi, C. Tanzarella, A. Antoccia, Cyogenetics effects in ag01522 human primary fibroblasts exposed to low-doses of radiations with different quality, Int. J. Radiat. Biol. 89 (2013) 698–707.
[175] F. Berardinelli, A. Antoccia, R. Buonsante, S. Gerardi, R. Cherubini, V.D. Nadal, C. Tanzarella, A. Sgura, The role of telomere length modulation in delayed chromosome instability induced by ionizing radiation in human primary fibroblasts, Environ. Mol. Mutagen. 54 (2013) 172–179.
[176] F. Berardinelli, A. Antoccia, R. Cherubini, V. De Nadal, S. Gerardi, C. Tanzarella, A. Sgura, Telomere alterations and genomic instability in long-term cultures of normal human fibroblasts irradiated with X rays and protons, Radiat. Prot. Dosim. 143 (2011) 274–278.
[177] P. Li, M. Hou, F. Lou, M. Bjorkholm, D. Xu, Telomere dysfunction induced by chemotherapeutic agents and radiation in normal human cells, Int. J. Biochem. Cell Biol. 44 (2012) 1531–1540.
[178] T. Maeda, K. Nakamura, K. Atsumi, M. Hirakawa, Y. Ueda, N. Makino, Radiation-associated changes in the length of telomeres in peripheral leukocytes from inpatients with cancer, Int. J. Radiat. Biol. 89 (2013) 106–109.
[179] M.A. Rubio, A.R. Davalos, J. Campisi, Telomere length mediates the effects of telomerase on the cellular response to genotoxic stress, Exp. Cell Res. 298 (2004) 17–27.
[180] A. Sgura, A. Antoccia, F. Berardinelli, R. Cherubini, S. Gerardi, C. Zilio, C. Tanzarella, Telomere length in mammalian cells exposed to low- and high-LET radiations, Radiat. Prot. Dosim. 122 (2006) 176–179.
[181] F. Berardinelli, A. Antoccia, R. Cherubini, V. De Nadal, S. Gerardi, G.A. Cirrone, C. Tanzarella, A. Sgura, Transient activation of the ALT pathway in human primary fibroblasts exposed to high-LET radiation, Radiat. Res. 174 (2010) 539–549.
[182] P. Belloni, P. Latini, F. Palitti, Radiation-induced bystander effect in healthy G(o) human lymphocytes: biological and clinical significance, Mutat. Res. 713 (2011) 32–38.
[183] F. Leteurtre, X. Li, E. Gluckman, E.D. Carosella, Telomerase activity during the cell cycle and in gamma-irradiated hematopoietic cells, Leukemia 11 (1997) 1681–1689.
[184] M. Terashima, Y. Ogawa, K. Toda, A. Nishioka, T. Inomata, I. Kubonishi, H. Taguchi, S. Yoshida, Y. Shizuta, Effects of irradiation on telomerase activity in human lymphoma and myeloma cell lines, Int. J. Mol. Med. 2 (1998) 567–571.
[185] R. Perez Mdel, D. Dubner, S. Michelin, F. Leteurtre, E.D. Carosella, P.A. Gisone, Radiation-induced up-regulation of telomerase in KG1a cells is influenced by dose-rate and radiation quality, Int. J. Radiat. Biol. 78 (2002) 1175–1183.
[186] R. Ram, O. Uziel, O. Eldan, E. Fenig, E. Beery, S. Lichtenberg, Y. Nordenberg, M. Lahav, Ionizing radiation up-regulates telomerase activity in cancer cell lines by post-translational mechanism via ras/phosphatidylinositol 3-kinase/Akt pathway, Clin. Cancer Res. 15 (2009) 914–923.
[187] D. Neuhof, A. Ruess, F. Wenz, K.J. Weber, Induction of telomerase activity by irradiation in human lymphoblasts, Radiat. Res. 155 (2001) 693–697.
[188] J. Xing, Y. Zhu, H. Zhao, H. Yang, M. Chen, M.R. Spitz, X. Wu, Differential induction in telomerase activity among bladder cancer patients and controls on gamma-radiation, Cancer Epidemiol. Biomark. Prev. 16 (2007) 606–609.
[189] C.N. Andreassen, E. Dikomey, M. Parliament, C.M. West, Will SNPs be useful predictors of normal tissue radiosensitivity in the future? Radiother. Oncol. 105 (2012) 283–288.
[190] M. Fernet, J. Hall, Genetic biomarkers of therapeutic radiation sensitivity, DNA Repair (Amst.) 3 (2004) 1237–1243.
[191] E. Pernot, J. Hall, S. Baatout, M.A. Benotmane, E. Blanchardon, S. Bouffler, H. El Saghire, M. Gomolka, A. Guertler, M. Harms-Ringdahl, P. Jeggo, M. Kreuzer, D. Laurier, C. Lindholm, R. Mkacher, R. Quintens, K. Rothkamm, L. Sabatier, S. Tapio, F. de Vathaire, E. Cardis, Ionizing radiation biomarkers for potential use in epidemiological studies, Mutat. Res. 751 (2012) 258–286.
[192] A. Genesca, M. Martin, L. Latre, D. Soler, J. Pampalona, L. Tusell, Telomere dysfunction: a new player in radiation sensitivity, Bioessays 28 (2006) 1172–1180.
[193] E. Gilson, A. Londono-Vallejo, Telomere length profiles in humans: all ends are not equal, Cell Cycle 6 (2007) 2486–2494.
[194] M. Castella, S. Puerto, A. Creus, R. Marcos, J. Surralles, Telomere length modulates human radiation sensitivity in vitro, Toxicol. Lett. 172 (2007) 29–36.
[195] S.D. Bouffler, M.A. Blasco, R. Cox, P.J. Smith, Telomeric sequences, radiation sensitivity and genomic instability, Int. J. Radiat. Biol. 77 (2001) 995–1005.
[196] M.A. Rubio, S.H. Kim, J. Campisi, Reversible manipulation of telomerase expression and telomere length. Implications for the ionizing radiation response and replicative senescence of human cells, J. Biol. Chem. 277 (2002) 28609–28617.
[197] F. Berardinelli, D. Nieri, A. Sgura, C. Tanzarella, A. Antoccia, Telomere loss, not average telomere length, confers radiosensitivity to TK6-irradiated cells, Mutat. Res. 740 (2012) 13–20.
[198] L. Latre, L. Tusell, M. Martin, R. Miro, J. Egozcue, M.A. Blasco, A. Genesca, Shortened telomeres join to DNA breaks interfering with their correct repair, Exp. Cell Res. 287 (2003) 282–288.
[199] D. Soler, J. Pampalona, L. Tusell, A. Genesca, Radiation sensitivity increases with proliferation-associated telomere dysfunction in nontransformed human epithelial cells, Aging Cell 8 (2009) 414–425.
[200] M. Nakamura, K. Masutomi, S. Kyo, M. Hashimoto, Y. Maida, T. Kanaya, M. Tanaka, W.C. Hahn, M. Inoue, Efficient inhibition of human telomerase reverse transcriptase expression by RNA interference sensitizes cancer cells to ionizing radiation and chemotherapy, Hum. Gene Ther. 16 (2005) 859–868.
[201] T. Hauguel, F. Bunz, Haploinsufficiency of hTERT leads to telomere dysfunction and radiosensitivity in human cancer cells, Cancer Biol Ther 2 (2003) 679–684.
[202] S. Wesbuer, C. Lanvers-Kaminsky, I. Duran-Seuberth, T. Bolling, K.L. Schafer, Y. Braun, N. Willich, B. Greve, Association of telomerase activity with radio- and chemosensitivity of neuroblastomas, Radiat. Oncol. 5 (2010) 66.
[203] O.A. Kovalenko, J. Kaplunov, U. Herbig, S. Detoledo, E.I. Azzam, J.H. Santos, Expression of (NES-)hTERT in cancer cells delays cell cycle progression and increases sensitivity to genotoxic stress, PLoS ONE 5 (2010) e10812.
[204] F.X. Zhou, J. Xiong, Z.G. Luo, J. Dai, H.J. Yu, Z.K. Liao, H. Lei, C.H. Xie, Y.F. Zhou, cDNA expression analysis of a human radiosensitive-radioresistant cell line model identifies telomere function as a hallmark of radioresistance, Radiat. Res. 174 (2010) 550–557.
[205] K. Kurvinen, V. Rantanen, S. Syrjanen, B. Johansson, Radiation-induced effects on telomerase in gynecological cancer cell lines with different radiosensitivity and repair capacity, Int. J. Radiat. Biol. 82 (2006) 859–867.
[206] V. Gorbunova, A. Seluanov, O.M. Pereira-Smith, Expression of human telomerase (hTERT) does not prevent stress-induced senescence in normal human fibroblasts but protects the cells from stress-induced apoptosis and necrosis, J. Biol. Chem. 277 (2002) 38540–38549.
[207] L.M. Pirzio, M.A. Freulet-Marriere, Y. Bai, B. Fouladi, J.P. Murnane, L. Sabatier, C. Desmaze, Human fibroblasts expressing hTERT show remarkable karyotype stability even after exposure to ionizing radiation, Cytogenet. Genome Res. 104 (2004) 87–94.
[208] R. Drissi, J. Wu, Y. Hu, C. Bockhold, J.S. Dome, Telomere shortening alters the kinetics of the DNA damage response after ionizing radiation in human cells, Cancer Prev. Res. (Phila.) 4 (2011) 1973–1981.
[209] K. Rothkamm, M. Lobrich, Evidence for a lack of DNA double-strand break repair in human cells exposed to very low X-ray doses, Proc. Natl. Acad. Sci. U. S. A. 100 (2003) 5057–5062.
[210] O.A. Sedelnikova, I. Horikawa, C. Redon, A. Nakamura, D.B. Zimonjic, N.C. Popescu, W.M. Bonner, Delayed kinetics of DNA double-strand break processing in normal and pathological aging, Aging Cell 7 (2008) 89–100.
[211] E. Cabuy, C. Newton, G. Joksic, L. Woodbine, B. Koller, P.A. Jeggo, P. Slijepcevic, Accelerated telomere shortening and telomere abnormalities in radiosensitive cell lines, Radiat. Res. 164 (2005) 53–62.
[212] E. Mladenov, S. Magin, A. Soni, G. Iliakis, DNA double-strand break repair as determinant of cellular radiosensitivity to killing and target in radiation therapy, Front. Oncol. 3 (2013) 113.
[213] D. Hanahan, R.A. Weinberg, Hallmarks of cancer: the next generation, Cell 144 (2011) 646–674.
[214] J.P. Pommier, J. Lebeau, C. Ducray, L. Sabatier, Chromosomal instability and alteration of telomere repeat sequences, Biochimie 77 (1995) 817–825.
[215] N.L. Komarova, D. Wodarz, The optimal rate of chromosome loss for the inactivation of tumor suppressor genes in cancer, Proc. Natl. Acad. Sci. U. S. A. 101 (2004) 7017–7021.
[216] B. van Steensel, A. Smogorzewska, T. de Lange, TRF2 protects human telomeres from end-to-end fusions, Cell 92 (1998) 401–413.
[217] B. van Steensel, T. de Lange, Control of telomere length by the human telomeric protein TRF1, Nature 385 (1997) 740–743.
[218] A. Smogorzewska, B. van Steensel, A. Bianchi, S. Oelmann, M.R. Schaefer, G. Schnapp, T. de Lange, Control of human telomere length by TRF1 and TRF2, Mol. Cell. Biol. 20 (2000) 1659–1668.
[219] H. Hu, Y. Zhang, M. Zou, S. Yang, X.Q. Liang, Expression of TRF1, TRF2, TIN2, TERT, KU70, and BRCA1 proteins is associated with telomere shortening and may contribute to multistage carcinogenesis of gastric cancer, J. Cancer Res. Clin. Oncol. 136 (2010) 1407–1414.
[220] M. Bellon, A. Datta, M. Brown, J.F. Pouliquen, P. Couppie, M. Kazanji, C. Nicot, Increased expression of telomere length regulating factors TRF1, TRF2 and TIN2 in patients with adult T-cell leukemia, Int. J. Cancer 119 (2006) 2090–2097.

[221] D. Loayza, T. De Lange, POT1 as a terminal transducer of TRF1 telomere length control, Nature 423 (2003) 1013–1018.
[222] S.H. Kim, P. Kaminker, J. Campisi, TIN2, a new regulator of telomere length in human cells, Nat. Genet. 23 (1999) 405–412.
[223] J.Z. Ye, T. de Lange, TIN2 is a tankyrase 1 PARP modulator in the TRF1 telomere length control complex, Nat. Genet. 36 (2004) 618–623.
[224] K. Ancelin, M. Brunori, S. Bauwens, C.E. Koering, C. Brun, M. Ricoul, J.P. Pommier, L. Sabatier, E. Gilson, Targeting assay to study the cis functions of human telomeric proteins: evidence for inhibition of telomerase by TRF1 and for activation of telomere degradation by TRF2, Mol. Cell. Biol. 22 (2002) 3474–3487.
[225] J. Karlseder, A. Smogorzewska, T. de Lange, Senescence induced by altered telomere state, not telomere loss, Science 295 (2002) 2446–2449.
[226] M. McKerlie, X.D. Zhu, Cyclin B-dependent kinase 1 regulates human TRF1 to modulate the resolution of sister telomeres, Nat. Commun. 2 (2011) 371.
[227] P. Martinez, J.M. Flores, M.A. Blasco, 53BP1 deficiency combined with telomere dysfunction activates ATR-dependent DNA damage response, J. Cell Biol. 197 (2012) 283–300.
[228] P. Munoz, R. Blanco, G. de Carcer, S. Schoeftner, R. Benetti, J.M. Flores, M. Malumbres, M.A. Blasco, TRF1 controls telomere length and mitotic fidelity in epithelial homeostasis, Mol. Cell. Biol. 29 (2009) 1608–1625.
[229] P. Martinez, M. Thanasoula, P. Munoz, C. Liao, A. Tejera, C. McNees, J.M. Flores, O. Fernandez-Capetillo, M. Tarsounas, M.A. Blasco, Increased telomere fragility and fusions resulting from TRF1 deficiency lead to degenerative pathologies and increased cancer in mice, Genes Dev. 23 (2009) 2060–2075.
[230] J. Karlseder, L. Kachatrian, H. Takai, K. Mercer, S. Hingorani, T. Jacks, T. de Lange, Targeted deletion reveals an essential function for the telomere length regulator Trf1, Mol. Cell. Biol. 23 (2003) 6533–6541.
[231] L.E. Donate, M.A. Blasco, Telomeres in cancer and ageing, Philos. Trans. R. Soc. Lond. B: Biol. Sci. 366 (2011) 76–84.
[232] A. Sfeir, S.T. Kosiyatrakul, D. Hockemeyer, S.L. MacRae, J. Karlseder, C.L. Schildkraut, T. de Lange, Mammalian telomeres resemble fragile sites and require TRF1 for efficient replication, Cell 138 (2009) 90–103.
[233] T. Iwano, M. Tachibana, M. Reth, Y. Shinkai, Importance of TRF1 for functional telomere structure, J. Biol. Chem. 279 (2004) 1442–1448.
[234] S.M. Bailey, M.N. Cornforth, A. Kurimasa, D.J. Chen, E.H. Goodwin, Strand-specific postreplicative processing of mammalian telomeres, Science 293 (2001) 2462–2465.
[235] O. Bombarde, C. Boby, D. Gomez, P. Frit, M.J. Giraud-Panis, E. Gilson, B. Salles, P. Calsou, TRF2/RAP1 and DNA-PK mediate a double protection against joining at telomeric ends, EMBO J. 29 (2010) 1573–1584.
[236] N. Dimitrova, T. de Lange, Cell cycle-dependent role of MRN at dysfunctional telomeres: ATM signaling-dependent induction of nonhomologous end joining (NHEJ) in G1 and resection-mediated inhibition of NHEJ in G2, Mol. Cell. Biol. 29 (2009) 5552–5563.
[237] J.Z. Ye, D. Hockemeyer, A.N. Krutchinsky, D. Loayza, S.M. Hooper, B.T. Chait, T. de Lange, POT1-interacting protein PIP1: a telomere length regulator that recruits POT1 to the TIN2/TRF1 complex, Genes Dev. 18 (2004) 1649–1654.
[238] M.F. Kendellen, K.S. Barrientos, C.M. Counter, POT1 association with TRF2 regulates telomere length, Mol. Cell. Biol. 29 (2009) 5611–5619.
[239] D. Hockemeyer, A.J. Sfeir, J.W. Shay, W.E. Wright, T. de Lange, POT1 protects telomeres from a transient DNA damage response and determines how human chromosomes end, EMBO J. 24 (2005) 2667–2678.
[240] T. Veldman, K.T. Etheridge, C.M. Counter, Loss of hPot1 function leads to telomere instability and a cut-like phenotype, Curr. Biol. 14 (2004) 2264–2270.
[241] R. Rai, J.M. Li, H. Zheng, G.T. Lok, Y. Deng, M.S. Huen, J. Chen, J. Jin, S. Chang, The E3 ubiquitin ligase Rnf8 stabilizes Tpp1 to promote telomere end protection, Nat. Struct. Mol. Biol. 18 (2011) 1400–1407.
[242] H. He, Y. Wang, X. Guo, S. Ramchandani, J. Ma, M.F. Shen, D.A. Garcia, Y. Deng, A.S. Multani, M.J. You, S. Chang, Pot1b deletion and telomerase haploinsufficiency in mice initiate an ATR-dependent DNA damage response and elicit phenotypes resembling dyskeratosis congenita, Mol. Cell. Biol. 29 (2009) 229–240.
[243] S.H. Kim, A.R. Davalos, S.J. Heo, F. Rodier, Y. Zou, C. Beausejour, P. Kaminker, S.M. Yannone, J. Campisi, Telomere dysfunction and cell survival: roles for distinct TIN2-containing complexes, J. Cell Biol. 181 (2008) 447–460.
[244] Y.J. Chiang, S.H. Kim, L. Tessarollo, J. Campisi, R.J. Hodes, Telomere-associated protein TIN2 is essential for early embryonic development through a telomerase-independent pathway, Mol. Cell. Biol. 24 (2004) 6631–6634.
[245] X. Guo, Y. Deng, Y. Lin, W. Cosme-Blanco, S. Chan, H. He, G. Yuan, E.J. Brown, S. Chang, Dysfunctional telomeres activate an ATM-ATR-dependent DNA damage response to suppress tumorigenesis, EMBO J. 26 (2007) 4709–4719.
[246] A.M. Tejera, M. Stagno d'Alcontres, M. Thanasoula, R.M. Marion, P. Martinez, C. Liao, J.M. Flores, M. Tarsounas, M.A. Blasco, TPP1 is required for TERT recruitment, telomere elongation during nuclear reprogramming, and normal skin development in mice, Dev. Cell 18 (2010) 775–789.
[247] T. Kibe, G.A. Osawa, C.E. Keegan, T. de Lange, Telomere protection by TPP1 is mediated by POT1a and POT1b, Mol. Cell. Biol. 30 (2010) 1059–1066.
[248] B. Li, S. Oestreich, T. de Lange, Identification of human Rap1: implications for telomere evolution, Cell 101 (2000) 471–483.
[249] M. Yamada, N. Tsuji, M. Nakamura, R. Moriai, D. Kobayashi, A. Yagihashi, N. Watanabe, Down-regulation of TRF1, TRF2 and TIN2 genes is important to maintain telomeric DNA for gastric cancers, Anticancer Res. 22 (2002) 3303–3307.
[250] B. Li, T. de Lange, Rap1 affects the length and heterogeneity of human telomeres, Mol. Biol. Cell 14 (2003) 5060–5068.
[251] M.S. O'Connor, A. Safari, D. Liu, J. Qin, Z. Songyang, The human Rap1 protein complex and modulation of telomere length, J. Biol. Chem. 279 (2004) 28585–28591.
[252] J. Sarthy, N.S. Bae, J. Scrafford, P. Baumann, Human RAP1 inhibits non-homologous end joining at telomeres, EMBO J. 28 (2009) 3390–3399.
[253] P. Martinez, M. Thanasoula, A.R. Carlos, G. Gomez-Lopez, A.M. Tejera, S. Schoeftner, O. Dominguez, D.G. Pisano, M. Tarsounas, M.A. Blasco, Mammalian Rap1 controls telomere function and gene expression through binding to telomeric and extratelomeric sites, Nat. Cell Biol. 12 (2010) 768–780.
[254] S. Kabir, A. Sfeir, T. de Lange, Taking apart Rap1: an adaptor protein with telomeric and non-telomeric functions, Cell Cycle 9 (2010) 4061–4067.
[255] D. Gilley, H. Tanaka, M.P. Hande, A. Kurimasa, G.C. Li, M. Oshimura, D.J. Chen, DNA-PKcs is critical for telomere capping, Proc. Natl. Acad. Sci. U. S. A. 98 (2001) 15084–15088.
[256] F.A. Goytisolo, E. Samper, S. Edmonson, G.E. Taccioli, M.A. Blasco, The absence of the DNA-dependent protein kinase catalytic subunit in mice results in anaphase bridges and in increased telomeric fusions with normal telomere length and G-strand overhang, Mol. Cell. Biol. 21 (2001) 3642–3651.
[257] H. Yasaei, Y. Gozaly-Chianea, P. Slijepcevic, Analysis of telomere length and function in radiosensitive mouse and human cells in response to DNA-PKcs inhibition, Genome Integr. 4 (2013) 2.
[258] S.M. Bailey, M.A. Brenneman, J. Halbrook, J.A. Nickoloff, R.L. Ullrich, E.H. Goodwin, The kinase activity of DNA-PK is required to protect mammalian telomeres, DNA Repair (Amst.) 3 (2004) 225–233.
[259] T.S. Fisher, V.A. Zakian, Ku: a multifunctional protein involved in telomere maintenance, DNA Repair (Amst.) 4 (2005) 1215–1226.
[260] E. Samper, F.A. Goytisolo, P. Slijepcevic, P.P. van Buul, M.A. Blasco, Mammalian Ku86 protein prevents telomeric fusions independently of the length of TTAGGG repeats and the G-strand overhang, EMBO Rep. 1 (2000) 244–252.
[261] L. Hu, Q.Q. Wu, W.B. Wang, H.G. Jiang, L. Yang, Y. Liu, H.J. Yu, C.H. Xie, Y.F. Zhou, F.X. Zhou, Suppression of Ku80 correlates with radiosensitivity and telomere shortening in the U2OS telomerase-negative osteosarcoma cell line, Asian Pac. J. Cancer Prev.: APJCP 14 (2013) 795–799.
[262] H.L. Hsu, D. Gilley, S.A. Galande, M.P. Hande, B. Allen, S.H. Kim, G.C. Li, J. Campisi, T. Kohwi-Shigematsu, D.J. Chen, Ku acts in a unique way at the mammalian telomere to prevent end joining, Genes Dev. 14 (2000) 2807–2812.
[263] T. de Lange, Protection of mammalian telomeres, Oncogene 21 (2002) 532–540.
[264] A. Smogorzewska, J. Karlseder, H. Holtgreve-Grez, A. Jauch, T. de Lange, DNA ligase IV-dependent NHEJ of deprotected mammalian telomeres in G1 and G2, Curr. Biol. 12 (2002) 1635–1644.
[265] F. Dantzer, M.J. Giraud-Panis, I. Jaco, J.C. Ame, I. Schultz, M. Blasco, C.E. Koering, E. Gilson, J. Menissier-de Murcia, G. de Murcia, V. Schreiber, Functional interaction between poly(ADP-Ribose) polymerase 2 (PARP-2) and TRF2: PARP activity negatively regulates TRF2, Mol. Cell. Biol. 24 (2004) 1595–1607.
[266] M. Gomez, J. Wu, V. Schreiber, J. Dunlap, F. Dantzer, Y. Wang, Y. Liu, PARP1 Is a TRF2-associated poly(ADP-ribose)polymerase and protects eroded telomeres, Mol. Biol. Cell 17 (2006) 1686–1696.
[267] Y. Bai, J.P. Murnane, Telomere instability in a human tumor cell line expressing NBS1 with mutations at sites phosphorylated by ATM, Mol. Cancer Res. 1 (2003) 1058–1069.
[268] C.L. Attwooll, M. Akpinar, J.H. Petrini, The mre11 complex and the response to dysfunctional telomeres, Mol. Cell. Biol. 29 (2009) 5540–5551.
[269] H. Zhang, M.H. Yang, J.J. Zhao, L. Chen, S.T. Yu, X.D. Tang, D.C. Fang, S.M. Yang, Inhibition of tankyrase 1 in human gastric cancer cells enhances telomere shortening by telomerase inhibitors, Oncol. Rep. 24 (2010) 1059–1065.
[270] S.J. Hsiao, S. Smith, Sister telomeres rendered dysfunctional by persistent cohesion are fused by NHEJ, J. Cell Biol. 184 (2009) 515–526.
[271] Y.J. Chiang, S.J. Hsiao, D. Yver, S.W. Cushman, L. Tessarollo, S. Smith, R.J. Hodes, Tankyrase 1 and tankyrase 2 are essential but redundant for mouse embryonic development, PLoS ONE 3 (2008) e2639.
[272] S.M. de Toledo, M. Buonanno, M. Li, N. Asaad, Y. Qin, G. Gonon, G. Shim, M. Galdass, Y. Boateng, J. Zhang, E.I. Azzam, The impact of adaptive and non-targeted effects in the biological responses to low dose/low fluence ionizing radiation: the modulating effect of linear energy transfer, Health Phys. 100 (2011) 290–292.

6 - DISCUSSION AND CONCLUSIONS

As presented in this thesis, there are inter-individual variations in radiosensitivity, measured in terms of IR-induced DNA DSBs (Section 3), which may be linked to age, gender, and inherent and IR-induced changes in telomere length (Section 4). These differences in individual radiosensitivity have important implications in biological dosimetry (discussed in detail in Section 2 and in **our recent paper** (Viau et al., 2015)) and radiotherapy (discussed in detail in Section 1.4.2), as a given dose of IR can induce significantly different levels of cellular damage in individuals of different radiosensitivities. In the following chapters, we discuss how individual radiosensitivity can influence long-term health following IR exposure, specifically focusing on the development of cardiovascular disease and the process of carcinogenesis. As we have demonstrated a link between these pathologies and telomeres (in Sections 5.1 and 5.2, respectively), we elaborate on the detailed model for carcinogenesis originally presented at the conclusion of **our original paper** (Shim et al., 2014) (presented in Section 5.2) to tie in how telomeres also play a key role in the development of cardiovascular diseases and how individual radiosensitivity may influence these processes. We then conclude with an argument on how telomeres could be useful in the prediction of individual sensitivity to identify hyper-radiosensitive individuals that may be more vulnerable to the induction of these pathologies following IR exposure.

6.1 Telomeres as key players in the process of radiation-induced carcinogenesis and cardiovascular disease, and the influence of individual radiosensitivity

The propagation of genomic instability can have a wide variety of biological consequences for the cell and the organism/being. As discussed in Section 1.2, IR exposure also induces a variety of other DNA and cellular damage, perhaps most notably DNA DSBs (which can lead to the formation of chromosomal aberrations) and mitochondrial dysfunction. We showed in this thesis that the extent of IR-induced DSBs (calculated based on the frequency of IR-induced chromosomal aberrations) varies among individuals of different levels of radiosensitivity (Section 3). Meanwhile, IR-induced mitochondrial dysfunction results in the production of excess ROS that goes on to cause further damage to the genome. Stress signals can be transmitted from irradiated cells to the progeny of irradiated cells, as well as to neighboring bystander cells and their progeny, and can cause ongoing oxidative stress, prolonged cellular injury, and the propagation of genomic instability (Azzam et al., 2012;Morgan and Sowa, 2015); telomeres themselves may play a role in the long-

term transmission of chromosomal instability (Shim et al., 2014). Depending on the level of genomic instability, cells may or may not be able to continue to proliferate. For the process of carcinogenesis, which requires accumulation and unmasking of recessive mutations at a combination of oncogenes and tumor suppressor genes, the mutations, chromosomal rearrangements, and other types of genetic alterations that are generated during the propagation of genomic instability may facilitate the unmasking of recessive mutations via loss of heterozygosity (LOH) and thereby fuel tumor progression (Hanahan and Weinberg, 2011). Meanwhile, in the development of cardiovascular diseases, the continuous mechanical, hemodynamic, and/or immunological damage (probably involving oxidative stress) to vascular endothelial cells during the age-related progression of atherosclerosis (a common underlying cause of cardiovascular diseases) could cause increased localized cellular turnover, accumulating levels of DNA/cellular damage and genomic instability, leading to cellular senescence, myocardial cell death, or fibrosis (Schultz-Hector and Trott, 2007;Little et al., 2008;Sabatino et al., 2012;Shah and Mahmoudi, 2015). Therefore, along the road to carcinogenesis, a careful level of genomic instability must be maintained, as 'too much' instability would be detrimental and would result in cell death or senescence, while 'too little' instability would slow the progression to tumorigenesis. Thus, ***we propose that just the right amount of genomic instability would minimize the rate of cell death/senescence while maximizing the rate of progression to carcinogenesis*** (Komarova and Wodarz, 2004). Meanwhile, ***we propose that the cell death/senescence induced from 'too much' genomic instability leads to pathologies associated with these cellular states, including cardiovascular disease***.

As discussed in Section 1.1, genomic instability can be induced by deregulation of telomere length, shelterin proteins, and DNA damage repair proteins, factors that have all been linked to cancer progression. We have also reviewed how dysfunction of these factors can be induced following direct and indirect (via bystander effects) IR exposure. Telomere length (which varies between individuals (Gilson and Londono-Vallejo, 2007;Hernandez et al., 2015;Lapham et al., 2015), different cell types in a single individual, as well as on individual chromosome arms within a single cell (Pommier and Sabatier, 2002)) continuously decreases naturally with each cell replication cycle (Harley et al., 1990). This telomere shortening can be accelerated following IR exposure either via increased levels of cell proliferation in order to replenish cells killed by IR exposure, or via IR-induced damages to telomeres (either through a direct hit or indirectly-induced oxidative damage) that prevents adequate telomere maintenance. Accelerated telomere shortening will be further induced by continuous exposure to other endogenous and exogenous DNA damaging agents throughout the cell lifespan (d'Adda di Fagagna et al., 2003;Jackson and Bartek, 2009;Lin et

al., 2012;Price et al., 2013). Considering that the heterogeneity of telomere lengths on each arm of individual chromosomes is maintained as telomeres shorten with each cell cycle, the shortest telomeres will eventually become critically short and dysfunctional, and could result in chromosome fusion and lead to chromosomal instability (Murnane, 2012). As shown in Figure 34, **we propose that the heterogeneity in telomere length, *continuous telomere shortening, and the triggering of DNA damage repair pathways and senescence due to dysfunctional telomeres play an essential role in the process of carcinogenesis and the development of cardiovascular diseases***.

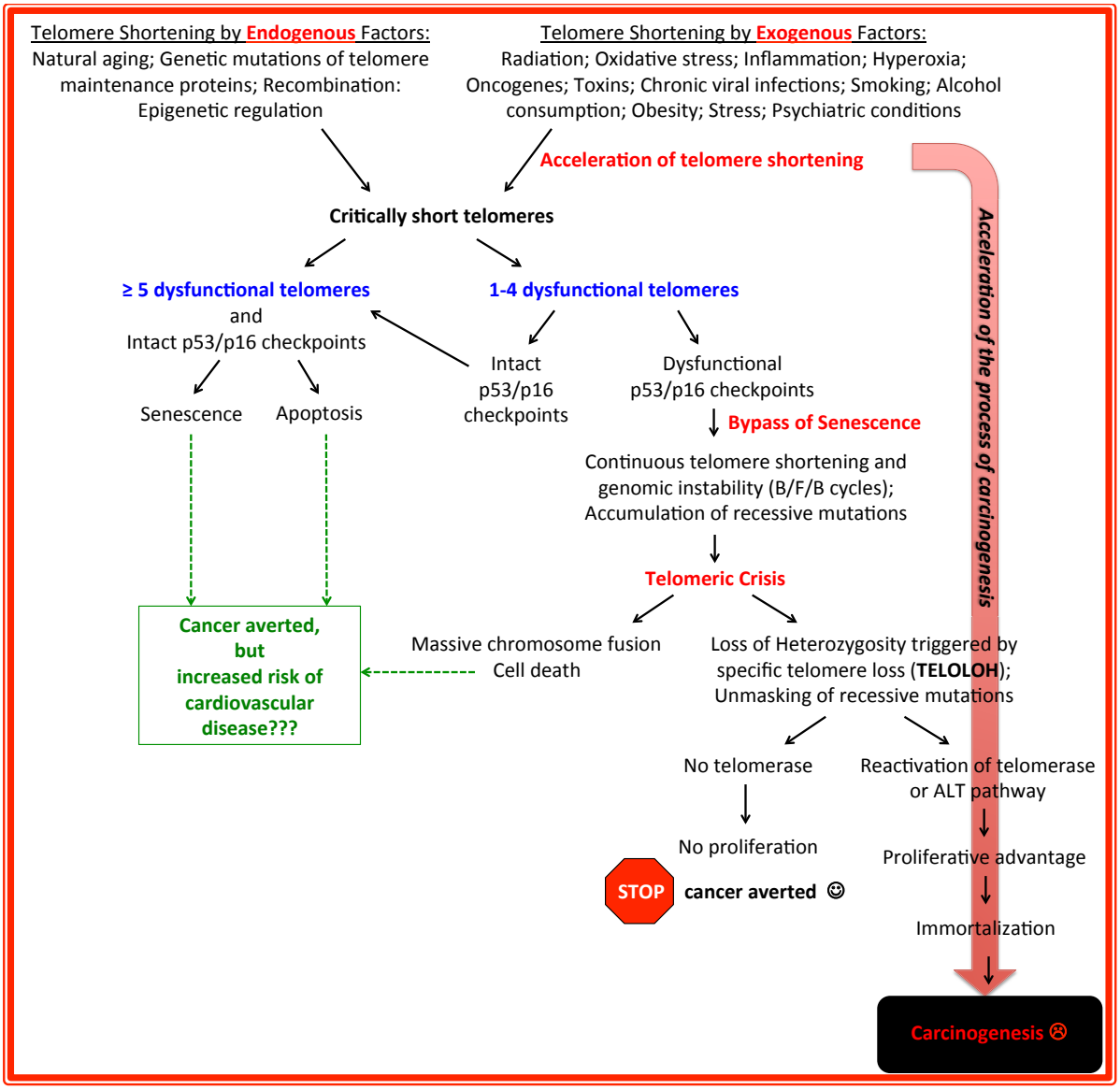

Figure 34. Our proposed model of the impact of telomere length heterogeneity on the processes of cellular aging, senescence, crisis, carcinogenesis, and the development of cardiovascular disease.

When the shortest telomeres become critically short and dysfunctional, these dysfunctional/uncapped telomeres are sensed as DNA damage and trigger DDR pathways, forming TIFs in normal cells with intact cell cycle checkpoints (Takai et al., 2003). An important study suggested that normal human cells are able to tolerate small numbers of dysfunctional telomeres, and cells can continue to proliferate until a ***threshold of five TIFs per cell*** is reached. In normal cells with intact cell cycle checkpoints, senescence or apoptosis is triggered when this threshold of 5 dysfunctional telomeres is reached. In cells that are unable to senesce due to the loss of cell cycle checkpoint proteins such as p53 or p16, senescence is temporarily bypassed, and cells continue to proliferate with further accumulation of chromosomal instability, TIFs, and telomere shortening, until "telomeric crisis" is reached. In virus-immortalized cells undergoing crisis, more than 5 dysfunctional telomeres were found (Kaul et al., 2012) along with massive chromosome fusion and cell death (Counter et al., 1992;Counter et al., 1994;Ducray et al., 1999), perhaps due to extreme telomere shortening and loss of shelterin proteins. ***We propose that this cell death due to 'too much' genomic instability halts the process of carcinogenesis, but is responsible for the increased risk of diseases related to cell death, such as cardiovascular diseases if cell death occurs in vascular tissues*** (Figure 34).

On the other hand, as shown in Figure 34, ***in the case of carcinogenesis, we propose that careful accrual of genomic instability when there are 1 to 4 dysfunctional telomeres in the presence of dysfunctional cell cycle checkpoints and/or DNA damage response mechanisms is key to the fate of the cell/being.*** As mentioned above, the process of carcinogenesis requires just the right amount of genomic instability to minimize the rate of cell death/senescence while maximizing the rate of progression to carcinogenesis. At these low levels of telomere dysfunction (1 to 4 dysfunctional telomeres), low levels of chromosomal instability may be allowed to persist, including the accumulation of recessive mutations in the genome with each successive generation that would allow the emergence of cells with a proliferative advantage if unmasked via loss of heterozygosity (LOH). With continuous telomere shortening with each cell cycle, telomeric crisis can lead to the loss of whole chromosomes or partial chromosomal arms, thereby unmasking in a single step via telomere-induced chromosomal imbalances the recessive mutations of hundreds of genes that have accumulated in the genome; these recessive mutations would otherwise remain silent unless the other, normal allele becomes mutated, a highly unlikely event. This phenomenon that we have coined "TELOLOH" is triggered by the shortest telomere that will first reach the threshold of instability (Pommier et al., 1995), and could lead to the emergence of cells with a proliferative advantage, especially if coupled with loss of tumor suppressor function and activation of telomerase and/or ALT pathways, leading to cell

immortalization and eventually carcinogenesis (Pommier et al., 1995;Sabatier et al., 1995;Raynaud et al., 2008b). Therefore, ***as telomere dysfunction (natural and/or IR-induced) may cause and propagate genetic instability and LOH, telomeres may be considered as a key player in the process of radiation-induced carcinogenesis***. The IR-induced acceleration of telomere shortening may lead to acceleration of this entire process to carcinogenesis or the development of cardiovascular diseases.

As the rate at which these processes occur will vary depending on the inherent heterogeneity of telomere length of the given individual, this factor may be considered as the cornerstone of individual predisposition to carcinogenesis or cardiovascular diseases. In other words, the starting point (i.e. the inherent telomere length and telomere length heterogeneity both per individual and within the individual) on the road to senescence, crisis (premature or not), and/or carcinogenesis, and/or cardiovascular diseases can determine whether that road is taken, and how long the journey will be. Furthermore, accumulation of IR-induced genomic damage may be of particular concern in highly radiosensitive individuals, as these individuals harbor more IR-induced damage in the genome (as shown in this thesis) that may not be properly repaired than in more radioresistant individuals. Conversely, radiosensitive individuals may be radiosensitive due to inherent genetic mutations (e.g. defects/deficiencies in genes involved in the DNA damage repair pathways or in proteins involved in the activation of cell cycle checkpoints or DNA replication/repair) that may also predispose them to IR-associated cancers or cardiovascular diseases. These considerations highlight the importance of identifying these highly radiosensitive individuals and adapting diagnostic radiology and radiation protection protocols based on individual radiosensitivity, as they may not be adequately protected under current guidelines, which utilize population averages in radiosensitivity (Advisory Group on Ionising Radiation, 2013).

6.2 Telomeres and telomere maintenance as a predictor of individual radiosensitivity

Several characteristics of telomeres and their maintenance mechanisms make this parameter a promising candidate as a predictive biomarker (see details and discussion in **our original paper** (Shim et al., 2014) presented in Section 5.2). In line with our paper (Shim et al., 2014), a recent paper (Mirjolet et al., 2015) highlights the potential of telomeres and telomere maintenance as key players in predicting individual radiosensitivity that can be applied to radiotherapy regimens to personalize treatment. The key points supporting telomeres as a predictive biomarker of individual radiosensitivity are summarized here:

- Telomere length (TL) varies between individuals and on individual chromosome arms. TL in somatic proliferative tissues naturally declines with each cell replication cycle, and thus with increasing age. The natural shortening of telomeres can be accelerated by endogenous factors (e.g. metabolic stress leading to point mutations or deletions in genes encoding proteins involved in telomere protection, as well as recombination and epigenetic regulation) and by external environmental stress and lifestyle factors that cause DNA DSBs or mis-replication of telomeres (e.g. IR and other oxidizing agents, oxidative stress, inflammation, hyperoxia, oncogenes, toxins, chronic viral infections, smoking, alcohol consumption, obesity, stress, and even psychiatric conditions). ***TL can therefore be considered as a prognostic marker that takes into account a set of all past events.***

- Reduced TL reflects the accumulation of previous insults from various damaging conditions and has been associated with numerous chronic diseases that are generally considered to be diseases of aging, such as diabetes, cancer, and heart disease (M'Kacher et al., 2015b). Abnormal telomerase activity and TL regulation have also been linked to the pathology of several age-related human diseases, as described in Section 1.1.3 (Armanios and Blackburn, 2012;Holohan et al., 2014). Telomerase is up-regulated in about 85% of human cancers (and is silent in most differentiated cells such as normal somatic cells), suggesting its important role in the process of cellular immortalization and tumorigenesis. ***This illustrates that telomeres and mechanisms of telomere maintenance play important roles at various stages in the initiation and development of cancer and other human pathologies.***

- Telomeric regions (and sub-telomeric regions) are particularly sensitive to IR-induced oxidative stress and are more prone to DSBs, perhaps due to their inappropriate processing: the presence of DNA damage within telomeric repeat sequences hinders telomere replication, leading to telomere shortening or loss, and the deficiency of DSB

repair near telomeres has been suggested to play a role in chromosomal instability associated with human cancers. ***This makes telomeres more sensitive to IR exposure than the rest of the genome, and thus to radiotherapy.***

- Telomeres and DDR mechanisms exhibit a co-dependent, bi-directional relationship, as dysfunctional telomeres are recognized as DSBs and trigger the DDR pathways, whose proteins are also involved in the normal maintenance and protection of telomeres (Section 1.1.2). ***As DDR processes are also closely linked to radiosensitivity, telomere maintenance is also likely to be closely linked to radiosensitivity.***

All of this evidence indicates that telomeres and telomere maintenance could be sensitive and reliable biomarkers of IR exposure, and could be a new parameter to predict individual radiosensitivity (Pernot et al., 2012;Shim et al., 2014;Mirjolet et al., 2015). As we have found that radiosensitivity could indeed be predicted by a combination of age and gender, as well as the combination of inherent and IR-induced changes in TL following TC-FISH analysis (Section 4.2), we postulate that these factors can be adapted to establish a clinical method of identifying radiosensitive individuals. The ability to reliably predict individual radiosensitivity would have important implications in biological dosimetry (discussed in detail in Section 1.4.3) and radiotherapy (discussed in detail in Section 1.4.2), as it would allow for refinement of radiation protection protocols to identify and especially protect highly radiosensitive individuals. Though the analysis of telomeres and TL using TC-FISH (or other methods) may be too complex (and time-consuming) to use as the actual biomarker to provide dose estimates based on its measurements for biodosimetry purposes (due to the intra- and inter-individual heterogeneity of TL), prior knowledge of an individual's radiosensitivity (i.e. those individuals that have already been classified as highly radiosensitive) can perhaps aid in the proper medical triage of these individuals. TC-FISH analysis of telomeres and TL to predict individual radiosensitivity could, however, be useful in the context of radiotherapy. Nevertheless, there remains the issue of how to effectively measure and rank individuals based on their radiosensitivity, as discussed in Section 1.4.3. Since the method that we use to create triage categories in the case of an emergency situation using global fluorescence of γH2AX at the time point of 4 hours post-irradiation allows for creation of such triage categories independently of individual radiosensitivity (Section 2), it foregoes the issue of ranking individuals based on their radiosensitivity. Though this method is rapid and capable of high-throughput analysis (both crucial in the case of a mass accident), this analysis is hindered by the time-sensitive nature of the measurement of γH2AX.

In the context of radiotherapy, as also highlighted in (Mirjolet et al., 2015), the ability to reliably predict individual radiosensitivity could allow for personalization of treatment. Additionally, as radiosensitivity has been associated with TL and telomerase activity, the management of TL and telomerase could be useful during radiotherapy. Indeed, shorter TL has been linked with increased radiosensitivity in many *in vivo* and *in vitro* studies in telomerase-deficient mouse and human cells. Down-regulation or inhibition of telomerase was shown to compromise the viability of cancer cells while minimally affecting normal cells; thus, the use of telomerase inhibitors during cancer therapy may sensitize cancer cells to chemotherapy and radiotherapy. On the other hand, radioresistant carcinoma cells exhibited up-regulation of telomerase activity and longer telomeres (Genesca et al., 2006;Ayouaz et al., 2008;Shim et al., 2014). The authors of Mirjolet *et al* also propose that TL and telomeric shelterin protein analysis in both cancer cells (to assess tumor sensitivity) and normal cells (to assess radiotherapy tolerance) could be useful in the personalization of radiotherapy treatments based on individual radiosensitivity. TL could be used to adjust doses per fraction, and the effectiveness and safety of radiotherapy could be enhanced with the use of pharmacological interference of telomere biology (e.g. reduce TL) in tumor cells (Mirjolet et al., 2015).

In the coming months, we aim to confirm the correlations between individual radiosensitivity and TL (presented in Section 4.2) in the PBL of a larger cohort of at least 30 donors (in an ad hoc study with approved funding from DoReMi). This cohort will be selected from a previously established biobank for a separate project (EpiRadBio). As mean inherent TL was previously determined for the EpiRadBio project, donors representing the extremes in terms of TL will be selected and subjected to *in vitro* irradiation. TL will be determined following telomere-PNA FISH staining before and after irradiation, and will be analyzed by automated image capture and analysis. Metaphase spreads will also be stained with TC-FISH, and radiosensitivity of the PBLs will be determined in terms of DSBs per cell following automated analysis with the software (TCScore) developed in our laboratory (previously discussed in Section 3, and presented in (M'Kacher et al., 2014)).

Telomeres, long considered the guardians of the genome, can arguably represent the potential overall health of a being, as it can represent a lifetime of exposures to various DNA damaging agents including ionizing radiation (as they are deficient in repair and therefore leads to accumulation of damages). Telomeres and mechanisms of their maintenance could therefore have important implications in long-term human health. As humans are constantly exposed to IR via natural and man-made sources, determining if/how telomeres play a role in the mechanisms of direct and indirect IR-induced biological effects, as well as their role in the transmission of these IR-induced effects during cell proliferation

can be critical to the determination of the long-term effects of IR on human health, and can contribute to our understanding of how IR-associated cancers and other human pathologies arise.

APPENDIX

A.1. *Materials and Methods for lymphocyte radiosensitivity studies*

A.1.1. Cell culture and irradiation

Peripheral blood lymphocytes (PBL) used in these studies were isolated from the whole blood of healthy blood donors (with negative viral status) from the Center of Blood Transfusions using the standard Ficoll isolation technique. After isolation, lymphocytes were frozen in liquid nitrogen (-196°C) until use. Lymphocytes were unfrozen 24 hours before irradiation and incubated at 37°C in an atmosphere of 5% CO_2 in RPMI 1640 medium (Gibco) supplemented with 20% fetal bovine serum (FBS; Eurobio) and antibiotics (penicillin/streptomycin; Gibco). Lymphocytes were irradiated at various doses at room temperature (RT) with γ-rays from a Cesium-137 source at the CEA Fontenay aux Roses, France (dose-rate of 2 Gy/min).

Carbon-13 irradiations were performed on the GANIL D1 high energy line with energy of 75 MeV/u. Lymphocytes were irradiated in small tubes with a glass wall of 2 mm thickness. Samples were irradiated at the plateau region of the Bragg peak curve; the mean LET at the sample was estimated to be approximately 36.5 keV/µm. The dosimetry was realized with the assistance of CIMAP-CIRIL physicists using a Faraday cup and an X-ray detector (5 µm stainless steel foil and photomultiplier). The photons emitted after traversal of the foil by the accelerated ions were counted, and a correlation at low fluences/doses was established with the real ion tracks measured on CR39 tracks detectors $(C_{12}H_{18}O_7)_n$. After exposure to the beam, the ion tracks in the CR39 were chemically etched for 8 to 12 min in 12 N KOH at 80°C. Several microscope fields were photographed using an Olympus Vanox-S, x100, equipped with a Cohn Pieper FK-7512-Q video camera. The tracks were then counted using a homemade image analysis application from the Aphelion® software. X-ray detector doses were also subsequently correlated to the doses measured with an ionizing chamber (Unidos 23332 or 23344, PTW Freiburg, Germany, depending on the ion atomic number and its track length) for further verification of the dose/fluence-ratio. The ionizing chamber was not used as reference dosimeter for the sample irradiations since it was designed for measuring photon fluxes (utilized in radiotherapy).

A.1.2. Collection of metaphase spreads

To obtain metaphases for cytogenetic analysis, isolated PBLs were stimulated immediately after irradiation using recombinant human interleukin 2 and phytohemagglutinin (PHA; Gibco), and bromodeoxyuridine (BrdU; Sigma-Aldrich) was added to the culture

medium. Lymphocytes were incubated with BrdU for 60 hours after irradiation at 37°C in an atmosphere of 5% CO_2. At 60 hours post-irradiation, 60 ng/mL colchicine (Gibco) was added into culture media for 2 hours at 37°C and 5% CO_2 to accumulate mitotic cells. Cells were harvested and centrifuged at RT at 1400 rpm for 7 min, almost all of the supernatant was aspirated, and cells were resuspended in 10 mL of 37°C 0.075 M KCl (hypotonic shock to swell the cells) and incubated for 20 min in a 37°C water bath. For prefixation, a few drops of fixative solution (3:1 v/v ethanol/acetic acid; both from VWR Chemicals) were added to each tube. Tubes were gently inverted several times to mix well, then centrifuged again at RT for 1400 rpm for 7 min. The KCl solution was removed after the second centrifugation step, and cells were resuspended in 10 mL of fixative solution. These fixation and centrifugation steps were repeated twice more, and samples were incubated in fresh fixative solution overnight at 4°C. Cells were washed once more with the fixative solution before metaphases were spread on ice cold, wet slides the next day. Slides with metaphase spreads were dried at RT overnight, and then stored in -20°C until use.

A.1.3. Telomere/centromere-FISH (TC-FISH)

Analysis of chromosomal aberrations was done as previously described (M'Kacher et al., 2014) on slides with metaphase spreads using telomere-specific Cyanine3-labeled protein nucleic acid (PNA) probe and centromere-specific FITC-labeled PNA probes (both from Panagene, Daejon, South Korea). Slides stored at -20°C were unfrozen and left at RT overnight before the experiment. Dry slides were soaked in PBS for at least 5 min, and then were fixed in 4% formaldehyde for 2 min followed by 3 successive washes in PBS for 5 min each. Pepsin (Gibco) was diluted in 1 N HCl pH 2 to a final concentration of 0.3 mg/mL, and 40 µL were deposited on each slide, covered with a plastic coverslip, and incubated in a humid (H_2O) chamber at 37°C for 7 min. Plastic coverslips were removed and slides were gently placed briefly (30 sec) in PBS. Slides were fixed again in 4% formaldehyde for 2 min, followed by 3 successive washes in PBS for 5 min each. Slides were dehydrated in 50%, 70%, and 100% ice cold ethanol for 5 min each, and slides were left to dry at RT for ~20 min. PNA telomere and centromere probes were diluted (1:100 dilution each) in home-made PNA hybridization buffer (70% formamide, 10 mM Tris pH 7.2), and 50 µL were deposited on each slide and covered with plastic coverslips. Slides were denatured for 3 min on a hot plate at 80°C, and then were left in dark humid chambers at RT for ~2 hours. Slides were washed twice for 15 min each in 70% formamide-10 mM Tris-HCl pH 7.2 solution, and then 3 times for 5 min each in solution containing 50 mM Tris-HCl pH 7.2, 150 mM NaCl, and 0.05% Tween-20. After counter-coloration of the DNA with 4´,6-diamidino-2-phenylindole (DAPI) for 5 min, slides were placed in PBS, and then mounted with coverslips with PPD (1

mg/mL *p*-phenylenediamine-90% glycerol-10% PBS). Slides were kept in a dark box at stored at -4°C until automated image capturing with MetaSystems, and images were analyzed using the MetaSystems ISIS software as previously described (M'Kacher et al., 2014).

A.1.4. Multicolor-FISH (M-FISH)

Slides were hybridized with a 24XCyte mFISH kit (Metasystems Altlussheim, Germany) according to the protocol recommended by the manufacturer. If previous hybridization was done on the slides, slides were soaked in PBS for 15-30 min to remove the glass coverslip. To denature the chromosomes, slides were rinsed for 1 min in 0.1xSSC pH 6.3 (15 mM NaCl + 0.15 mM Tris sodium citrate) at RT, followed by 30 min in 2xSSC pH 6.3 (300 mM NaCl + 30 mM Tris sodium citrate) at 70°C. The 2xSSC with the slides inside was cooled to 37°C, and slides were rinsed for 1 min each in 0.1xSSC pH 6.3 at RT, 0.07 N NaOH at RT, 0.1xSSC pH 6.3 at 4 °C, and 2xSSC pH 6.3 at 4°C. Slides were then dehydrated in 30%, 50%, 70%, and 100% ethanol for 1 min each at RT, and were dried at RT for at least 15 min. The probe was denatured for 5 min in 75°C, and pre-hybridized for 30 min at 37°C. The probe was then centrifuged and vortexed, and ~10 µL was deposited onto each slide and covered with a plastic coverslip. Slides were incubated in a humid chamber of 50% formamide at 37°C for ~4 nights. Post-hybridization, slides were placed in pre-warmed 0.4xSSC pH 7.0 at 72°C for 2 min, followed by 30 sec in 2xSSCT (2xSSC pH 7.0 and 0.05% Tween-20) at RT. After counter-coloration of the DNA with DAPI for 5 min, slides were placed in PBS, and then mounted with coverslips with PPD. Slides were kept in a dark box at stored at -4°C until automated image capturing with MetaSystems, and images were analyzed using the MetaSystems ISIS software.

A.1.5. γH2AX immunofluorescence

At specified time points (0.5, 1, 2, and 24 hours) following γ-irradiation (0, 0.2, 2, and 8 Gy), lymphocytes (approximately 100,000 cells) were fixed onto polylysine slides using Cytospin®. Cells were then fixed for 15 min in 0.4% paraformaldehyde (PFA), which stops cell metabolism. Slides were then placed in a permeabilization buffer (20 mM Hepes pH 7.9, 50 mM sodium chloride, 3 mM magnesium chloride, 300 mM sucrose, and 0.5% Triton) for 30 min, followed by 1 hour at 37°C in blocking buffer I (Boehringer Ingelheim 1% Blocking Reagent®, 5% FBS, and 0.5% Triton in PBS). Slides were incubated with primary antibody (Upstate anti-phosphorylated H2AX from mice, 2 µg/mL) diluted in blocking buffer I for 1 hour at 37°C. Excess antibody was removed by three successive rinses in PBS-0.5% triton

for 5 min each, and slides were blocked once more in blocking buffer II (Boehringer Ingelheim 1% Blocking Reagent® and 0.1% Triton in PBS) for 10 min at RT. Slides were then hybridized with anti-mouse secondary antibody coupled to Cyanine-3 (Upstate) in blocking buffer II for 1 hour at 37°C, and excess secondary antibody was removed with three rinses in PBS-0.5% Triton for 5 min each. Slides were washed briefly in PBS, counterstained with DAPI, and then mounted with coverslips with PPD. Slides were kept in a dark box and stored at -4°C until capture with MetaSystems.

A.1.6. Imaging using MetaSystems, and analysis using ISIS

Images of hybridized slides were captured with a charge-coupled device camera (Zeiss, Thornwood, NY) coupled to a Zeiss Axioplan microscope. Two MetaSystems softwares allow automatic image scanning. “MetaCyte" photographs interphasic nuclei under 10X objective and quantifies the cellular intensity of fluorescence markers of interest (e.g. telomeric PNA probes, γH2AX); this software rapidly photographs thousands of interphasic nuclei, and pooled data summaries or data of each individual nucleus could be directly exported for statistical analyses using Microsoft Excel or other statistical software. MetaCyte parameters used to capture γH2AX global fluorescence is described in our recently published paper (Viau et al., 2015). “AutoCapt" photographs metaphases hybridized with fluorescent probes (e.g. TC-FISH and M-FISH) under 63X objective; images were then exported for analysis using the MetaSystems ISIS software or other imaging software.

Images of individual nuclei (e.g. for manual γH2AX foci scoring) can also be captured manually under 63X objective using the “Metafer4” software (MetaSystems). For the manual scoring of γH2AX foci, the integration time for DAPI was set to automatic, and the integration time for SpO to capture Cyanine-3 labeled foci was fixed to 0.003 sec. Additionally, to take into account the roundness of the interphasic nuclei of lymphocytes, images were captured in 8 stacks, 5 µm apart; the MetaSystems software automatically compiled these stacks into a single image per nucleus. Images were exported in JPEG format for analysis using Image J: upon opening the JPEG images in ImageJ, each nucleus was cropped, subjected to RGB split, and the number of foci was counted.

A.2. *Supplemental figures*

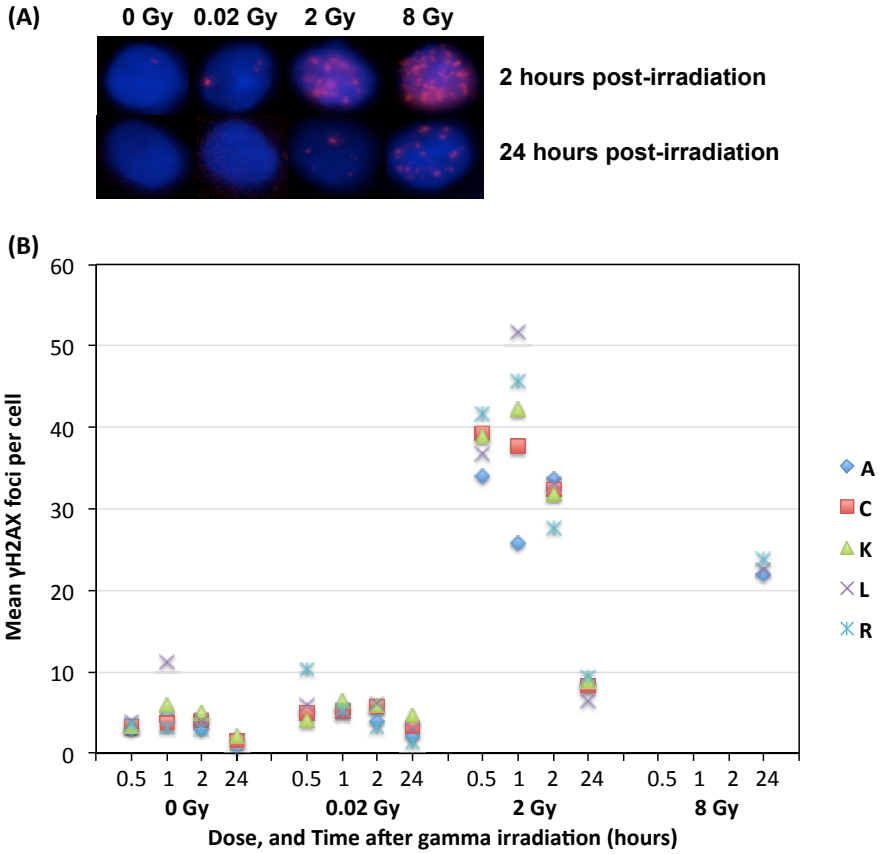

Figure A-1. (A) Representative images of γH2AX foci for manual scoring in interphasic lymphocyte nuclei irradiated with γ-rays from a Cesium-137 source at the indicated doses (0 to 8 Gy) at 2 and 24 hours post-irradiation. Images of nuclei for manual scoring of foci was captured under 63X magnification using Metafer® software (MetaSystems®). Foci were manually scored using ImageJ software. (B) Dispersion of manually scored γH2AX foci in lymphocytes from 5 blood donors (increasing radiosensitivity measured using cytogenetic analysis associated with labels from A to R, presented in Section 3.1.1 of this thesis). Lymphocytes were irradiated with γ-rays from a Cesium-137 source at the indicated doses (0 to 8 Gy) and placed at 37°C for repair. Cells were harvested at the indicated times (0.5–24 hours post-irradiation) for staining. Data points represent results obtained for one experiment with each donor. γH2AX foci following irradiation with 8 Gy at 0 to 2 hours post-irradiation was not quantifiable due to fluorescence saturation of nuclei; however, foci following 8 Gy irradiation were quantifiable at 24 hours post-irradiation. Large inter-individual variability can be observed; this variability increases with dose, with maximum variability at 1 hour after 2 Gy irradiation, and decreases with time post-irradiation. Basal levels of γH2AX (0 Gy) are not negligible (Complementary results of (Viau et al., 2015)).

Table A-1. Correlations between radiosensitivity (DSBs per cell) and induction of γH2AX (at several time points between 0.5 and 24 hours post-irradiation) to 2 Gy of γ-rays or carbon ions. γH2AX induction was measured in terms of global fluorescence in 8 donors (Donors A, B, G, H, K, M, Q, R) of the cohort discussed in Sections 3.1 and 3.2. Radiosensitivity to 2 Gy of γ-rays and γH2AX induction at 0.5 hours post-irradiation to 2 Gy of γ-rays show moderate correlation (R^2 = 0.595, red text); however, these results remain to be confirmed in a larger cohort. This correlation is also plotted in Figure A-2 below. No other correlations were observed.

	Time post-irradiation (hours)	R^2 values (8 donors)	
		DSB/Cell Gamma 2Gy	DSB/Cell Carbon 2Gy
γH2AX - gamma 2Gy	0.5	0.595*	0.329
	3	0.012*	0.082
	6	0.002*	0.114
	24	0.010	0.239
γH2AX - carbon 2Gy	0.5	0.140	0.368
	3	0.004	0.000**
	24	0.001	0.076

* Data for Donor H missing. ** Data for Donor G missing.

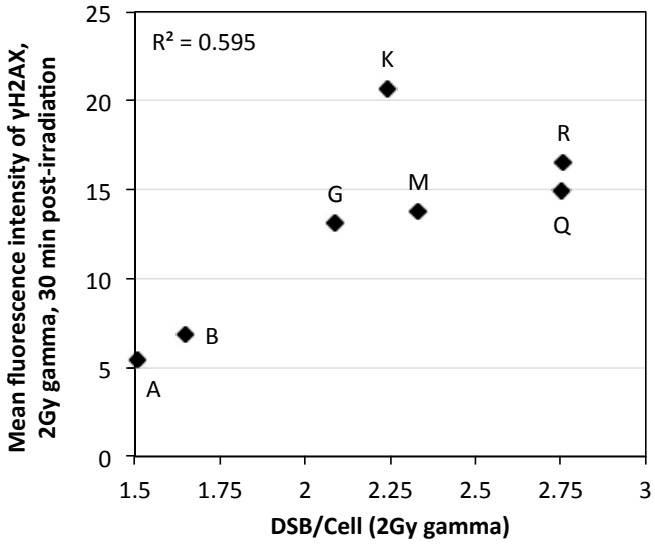

Figure A-2. Moderate correlation (R^2 = 0.595) between radiosensitivity to 2 Gy of γ-rays and γH2AX induction at 0.5 hours post-irradiation to 2 Gy of γ-rays. Induction of γH2AX was measured in terms of global fluorescence in 7 donors (Donors A, B, G, K, M, Q, R) of the cohort discussed in Sections 3.1 and 3.2. These results remain to be confirmed in a larger cohort.

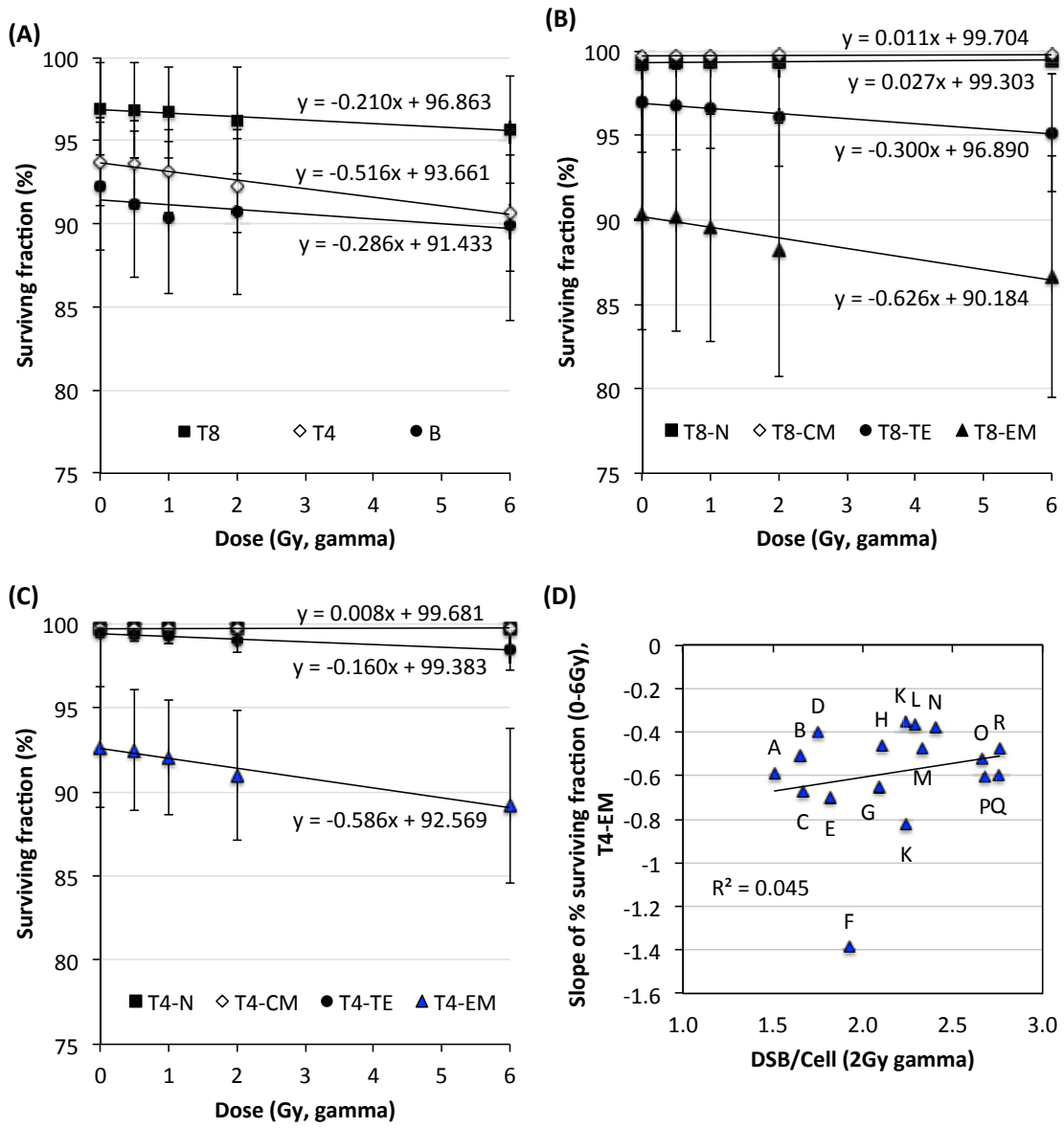

Figure A-3. Sensitivity to IR-induced apoptosis after *in vitro* γ-irradiation (0 to 6 Gy) in lymphocyte subpopulations of 17 healthy blood donors (Donors A-H, J-R) of the cohort discussed in Section 3.1. Apoptosis (Annexin V) in quiescent lymphocytes was determined using 8-color flow cytometry [method details are given in (Schmitz et al., 2007)]. T and non-T lymphocytes were identified based on phycoerythrin-Texas-red fluorescence (CD3). A phycoerythrincyanin 7 (CD4) versus APC-cyanin 7 (CD8) histogram allowed for the identification of T4 and T8 lymphocytes. T4 and T8 subpopulations were discriminated using an APC (CD45RA) versus phycoerythrin (CD62L) histogram as follows: central memory (CM; CD62L+ CD45RA-), effector memory (EM; CD62L- CD45RA-), naive (N; CD62L+ CD45RA+), and terminal effector (TE; CD62L- CD45RA+). B cells were determined on a bivariate histogram of APC (CD45RA) vs. phycoerythrin-cyanin 5 (CD19) of non-T lymphocytes. Average surviving fractions (%) and standard deviation (error bars) are presented as a function of dose (Gy) of γ-irradiation for (A) B-, T4-, and T8- lymphocyte subpopulations, and for (B) T8 and (C) T4 subpopulations. Surviving fractions at 0 Gy were not normalized to 100% to illustrate basal (spontaneous) levels of apoptosis. As the *susceptibility* to IR-induced apoptosis in the T4-EM subpopulation was found to be correlated with radiosensitivity following γ-irradiation (Schmitz et al., 2007), we looked at whether the *slope* of IR-induced apoptosis in T4-EM lymphocytes between the doses of 0 and 6 Gy of γ-irradiation (blue data points in panel (C)) correlates to individual radiosensitivity to 2 Gy of γ-irradiation (Figure 17A); as shown in panel (D), no correlations were found (R^2=0.045).

Table A-2. No correlations (R2 coefficients) between radiosensitivity (DSBs per cell) to 2 Gy of γ-rays or carbon ions and sensitivity to spontaneous (0 Gy) or IR-induced apoptosis (2 Gy of γ-rays). Results of individual donors that were included in the analysis shown in Figure A-3 were correlated with radiosensitivity results discussed in Sections 3.1 and 3.2. Correlations with radiosensitivity to 2 Gy of γ-rays included 17 donors (Donors A-H, J-R), and correlations with radiosensitivity to 2 Gy of carbon ions included 13 donors (Donors A-C, E-H, J-M, Q, R).

	% Surviving fraction at 0 Gy		% Surviving fraction at 2 Gy γ-irradiation	
	DSB/Cell Gamma 2Gy	DSB/Cell Carbon 2 Gy	DSB/Cell Gamma 2Gy	DSB/Cell Carbon 2 Gy
B	0.000	0.005	0.003	0.084
T4	0.088	0.257	0.052	0.298
T4-TE	0.015	0.466	0.013	0.304
T4-N	0.023	0.322	0.045	0.121
T4-CM	0.001	0.023	0.000	0.021
T4-EM	0.080	0.227	0.048	0.262
T8	0.025	0.299	0.037	0.231
T8-TE	0.006	0.218	0.000	0.236
T8-N	0.067	0.110	0.072	0.050
T8-CM	0.051	0.000	0.057	0.020
T8-EM	0.024	0.266	0.033	0.185

Table A-3. No correlations (R^2 coefficients) between radiosensitivity (DSBs per cell) to 2 Gy of γ-rays or carbon ions and sensitivity to IR-induced apoptosis at other doses of γ-irradiation (0.5, 1, 6 Gy). Results of individual donors that were included in the analysis shown in Figure A-3 were correlated with radiosensitivity results discussed in Sections 3.1 and 3.2. Correlations with radiosensitivity to 2 Gy of γ-rays included 17 donors (Donors A-H, J-R), and correlations with radiosensitivity to 2 Gy of carbon ions included 13 donors (Donors A-C, E-H, J-M, Q, R).

	% Surviving fraction at 0.5 Gy γ-irradiation		% Surviving fraction at 1 Gy γ-irradiation		% Surviving fraction at 6 Gy γ-irradiation	
	DSB/Cell Gamma 2Gy	DSB/Cell Carbon 2 Gy	DSB/Cell Gamma 2Gy	DSB/Cell Carbon 2 Gy	DSB/Cell Gamma 2Gy	DSB/Cell Carbon 2 Gy
B	0.010	0.004	0.006	0.081	0.012	0.092
T4	0.071	0.277	0.084	0.266	0.071	0.230
T4-TE	0.024	0.388	0.021	0.386	0.002	0.232
T4-N	0.055	0.220	0.030	0.053	0.126	0.020
T4-CM	0.004	0.000	0.002	0.047	0.027	0.103
T4-EM	0.070	0.253	0.080	0.240	0.078	0.192
T8	0.033	0.274	0.042	0.242	0.018	0.226
T8-TE	0.003	0.242	0.001	0.236	0.008	0.200
T8-N	0.030	0.150	0.014	0.014	0.005	0.029
T8-CM	0.016	0.002	0.012	0.045	0.012	0.059
T8-EM	0.027	0.247	0.034	0.184	0.010	0.150

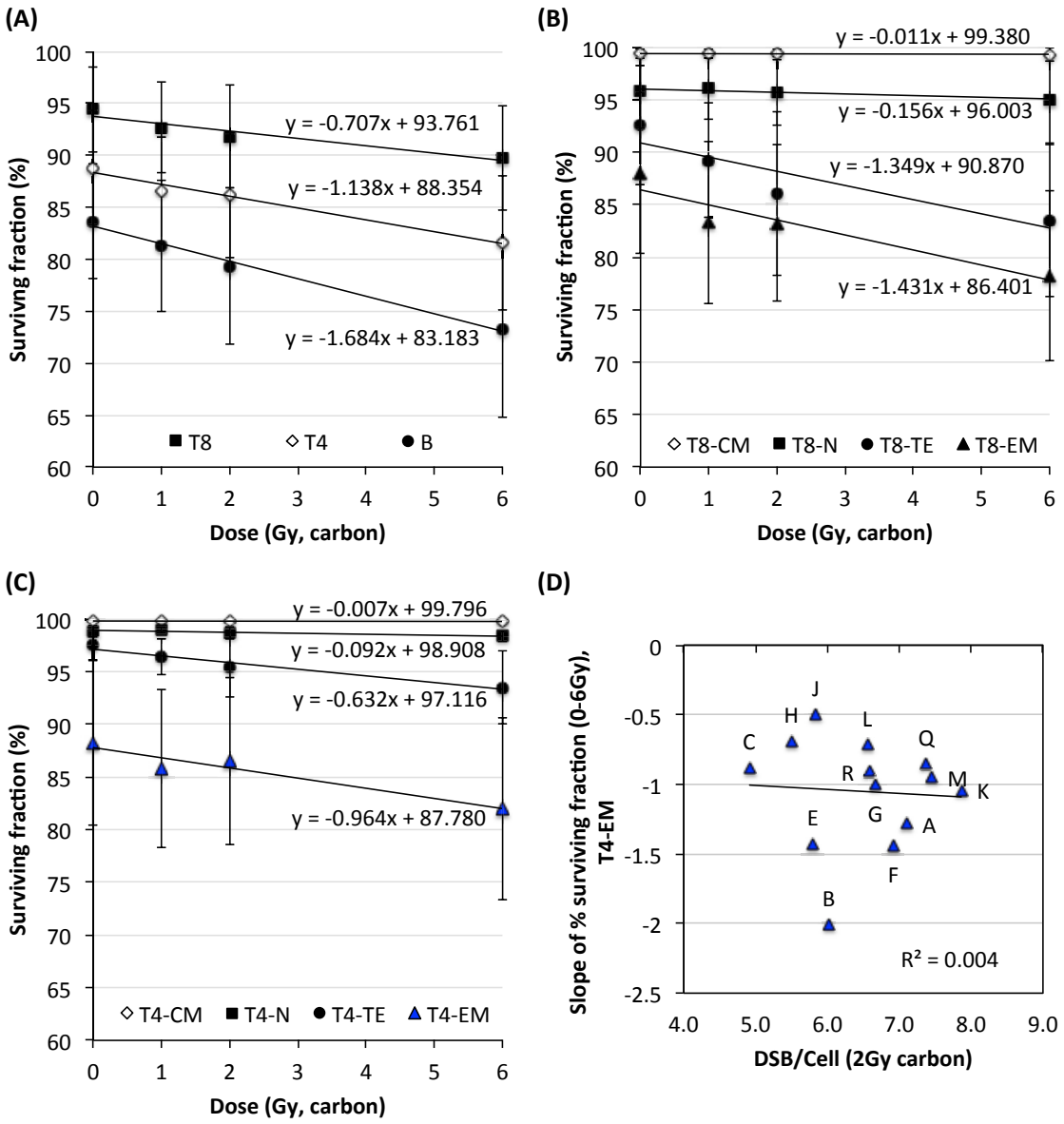

Figure A-4. Sensitivity to IR-induced apoptosis after in vitro carbon irradiation (0 to 6 Gy) in lymphocyte subpopulations of 16 healthy blood donors (Donors A-H, J-O, Q, R) of the cohort discussed in Section 3.2. Apoptosis (Annexin V) in quiescent lymphocytes was determined using 8-color flow cytometry [method details are given in (Schmitz et al., 2007)]. T and non-T lymphocytes were identified based on phycoerythrin-Texas-red fluorescence (CD3). A phycoerythrincyanin 7 (CD4) versus APC-cyanin 7 (CD8) histogram allowed for the identification of T4 and T8 lymphocytes. T4 and T8 subpopulations were discriminated using an APC (CD45RA) versus phycoerythrin (CD62L) histogram as follows: central memory (CM; CD62L+ CD45RA-), effector memory (EM; CD62L- CD45RA-), naive (N; CD62L+ CD45RA+), and terminal effector (TE; CD62L- CD45RA+). B cells were determined on a bivariate histogram of APC (CD45RA) vs. phycoerythrin-cyanin 5 (CD19) of non-T lymphocytes. Average surviving fractions (%) and standard deviation (error bars) are presented as a function of dose (Gy) of carbon ions for (A) B-, T4-, and T8- lymphocyte subpopulations, and for (B) T8 and (C) T4 subpopulations. Surviving fractions at 0 Gy were not normalized to 100% to illustrate basal (spontaneous) levels of apoptosis. (D) No correlations were found (R^2=0.004) between the susceptibility to IR-induced apoptosis (i.e. slope of IR-induced apoptosis between the doses of 0 and 6 Gy of carbon irradiation, the blue data points in panel (C)) in the T4-EM subpopulation and radiosensitivity following 2 Gy carbon irradiation (Figure 21A).

Table A-4. No correlations (R^2 coefficients) between radiosensitivity (DSBs per cell) to 2 Gy of γ-rays or carbon ions and sensitivity to spontaneous (0 Gy) or IR-induced apoptosis (2 Gy of carbon ions). Results of individual donors that were included in the analysis shown in Figure A-4 were correlated with radiosensitivity results discussed in Sections 3.1 and 3.2. Correlations with radiosensitivity to 2 Gy of γ-rays included 16 donors (Donors A-H, J-O, Q, R), and correlations with radiosensitivity to 2 Gy of carbon ions included 13 donors (Donors A-C, E-H, J-M, Q, R).

	% Surviving fraction at 0 Gy		% Surviving fraction at 2 Gy carbon irradiation	
	DSB/Cell Gamma 2Gy	DSB/Cell Carbon 2 Gy	DSB/Cell Gamma 2Gy	DSB/Cell Carbon 2 Gy
B	0.001	0.011	0.011	0.024
T4	0.201	0.001	0.220	0.015
T4-TE	0.033	0.053	0.044	0.117
T4-N	0.000	0.040	0.027	0.047
T4-CM	0.096	0.138	0.092	0.102
T4-EM	0.177	0.002	0.199	0.000
T8	0.025	0.124	0.055	0.150
T8-TE	0.113	0.050	0.144	0.078
T8-N	0.002	0.076	0.024	0.118
T8-CM	0.066	0.016	0.093	0.065
T8-EM	0.040	0.040	0.072	0.074

Table A-5. No correlations (R^2 coefficients) between radiosensitivity (DSBs per cell) to 2 Gy of γ-rays or carbon ions and sensitivity to IR-induced apoptosis at other doses of carbon irradiation (1, 6 Gy). Results of individual donors that were included in the analysis shown in Figure A-4 were correlated with radiosensitivity results discussed in Sections 3.1 and 3.2. Correlations with radiosensitivity to 2 Gy of γ-rays included 16 donors (Donors A-H, J-O, Q, R), and correlations with radiosensitivity to 2 Gy of carbon ions included 13 donors (Donors A-C, E-H, J-M, Q, R).

	% Surviving fraction at 1 Gy carbon irradiation		% Surviving fraction at 6 Gy carbon irradiation	
	DSB/Cell Gamma 2Gy	DSB/Cell Carbon 2 Gy	DSB/Cell Gamma 2Gy	DSB/Cell Carbon 2 Gy
B	0.011	0.040	0.000	0.039
T4	0.253	0.001	0.200	0.009
T4-TE	0.034	0.101	0.017	0.131
T4-N	0.032	0.098	0.004	0.099
T4-CM	0.170	0.215	0.368	0.143
T4-EM	0.204	0.000	0.213	0.000
T8	0.015	0.143	0.035	0.146
T8-TE	0.121	0.068	0.118	0.070
T8-N	0.023	0.058	0.013	0.001
T8-CM	0.108	0.005	0.081	0.010
T8-EM	0.028	0.046	0.036	0.052

A.3. ***Additional original bibliographies***

A.3.1. The impact of adaptive and non-targeted effects in the biological responses to low dose/low fluence ionizing radiation: The modulating effect of linear energy transfer

In the following abstract (de Toledo et al., 2011), we discuss in detail evidence from mechanistic studies of the influence of radiation LET on the induction of the adaptive response and non-targeted effects following exposure to low doses of IR.

Summary of the key points of this abstract:

- Normal human or rodent cells exposed to low chronic doses of low-LET IR were better able to correctly repair DNA lesions resulting from endogenous metabolism or a subsequent challenge exposure to IR, and were less likely to transform to the neoplastic phenotype.
- In contrast, cells exposed to low-doses of high-LET IR (including alpha and heavy ion particles) did not induce adaptive responses, but instead showed persistent stressful effects such as oxidative stress, mitochondrial dysfunction, and genomic DNA damage in both the directly targeted cell as well as their neighboring, bystander cells and their progeny. I aided in the development and optimization of the assays used to measure antioxidant enzyme activity in normal human cells and mice tissue; these assays were used in many of these studies in correlation to oxidative stress and levels of ROS.
- The data strongly support a role for IR dose and quality (i.e. LET) in determining the nature of the induced IR effects at low doses.

Abstract

THE IMPACT OF ADAPTIVE AND NON-TARGETED EFFECTS IN THE BIOLOGICAL RESPONSES TO LOW DOSE/LOW FLUENCE IONIZING RADIATION: THE MODULATING EFFECT OF LINEAR ENERGY TRANSFER

Sonia M. de Toledo, Manuela Buonanno, Min Li, Nesrin Asaad, Yong Qin, Geraldine Gonon, Grace Shim, Mariann Galdass, Yaa Boateng, Jie Zhang, and Edouard I. Azzam*

A large volume of laboratory and human epidemiological studies have shown that high doses of ionizing radiation engender significant health risks. In contrast, the health risks of low level radiation remain ambiguous and have been the subject of intense debate. To reduce the uncertainty in evaluating these risks, research advances in cellular and molecular biology are being used to characterize the biological effects of low dose radiation exposures and their underlying mechanisms. Radiation type, dose rate, genetic susceptibility, cellular redox environment, stage of cell growth, level of biological organization and environmental parameters are among the factors that modulate interactions among signaling processes that determine short- and long-term outcomes of low dose exposures. Whereas recommended radiation protection guidelines assume a linear dose-response relationship in estimating radiation cancer risk, in vitro and in vivo investigations of phenomena such as adaptive responses and non-targeted effects, namely bystander effects and genomic instability, suggest that low dose/low fluence-induced signaling events act to alter linearity of the dose-response relationship as supported by the biophysical argument. The latter predicts that increases in dose simply increase the probability that a given cell in a tissue will be intersected by an electron track, and by corollary, each unit of radiation, no matter how small, would increase risk. These predictions assume that similar molecular events mediate both low and high dose radiobiological effects, and the cumulative risk from two sequential radiation exposures can never be less than one alone.

Using normal human or rodent cells maintained in culture and a variety of biological endpoints, studies have shown that exposure to low dose/low linear energy transfer (LET) radiation delivered at low dose-rates ($\leq$ 10 cGy from ^{137}Cs or ^{60}Co γ-rays delivered at $\leq$ 0.2 cGy γ h^{-1}), triggers signaling events that protect cells from endogenous oxidative damage or damage due to a subsequent challenge dose of ionizing radiation (Azzam et al. 1994a and b, 1996; de Toledo et al. 2006). Similar effects were observed in cells exposed to acute low doses of γ-rays that were followed by incubation at 37°C for periods extending up to 48 h. Accumulating data indicate that DNA repair, oxidative metabolism, and cell cycle checkpoints are implicated in the observed biological responses and involve differential regulation of signaling processes. Significantly, proteomic analyses have shown that several proteins are distinctly sensitive to low, but not high, dose γ-rays. Furthermore, dissimilar epigenetic events were detected in low- or high dose-irradiated cells and in cells exposed to doses from low or high LET radiations that result in similar survival levels. Notably, studies show that reactive oxygen species (ROS) produced by low dose γ-radiation exert similar biological effects as those generated by normal oxidative metabolism (Venkatachalam et al. 2008). The exposure to low dose/low dose rate γ-rays restored normal progression in the cell cycle of human fibroblasts wherein signaling pathways that regulate growth under homeostatic conditions were perturbed by the effect of inhibiting NADP(H) oxidase, an important source of ROS in various cell types (Venkatachalam et al. 2008).

With relevance to the assessment of health risks, exposure to low dose/low dose rate ^{60}Co γ-rays in the

* Department of Radiology, UMDNJ-New Jersey Medical School Cancer Center, 205 South Orange Avenue, Newark, NJ 07103.

For correspondence contact Edouard I. Azzam, Department of Radiology, UMDNJ-New Jersey Medical School Cancer Center, 205 South Orange Avenue, Newark, NJ 07103, or email at azzamei@umdnj.edu.

(*Manuscript accepted* 23 *November* 2010)
0017-9078/10/0

DOI: 10.1097/HP.0b013e31820832d8

range of 0.1 to 10 cGy significantly ($p < 1.9 \times 10^{-5}$) reduced the frequency of neoplastic transformation to below the spontaneous level in C3H 10T1/2 mouse embryo fibroblasts (Azzam et al. 1996). Interestingly, a dose of 0.1 cGy is in the range of a typical occupational exposure and represents, on average, about one track per cell that is hit, the lowest possible dose that a cell can receive (Bond et al. 1988). Hence, neoplastic transformation data imply that a single low dose exposure, in the background or occupational dose range, can in some circumstances induce processes that reduce rather than increase carcinogenic risk, which is similar to extensive findings by others (Redpath and Antoniono 1998; Redpath et al. 2001).

In experiments designed to examine the propagation of protective effects induced in low dose/low LET irradiated cells, studies in confluent cultures consisting of irradiated and unirradiated normal human cells showed that adaptive effects induced by low dose/low LET radiations, including short-range β particles from incorporated tritium, ^{137}Cs γ-rays, or 1 GeV protons, were communicated to neighboring non-targeted cells and protected the latter against DNA damages from challenge exposures to γ-rays or high charge/high energy (HZE) particles, a high LET radiation.

Using mice, studies have shown that oxidative metabolism and intercellular communication are major mediators of tissue responses to low dose/low dose rate γ-rays. Mitochondria, which are active participants in oxidative metabolism, play a crucial role in the induced adaptive responses, which appear to be transient and tissue-dependent. Whereas exposure to acute low doses (10 cGy) transiently decreased some mitochondrial functions (e.g., mitochondrial protein import), exposure to low dose/low dose-rate γ-rays enhanced these functions. Accordingly, the observed decreases following acute low dose γ-rays may be a protective compensatory response to the initial induced oxidative stress; they occurred in normal cells and not in transformed or cancer cells.

Collectively, the results show that cells can adapt when exposed to low chronic doses of low LET radiation, and the adapted cells are better able to correctly repair DNA lesions resulting from endogenous metabolism or a subsequent challenge exposure to radiation, and thus are less likely to be transformed to the neoplastic phenotype.

In contrast to adaptive responses detected in cells/tissues targeted with low dose/low LET radiations, persistent stressful effects were observed in cells/tissues targeted with high LET radiations, including alpha and HZE particles. Oxidative stress as judged by increased levels of ROS, protein carbonylation and lipid peroxidation, as well as mitochondrial dysfunction and genomic DNA damage were not only confined to the target but were also propagated to neighboring cells/tissues. Direct intercellular communication through gap junctions (Azzam et al. 1998, 2001) and indirect communication involving inflammatory cytokines were involved in the propagation of the observed stressful effects, which also persisted in the progeny of bystander cells and led to their transformation to the neoplastic phenotype.

In conclusion, the data support the argument that biological responses together with biophysical considerations predict the outcome of exposure of human and non-human biota to ionizing radiation. While similar mediators may modulate the same endpoint in low dose-induced adaptive responses, bystander effects or genomic instability phenomena, the occurrence of opposite effects, such as pro-survival rather than cytotoxic/carcinogenic effects, may reflect changes in concentration of the inducing factor(s), and may also involve distinct mediating factors/mechanisms. The data strongly support a role for radiation dose and radiation quality (i.e., LET) in determining the nature of the induced effect.

Coupled with epidemiology, knowledge of cellular and molecular processes underlying low dose radiation-induced biological effects should further refine estimates of radiation risks at low doses. These studies are consistent with the concept that mechanistic investigations constitute a significant guide to empirical epidemiological analyses in areas where there is uncertainty. Health Phys. 100(3):290–292; 2011

Key words: dose, low; health effects; hormesis; linear hypothesis

REFERENCES

Azzam EI, de Toledo SM, Gooding T, Little JB. Intercellular communication is involved in the bystander regulation of gene expression in human cells exposed to very low fluences of alpha particles. Radiat Res 150:497–504; 1998.

Azzam EI, de Toledo SM, Little JB. Direct evidence for the participation of gap-junction mediated intercellular communication in the transmission of damage signals from alpha-particle irradiated to non-irradiated cells. Proc Natl Acad Sci USA 98:473–478; 2001.

Azzam EI, de Toledo SM, Raaphorst GP, Mitchel RE. Réponse adaptative au rayonnement ionisant des fibroblastes de peau humaine. Augmentation de la vitesse de réparation de l'ADN et variation de l'expression des gènes. J Chim Phys 91:931–936; 1994a [in French].

Azzam EI, de Toledo SM, Raaphorst GP, Mitchel RE. Low-dose ionizing radiation decreases the frequency of neoplastic transformation to a level below the spontaneous rate in C3H 10T1/2 cells. Radiat Res 146:369–373; 1996.

Azzam EI, Raaphorst GP, Mitchel RE. Radiation-induced adaptive response for protection against micronucleus formation and neoplastic transformation in C3H 10T1/2 mouse embryo cells. Radiat Res 138:S28–S31; 1994b.

Bond VP, Feinendegen LE, Booz J. What is a 'low dose' of radiation? Int J Radiat Biol Relat Stud Phys Chem Med 53:1–12; 1988.

de Toledo SM, Asaad N, Venkatachalam P, Li L, Spitz DR, Azzam EI. Adaptive responses to low-dose/low-dose-rate gamma rays in normal human fibroblasts: the role of growth architecture and oxidative metabolism. Radiat Res 166:849–857; 2006.

Redpath JL, Antoniono RJ. Induction of an adaptive response against spontaneous neoplastic transformation in vitro by low-dose gamma radiation. Radiat Res 149:517–520; 1998.

Redpath JL, Liang D, Taylor TH, Christie C, Elmore E. The shape of the dose-response curve for radiation-induced neoplastic transformation in vitro: evidence for an adaptive response against neoplastic transformation at low doses of low-LET radiation. Radiat Res 156:700–707; 2001.

Venkatachalam P, de Toledo SM, Pandey BN, Tephly LA, Carter AB, Little JB, Spitz DR, Azzam EI. Regulation of normal cell cycle progression by flavin-containing oxidases. Oncogene 27:20–31; 2008.

■ ■

A.3.2. Book Chapter – Bystander effects and adaptive responses modulate in vitro and in vivo biological responses to low dose ionizing radiation

In this book chapter (Zhang et al., 2012), we provide a more detailed review of topics discussed in the preceding paper above (de Toledo et al., 2011). We characterize biological effects that are induced in normal mammalian cells and tissues exposed to low doses/low fluences of IR of various LET.

Summary of the key points of this chapter:

- There is strong evidence of bystander and adaptive responses.
- The LET of the IR has been shown to play a critical role in triggering either protective or stressful effects at low doses of IR exposure.
- The data strongly support a role for intercellular communication and oxidative metabolism in the mediation of IR-induced non-targeted effects. As above, I aided in the development and optimization of the assays used to measure antioxidant enzyme activity, which were used in many of these studies in correlation to oxidative stress and levels of ROS.
- Our data suggest that biological responses to low doses of IR exposure alter the linearity of the dose-response relationship that is predicted by biophysical arguments.

BYSTANDER EFFECTS AND ADAPTIVE RESPONSES MODULATE IN VITRO AND IN VIVO BIOLOGICAL RESPONSES TO LOW DOSE IONIZING RADIATION[♣]

JIE ZHANG, MANUELA BUONANNO, GERALDINE GONON,
MIN LI, MARIANN GALDASS, GRACE SHIM,
SONIA M. DE TOLEDO, EDOUARD I. AZZAM[*]
Department of Radiology, UMDNJ-New Jersey Medical School Cancer Center, 205 South Orange Avenue, Newark, NJ 07103, USA

Abstract. We have utilized cellular and molecular approaches to characterize biological effects that are induced in normal mammalian cells and tissues exposed to low doses/low fluences of ionizing radiations that differ in their quality (i.e. linear energy transfer; LET). In human cells exposed to particulate radiations with high, but not low, LET character, the induced stressful effects were not only confined to the cells that have been directly targeted by the radiation, but involved a number of non-targeted and delayed effects. Chromosomal damage and oxidative changes in proteins and lipids were detected in cells exposed to alpha and high charge and high energy (HZE) particles and in their neighboring bystanders. Signaling events mediated via inflammatory cytokines and/or intercellular channels that comprise gap junctions were critical for the expression of the induced non-targeted effects. With relevance to health risks, the stressful changes in bystander cells were propagated to their progeny. In contrast, induced DNA repair and antioxidant defense mechanisms often attenuated the basal level of DNA damage and oxidative stress to below the spontaneous rate in tissues of animals and in cultured rodent and human cells exposed to low dose/low dose-rate γ rays, a low LET radiation. Together, our data suggest that low dose radiation-induced signaling events act to alter the linearity of the dose-response relation that is predicted by biophysical arguments. They show that the nature of the altered responses strongly depend on radiation quality.

Keywords: Low dose ionizing radiation, bystander effect, adaptive response, health risks, linear energy transfer

[♣] Radiobiology and Environmental Security / Eds. C.Mothersill, V.Korogodina, C.Seymour. Springer, 2012. P.71-88
[*] To whom the correspondence should be addressed

1. Introduction

Although recent advances in biochemical, molecular, and epidemiological techniques have increased our understanding of the biological effects and health risks of low dose ionizing radiation (<100 mSv), great ambiguities in knowledge still remain. The quality (i.e. linear energy transfer; LET), dose and dose-rate of the radiation, the types of irradiated cells, their microenvironment and their metabolic state, as well as the variations in inherent radiation sensitivity are among the factors that can modulate the responses to low dose radiation. These characteristics and others are under intense investigation in many laboratories, including ours; the results are yielding a wealth of novel insights into the mechanisms that underlay cell and tissue responses to low dose/low fluence ionizing radiation[1]. It is hoped that the elucidation of the mechanisms involved may alleviate the uncertainties in estimating low dose radiation effects on human health[2]. Typically, human epidemiological studies would be ideal to assess such effects; however, they currently have limited statistical power due to the small size of the cohorts under study[3].

Understanding the biological effects of low dose radiation is of immense, public, scientific and regulatory interest, as the frequency of human exposure to low dose radiation has been on the increase. In addition to exposures from natural sources (e.g. inhaled radon gas), the human population may be subjected to ionizing radiation during activities related to nuclear technology, mining, air travel and space exploration. Perhaps of greatest significance is the explosive growth in diagnostic radiology use where an increasing number of individuals, including children, are being *repeatedly* exposed to low dose radiation[4].

Currently, for the purposes of radiation protection, the deleterious effects of ionizing radiation are assumed to have a linear dose response with no threshold[2]. Two radiation-induced phenomena that were particularly recognized in the past three decades, namely adaptive and bystander effects, are thought to cause a challenge to these assumptions[5]. The propagation of damaging effects from irradiated to non-irradiated bystander cells would, presumably, result in supra-linear dose-response relationships. In contrast, the expression of adaptive responses that mitigate the initial damaging effects induced by radiation would suggest an infra-linear dose-response relationship or the existence of a threshold dose, below which there would be no risk. Although widely observed, the data confirming the expression of these two phenomena are not universal[6-9]. Moreover, the exact molecular steps by which adaptive and bystander effects are elicited remain unclear. Elucidation of these steps would clearly increase our understanding of the role of cellular processes that impact the health risks of low dose radiation exposures.

We have been intensely involved in examining the mechanisms underlying radiation-induced bystander and adaptive responses by using model cells and rodent tissues. Here, we summarize some of our findings in the context of a brief review of the latter phenomena. These findings provide strong support for the expression of both bystander and adaptive responses and reveal a critical role of the quality of the radiation in triggering either protective or stressful effects at low doses. Whereas, low doses of low LET radiations (highly energetic X rays, γ rays or protons) triggered processes that mitigated not only stressful effects induced by subsequent challenge doses of radiation, but also stressful effects due to endogenous oxidative metabolism[10-13], high LET radiations (α particles and high charge, high energy (HZE) particles) resulted in the propagation of stressful effects from irradiated to non-irradiated bystander cells[14-16]. The data strongly support a role for intercellular communication and oxidative metabolism in the mediation of these responses. Induction of genomic instability and low dose hypersensitivity are other phenomena that are also thought to impact the health risks of exposure to low dose radiation. These phenomena are being investigates in different laboratories[17-20].

2. Interactions of Ionizing Radiation with Biological Matter

Ionizing radiation is energetic and penetrating. Many of its chemical effects in biological matter are due to the geometry of the initial physical energy deposition events, referred to as the track structure. The transfer of radiation energy to living tissues causes ionization of atoms and molecules and breaks chemical bonds, which initiates a series of biochemical and molecular signaling events that culminate in transient or permanent physiological changes[21].

Ionizing radiation exists in either particulate or electromagnetic types. The ionizations and excitations that it produces tend to be localized, along the tracks of individual charged particles, in a pattern that depends on the type of radiation involved. Whereas the ionization events produced by fast electrons ejected from molecules traversed by high energy X rays or γ rays are well separated in space, those produced by certain charged particles, such as α and HZE particles, occur in dense columns along the particle path[22]. Such differences in ionization patterns mainly arise from differences in charge-to-mass ratio of the impacting particles.

Effects due to the track structure define the quality of the radiation and are commonly called linear energy transfer (LET) effects. In irradiated mammalian cells, which consist mainly of water, single energy deposition events cause bursts of reactive oxygen species (ROS) in and around the radiation track as well as in the intercellular matrix. Depending on the physiological state of the cell, these bursts of reactive species may alter the cellular redox environment, modify signaling cascades and normal biochemical reactions, and generate damage to cellular molecules and organelles[23]. In

addition to the damages caused by water radiolysis products (i.e. the indirect effect), cellular damage may also involve reactive nitrogen species (RNS) and other species[24], and can occur also as a result of ionization of atoms on constitutive key molecules (e.g. DNA). The latter is known as the direct effect[21]. The ultimate result, of direct and indirect effects, is the development of biological and physiological alterations that may manifest themselves seconds or decades later. Genetic and epigenetic changes may be involved in the evolution of these alterations[25, 26]. Intercellular communication among the irradiated cells[27], and between irradiated and non-irradiated cells[14, 28], as well as oxidative metabolism and DNA repair mechanisms are major mediators of the *system* responses to ionizing radiation exposure[29].

Because high LET radiation deposits greater amounts of energy per unit length of matter traversed, the possibility of multiple lesions in close proximity and short time frame is high[30]. Consequently, for the same total dose absorbed, high LET radiation is more damaging to cells than low LET radiation[21]. The effects of LET, dose, and dose-rate in the cellular responses to low dose/low fluence ionizing radiation exposures continue to be intensely investigated. Here, we highlight the relevance of the latter charactersitics of radiation in the expression of adaptive responses and in the nature of the biological effect propagated from irradiated to bystander cells in the exposed cell populations.

3. Ionizing Radiation-Induced Bystander Effects

The ionizing radiation-induced bystander effect is broadly defined as the occurrence of biological effects in unirradiated cells as a result of exposure of other cells in the population to radiation. Bystander effects have been mainly observed in high density cell cultures exposed to low fluences of α particles wherein only a small fraction of cells is irradiated[31]. Emerging data also indicate that bystander effects exist in cell cultures exposed to low doses of HZE particles[32]. They have also been noted in co-cultures of irradiated and unirradiated cells[33, 34]. Stressful effects including up-regulation of stress-responsive proteins, genetic changes, induction of cell cycle checkpoints and cell death occur in both irradiated and non-irradiated cells of human and rodent origin at different stages of growth (reviewed in[1, 18, 35-37]). More recently, strong evidence for bystander responses *in vivo* has been presented[38, 39]. A few studies have also indicated that radiation-induced protective responses are mediated in a bystander manner in cell cultures exposed to low doses of low LET radiations[40] (and our unpublished data).

By using several biological endpoints to investigate non-targeted effects, including induction of DNA damage and various parameters of oxidative stress, our studies strongly support a role for LET, dose-rate and total absorbed dose in determining the nature and magnitude of the radiation-induced bystander effect and its persistence in progeny cells[13, 41, 42]. Together with results generated by others, the data clearly show

that a given cell need not be directly irradiated to experience an ionizing radiation-induced biological response. Depending on cell type and radiation characteristics, distinct molecular interactions lead to propagation of either damaging or protective effects from irradiated to unirradiated cells and between irradiated cells. Gap-junction selectivity, secreted diffusible factors and oxidative metabolism are mediators of these effects[35].

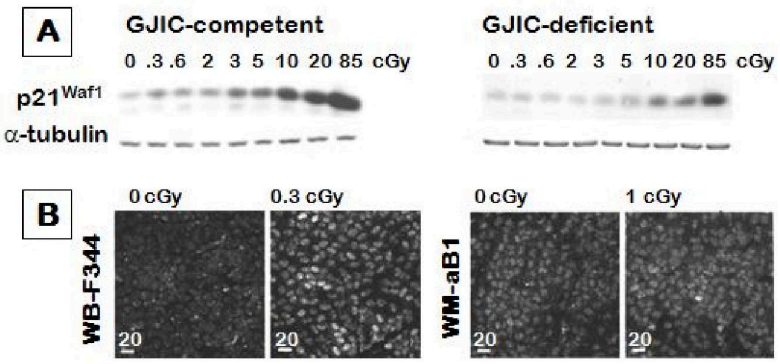

Figure 1 **(A)** Expression of $p21^{Waf1}$ in protein lysates from gap junction communication-competent WB-F344 or gap junction communication-deficient WM-aB1 confluent cultures following exposure to α particles. Cells were harvested 4h after the exposure and proteins were examined by western blot analyses **(B)** *In situ* immunofluorescence detection of $p21^{Waf1}$ expression in control non-irradiated WB-F344 cultures and in cultures exposed to 0.3 cGy of α particles. Expression of $p21^{Waf1}$ in control non-irradiated and in 1 cGy-exposed cultures of GJIC-deficient WM-aB1 cells[15]

A direct evidence for the role of gap-junction intercellular communication (GJIC) in these processes was shown by our group and by others[14, 15, 28]. The modulation of proteins involved in the $p53/p21^{Waf1}$ stress-induced signaling pathway and induction of DNA damage in bystander cells were observed only in GJIC-proficient cell cultures. The data in Figure (1) describe $p21^{Waf1}$ expression in sham-exposed and α particle-irradiated cultures from two related rat epithelial cell lines that differ in their ability to communication via gap junctions. The WB-F344 cells are GJIC-competent, a function that is sensitive to inhibition by lindane and other chemicals that block junctional communication[43, 44]. The WM-aB1 cells were derived from WB-F344 cells, but are deficient in GJIC[15, 45]. Similar to WB-F344 cells, WM-aB1 cells express connexin43, a structural protein of gap junctions, however they are deficient in the ability to phoshorylate it, which renders them deficient in functional GJIC[15, 45]. The western blot analyses data in Fig. (1A) show an increase in $p21^{Waf1}$ levels in confluent WB-F344 cultures exposed to mean doses as low as 0.3 cGy. In WM-aB1 cell cultures, an increase in $p21^{Waf1}$ levels is

significant only at mean doses of 5 cGy or higher. Therefore, the magnitude of the response in the GJIC-competent cells and the lack of $p21^{Waf1}$ up-regulation in WM-aB1 GJIC-deficient cultures exposed to low mean doses strongly support the involvement of GJIC in the bystander gene expression response. This is further confirmed by the *in situ* immunofluorescence data in Fig. (1B) showing induction of $p21^{Waf1}$ in confluent cultures exposed to a mean dose of 0.3 cGy. While small clusters of responding cells were observed in WB-F344 cells, only single isolated and presumably irradiated WM-aB1 cells invariably exhibited up-regulation of $p21^{Waf1}$ after exposure to doses in the range of 0.3 to 1.0 cGy (Fig. 1B). At these mean doses to the monolayer, 1% or less of the WB-F344 or WM-aB1 cells would have their nuclei traversed by an α particle.

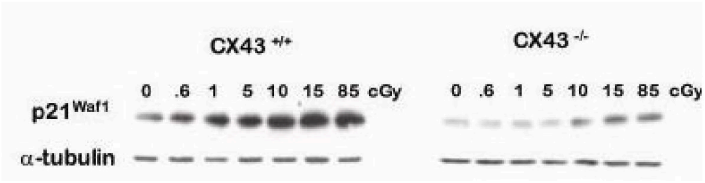

Figure 2 Western analyses of $p21^{Waf1}$ level in lysates from isogenic wt or connexin43-/- MEF cultures exposed to α particles. Cells were harvested 4h after the exposure[15].

The WM-aB1 cells were transformed by mutagenesis of the WB-F344 parental cell line[46]. To exclude effects due to mutagenesis other than loss of GJIC, we tested the induction of the p53/$p21^{Waf1}$ signaling pathway after low fluence α particle irradiation of low passage mouse embryo fibroblasts (MEFs) from wt and isogenic knockout embryos for connexin43. Similar to WB-F344 and WM-aB1 cells (Fig. 1), the data in Fig. (2) indicate a lack of detectable increase in $p21^{Waf1}$ level in connexin43$^{-/-}$ cell cultures exposed to mean doses less than 10 cGy. In contrast, $p21^{Waf1}$ was induced in wt cell cultures exposed to mean doses as low as 0.6 cGy. Collectively, these data support strongly the involvement of GJIC in the bystander gene expression response observed in confluent, density-inhibited cell cultures exposed to low fluences of α particles. They are relevant to estimation of the health risks of exposure to environmental radon. Radon accounts for 55% of the average annual radiation dose to the public in the USA and is considered to be the single largest naturally occurring environmental hazard. In fact, ~ 10-14% of lung cancer fatalities in the USA may be linked to radon and its α particle-emitting decay[47].

In addition to α particles, and with relevance to space exploration, we have also observed prominent stressful bystander effects in cell cultures exposed to low fluenes of HZE particles[48]. Our published and unpublished data indicate prominent induction of DNA damage, protein oxidation, lipid peroxidation and perturbations in mitochondrial functions, including mitochondrial protein transport and inactivation of the metabolic enzyme aconitase in bystander cells and in their progeny. Gap-junction communication was a major mediator of the propagation of these effects in the tissue culture systems used in our studies.

3.1. GAP-JUNCTION CHANNELS AND THE CELLULAR RESPONSE TO IONIZING RADIATION

Gap junctions are dynamic structures that are critical for diverse physiological functions[49]. The intercellular channels that comprise gap junctions are formed by *connexin* protein. Each of the ~20 isoforms of connexin forms channels with distinct permeability properties. Though the properties of channels formed by each isoform differ, connexin pores, which vary in diameter, usually allow permeation of molecules up to ~1000Da, well above the size of most second messengers. Connexin channels have been shown to be highly selective among molecular permeants[49].

Evidence for the involvement of GJIC in propagation of bystander effects has been derived from studies with α particle, β particle, γ, and HZE radiations. These studies highlight the relevance of bystander responses to radiotherapy, diagnostic radiology, and risk of environmental and occupational exposures[50]. Manipulation (↓↑) of connexin expression/gap-junction gating by pharmacological agents, forced expression by transfection, and connexin gene knockout studies have provided evidence for the participation of GJIC in radiation-induced bystander effects[35]. This is particularly supported by the stabilization and up-regulation of connexin mRNA and protein by ionizing radiation Fig. (3)[51]. Examination by Northern and Western analyses of AG1522 normal human fibroblast cultures exposed to low fluences of α particles indicated that the *CONNEXIN43* gene is indeed activated. Relative to sham-irradiated controls, *CONNEXIN43* mRNA (Fig. 3A) and protein levels (Fig. 3B) were increased after exposure to mean doses ranging from 1 to 24 cGy. The similar increases at all doses suggest that low fluences of α particles induce molecular pathways that lead to maximal up-regulation of *CONNEXIN43*. The data in Fig. (3B) indicate increased expression in three protein bands detected by the antibody used. These bands were previously described to represent the native, phosphorylated and hyperphosphorylated isoforms of connexin43[52]. Low fluences of α particles up-regulate both the native and the post-translationally modified isoforms in confluent normal human fibroblasts[51].

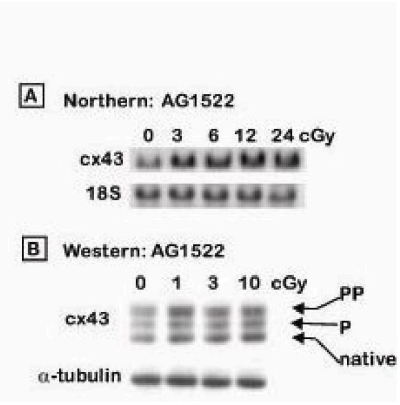

Figure 3. Upregulation of *CONNEXIN43* in α-particle-irradiated cell cultures. **(A)** Northern analyses of *connexin43* expression in AG1522 fibroblast cultures exposed to α-particles doses ranging from 0 to 24 cGy and held at 37°C for 6 h. **(B)** Western analyses of connexin43 in AG1522 confluent cultures at 3 h after exposure to α particle doses ranging from 0 to 10 cGy under normal growth conditions[51].

Participation of GJIC in stress-induced bystander effects is not unique to ionizing radiation; it has also been described in high density cell populations exposed to chemotherapeutic agents. Toxicity of these compounds was enhanced by functional gap-junction communication in target cells [53]. Thus, many systems show that GJIC enhances the effects of toxic agents on targeted and untargeted cells. Direct intercellular communication may also lead to induction of protective effects that attenuate damage in targeted cells[54]. The determinants and mechanism(s) of these effects, however, remain largely undefined. Our emerging data indicate that permeability properties of gap-junction channels have affect the nature of the induced bystander response. Different connexins form channels with *different* selectivities for various molecules including ions and highly similar second messengers[55].

Direct intercellular communication is not unique in propagating radiation-induced non-targeted effects. A wealth of data has also shown the critical importance of secreted diffusible factors in the expression of radiation-induced non-targeted effects[36]. TGF-β, interleukin-8, serotonin and others have been implicated in propagation of bystander effects[56, 57].

3.2. OXIDATIVE METABOLISM AND BYSTANDER EFFECTS

Normal oxidative metabolism is a key endogenous generator of reactive oxygen and nitrogen species[58], and homeostatic control of normal cellular growth pathways is tightly dependent on oxidants[59]. A disruption of the balance between oxidant production

and antioxidant defense alters the homeostatic cellular redox environment, resulting in a state of oxidative stress that promotes several pathological conditions including degenerative diseases and cancer[60]. The endogenous targets of oxidants are diverse and include nucleic acids, proteins and lipids.

There is a strong connection between the generation of ROS and RNS and the damage that follows radiation exposure. Whereas ~60 ROS per nanogram of tissue were estimated to be generated from a hit caused by ^{137}Cs γ rays[67, 68], we can estimate that over 2000 ROS are generated from an α particle traversal, corresponding to a ROS concentration of ~19 n*M* in the nucleus of a normal human AG1522 cells[27]. Such a ROS concentration can obviously cause extensive oxidative damage and may constitute a signaling event that triggers the spread of stressful effects from irradiated to neighboring bystander cells.

The involvement of ROS in the ionizing radiation induced bystander response was postulated by Nagasawa and Little[31] in their initial report describing the induction of sister-chromatid exchanges (SCE) in bystander Chinese hamster ovary cells present in cultures exposed to fluences of α particles by which less than 1% of the nuclei were directly targeted. Evidence for such involvement was subsequently generated in studies involving various biological endpoints and irradiation modalities[35]. Induction of stress responsive proteins, lethality and genetic changes (SCEs, mutations, chromosomal aberrations) in bystander cells was inhibited by superoxide dismutase (SOD) and other antioxidants[35].

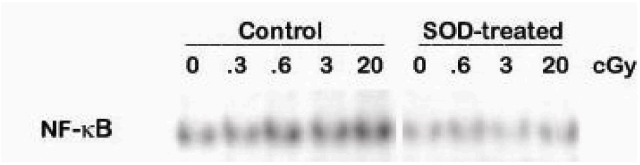

Figure 4. Electrophoretic mobility shift assay in α particle-irradiated AG1522 fibroblast cultures indicates activation of NFκB DNA-binding by low mean doses at 30 min after exposure[16].

ROS act as second messengers that regulate gene expression by signaling processes that involve activation of redox sensitive transcription factors[61-67]. Consistent with a role for radiation-induced alterations in redox sensitive transcription factor activation in bystander cells in cultures exposed to low fluences of α particles, increases in the DNA-binding activity of NFκB were observed in AG1522 normal human cell cultures exposed to doses as low as 0.3 cGy (Fig. 4). A similar level of increased DNA-binding activity was observed at 0.6 and 3 cGy although a 5-fold greater fraction of cell nuclei are traversed at 3 cGy than at 0.6 cGy. Importantly, when SOD (100 μg/ml, 300 U/ml) was added to the culture 30 min prior to irradiation, the increase in NFκB DNA-binding activity was inhibited (Fig. 4), further supporting the role of $O_2^{\bullet-}$ in the bystander response of AG1522 cells.

Extensive data now indicate that the intracellular production of superoxide anions and hydrogen peroxide in both irradiated and bystander cells involves both the plasma bound NADPH-oxidase and mitochondria[16]. Of particular significance, our data strongly indicate that increased ROS levels following cellular exposure to α or HZE particles persist in progeny cells for many generations. This is manifested by increased oxidation of cellular proteins and disruption of mitochondrial physiology. In particular, decreased aconitase activity, which is involved in electron transport and regulation of gene expression, was observed, in bystander cells, 20 population doublings after exposure[48]. Ectopic over-expression at the time of irradiation of the antioxidant enzymes superoxide dismutase or glutathione peroxidase, in bystander or irradiated cells, attenuated DNA damage and induction of stress-responsive proteins in the bystander cells (our data, unpublished). These results show that oxidative metabolism modulates non-targeted effects at the level of the irradiated and bystander cells.

Through *in vivo* experiments consisting of partial body irradiation of male Sprague-dawley rats with low fluences of HZE particles (energetic titanium or oxygen ions), stressful effects involving mitochondrial dysfunction were observed in non-targeted tissues 20 months after the exposure[38]. Decreases in mitochondrial protein import as well as increases in antioxidant defense in non-targeted tissues were associated with perturbations in immune responses and inflammatory cytokines levels (e.g. interleukin-6) (unpublished). These data are consistent with the findings of others who showed that inflammatory-type responses involving oxidative stress occur after exposure to ionizing radiation[68, 69]. In these *in vivo* experiments, activation of macrophages and neutrophil infiltration were not a direct effects of irradiation, but were a consequence of the recognition and clearance of radiation-induced apoptotic cells. The occurrence of such a response has been suggested to provide a mechanism for the interactions between irradiated and non-irradiated haemopoietic cells[68, 69]. Such interaction was also observed in out of field experiments examining the genetic effects of partial organ irradiation. Antioxidants and nitric oxide synthase inhibitors attenuated these effects[70] strongly supporting the role of ROS and RNS in mediating bystander effects[71, 72].

Overall, several studies challenge the traditional paradigm that the important biological effects of ionizing radiation are due to DNA damage induced as a result of direct interaction of the radiation track with the cell nucleus. They indicate that irradiated and non-irradiated cells interact, and oxidative metabolism and intercellular communication have an essential role in signaling events leading to radiation-induced bystander effects. However, clear evidence explaining how these events occur is still lacking. Regardless, the occurrence of bystander effects implies that the modeling of dose response relationships based on the number of irradiated cells may not be a valid approach[17].

4. Low LET Radiation-Induced Adaptive Responses

The "adaptive response" is a phenomenon generally induced by low dose/low LET radiation that protects cells and whole organisms against endogenous damage or damage due to a subsequent dose of radiation[73]. Data generated over the last three decades suggest that exposure of mammalian cells, including human cells, to low doses of low LET radiation (e.g. X rays, γ rays, β particles) induces molecular processes that are different from those induced by high dose radiation[74]. Such processes were found to be protective against stress measured by several biological endpoints[5]. Radiation-induced adaptive responses were dependent on the adapting dose, dose rate, expression time, culture conditions and stage of the cell cycle[75]. Adaptive responses seem to be evolutionarily conserved as effects that protect against DNA damage in mammalian cells[76] mirror the evidence of radiation-induced protective mechanisms in prokaryotes and lower eukaryotes[77]. Adaptive responses to ionizing radiation have also been dtected *in vivo*[78, 79].

Of particular relevance to risk assessment, it was observed that low-dose/low LET radiation (0.1 – 10 cGy) decreases the frequency of neoplastic transformation to a level below the spontaneous rate in C3H 10T½ mouse embryo fibroblasts (MEFs) and in HeLa human hybrid cells[11, 80]. It is noteworthy that these protective effects were seen only in irradiated cells that were allowed to incubate at 37°C before release from contact inhibition (Fig. 5), which suggests that time is required for expression of the protective effects.

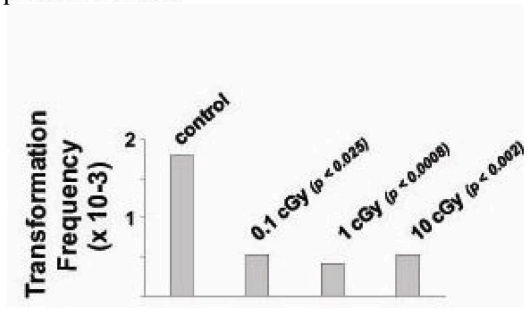

Figure 5. Low dose/low dose rate γ rays decrease the frequency of neoplastic transformation to a level below the spontaneous rate in C3H 10T½ mouse embryo fibroblasts[11].

Chronic exposure of C3H 10T½ MEFs to ^{60}Co γ-radiation at doses as low as 10 cGy protected the cells not only against damage from endogenous metabolic processes, but also against neoplastic transformation by a subsequent large acute radiation exposure[12]. The induced resistance to neoplastic transformation correlated with increased ability to repair radiation-induced chromosome breaks[10]. Significantly, our recent proteomic

studies have identified novel proteins that were distinctly induced by low and not high dose γ rays. We have uncovered a role in DNA repair for the translationally controlled tumor protein, which was induced by almost 10-folds in cell cultures exposed to doses as low as 1 cGy (Zhang *et al.*, manuscript in preparation).

In addition to up-regulation of DNA repair mechanisms[81], other processes may also modulate cellular responses to low dose/low dose-rate irradiation. Irradiation, under such conditions may affect the overall redox-state of the cell and its anti-oxidation potential, and may alter chromatin conformation, hence affecting the accessibility of DNA lesions to components of the DNA repair machinery. It may also induce mechanisms (e.g. apoptosis) that eliminate heavily damaged cells from the irradiated cell population[82]. Our data indicate that direct intercellular communication by gap-junctions[13] is an important modulator of these effects. In addition, the induction of cell cycle checkpoints presumably provides more time for repair of radiation damage. Such effects may involve epigenetic events that could be transmitted to the progeny of low dose irradiated cells (Chaudhry *et al.*, manuscript in preparation).

Similar to its role in modulating bystander effects, oxidative metabolism is also a significant mediator of low dose, low LET radiation effects. Exposure of normal human fibroblasts maintained in 3-dimensional architecture to 10 cGy from γ rays delivered over 48 h reduced the frequency of micronucleus formation (a form of DNA damage) to levels similar or lower than background[13]. The effects correlated with up-regulation of cellular content of the antioxidant glutathione[13]. Extensive data have also shown that whole-body exposure of mice to low dose/low dose-rate γ rays up-regulates superoxide dismutase and alters mitochondrial functions in a manner that attenuates the generation of ROS (Li *et al.*, manuscript in preparation). We predict that such alterations provide a defense mechanism that allows the organism to cope with the radiation-induced oxidative stress. Together, the data suggest that mitochondria, which are active participants in oxidative metabolism, play a crucial role in low dose-induced adaptive responses.

5. Conclusions

Some of the mechanisms (e.g. junctional communication, oxidative metabolism) that underlie the bystander effect have been also implicated in the adaptive response to ionizing radiation. However, classical adaptive response protocols involving low LET radiation are clearly distinct from those of bystander studies conducted mainly with high LET radiation. In the adaptive response, cells are exposed to a small dose of low LET radiation. In contrast, cells traversed by an α or a HZE particle receive a substantial dose (10-70 cGy) and undergo a complex type of DNA damage. While similar mediators may modulate the same endpoint in both phenomena, the occurrence of opposite effects, such as pro-survival rather than cytotoxic effect, may reflect

changes in concentration of the inducing factor(s). For example, ROS have been shown to be a double-edged sword capable of inducing both proliferative or cell death effects depending on their concentration. Moreover, recent studies emphasized the effect of LET on the yield of water radiolysis products[83]. Prevalence of different radiolysis species at the time of irradiation may induce dissimilar effects. However, the bystander effect and adaptive response could also be mediated by distinct mechanisms/mediating factors.

Due to limitations in the statistical power of current human epidemiological studies in assessing the health risks of low dose radiation exposures, mechanistic studies may be essential to understanding biological effects, and to help evaluating risks at low doses. Coupled with epidemiology, the knowledge of cellular and molecular processes that underlay low dose radiation-induced biological effects should further refine our estimates of radiation risks at low doses. The expression of stressful bystander effects in cell populations exposed to low fluences of high LET particles may contribute to the understanding of lung cancer incidence from environmental radon and degenerative diseases that may occur following deep space travel[84]. Bystander effect studies may also enhance our understanding of biological effects that result from non-uniform distribution of incorporated radioactivity such as α particles emitted from radionuclides used in therapeutic nuclear medicine or released during nuclear accidents or terrorist activities[50]. In particular, they offer avenues to characterize the nature of communicated signaling molecules and formulate strategies to protect normal tissue surrounding irradiated tumor targets. In contrast, the expression of adaptive responses in low dose/low LET exposed cell populations and the propagation of protective effects from irradiated to non-irradiated cells present in these populations may explain reported hormetic effects. They indicate that for some individuals, the risk from very small doses of radiation delivered at low dose-rate may be inexistent.

In conclusion, it is apparent that extensive *in vitro* and *in vivo* experimental evidence suggests that biological responses together with biophysical considerations likely determine the outcome of cellular exposure to ionizing radiation. Collectively, these studies should further contribute to the setting of radiation protection standards that would be effective in different exposure scenarios, applicable to men and women of all ages, and that must protect radiosensitive persons.

Acknowledgements

This research was supported by Grants DE-FG02-07ER64344 from the US Department of Energy (Low Dose Radiation Research Program), CA049062 from the NIH and NNJ06HD91G from NASA.

References

1. N. Hamada , M. Maeda , K. Otsuka and M. Tomita, Signaling Pathways Underpinning the Manifestations of Ionizing Radiation-Induced Bystander Effects, *Current molecular pharmacology*, (2010).
2. BEIR-VII *Health Risks from Exposure to Low Levels of Ionizing Radiation*; National Research Council of the National Academies: Washington, D.C., 2005.
3. D. Averbeck, Does scientific evidence support a change from the LNT model for low-dose radiation risk extrapolation?, *Health Phys 97*(5), 493-504 (2009).
4. D. J. Brenner and E. J. Hall, Computed tomography--an increasing source of radiation exposure, *N Engl J Med 357*(22), 2277-84 (2007).
5. S. M. de Toledo and E. I. Azzam, Adaptive and bystander responses in human and rodent cell cultures exposed to low level ionizing radiation: the impact of linear energy transfer, *Dose Response 4*(4), 291-301 (2006).
6. B. J. Blyth , E. I. Azzam , R. W. Howell , R. J. Ormsby , A. H. Staudacher and P. J. Sykes, An adoptive transfer method to detect low-dose radiation-induced bystander effects in vivo, *Radiat Res 173*(2), 125-37
7. C. Fournier , P. Barberet , T. Pouthier , S. Ritter , B. Fischer , K. O. Voss , T. Funayama , N. Hamada , Y. Kobayashi and G. Taucher-Scholz, No evidence for DNA and early cytogenetic damage in bystander cells after heavy-ion microirradiation at two facilities, *Radiat Res 171*(5), 530-40 (2009).
8. M. B. Sowa , W. Goetz , J. E. Baulch , A. J. Lewis and W. F. Morgan, No Evidence for a Low Linear Energy Transfer Adaptive Response in Irradiated Rko Cells, *Radiat Prot Dosimetry*, (2011).
9. M. B. Sowa , W. Goetz , J. E. Baulch , D. N. Pyles , J. Dziegielewski , S. Yovino , A. R. Snyder , S. M. de Toledo , E. I. Azzam and W. F. Morgan, Lack of evidence for low-LET radiation induced bystander response in normal human fibroblasts and colon carcinoma cells, *Int J Radiat Biol 86*(2), 102-13 (2010).
10. E. I. Azzam , S. M. de Toledo , G. P. Raaphorst and R. E. Mitchel, Réponse adaptative au rayonnement ionisant des fibroblastes de peau humaine. Augmentation de la vitesse de réparation de l'ADN et variation de l'expression des gènes, *J Chim Phys 91*(7/8), 931-936 (1994).
11. E. I. Azzam , S. M. de Toledo , G. P. Raaphorst and R. E. Mitchel, Low-dose ionizing radiation decreases the frequency of neoplastic transformation to a level below the spontaneous rate in C3H 10T1/2 cells, *Radiat Res 146*(4), 369-73 (1996).
12. E. I. Azzam , G. P. Raaphorst and R. E. Mitchel, Radiation-induced adaptive response for protection against micronucleus formation and neoplastic transformation in C3H 10T1/2 mouse embryo cells, *Radiat Res 138*(1 Suppl), S28-31 (1994).
13. S. M. de Toledo , N. Asaad , P. Venkatachalam , L. Li , D. R. Spitz and E. I. Azzam, Adaptive responses to low-dose/low-dose-rate gamma rays in normal human fibroblasts: The role of growth architecture and oxidative metabolism, *Radiat Res 166*, 849-857 (2006).
14. E. I. Azzam , S. M. de Toledo , T. Gooding and J. B. Little, Intercellular communication is involved in the bystander regulation of gene expression in human cells exposed to very low fluences of alpha particles, *Radiat. Res. 150*, 497-504 (1998).

15. E. I. Azzam , S. M. de Toledo and J. B. Little, Direct evidence for the participation of gap-junction mediated intercellular communication in the transmission of damage signals from alpha-particle irradiated to non-irradiated cells, *Proc Natl Acad Sci U S A 98*(2), 473-478 (2001).
16. E. I. Azzam , S. M. de Toledo , D. R. Spitz and J. B. Little, Oxidative metabolism modulates signal transduction and micronucleus formation in bystander cells from alpha-particle-irradiated normal human fibroblast cultures, *Cancer Res 62*(19), 5436-42 (2002).
17. J. B. Little, Genomic instability and bystander effects: a historical perspective, *Oncogene 22*(45), 6978-87 (2003).
18. W. F. Morgan, Non-targeted and delayed effects of exposure to ionizing radiation: I. Radiation-induced genomic instability and bystander effects *in vitro*, *Radiat Res 159*(5), 567-80 (2003).
19. H. Matsumoto , N. Hamada , A. Takahashi , Y. Kobayashi and T. Ohnishi, Vanguards of paradigm shift in radiation biology: radiation-induced adaptive and bystander responses, *J Radiat Res (Tokyo) 48*(2), 97-106 (2007).
20. M. C. Joiner , P. Lambin , E. P. Malaise , T. Robson , J. E. Arrand , K. A. Skov and B. Marples, Hypersensitivity to very-low single radiation doses: its relationship to the adaptive response and induced radioresistance, *Mutat Res 358*(2), 171-83 (1996).
21. E. J. Hall, *Radiobiology for the Radiologist*. 5 ed.; J. B. Lippincott Co.: Philadelphia, 2000.
22. D. T. Goodhead, Spatial and temporal distribution of energy, *Health Phys. 55*, 231-240 (1988).
23. D. R. Spitz , E. I. Azzam , J. J. Li and D. Gius, Metabolic oxidation/reduction reactions and cellular responses to ionizing radiation: a unifying concept in stress response biology, *Cancer Metastasis Rev 23*(3-4), 311-22 (2004).
24. P. Wardman, The importance of radiation chemistry to radiation and free radical biology (The 2008 Silvanus Thompson Memorial Lecture), *Br J Radiol 82*(974), 89-104 (2009).
25. R. L. Jirtle and M. K. Skinner, Environmental epigenomics and disease susceptibility, *Nat Rev Genet 8*(4), 253-62 (2007).
26. I. Koturbash , K. Kutanzi , K. Hendrickson , R. Rodriguez-Juarez , D. Kogosov and O. Kovalchuk, Radiation-induced bystander effects in vivo are sex specific, *Mutat Res 642*(1-2), 28-36 (2008).
27. N. Autsavapromporn , S. M. De Toledo , J. B. Little , J. P. Jay-Gerin , A. L. Harris and E. I. Azzam, The role of gap-junction communication and oxidative stress in the propagation of toxic effects among high dose alpha particle-irradiated human cells, *Radiat. Res. in press* (2011).
28. H. N. Zhou , M. Suzuki , R. Randers-Pehrson , G. Chen , J. Trosko , D. Vannais , C. A. Waldren , E. J. Hall and T. K. Hei, Radiation risk at low doses may be greater than we thought, *Proc. Natl. Acad. Sci. USA 98*(25), 14410-5 (2001).
29. L. Feinendegen , P. Hahnfeldt , E. E. Schadt , M. Stumpf and E. O. Voit, Systems biology and its potential role in radiobiology, *Radiat Environ Biophys 47*(1), 5-23 (2008).
30. F. A. Cucinotta , H. Wu , M. R. Shavers and K. George, Radiation dosimetry and biophysical models of space radiation effects, *Gravit Space Biol Bull 16*(2), 11-8 (2003).
31. H. Nagasawa and J. B. Little, Induction of sister chromatid exchanges by extremely low doses of alpha-particles, *Cancer Res. 52*, 6394-6396 (1992).
32. K. D. Held, Effects of low fluences of radiations found in space on cellular systems, *Int J Radiat Biol 85*(5), 379-90 (2009).

33. A. Bishayee , H. Z. Hill , D. Stein , D. V. Rao and R. W. Howell, Free-radical initiated and gap junction-mediated bystander effect due to nonuniform distribution of incorporated radioactivity in a three-dimensional tissue culture model, *Radiat. Res. 155*, 335-344 (2001).
34. B. I. Gerashchenko and R. W. Howell, Cell proximity is a prerequisite for the proliferative response of bystander cells co-cultured with cells irradiated with gamma-rays, *Cytometry 56A*, 71-80 (2003).
35. E. I. Azzam , S. M. de Toledo and J. B. Little, Oxidative metabolism, gap junctions and the ionizing radiation-induced bystander effect, *Oncogene 22*(45), 7050-7 (2003).
36. C. Mothersill and C. B. Seymour, Radiation-induced bystander effects--implications for cancer, *Nat Rev Cancer 4*(2), 158-64 (2004).
37. K. M. Prise and J. M. O'Sullivan, Radiation-induced bystander signalling in cancer therapy, *Nat Rev Cancer 9*(5), 351-60 (2009).
38. M. R. Jain , M. Li , W. Chen , T. Liu , S. M. de Toledo , B. N. Pandey , H. Li , B. M. Rabin and E. I. Azzam, In Vivo Space Radiation-Induced Non-Targeted Responses: Late Effects On Molecular Signaling In Mitochondria, *Current molecular pharmacology*, (2010).
39. M. Mancuso , E. Pasquali , S. Leonardi , M. Tanori , S. Rebessi , V. Di Majo , S. Pazzaglia , M. P. Toni , M. Pimpinella , V. Covelli and A. Saran, Oncogenic bystander radiation effects in Patched heterozygous mouse cerebellum, *Proc Natl Acad Sci U S A 105*(34), 12445-50 (2008).
40. H. Klammer , M. Kadhim and G. Iliakis, Evidence of an adaptive response targeting DNA nonhomologous end joining and its transmission to bystander cells, *Cancer Res 70*(21), 8498-506 (2010).
41. M. Boyd , A. Sorensen , A. G. McCluskey and R. J. Mairs, Radiation quality-dependent bystander effects elicited by targeted radionuclides, *The Journal of pharmacy and pharmacology 60*(8), 951-8 (2008).
42. M. Pinto , E. I. Azzam and R. W. Howell, Bystander responses in three-dimensional cultures containing radiolabeled and unlabeled human cells, *Radiat. Prot. Dosim.*, In press (2006).
43. K. A. Criswell and R. Loch-Caruso, Lindane-induced elimination of gap junctional communication in rat uterine monocytes is mediated by an arachdonic acid-sensitive cAMP-independent mechanism, *Toxicol. Appl. Pharmacol. 135*, 127-138 (1995).
44. R. Li and J. P. Mather, Lindane, an inhibitor of gap junction formation, abolishes oocyte directed follicle organizing activity in vitro, *Endocrinology 138*(10), 4477-80 (1997).
45. S. Y. Oh , E. Dupont , B. V. Madhukar , J. P. Briand , C. C. Chang , E. Beyer and J. Trosko, Characterization of gap junctional communication-deficient mutants of a rat liver epithelial cell line, *Eur. J. Cell Biol. 60*, 250-255 (1993).
46. G. Tsushimoto , C. C. Chang , J. E. Trosko and F. Matsumura, Cytotoxicity , mutagenic, and cell-cell communication inhibitory properties of DDT, lindane, and chlordane on hamster cells in vitro, *Arch. Environ. Contam. Toxicol. 12*, 721-730 (1983).
47. BEIR-VI *Health Effects of Exposure to Radon (BEIR VI)*; National Academy Press: Washington, D.C., 1998.
48. M. Buonanno , S. M. De Toledo , D. Pain and E. I. Azzam, Long-Term Consequences of Radiation-Induced Bystander Effects Depend on Radiation Quality and Dose and Correlate with Oxidative Stress, *Radiation Research In press*, (2011).

49. A. L. Harris, Emerging issues of connexin channels: biophysics fills the gap, *Q Rev Biophys 34*(3), 325-472 (2001).
50. R. W. Howell , P. V. Neti , M. Pinto , B. I. Gerashchenko , V. R. Narra and E. I. Azzam, Challenges and progress in predicting biological responses to incorporated radioactivity, *Radiat Prot Dosimetry 122*(1-4), 521-7 (2006).
51. E. I. Azzam , S. M. de Toledo and J. B. Little, Expression of CONNEXIN43 is highly sensitive to ionizing radiation and environmental stresses, *Cancer Res 63*(21), 7128-7135 (2003).
52. P. D. Lampe and A. F. Lau, Regulation of gap junctions by phosphorylation of connexins, *Arch Biochem Biophys 384*(2), 205-15 (2000).
53. R. Jensen and P. M. Glazer, Cell-interdependent cisplatin killing by Ku/DNA-dependent protein kinase signaling transduced through gap junctions, *Proc Natl Acad Sci U S A 101*(16), 6134-9 (2004).
54. M. R. Wygoda , M. R. Wilson , M. A. Davis , J. E. Trosko , A. Rehemutulla and T. S. Lawrence, Protection of herpes simplex virus thymidine kinase-transduced cells from ganciclovir-mediated cytotoxicity by bystander cells: The good samaritan effect, *Cancer Res. 57*, 1699-1703 (1997).
55. C. G. Bevans , M. Kordel , S. K. Rhee and A. L. Harris, Isoform composition of connexin channels determines selectivity among second messengers and uncharged molecules, *J Biol Chem 273*(5), 2808-16 (1998).
56. B. E. Lehnert and E. H. Goodwin, Extracellular factor(s) following exposure to alpha particles can cause sister chromatid exchanges in normal human cells, *Cancer Res. 57*, 2164-2171 (1997).
57. C. Mothersill , R. Saroya , R. W. Smith , H. Singh and C. B. Seymour, Serum serotonin levels determine the magnitude and type of bystander effects in medium transfer experiments, *Radiat Res 174*(1), 119-23
58. W. Droge, Free radicals in the physiological control of cell function, *Physiol Rev 82*(1), 47-95 (2002).
59. R. H. Burdon, Control of cell proliferation by reactive oxygen species, *Biochem Soc Trans 24*(4), 1028-32 (1996).
60. T. Finkel and N. J. Holbrook, Oxidants, oxidative stress and the biology of ageing, *Nature 408*(6809), 239-47 (2000).
61. R. V. Blackburn , D. R. Spitz , X. Liu , S. S. Galoforo , J. E. Sim , L. A. Ridnour , J. C. Chen , B. H. Davis , P. M. Corry and Y. J. Lee, Metabolic oxidative stress activates signal transduction and gene expression during glucose deprivation in human tumor cells, *Free Radic Biol Med 26*(3-4), 419-30. (1999).
62. D. R. Spitz , J. E. Sim , L. A. Ridnour , S. S. Galoforo and Y. J. Lee, Glucose deprivation-induced oxidative stress in human tumor cells. A fundamental defect in metabolism?, *Ann N Y Acad Sci 899*, 349-62 (2000).
63. V. Adler , Z. Yin , K. D. Tew and Z. Ronai, Role of redox potential and reactive oxygen species in stress signaling, *Oncogene 18*(45), 6104-11 (1999).
64. K. Schulze-Osthoff , M. Bauer , M. Vogt , S. Wesselborg and P. A. Baeuerle, Reactive Oxygen Intermediates as Primary Signals and Second Mesengers in the Activation of transcription Factors. In *Oxidative Stress and Signal Transduction*, Forman, H. J.; Cadenas, E., Eds. Chapman & Hall: New York, 1997; pp 239-259.

65. H. C. Liou and D. Baltimore, Regulation of the NF-kappa B/rel transcription factor and I kappa B inhibitor system, *Curr Opin Cell Biol 5*(3), 477-87. (1993).
66. R. Schreck , P. Rieber and P. A. Baeuerle, Reactive oxygen intermediates as apparently widely used messengers in the activation of the NF-kappa B transcription factor and HIV-1, *Embo J 10*(8), 2247-58. (1991).
67. N. Li and M. Karin, Is NF-kappaB the sensor of oxidative stress?, *Faseb J 13*(10), 1137-43. (1999).
68. P. J. Coates , J. I. Robinson , S. A. Lorimore and E. G. Wright, Ongoing activation of p53 pathway responses is a long-term consequence of radiation exposure in vivo and associates with altered macrophage activities, *The Journal of pathology 214*(5), 610-6 (2008).
69. S. A. Lorimore , P. J. Coates , G. E. Scobie , G. Milne and E. G. Wright, Inflammatory-type responses after exposure to ionizing radiation in vivo: a mechanism for radiation-induced bystander effects?, *Oncogene 20*(48), 7085-95 (2001).
70. M. A. Khan , R. P. Hill and J. Van Dyk, Partial volume rat lung irradiation: an evaluation of early DNA damage, *Int J Radiat Oncol Biol Phys 40*(2), 467-76 (1998).
71. H. Matsumoto , S. Hayashi , M. Hatashita , K. Ohnishi , H. Shioura , T. Ohtsubo , R. Kitai , T. Ohnishi and E. Kano, Induction of radioresistance by a nitric oxide-mediated bystander effect, *Radiat Res 155*(3), 387-96 (2001).
72. C. Shao , V. Stewart , M. Folkard , B. D. Michael and K. M. Prise, Nitric oxide-mediated signaling in the bystander response of individually targeted glioma cells, *Cancer Res 63*(23), 8437-42 (2003).
73. S. Wolff, Failla Memorial Lecture. Is radiation all bad? The search for adaptation, *Radiat Res 131*(2), 117-23. (1992).
74. L. E. Feinendegen , M. Pollycove and R. D. Neumann, Whole-body responses to low-level radiation exposure: new concepts in mammalian radiobiology, *Exp Hematol 35*(4 Suppl 1), 37-46 (2007).
75. J. D. Shadley, Chromosomal adaptive response in human lymphocytes, *Radiat Res 138*(1 Suppl), S9-12. (1994).
76. G. Olivieri , J. Bodycote and S. Wolff, Adaptive response of human lymphocytes to low concentrations of radioactive thymidine, *Science 223*(4636), 594-7 (1984).
77. L. Samson and J. Cairns, A new pathway for DNA repair in Escherichia coli, *Nature 267*(5608), 281-3. (1977).
78. L. Cai and S. Z. Liu, Induction of cytogenetic adaptive response of somatic and germ cells in vivo and in vitro by low-dose X-irradiation, *Int J Radiat Biol 58*(1), 187-94 (1990).
79. R. E. Mitchel , J. S. Jackson , R. A. McCann and D. R. Boreham, The adaptive response modifies latency for radiation-induced myeloid leukemia in CBA/H mice, *Radiat Res 152*(3), 273-9 (1999).
80. J. L. Redpath and R. J. Antoniono, Induction of an adaptive response against spontaneous neoplastic transformation in vitro by low-dose gamma radiation, *Radiat Res 149*(5), 517-20 (1998).
81. I. Szumiel, Adaptive response: stimulated DNA repair or decreased damage fixation?, *Int J Radiat Biol 81*(3), 233-41 (2005).
82. S. Wolff, The adaptive response in radiobiology: evolving insights and implications, *Environ Health Perspect 106 Suppl 1*, 277-83 (1998).

83. J. P. Jay-Gerin , J. Meesungnoen , P. Banville and S. Mankhetkorn, Comment on "The radiation-induced lesions which trigger the bystander effect" by J.F. Ward [Mutat. Res. 499 (2002) 151-154], *Mutat Res 525*(1-2), 125-7 (2003).
84. F. A. Cucinotta and L. J. Chappell, Non-targeted effects and the dose response for heavy ion tumor induction, *Mutat Res 687*(1-2), 49-53 (2010).

A.3.3. Encyclopedia Entry – Telomere

This encyclopedia entry, published in the Encyclopedia of Pathology, provides an overview of telomeres, mechanisms of telomere maintenance, and the roles of telomeres and telomerase in human pathology (Frenzel et al., 2014). I have contributed to the development of the manuscript and provided Figure 2 in the entry.

Summary of the key points of this article:

- Telomeres and their structure and functions are defined.
- The role of telomeres in replicative senescence, the mechanisms of telomere maintenance, and consequences of telomere dysfunction and chromosomal instability are outlined.
- Finally, the roles of telomeres and telomerase activity in carcinogenesis are discussed.

T

Telomere

Monika Frenzel, Corina Cuceu, Grace Shim, Michelle Ricoul and Laure Sabatier
Laboratory of Radiobiology and Oncology, Commissariat à l'Energie Atomique (CEA), DSV/IRCM/SRO, Fontenay aux Roses, France

Synonyms

Chromosomal extremity; Chromosomal terminus; End of chromosome; Shelterin complex; Telomeric DNA

Definition

Telomeres are specialized nucleoprotein structures located at the ends of linear eukaryotic chromosomes. The name "telomere" was derived from the Greek roots *telos* (τέλος), meaning "*end*," and *meros* (μέρος, root: μερ-), meaning "*part*." Telomeres were first described more than 70 years ago by the pioneering studies of the geneticists Hermann Joseph Muller and Barbara McClintock in the fruit fly *Drosophila melanogaster* and maize, respectively. Since then, telomeres have proven to be critical structures for maintaining genetic stability and integrity and have thus been established as guardians of the genome (Fig. 1).

Principle

Telomere Structure and Function

The structure of telomeres in all vertebrates consists of tandem repeats of (TTAGGG/AATCCC)n DNA sequences, first identified by Moyzis in 1988, and several associated proteins. Together, they form a protective cap called the *shelterin complex* (Fig. 2). The complex is found as a looped structure known as the T-loop, which is formed when the 3-prime overhang of the G-rich strand of about 50–500 nucleotides folds back and invades the double-stranded region of the telomeric DNA. As the single-stranded telomeric DNA is G-rich, this region may also form G-quadruplexes, which are formed from a series of G-quartets, each containing four guanine bases arranged in a helical fashion.

The shelterin complex in humans includes six proteins that are associated with telomeric DNA: TRF1, TRF2, TIN2, POT1 [POT1a/b in rodents], TPP1, and RAP1 (reviewed in Palm and de Lange 2008). Each of these proteins has evolved specific functions for telomere maintenance, including the regulation of telomerase access and activity as well as the interaction with many DNA repair/recombination factors. TRF1 and TRF2 bind independently (both as homodimers or oligomers) to the double-stranded regions of telomeres, while POT1 binds to the 3′ single-stranded G-rich overhang. Interactions between TRF1 and TRF2 with POT1 occur via TIN2 and TPP1. TPP1 contains a telomerase binding domain and may be involved in the process of telomere elongation. Finally, RAP1 is not

H.V. Krieken (ed.), *Encyclopedia of Pathology*,
DOI 10.1007/978-3-642-04978-1, © Springer-Verlag Berlin Heidelberg 2014

essential for the formation of the shelterin complex but stabilizes the structure itself by binding to TRF2.

The protective cap formed by the shelterin complex at the telomeres is known to serve at least three essential functions. First, they protect natural chromosomal DNA ends from being inappropriately recognized as double-strand breaks (DSBs) and therefore prevent unwanted activation of DNA damage response (DDR) pathways. Secondly, telomeres protect chromosomal ends from inappropriate enzymatic degradation. Lastly, they prevent chromosomal end-to-end fusions. Therefore, telomeres play a crucial role in maintaining the stability and integrity of the genome.

Methodology

Telomeres and Replicative Senescence

In 1961, Hayflick and Moorhead demonstrated that human diploid cells have a limited lifespan and cells stop dividing after a certain number of replication cycles. Then in 1990, Harley et al. observed that telomere length naturally decreases with each round of cell division and finally affirmed the hypothesis that telomere length in somatic cells reflects the replicative history of a cellular lineage. More recently, the research on telomere features and the line of evidence that led to the concept that telomerase activity exists has been recompensed in 2009 with a Nobel Prize to Elizabeth H. Blackburn, Carol W. Greider, and Jack W. Szostak (see also Blackburn Nobel Lecture).

Telomere length varies between organisms; in humans, the mean length of the double-stranded end at birth is ~15 kilobases (kb) (Wright et al. 1996). Telomere length also varies on individual chromosome arms, and this inherent heterogeneity is conserved during life. Telomere length in somatic proliferative tissues naturally declines at a rate of approximately 20–300 base pairs per population, doubling (varying with cell type) due to the incomplete replication of telomere ends by conventional DNA polymerases, a situation known as the "DNA end-replication problem." After many rounds of cell division, telomeres eventually pass their size "threshold" and become critically short or dysfunctional. In normal cells with intact p53 functions and cell cycle checkpoints, these dysfunctional/uncapped telomeres are sensed as DNA damage and trigger DDR pathways, which prevent the cell from further division, and cells enter a stage of permanent growth arrest called "replicative senescence." Progressive loss of telomeric DNA therefore acts as an internal "molecular clock" that limits the number of cell divisions and therefore limits the lifespan of normal cells. Since senescent and potentially damaged cells are eliminated or do not give rise to viable progeny, this mechanism works as an important tumor suppressor.

Mechanisms of Telomere Maintenance

The persistent shortening of telomeres can be offset in different cell types (i.e., stem cells, germ cells, or cancer cells) via two mechanisms of telomere elongation: (1) telomerase, a specialized reverse transcriptase that elongates telomeres by adding TTAGGG DNA sequence repeats to the 3′ G-strand overhang, and (2) homologous recombination of telomeres via "alternative lengthening of telomeres" (ALT), a pathway independent of telomerase activity.

Telomeres are primarily elongated by telomerase. The enzyme is a ribonucleic protein complex composed of two core components: the telomerase reverse transcriptase (TERT) protein, which reversely transcribes the template region of the second component, the RNA subunit (TERC), onto the 3′ end of the telomeric DNA. Telomerase is essential for the long-term proliferation potential of stem cells and germ line cells and for tissue renewal. The enzyme is also constantly expressed in normal somatic cells at low concentrations; however, telomerase is unable to bind to and exert its elongating functions at the telomeres due to the protective function of the shelterin complex, thereby resulting in telomere shortening after each round of cell division. In cell culture, telomerase activation increases the ability of cells to divide continuously and therefore extends their lifespan as shown by Bodnar in 1998.

ALT-positive immortalized cell lines are able to maintain their telomere length throughout many cell doublings in the absence of telomerase activity. ALT involves homologous recombination-mediated DNA replication and requires the activity of the MRE11/RAD50/NBS1 recombination complex. The typical ALT phenotype has only been found in abnormal situations, including immortalized human cell lines, human tumors, and tumors or cell lines derived from telomerase null mice, suggesting that this is an anomalous telomere phenotype.

Quality Aspects

Telomere Dysfunction and Chromosomal Instability

Loss of telomeric functions can arise due to loss of telomeric DNA or from mutations at crucial telomere protein components. Depending on the type of mutation, the uncapping process differs and telomeres undergo progressive shortening. Excessive telomere shortening and/or telomere loss enables gene amplification and chromosomal imbalances and may eventually lead to chromosomal instability, characterized by increased levels of chromosomal aberrations that danger the integrity of the genome (Fig. 3).

Telomere loss that is not rapidly repaired causes chromosomal instability due to degradation of DNA from the end of the chromosome. Lost telomeres can be recovered via several mechanisms. First, telomere sequences can be added directly to the open ends of broken chromosomes with the help of telomerase; this process, termed chromosome healing, results in a terminal deletion. Secondly, sister-chromatid fusions after telomere loss, followed by propagation of chromosomal instability via breakage/fusion/bridge (BFB) cycles (McClintock 1941), result in terminal deletions, inverted duplications, DNA amplification, duplications, and nonreciprocal translocations; all of these types of chromosomal rearrangements related to telomere instability have been associated with human cancer. Additionally, anaphase bridges during BFB cycles can also cause losses of whole chromosomes, leading to aneuploidy (or an abnormal number of chromosomes). Moreover, telomeres can be acquired through telomere capture, involving the translocation of the ends of other chromosomes via break-induced replication (BIR). Finally, chromosomal rearrangements that do not involve telomere restoration may arise, without compensating for telomere loss, such as rings or dicentric chromosomes, which are usually unstable in mammalian cells.

Higher levels of chromosomal instability and structural chromosomal alterations after telomere loss are often associated with functional loss of cell cycle control mechanisms, such as p53 or p16. Dicentric chromosomes that are formed by BFB cycles cause cell cycle arrest in normal cells with intact cell cycle checkpoints; however, cells lacking normal checkpoints continue to divide, and the unstable dicentric chromosomes break during cell division, leading to further genetic instability.

Applications

Telomeres and Carcinogenesis

Telomeres and telomere length are involved in the pathology of several age-related human diseases and carcinogenesis (reviewed in Shim et al. 2014) via (1) loss of cell cycle checkpoints that allow the bypass of senescence and continued cell proliferation that may eventually lead to carcinogenesis or (2) abnormal regulation of telomere length, including abnormal telomerase activity or activation of ALT pathways. Telomerase is upregulated in about 85 % of human cancers, suggesting its important role in the process of cellular immortalization and tumorigenesis. Its downregulation or inhibition would therefore target and impair telomerase-positive malignant cancers, while normal somatic cells, which do not express telomerase, are minimally affected. Clinical trials including telomerase inhibitors in cancer treatments already demonstrated that the use of these inhibitors hindered tumor growth and spread of metastases. Additionally, inhibition of telomerase may sensitize tumors to conventional

chemotherapy agents. Therefore, telomerase inhibition may be most effective when used in combination with conventional chemotherapy and/or radiotherapy regimens, since telomerase inhibitors may require a period of treatment before chemotherapy or radiotherapy to produce telomeres that are short enough to trigger death in cancer cells.

On the other hand, telomerase deficiency in stem cells can lead to untimely telomere shortening; a variety of degenerative disorders, including dyskeratosis congenita, pulmonary fibrosis, and bone marrow failure, are all characterized by the presence of short telomeres (reviewed in Armanios et al. 2012).

Additionally, a significant subset of human tumors (10–15 %) employs the telomerase-independent ALT pathway. Whether the cancer cell uses telomerase activation or the ALT pathway appears to depend on the origin of the tumor. This pathway can coexist with telomerase activity in some tumors, rendering these tumors resistant to treatment with telomerase inhibitors (Reddel et al. 2001).

Telomerase Activity in Tissues

The appearance of various cancers (colon, skin, thyroid, breast, etc.) is accompanied by changes in the telomere status including either an increase or decrease of telomere length. There is evidence that the quantification of telomerase activity – playing a major role in the telomere maintenance – allows the characterization and analysis of cancerous tissue. To perform these analyses, the amount of human TERT (hTERT) is quantified, assuming that the level of expression is correlated with its in vitro activity (Hao et al. 2005).

Telomerase expression is studied, i.e., by immunohistochemical staining of tissue sections (Volpi et al. 2005) or real-time polymerase chain reaction (RT-PCR) and PCR-ELISA mostly performed in liquid nitrogen-frozen tissues (Ayiomamitis et al. 2014; Capezzone et al. 2011). With the latter two protocols, overall hTERT expression is analyzed, while individual cells with telomerase activity can be identified and distinguished from normal cells only in tissue sections by colorimetric differences. Quantification of telomerase activity could help to classify histologic grades of carcinomas. This represents an important feature to evaluate the cancer status and therewith the need and type of follow-up. The expression level of hTERT can be used as a new marker for an early diagnosis for certain types of cancer (Bautista et al. 2007).

Studies of telomerase activity for a spectrum of colorectal tumors (hyperplastic polyps, adenomas, and carcinomas) – characterized in the majority of publications by short telomeres – show an increase of hTERT expression compared to adjacent healthy tissue, and stronger staining correlated proportionally with the histological grade (Simsek et al. 2010).

A clinical approach for the early detection of invasive bladder cancer was described by Soria et al. (2002). Epithelial cells have been isolated from the blood by magnetic beads coated with highly specific antibodies. Telomerase expression was detected using the telomerase-PCR-enzyme-linked immunosorbent assay test for the majority (90 %) of patients with high-grade, muscle-invasive, or metastatic bladder cancer but in none of the healthy donors. This diagnostic protocol may have great value for monitoring cancer progression and might be adjusted with regard to the type of cancer.

References and Further Reading

Blackburn, E. H. (1991). Structure and function of telomeres. *Nature, 350*, 569–573.

Günes, C., & Rudolph, K. L. (2013). The role of telomeres in stem cells and cancer. *Cell, 152*, 390–393. doi:10.1016/j.cell.2013.01.010. Review. PubMed PMID: 23374336.

McClintock, B. (1941). The stability of broken ends of chromosomes in Zea mays. *Genetics, 41*, 234–282.

Reddel, R. R., Bryan, T. M., Colgin, L. M., Perrem, K. T., & Yeager, T. R. (2001). Alternative lengthening of telomeres in human cells. *Radiation Research, 155*, 194–200.

Shim, G., Ricoul, M., Hempel, W. M., Azzam, E., & Sabatier, L. (2014). Crosstalk between telomere maintenance and radiation effects: A key player in the process of radiation-induced carcinogenesis. *Mutation Research/Reviews in Mutation Research, 760*, 1–17.

Soria, J. C., Morat, L., Durdux, C., Housset, M., Cortez, A., Blaise, R., & Sabatier, L. (2002). The molecular detection of circulating tumor cells in bladder cancer using telomerase activity. *The Journal of Urology, 167*(1), 352–356.

Wright, W. E., Piatyszek, M. A., Rainey, W. E., Byrd, W., & Shay, J. W. (1996). Telomerase activity in human germline and embryonic tissues and cells. *Developmental Genetics, 18*, 173–179.

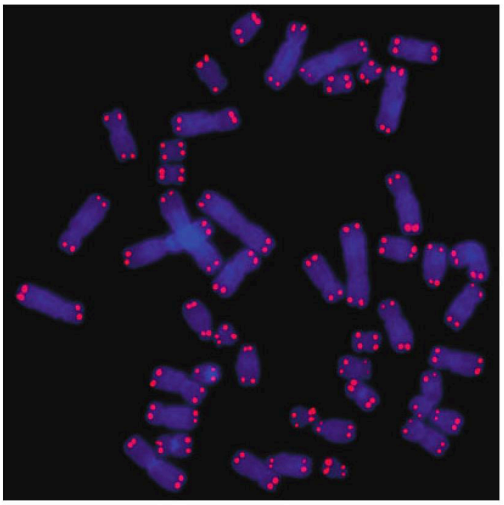

Telomere, Fig. 1 Visualization of telomeres in metaphasic chromosomes using PNA (peptide nucleic acid)-telomere-FISH (fluorescence in situ hybridization) staining. Telomeric regions are marked quantitatively with PNA probes corresponding to the telomeric sequence that is labeled with the fluorescent dye cyanine-3 (550 nm excitation, 570 nm emission)

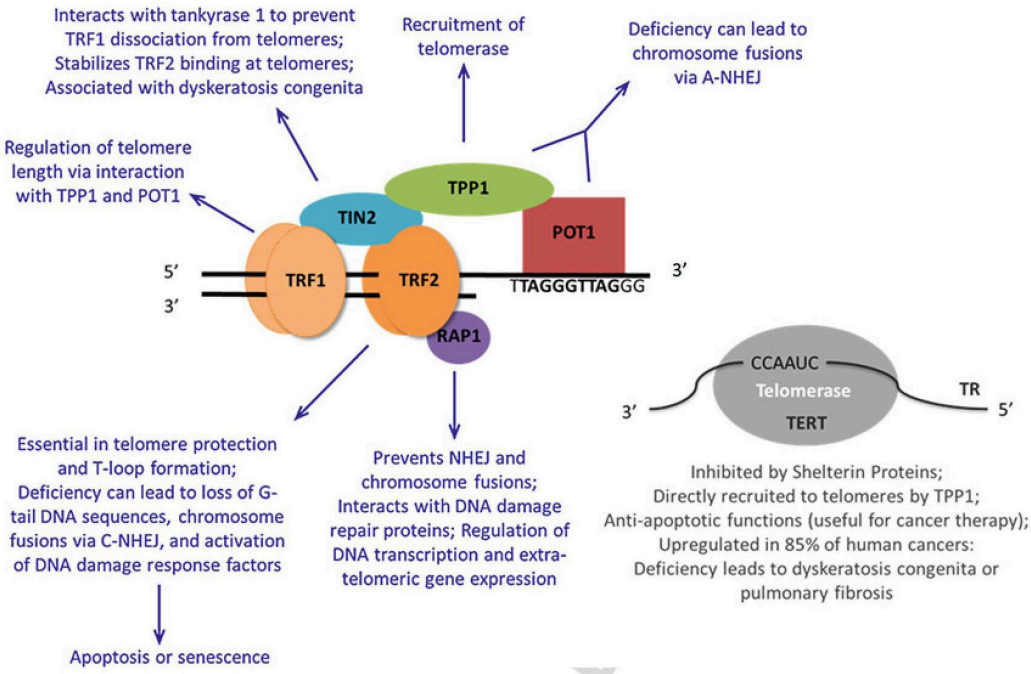

Telomere, Fig. 2 Composition of the shelterin complex: TRF1 and TRF2 are associated with the double-stranded region of telomeric DNA, while POT1 is associated with the single-stranded region and interacts with TRF1 and TRF2 with the help of TIN2 and TPP1. RAP1 increases the stability of the shelterin complex

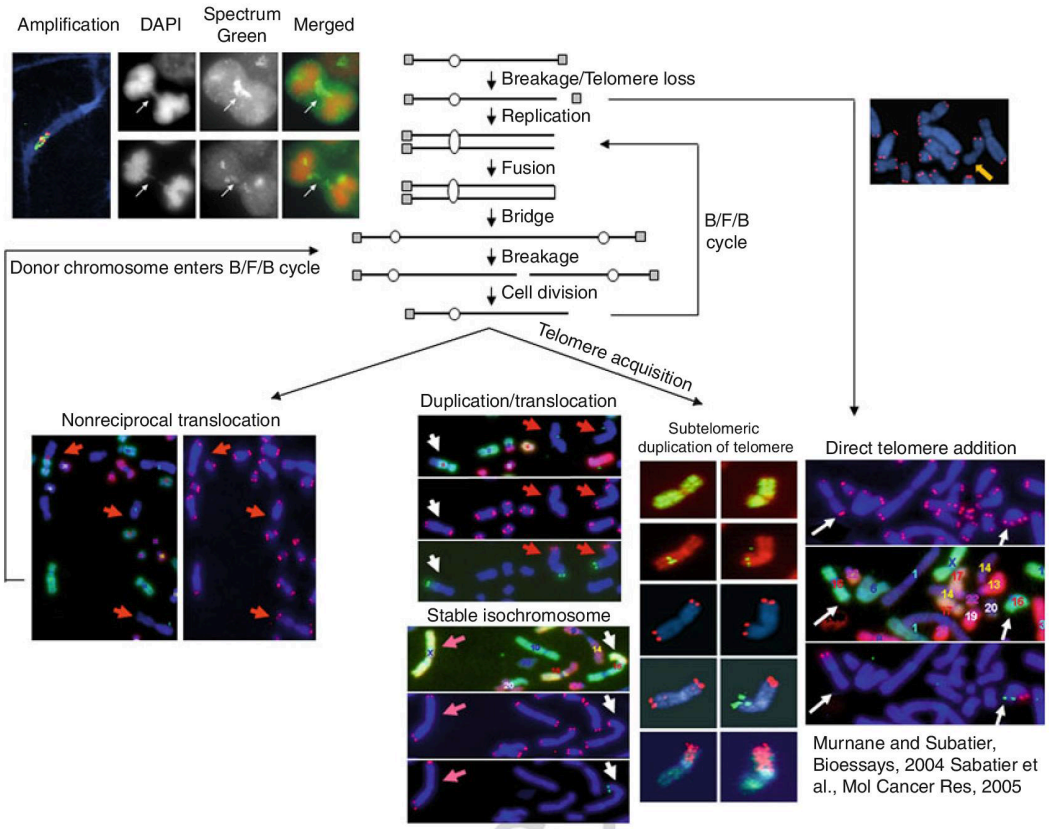

Telomere, Fig. 3 The B/F/B cycle is initiated when sister chromatids fuse after the loss of a telomere (*gray squares*). Due to the presence of two centromeres (*circles*), the fused sister chromatids form anaphase bridges that break when the cell attempts to divide. Breakage occurs at locations other than the site of fusion, resulting in amplification of sequences in one daughter cell and deletions in the other. Lost telomeres can be restored by sister-chromatid fusion following DNA replication or different mechanisms of telomere acquisition: duplication/translocation, formation of stable isochromosomes, subtelomeric duplication, or direct telomere addition by the telomerase. The translocations can be also nonreciprocal, leaving one uncapped, damaged chromosome. The loss of the telomere from the donating chromosome can initiate new B/F/B cycles. Therefore, a loss of a single telomere can lead to cascades of instability involving multiple chromosomes

A.3.4. Lead exposure induces telomere instability in human cells

In the following paper (Pottier et al., 2013), we present evidence that lead (Pb) neurotoxicity is due to Pb-induced "telomere-induced foci" (TIFs), which leads to telomere instability and loss of telomere maintenance. In this thesis, we expand upon the analysis of basal levels of telomere abnormalities (telomere loss or doublets) in 20 healthy individuals included in this paper (shown in Figure S2 in the paper) as we analyze a cohort of 35 healthy individuals (age range of 23 to 58, mean age of 39.5); these results are described in Section 0 of this thesis.

Summary of the key points of this paper:

- While *in vitro* Pb exposure (in the form of lead nitrate) did not increase intra-chromosomal γH2AX foci, it significantly increased the frequency of TIFs, which are formed when DNA repair machinery (e.g. γH2AX) recognize short or dysfunctional telomeres (uncapped or damaged telomeres) as DSBs, thus leading to γH2AX localization at these (intact) telomeres.
- The formation of TIFs at these intact telomeres likely leads to their loss due to perturbations of telomere replication, particularly on the lagging DNA strand.
- We propose a model for telomere instability following Pb exposure that could explain Pb-induced neurotoxicity.
- As numerous studies have demonstrated a role for telomere maintenance in brain development and tissue homeostasis, our results provide novel insight into the link between Pb exposure, telomere maintenance, and the biological responses that lead to the permanent neurotoxic effects.

OPEN ACCESS Freely available online

PLOS ONE

Lead Exposure Induces Telomere Instability in Human Cells

Géraldine Pottier, Muriel Viau, Michelle Ricoul, Grace Shim, Marion Bellamy, Corina Cuceu, William M. Hempel, Laure Sabatier*

Commissariat à l'Energie Atomique (CEA), Laboratoire de Radiobiologie et Oncologie (LRO), Fontenay-aux-Roses, France

Abstract

Lead (Pb) is an important environmental contaminant due to its widespread use over many centuries. While it affects primarily every organ system of the body, the most pernicious effects of Pb are on the central nervous system leading to cognitive and behavioral modification. Despite decades of research, the mechanisms responsible for Pb toxicity remain poorly understood. Recent work has suggested that Pb exposure may have consequences on chromosomal integrity as it was shown that Pb exposure leads to the generation of γH2Ax foci, a well-established biomarker for DNA double stranded break (DSB formation). As the chromosomal localization of γH2Ax foci plays an important role in determining the molecular mechanism responsible for their formation, we examined the localization of Pb-induced foci with respect to telomeres. Indeed, short or dysfunctional telomeres (uncapped or damaged telomeres) may be recognized as DSB by the DNA repair machinery, leading to "telomere-Induced Foci" (TIFs). In the current study, we show that while Pb exposure did not increase intra-chromosomal foci, it significantly induced TIFs, leading in some cases, to chromosomal abnormalities including telomere loss. The evidence suggests that these chromosomal abnormalities are likely due to perturbation of telomere replication, in particular on the lagging DNA strand. We propose a mechanism by which Pb exposure leads to the loss of telomere maintenance. As numerous studies have demonstrated a role for telomere maintenance in brain development and tissue homeostasis, our results suggest a possible mechanism for lead-induced neurotoxicity.

Citation: Pottier G, Viau M, Ricoul M, Shim G, Bellamy M, et al. (2013) Lead Exposure Induces Telomere Instability in Human Cells. PLoS ONE 8(6): e67501. doi:10.1371/journal.pone.0067501

Editor: Arthur J. Lustig, Tulane University Health Sciences Center, United States of America

Received November 27, 2012; **Accepted** May 20, 2013; **Published** June 26, 2013

Funding: M.V. is supported by the European 7th framework grant BOOSTER: grant agreement no. 242361 (http://ec.europa.eu/research/fp7/index_en.cfm). W.H. is supported by the European 7th framework grant DoReMi: grant agreement no. 249689 (http://ec.europa.eu/research/fp7/index_en.cfm). This work was supported by the grants from the Agence Nationale de la Recherche (ANR) (http://www.agence-nationale-recherche.fr/) and the Institute National Du Cancer (INCa) (http://www.e-cancer.fr/recherche), Hemi-BREAKS and HEMIBREAKS-T. The funders had no role in study design, data collection and analysis, decision to publish, or preparation of the manuscript.

Competing Interests: The authors have declared that no competing interests exist.

* E-mail: laure.sabatier@cea.fr

Introduction

Lead (Pb) is a naturally occurring metal which has been used for over 8000 years in a wide range of applications [1]. As Pb is non-biodegradable, it has historically been an important environmental pollutant in air and water, and while environmental Pb levels have decreased in western countries, due to strict regulatory policies, it remains a problem in developing countries, and inner city neighborhoods.

The first accurate description of symptoms from Pb poisoning was probably provided by Nicander, a little known poet of the 2nd century BC [2]. Since then, numerous studies have demonstrated that while Pb affects essentially every organ system in the body, including the hematopoietic, cardiovascular, renal and skeletal systems, it is the central nervous system which is particularly sensitive to the effects of Pb [3]. Alterations in cognitive function and behavior due to the neurotoxic effects following Pb poisoning have long been recognized [4]. Animal studies have shown that chronic lead exposure indeed affects neuronal development and adult neurogenesis [5]. Importantly, a lower threshold for the effects of Pb on the nervous system has not been determined [6]. Persistent low-level environmental contamination of this heavy metal has ensured that Pb contamination remains a significant public health issue. Lead has also been identified as a probable carcinogen [7].

Despite the fact that Pb exposure has been the subject of intense research over many decades, the mechanisms responsible for its far reaching and persistent neurotoxic effects are still poorly understood. In humans, as in animal models, Pb contamination is associated with generalized oxidative stress observed through biomarkers such as GSH status, lipid peroxidation, and an increase in the activity of glutathione reductase and peroxidase, catalase, superoxide dismutase… (reviewed in [8]). Lead serves no biological function in humans but its high electronegativity favors interactions with proteins, notably those with metal binding sites (rich in oxygen and sulfur).

More recently, the genotoxic effects of lead exposure have also been the subject of a number of studies. Using a variety of different experimental models, conditions, and endpoints, these studies have generated largely contradictory findings [9]. Nonetheless, a recently published study has reported the emergence of γH2Ax foci, commonly correlated with the formation of double-stranded DNA breaks (DSB), some hours after cell exposure to Pb [10]. Furthermore, the same study provides evidence suggesting close association between Pb molecules and DNA in the cells, suggesting that Pb directly affects DNA/chromosomal integrity.

The apparition of γH2Ax foci may arise from different mechanisms depending on the chromosomal localization. γH2Ax foci in intra-chromosomal regions are generally due to the presence of DSBs [11], whereas those at or near telomeres may also be due to telomere shortening, which has been shown to lead to γH2Ax foci formation in the absence of bona fide DSBs [12]. Telomeres are DNA-protein complexes containing long 6 base pair repeats added onto the ends of chromosomes by the enzyme telomerase. Telomeres serve multiple functions including protecting the ends of chromosomes and preventing chromosome fusion. Telomeres are maintained in germline cells, but shorten with each progressive cell division in somatic cells. Telomere shortening in somatic cells is a signal of replicative cell senescence which results from the inability of the telomere to form a cap that protects the end of the chromosome. When this occurs, the cells cease to divide and often undergo apoptosis. However, if the checkpoint pathways are deficient, cells continue to divide until they reach the stage of telomeric crisis which often leads to cell death or significant genomic instability (reviewed in [13]. When several chromosomes contain very short telomeres, their extremities tend to undergo end-to-end fusion leading to the generation of dicentric chromosomes. A correlation between reduced telomere length and dicentric chromosome frequency has been demonstrated in human senescent fibroblasts [14]. In the segregation phase of mitosis, dicentric chromosomes often form an anaphase bridge that results in chromosome breakage, increased chromosomal rearrangements and chromosomal abnormalities [15].

This association between Pb exposure and the generation of γH2Ax foci led us to study the cytogenetic consequences related to telomere maintenance. Indeed, short or dysfunctional telomeres (uncapped or damaged telomeres) may be recognized as DSB by the DNA repair machinery, leading to "telomere-Induced Foci" (TIFs). In the current study, we show that while Pb exposure did not increase intra-chromosomal foci, it significantly induced TIFs leading in some cases to chromosomal abnormalities including telomere loss. The evidence suggests that these chromosomal abnormalities are likely due to perturbation of telomere replication, in particular on the lagging DNA strand.

Materials and Methods

Cell Culture

Clone B3 was isolated from the human EJ30 bladder cell carcinoma cell line (obtained from Dr. William Dewey, University of California, San Francisco). The origin, derivation and use of this cell line are described in [15,43–49]. Cells were grown in alpha-MEM medium (Gibco®), supplemented with 10% fetal calf serum (Eurobio) and antibiotic antimycotic (Gibco®). For the detection of γH2Ax foci in interphase nuclei, cells were seeded at 6×10^4/slide, cultured for 24 h in the absence of Pb and a further 24 h in the presence of the indicated concentrations of $Pb(NO_3)_2$ before processing for immunofluorescence. For the detection of γH2Ax foci and/or telomeres in metaphase spreads, cells were seeded at 5×10^5 cells/T25 flask, cultured for 24 h in the absence of Pb and a further 24 h in the presence of the indicated concentrations of $Pb(NO_3)_2$. Colchecine (6 μg/mL) was included during the last 5 hours of culture to accumulate mitotic cells before processing for FISH or IF FISH.

Preparation of Pb Solution

Lead nitrate (Sigma Chemical) solution was prepared by dissolving 3.31 g Pb nitrate in 100 ml of distilled water (i.e. 100 mM solution).

Chromosome Analysis

Preparation of metaphase chromosome for *in situ* hybridization was performed as previously described [50]. Cytogenetic analyses were performed in two steps, consisting of hybridization with a protein nucleic acid (PNA) telomere probe followed by M-FISH for all chromosome painting. Telomere analysis was performed as previously described [51] using telomere specific PNA probes labelled with CY3 (Perspective Biosystems). M-FISH was performed using multi-FISH probes (Metasystems Gmbh, Althusseim, Germany), according to the manufacturer's recommendations. Images of hybridized metaphases were captured with a charge-coupled device camera (Zeiss, Thornwood, NY) coupled to a Zeiss Axioplan microscope and processed using ISIS software (Metasystems). In all cases, 50 metaphases were analysed per experiment.

Co-FISH

Chromosome Orientation FISH (CO-FISH) consists of a FISH technique that uses single-stranded DNA probes to produce strand-specific hybridization and was performed as previously described [18]. The technique relies on labelling by 5′-bromodeoxyuridine (BrdU) (Sigma) incorporation on one strand of DNA during S-phase. Metaphase chromosomes were prepared 24 h (1 cell cycle) after the addition of 1×10^{-5} M BrdU. After rinsing the slides with SSC (Saline Sodium Citrate), they were incubated for 15 min in 5 μg/ml Hoechst 33258 (Sigma) to allow intercolation of the dye into the newly synthesized DNA. The slides were then subjected to 45 min of UV irradiation, in a bath of 2×SSC, to introduce nicks at the sites of BrdU incorporation. The nicks were enlarged by incubating the slides in 10 U/μl ExoIII (Promega) for 15 min at 37°C, leaving the parental strand as a single-stranded template for the hybridization procedure. After dehydration in successive baths of μ50, 70, and 100% ethanol for 5 min each, on ice, the slides were incubated for 1 h30 with the PNA probe T_2AG_3 (FITC, Fluorescein IsoThioCyanate) and then with the probe C_3TA_2 (Cy3) for another 1 h30. After hybridization, the slides were counterstained with DAPI (1 μg/ml).

Immunofluorescence

Cells were fixed with methanol/acetone (1 V/1 V) for 10 min and permeabilized in 20 mM HEPES pH 7.9, 50 mM NaCl, 3 mM $MgCl_2$, 300 mM sucrose 0.5% TRITON X-100 (Sigma) for 30 min. Cells were then incubated 1 h at 37°C in PBS-TRITON 0.5% with anti- γH2Ax ^{ser139} antibody (1/800; Upstate). After washing in PBS, cells were incubated with an anti-mouse CY3 secondary antibody (1/300) at 37°C for 45 min. Cells were mounted in p-phenylene diamine after counterstaining with 4,6-diamidino-2-phenylindole (Sigma).

IF-FISH

Immunofluorescent-FISH (IF-FISH) was performed using a protocol similar to one described previously [17]. Cells were cytospun at 112×g after 5 h of colchicine (0.09 μg/ml) treatment at 37°C in a humidified atmosphere of 5% CO2. The pellet was washed in 1×PBS at 37°C and re-centrifuged. The cells were subjected to hypertonic shock by resuspension in 34 mM citrate at 37°C to obtain a suspension of cells at a concentration of 6×10^5 cells/ml and incubated for 1 h at 37°C. 200 μl of the suspension was subsequently applied to polylysine slides by centrifugation. Following fixation (PFA 3%, sucrose 2%), cells were immunostained as already described. Prior to telomere hybridization with the PNA probe $(CCCTAA)_3$- FITC, cells were successively fixed

(PFA 4%, 2 min), washed in PBS and dehydrated (50/70/100 ethanol).

Statistical Analysis

Statistical analyses of the results were performed using the student t-test for two unpaired independent sample sets (treated and untreated cells), and the standard error was calculated for chromosomal alteration frequencies between the two sample sets. The formula used to compare the two averages is shown below where s = the common variance to both sample sets, N = the number of samples.

$$t = \frac{m_1 - m_2}{\sqrt{\frac{s^2}{N_1} + \frac{s^2}{N_2}}}$$

Results

Lead Induces γH2Ax foci that are Mainly Localized in Telomere Regions

The induction of DNA damage following Pb nitrate exposure has been previously described, based on the quantification of nuclear foci formed following H2Ax phosphorylation by immunofluorescence (IF) [10]. They deduced that Pb induces DSB that they called HEMI-breaks for Heavy Metal Induced breaks that reached a maximum level after 24 hours of treatment. Indeed, the number of nuclear foci has been previously shown to directly correlate in a one to one ratio with the number of DSB following irradiation [16]. As γH2Ax foci formation reached a maximum level after 24 hours of Pb exposure in the paper published by Gestaldo et al, we chose to focus on the same time point for the current study. Our results confirm the generation of γH2Ax foci in human B3 cells following exposure to increasing concentrations of Pb nitrate after 24 h of treatment (**Figure 1A**). A dose dependent increase of the mean number of γH2Ax foci was observed that achieved significance starting with exposure of the cells to 100 μM Pb compared to non-exposed cells ($p<0.05$). Interestingly, there was a heterogeneous distribution of γH2Ax foci amongst the nuclei of B3 cells (**Figure 1B**). In untreated cells, more than 50% of nuclei contained 0–9 foci, whereas only a very small percentage contained over 30 foci. Following lead exposure, however, there was a significant increase in the percentage of nuclei containing over 30 foci starting from 100 μM ($p = .0.004$). Based on these results, subsequent experiments were performed with the lowest effective Pb nitrate concentration (100 μM) in order to study the mechanism and the downstream consequences of γH2Ax foci formation.

In order to position the induced γH2Ax foci on the chromosomes, we adapted the Immunofluorescence (IF)-FISH method [17] allowing simultaneous telomere hybridization and immunofluorescent staining of γH2Ax on the same metaphase chromosomes (**Figure 2A**). Using this approach it is possible to co-localize telomeres and chromosomal γH2Ax foci, distinguish internal from telomeric γH2Ax foci, and observe telomere loss. Several examples of the chromosomal localisation of the γH2Ax foci (telomeric or intra-chromosomal) after 24 h exposure with Pb nitrate are shown in **Figure 2A**, and the comprehensive data is represented in **Figure 2B**. Several staining patterns were observed including intra-chromosomal foci or telomeric foci on one or both chromosomal arms with or without telomere staining (see next section). Surprisingly, Pb nitrate treatment (100 μM) did not impact the percentage of intra-chromosomal foci, while the percentage of telomeric γH2Ax foci (co-localized γH2Ax and telomere staining) was increased. It is important to note that the co-localisation of telomere staining and γH2Ax foci indicate that γH2Ax formation has occurred in the absence of DSBs, as if this was the case, the telomere would most likely be lost. These results strongly suggest that Pb nitrate preferentially impacts the telomeric region, leading to telomere dysfunction signalled initially as a DSB in the intact telomere.

Lead Induces Telomere Instability

The results obtained from the above study suggest, that in some cases, Pb exposure of B3 cells leads to telomere loss. Indeed, the preferential localization of γH2Ax foci on telomeres may indicate the presence of extremely short or dysfunctional telomeres (uncapped or damaged telomeres) that are recognized as DSB by the DNA repair machinery [12], leading to "telomere-Induced Foci" (TIFs). As Pb is cytotoxic, it was necessary to first calculate the mitotic index of cells in the presence of the different concentrations of Pb (**Figure 3A**). Pb nitrate decreased the mitotic index of treated cells. The effect was dose-dependent and statistically significant starting with exposure of the cells to 100 μM compared to non-exposed cells ($p<0.05$). These data were thereafter taken into consideration and the subsequent experiments were normalized for the decrease of the mitotic index by dividing the percentage of chromosomes exhibiting telomere loss by the mitotic index for each concentration of Pb. The telomeric status of the cells was assessed after 24 h exposure with the same concentrations of Pb nitrate. The rates of telomere loss are presented in **Figure 3B–C**. Lead exposure induced a dose-dependent increase of telomere loss which was significant from 100 μM for one chromatid. Based on these analyses, it is not possible to determine if the loss of signal for two telomeres is due to a break in the subtelomeric region or intra-chromosomally. There was also an increase in telomere doublet formation which was maximal at 100 μM but not dose dependent (see **Figure S1**). In preliminary studies, Pb induced telomere loss and doublet formation were also observed in fresh human lymphocytes (see **Figure S2**) demonstrating that Pb exposure also leads to telomere dysfunction in primary cells. Interestingly, the level of spontaneous telomere loss in, and doublet formation and the subsequent effects of Pb exposure on human lymphocytes were highly dependent on the specific donor. The mechanism behind the donor-specific variability for the effects of Pb on telomere stability is currently under investigation.

In order to determine if the observed losses were limited to the telomeric region we performed sub-telomere staining (**Figure 3D**, middle panels) on the same slides that were used for the previous study (**Figure 3D**, top panels). Unlike the telomere probe, the sub-telomere probes are chromosome-specific, necessitating chromosome identification using the multi-FISH method prior to sub-telomere staining (**Figure 3D**, lower panels). To aid in the analysis, we decided to focus on chromosomes which demonstrated an elevated frequency of telomere loss. In addition, sub-telomere probes were not available for both arms of all chromosomes, further limiting the choice of chromosomes for analysis. Based on these constraints, we selected chromosomes 3, 5, 8 and X. Representative images in **Figure 3D** show that sub-telomere staining was preserved for chromosome 5 (left panels) and chromosome 8 (right panels). These results demonstrate that the observed loss of chromosome ends following Pb nitrate treatment is strictly limited to the telomeric region as subtelomeres are the most distal regions of unique DNA sequence found on chromosomes.

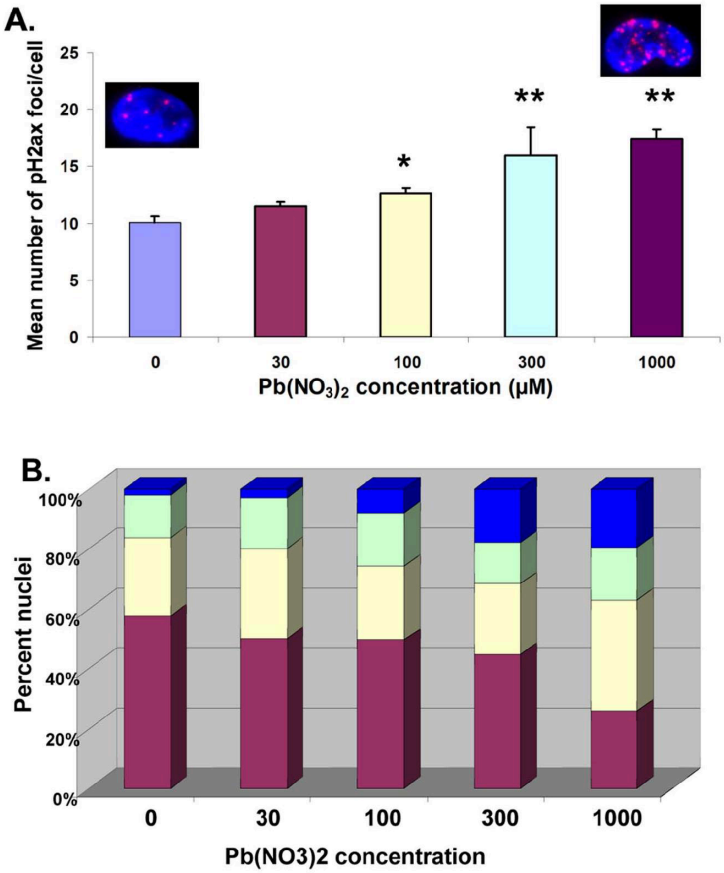

Figure 1. Lead induces γH2Ax foci in B3 cells. Results obtained with B3 cells following 24 h exposure with the indicated $Pb(NO_3)_2$ concentrations. **A.** Number of γH2Ax foci per cell. Inserts show representative γH2Ax signals observed for 0 and 1 mM $Pb(NO_3)_2$. **B.** Distribution of the number of γH2Ax foci per nucleus as a function of Pb concentration. Violet, 0–9 foci/nucleus; Yellow, 10–19 foci/nucleus; Green, 20–29 foci/nucleus; Blue, >30 foci/nucleus.
doi:10.1371/journal.pone.0067501.g001

Lead Preferentially Targets the Lagging Strand

As the leading and lagging strands of telomeres have dissimilar structures (reviewed in [13]), it seemed plausible that Pb may preferentially target one strand over the other. The telomeric probe used in the experiments described up to this point consisted of protein nucleic acid (PNA) bearing the specific sequence of one telomere strand. Chromosome orientation-FISH (CO-FISH) was used to differentiate the chromosomal strands [18] (lagging and leading) by the detection of their specific sequence (T_2AG_3 and C_3TA_2 respectively) with the complementary sequence (red and green respectively in **Figure 4A**). We analyzed the involvement of the leading and lagging strands in the loss of telomeres and the formation of doublets (**Figure 4B**). The presence of Pb nitrate in the cell culture medium induced a slight increase in all of the telomere aberrations analyzed. However, the increase was only statistically significant for the loss of the lagging strand ($p<0.05$). It is worth noting that FITC (green probe) is less efficient than Cy3 (red probe), and thus the loss of staining of the leading strand may be partially due to poor telomere staining, whereas the loss of staining of the lagging strand is more significant as it is likely to be a true measure of telomere loss. Interestingly, in the case of telomere doublet formation, neither strand seemed to be preferentially affected suggesting that the mechanism of doublet formation is strand-independent. These results show that exposure to Pb nitrate perturbs telomere stability and the lagging strand seems to be the preferential target of Pb nitrate induced telomere loss.

Discussion

Despite being the subject of vigorous research, the mechanism of Pb toxicity and/or carcinogenicity remains unknown. A recent study demonstrated the appearance of γH2Ax foci, a known biomarker for DSB formation, reached a maximum 24 hours after Pb contamination [10]. In the present study we have applied cytogenetic approaches to investigate the consequences of Pb-induced γH2Ax foci formation on human B3 cells.

The mechanism behind the formation of γH2Ax foci may be quite different depending on their chromosomal localization. Intra-chromosomal foci are primarily due to DSB whereas those found at telomeres may be due to short or dysfunctional telomeres, such as those which are uncapped [19] or damaged [20]. Our

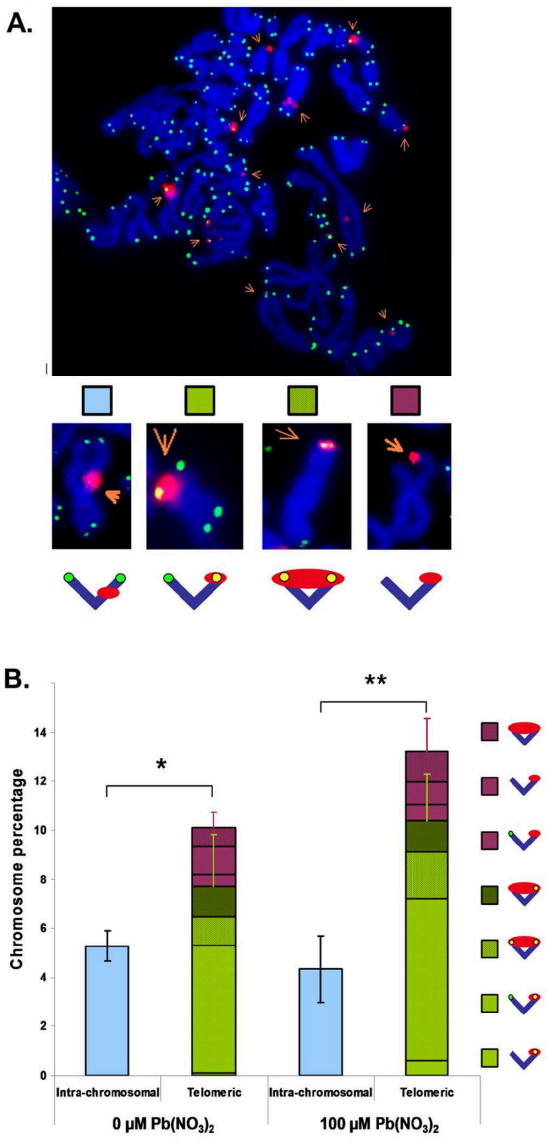

Figure 2. Lead induces Telomere-Induced Foci (TIFs). Results obtained with B3 cells following 24 h exposure with the indicated $Pb(NO_3)_2$ concentrations. **A.** Representative images obtained following IF-FISH. TIFs (yellow) represent co-localisation of γH2Ax (red) and telomere (green) signals. The upper panel shows a representative image of a single metaphase. The lower panel shows representative images of each type of staining pattern obtained from several metaphases **B.** Localisation of γH2Ax and telomere staining using IF-FISH. *$p<0.05$, ** $p<0.01$. The different combinations of staining are shown in the legend on the right.
doi:10.1371/journal.pone.0067501.g002

results indicate that the Pb-induced γH2Ax foci form mostly at the end of chromosomes at or near the telomeres suggesting that Pb exposure may induce telomere instability most likely due to a defect in telomere maintenance resulting in the emergence of doublets and telomere loss. Sub-telomere staining confirmed that the loss is strictly limited to telomeric sequences and the Co-FISH method allowed the identification of the lagging strand as the preferential target of these losses.

Indeed, in the previous study demonstrating the appearance of γH2Ax foci following Pb administration [10], it was never conclusively proven that Pb exposure directly led to the formation of DSB despite a concerted effort to do so. The authors concluded that DSB formation was not a direct consequence of lead exposure, but only occurred at a relatively late time point due to oxidative stress and the accumulation of single stranded breaks. Indeed, the relatively late appearance of γH2Ax foci would argue against the direct formation of DSBs following lead exposure, as intra-chromosomal DSB formation normally occurs relatively rapidly following, for example exposure of cells to ionizing radiation, and are almost completely repaired at 24 hours. In light of the results of the current study, it is likely that the γH2Ax foci observed by Gastaldo et al. were actually due to the presence of dysfunctional telomeres, in the absence of DSB, following Pb exposure.

In somatic cells, telomeres shorten at each cell division representing a mitotic clock of the senescence process. Telomeres are highly sensitive to oxidative stress due to less effective DNA repair than for intra-chromosomal sequences [21] and Pb is known to perturb the oxidative status of cells (reviewed in [8]) notably through its interaction with proteins [22]. The specific targeting of telomeres could thus be indirectly attributed to Pb-induced oxidative stress. The specific alteration of this chromosomal region may have drastic consequences on the formation and the long term transmission of chromosomal rearrangements via their interplay with the natural aging of the cells [21].

The preferential targeting of Pb to the lagging strand is intriguing. The particularity of this strand is the repetition of a well conserved G-rich sequence ($d[T_{1-3}\text{-}(T/A)\text{-}G_{3-4})_n$) which has been shown to form G-quadruplexes *in vitro* under physiological conditions. G quadruplexes are 4 stranded nucleic acid structures which can be formed by G rich sequences and can readily form in vitro and have also been demonstrated in vivo, notably associated with telomeres. Once formed, G-quadruplexes are highly stable and have to be processed by enzymes to unwind the DNA, notably to allow telomere replication. Several enzymes have been shown to have this property: BLM, WRN, DHX36, GQN1, MRE11 and FANCJ … (reviewed in [23]; [24]). Interestingly, G-quadruplex-interacting compounds, which stabilize the G-quadruplex structure, have been shown to induce the loss of telomere maintenance leading to the induction of apoptosis in normal or tumoral cells [25–27].

The presence of monovalent cations is an imperative requirement for G-quadruplex formation ($K^+ > Na^+ > Cs^+ > Li^+$). G-quadruplexes can also be stabilized by divalent ions, sometimes more strongly than by monovalent ions because of the increase in charge. G-quadruplex structures obtained with Pb^{2+} are more compact, the hydrogen bonds are more stable than with K^+ [28] and far fewer Pb^{2+} ions are needed to stabilize a G-rich sequence into a G-quadruplex structure.

Based on the results of the present study, it is tempting to speculate that Pb may displace the physiological ions in already formed G-quadruplexes and possibly induces the formation of additional G-quadruplex structures. In the case of DNAzymes, the replacement of K^+ by Pb^{2+} may inhibit the enzymatic activity because of the induced conformation changes [29]. The high selectivity of many G-quadruplex-unwinding enzymes coupled with their high affinity for these structures could lead to their

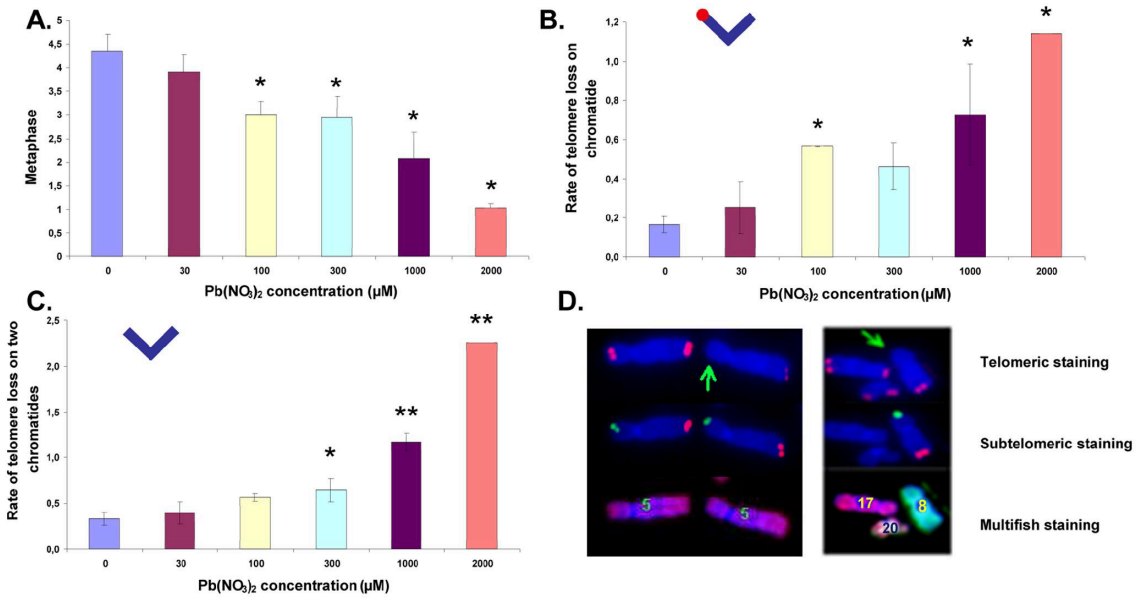

Figure 3. Lead induces telomere instability. A–C. Mean telomere loss observed in B3 cells after 24 h exposure with the indicated $Pb(NO_3)_2$ concentrations and normalized to the correspondent mitotic index. **A.** Mitotic index. **B.** Loss of one telomere on one chromatid. **C.** Loss of two telomeres on two chromatids. **D.** Representative images obtained with B3 cells following the indicated fluorescent *in situ* hybridization procedure. Subtelomere markers are: p-arm (FITC), q-arm (Texas Red).
doi:10.1371/journal.pone.0067501.g003

inability or a reduced ability to recognize and/or cleave the Pb-compacted G-quadruplexes.

Several studies have shown that cells carrying defective G-quadruplex-unwinding enzymes demonstrate telomere instability. For example, cells deficient for the Werner Syndrome RecQ Helicase (WRN), known to be critical in the processing of G quadruplexes, are characterized by the preferential loss of telomeres from the lagging strand [30]. The telomere instability observed in the present study could be correlated with the persistence of the G-quadruplexes during replication, underling a defect in telomere maintenance during replication.

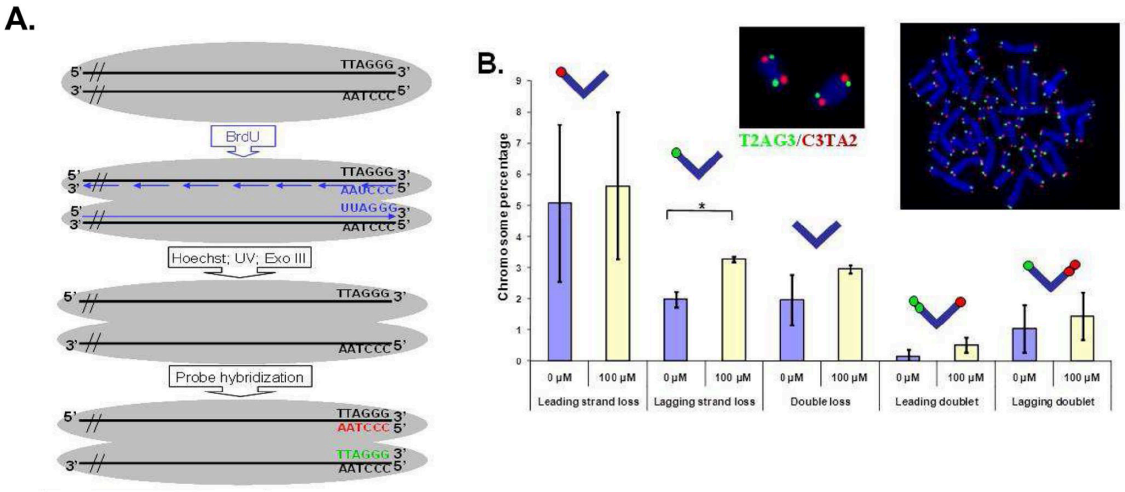

Figure 4. Lead induces mainly lagging strand instability. A. Principle of telomere hybridization by CO-FISH. **B.** Mean telomere instability observed with B3 cells after 24 h exposure with indicated $Pb(NO_3)_2$ concentrations. *$p<0.05$. Representative images obtained with B3 cells are shown in the inset.
doi:10.1371/journal.pone.0067501.g004

The effects of lead exposure on telomere maintenance are also intriguing in light of numerous recent studies which demonstrate a role for telomere maintenance in brain development and tissue homeostasis suggesting a possible mechanism for lead-induced neurotoxicity. Studies in mice in which either the telomerase mRNA component (mTR) [31] or telomerase reverse trascriptase (mTERT) [32] have been deleted demonstrate progressively shorter telomeres leading to numerous problems in organs with high cellular turnover after 4–6 generations [33,34]. In addition, starting from the 4th generation, developing embryos exhibit a failure in neural tube closure [35]. Furthermore, telomere shortening in neural stem cells has been shown to disrupt neurogenesis [36]. Interestingly, the effects of TERT deletion can be reversed in aging mice by inducible expression of TERT, leading to an increase in telomere length, and the reversal of tissue degeneration including in the central nervous system [37]. More recently, a strong link between levels of TERT activity in the hippocampus and depression has been demonstrated in a chronic mild stress mouse model [38].

In humans, perceived chronic stress [39] and high phobic anxiety [40] have been shown to be associated with telomere shortening of blood lymphocytes suggesting a link between environmental stressors, disruption of telomere maintenance, and psychological state. Recently, an age-independent association was also demonstrated between telomere length and cognitive function in a cohort of elderly subjects [41]. It is noteworthy that similar psychological and cognitive effects have been linked to childhood Pb exposure.

Finally, a recently published study has demonstrated that occupational exposure is associated with telomere shortening in the peripheral white blood cells of Chinese battery manufacturing plant workers [42] that was directly proportional to the body lead burden, suggesting a link between occupational lead exposure and the loss of telomere maintenance. While this study only demonstrates an association between lead exposure and telomere disruption, these results take on new significance in light of the results presented here which strongly suggest a causal link between lead exposure at the cellular level and the loss of telomere maintenance.

A model for telomere instability following Pb exposure which could explain Pb-induced neurotxicity can be proposed. The greater affinity of Pb for G-rich sequences may induce the displacement of the physiological ions (K^+ or Na^+) to form tighter G-quadruplex complexes [29]. The complexes need to be processed to permit telomere replication but the highly specific unwinding enzymes [23] may not function properly due to the more highly compacted form of the complex. Alternative mechanisms are perhaps then recruited to obtain linear DNA, notably with the intervention of nucleases that perturb telomere integrity leading to their recognition as DSBs (γH2Ax staining). We propose that the first anomaly is the emergence of telomere doublets subsequent to processing by the alternative unwinding enzymes. The loss of telomere integrity then leads to the loss of the telomeric sequence on one or sometimes two chromatids. This hypothesis is consistent with the results observed where the rate of doublet formation is not dose-dependent and with the γH2Ax staining at telomeres while telomere sequences are still detectable. The subsequent impaired telomere maintenance induces genomic and chromosomal instability that may lead to a perturbation in neurogenesis resulting in Pb-induced neurotoxicity. The loss of telomere maintenance may also be directly neurotoxic, but this remains to be demonstrated.

In light of our current knowledge of telomeres and the critical role that they play in cellular aging as well as in the development and maintenance of the central nervous system, and the downstream repercussions for cognitive and psychological status, the results presented from the current study suggest a promising novel avenue of inquiry to better understand the link between Pb exposure, telomere maintenance, and the biological responses leading to the permanent nature of the resulting neurotoxic effects.

Supporting Information

Figure S1 Lead induces the appearance of telomere doublets. Appearance of telomere doublets observed in B3 cells after 24 h exposure with the indicated $Pb(NO_3)_2$ concentrations and normalized to the corresponding mitotic index.
(TIF)

Figure S2 Lead induces telomere instability in primary human blood lymphocytes. To measure inter-individual variability, the spontaneous level of telomere loss and doublet formation were measured in the blood lymphocytes of 20 healthy donors (Panels A and B). The values represent the mean of the independent analyses of 3 different evaluators. The effect of Pb on telomere loss and doublet formation were measured in human blood lymphocytes of 7 donors after 24 h exposure with the indicated $Pb(NO_3)_2$ concentrations (Panels C and D). *$p<0.05$, ** $p<0.01$. In all cases, 50 metaphase spreads were analyzed.
(TIF)

Acknowledgments

We thank Dr. John P. Murnane for providing the B3 cell line which was derived from the EJ30 bladder cancer cell line. We are indebted to Radhia M'Kacher who kindly allowed us use her bank of human lymphocyte slides. We are grateful to Emmanuel Paul and Carolina Calderon for their help in the analysis of the human lymphocytes. We thank Nicolas Foray for stimulating discussions.

Author Contributions

Conceived and designed the experiments: LS MR. Performed the experiments: GP MR GS MB CC. Analyzed the data: GP MV MR WMH LS GS MB CC. Wrote the paper: GP MV MR WMH LS.

References

1. Gilbert SG, Weiss B (2006) A rationale for lowering the blood lead action level from 10 to 2 microg/dL. Neurotoxicology 27: 693–701.
2. Needleman H (2004) Lead poisoning. Annu Rev Med 55: 209–222.
3. White LD, Cory-Slechta DA, Gilbert ME, Tiffany-Castiglioni E, Zawia NH, et al. (2007) New and evolving concepts in the neurotoxicology of lead. Toxicol Appl Pharmacol 225: 1–27.
4. Bellinger DC, Bellinger AM (2006) Childhood lead poisoning: the torturous path from science to policy. J Clin Invest 116: 853–857.
5. Sanders T, Liu Y, Buchner V, Tchounwou PB (2009) Neurotoxic effects and biomarkers of lead exposure: a review. Rev Environ Health 24: 15–45.
6. Brown MJ, Margolis S (2012) Lead in drinking water and human blood lead levels in the United States. MMWR Surveill Summ 61: 1–9.
7. Silbergeld EK (2003) Facilitative mechanisms of lead as a carcinogen. Mutat Res 533: 121–133.
8. Verstraeten SV, Aimo L, Oteiza PI (2008) Aluminium and lead: molecular mechanisms of brain toxicity. Arch Toxicol 82: 789–802.
9. Garcia-Leston J, Mendez J, Pasaro E, Laffon B (2010) Genotoxic effects of lead: an updated review. Environ Int 36: 623–636.
10. Gastaldo J, Viau M, Bencokova Z, Joubert A, Charvet AM, et al. (2007) Lead contamination results in late and slowly repairable DNA double-strand breaks and impacts upon the ATM-dependent signaling pathways. Toxicol Lett 173: 201–214.
11. Redon C, Pilch D, Rogakou E, Sedelnikova O, Newrock K, et al. (2002) Histone H2A variants H2AX and H2AZ. Curr Opin Genet Dev 12: 162–169.

12. d'Adda di Fagagna F, Reaper PM, Clay-Farrace L, Fiegler H, Carr P, et al. (2003) A DNA damage checkpoint response in telomere-initiated senescence. Nature 426: 194–198.
13. Verdun RE, Karlseder J (2007) Replication and protection of telomeres. Nature 447: 924–931.
14. Counter CM, Avilion AA, LeFeuvre CE, Stewart NG, Greider CW, et al. (1992) Telomere shortening associated with chromosome instability is arrested in immortal cells which express telomerase activity. EMBO J 11: 1921–1929.
15. Lo AW, Sabatier L, Fouladi B, Pottier G, Ricoul M, et al. (2002) DNA amplification by breakage/fusion/bridge cycles initiated by spontaneous telomere loss in a human cancer cell line. Neoplasia 4: 531–538.
16. Rothkamm K, Lobrich M (2003) Evidence for a lack of DNA double-strand break repair in human cells exposed to very low x-ray doses. Proc Natl Acad Sci U S A 100: 5057–5062.
17. Ye J, Lenain C, Bauwens S, Rizzo A, Saint-Leger A, et al. (2010) TRF2 and apollo cooperate with topoisomerase 2alpha to protect human telomeres from replicative damage. Cell 142: 230–242.
18. Williams ES, Cornforth MN, Goodwin EH, Bailey SM (2011) CO-FISH, COD-FISH, ReD-FISH, SKY-FISH. Methods Mol Biol 735: 113–124.
19. Takai H, Smogorzewska A, de Lange T (2003) DNA damage foci at dysfunctional telomeres. Curr Biol 13: 1549–1556.
20. Nakamura AJ, Redon CE, Bonner WM, Sedelnikova OA (2009) Telomere-dependent and telomere-independent origins of endogenous DNA damage in tumor cells. Aging (Albany NY) 1: 212–218.
21. Ayouaz A, Raynaud C, Heride C, Revaud D, Sabatier L (2008) Telomeres: hallmarks of radiosensitivity. Biochimie 90: 60–72.
22. Magyar JS, Weng TC, Stern CM, Dye DF, Rous BW, et al. (2005) Reexamination of lead(II) coordination preferences in sulfur-rich sites: implications for a critical mechanism of lead poisoning. J Am Chem Soc 127: 9495–9505.
23. Maizels N (2006) Dynamic roles for G4 DNA in the biology of eukaryotic cells. Nat Struct Mol Biol 13: 1055–1059.
24. London TB, Barber LJ, Mosedale G, Kelly GP, Balasubramanian S, et al. (2008) FANCJ is a structure-specific DNA helicase associated with the maintenance of genomic G/C tracts. J Biol Chem 283: 36132–36139.
25. Salvati E, Leonetti C, Rizzo A, Scarsella M, Mottolese M, et al. (2007) Telomere damage induced by the G-quadruplex ligand RHPS4 has an antitumor effect. J Clin Invest 117: 3236–3247.
26. Tahara H, Shin-Ya K, Seimiya H, Yamada H, Tsuruo T, et al. (2006) G-Quadruplex stabilization by telomestatin induces TRF2 protein dissociation from telomeres and anaphase bridge formation accompanied by loss of the 3′ telomeric overhang in cancer cells. Oncogene 25: 1955–1966.
27. Pennarun G, Granotier C, Gauthier LR, Gomez D, Hoffschir F, et al. (2005) Apoptosis related to telomere instability and cell cycle alterations in human glioma cells treated by new highly selective G-quadruplex ligands. Oncogene 24: 2917–2928.
28. Kotch FW, Fettinger JC, Davis JT (2000) A lead-filled G-quadruplex: insight into the G-Quartet's selectivity for Pb(2+) over K(+). Org Lett 2: 3277–3280.
29. Li T, Wang E, Dong S (2009) Potassium-lead-switched G-quadruplexes: a new class of DNA logic gates. J Am Chem Soc 131: 15082–15083.
30. Crabbe L, Verdun RE, Haggblom CI, Karlseder J (2004) Defective telomere lagging strand synthesis in cells lacking WRN helicase activity. Science 306: 1951–1953.
31. Blasco MA, Lee HW, Hande MP, Samper E, Lansdorp PM, et al. (1997) Telomere shortening and tumor formation by mouse cells lacking telomerase RNA. Cell 91: 25–34.
32. Liu Y, Snow BE, Hande MP, Yeung D, Erdmann NJ, et al. (2000) The telomerase reverse transcriptase is limiting and necessary for telomerase function in vivo. Curr Biol 10: 1459–1462.
33. Lee HW, Blasco MA, Gottlieb GJ, Horner JW, 2nd, Greider CW, et al. (1998) Essential role of mouse telomerase in highly proliferative organs. Nature 392: 569–574.
34. Hao LY, Armanios M, Strong MA, Karim B, Feldser DM, et al. (2005) Short telomeres, even in the presence of telomerase, limit tissue renewal capacity. Cell 123: 1121–1131.
35. Herrera E, Samper E, Blasco MA (1999) Telomere shortening in mTR−/− embryos is associated with failure to close the neural tube. EMBO J 18: 1172–1181.
36. Ferron SR, Marques-Torrejon MA, Mira H, Flores I, Taylor K, et al. (2009) Telomere shortening in neural stem cells disrupts neuronal differentiation and neuritogenesis. J Neurosci 29: 14394–14407.
37. Jaskelioff M, Muller FL, Paik JH, Thomas E, Jiang S, et al. (2011) Telomerase reactivation reverses tissue degeneration in aged telomerase-deficient mice. Nature 469: 102–106.
38. Zhou QG, Hu Y, Wu DL, Zhu LJ, Chen C, et al. (2011) Hippocampal telomerase is involved in the modulation of depressive behaviors. J Neurosci 31: 12258–12269.
39. Epel ES, Blackburn EH, Lin J, Dhabhar FS, Adler NE, et al. (2004) Accelerated telomere shortening in response to life stress. Proc Natl Acad Sci U S A 101: 17312–17315.
40. Okereke OI, Prescott J, Wong JY, Han J, Rexrode KM, et al. (2012) High phobic anxiety is related to lower leukocyte telomere length in women. PLoS One 7: e40516.
41. Canela A, Vera E, Klatt P, Blasco MA (2007) High-throughput telomere length quantification by FISH and its application to human population studies. Proc Natl Acad Sci U S A 104: 5300–5305.
42. Wu Y, Liu Y, Ni N, Bao B, Zhang C, et al. (2012) High lead exposure is associated with telomere length shortening in Chinese battery manufacturing plant workers. Occup Environ Med 69: 557–563.
43. Fouladi B, Sabatier L, Miller D, Pottier G, Murnane JP (2000) The relationship between spontaneous telomere loss and chromosome instability in a human tumor cell line. Neoplasia 2: 540–554.
44. Bai Y, Murnane JP (2003) Telomere instability in a human tumor cell line expressing NBS1 with mutations at sites phosphorylated by ATM. Mol Cancer Res 1: 1058–1069.
45. Sabatier L, Ricoul M, Pottier G, Murnane JP (2005) The loss of a single telomere can result in instability of multiple chromosomes in a human tumor cell line. Mol Cancer Res 3: 139–150.
46. Kulkarni A, Zschenker O, Reynolds G, Miller D, Murnane JP (2010) Effect of telomere proximity on telomere position effect, chromosome healing, and sensitivity to DNA double-strand breaks in a human tumor cell line. Mol Cell Biol 30: 578–589.
47. Kato T, Irwin RJ, Jr., Prout GR., Jr. (1977) Cell cycles in two cell lines of human bladder carcinoma. Tohoku J Exp Med 121: 157–164.
48. O'Toole CM, Povey S, Hepburn P, Franks LM (1983) Identity of some human bladder cancer cell lines. Nature 301: 429–430.
49. Leonhardt EA, Trinh M, Forrester HB, Johnson RT, Dewey WC (1997) Comparisons of the frequencies and molecular spectra of HPRT mutants when human cancer cells were X-irradiated during G1 or S phase. Radiat Res 148: 548–560.
50. Dutrillaux B, Viegas Pequignot E, Aurias A, Prod'homme M, Sportes M, et al. (1981) Tentative estimate of the risk of chromosomal disease due to radiation-induced translocations in man. Mutat Res 82: 191–200.
51. Lansdorp PM, Verwoerd NP, van de Rijke FM, Dragowska V, Little MT, et al. (1996) Heterogeneity in telomere length of human chromosomes. Hum Mol Genet 5: 685–691.

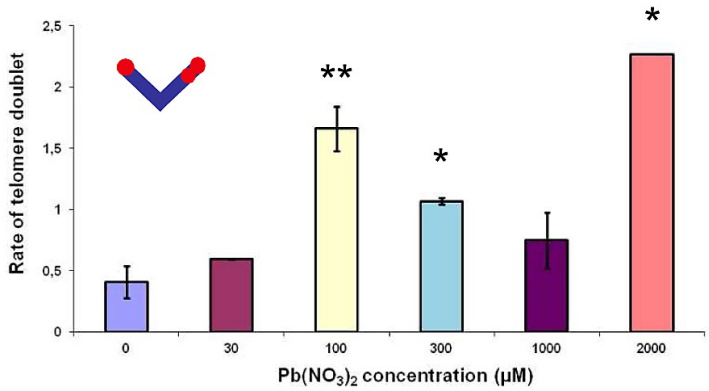

Figure S1. Lead induces the appearance of telomere doublets. Appearance of telomere doublets observed in B3 cells after 24 h exposure with the indicated $Pb(NO_3)_2$ concentrations and normalized to the corresponding mitotic index.

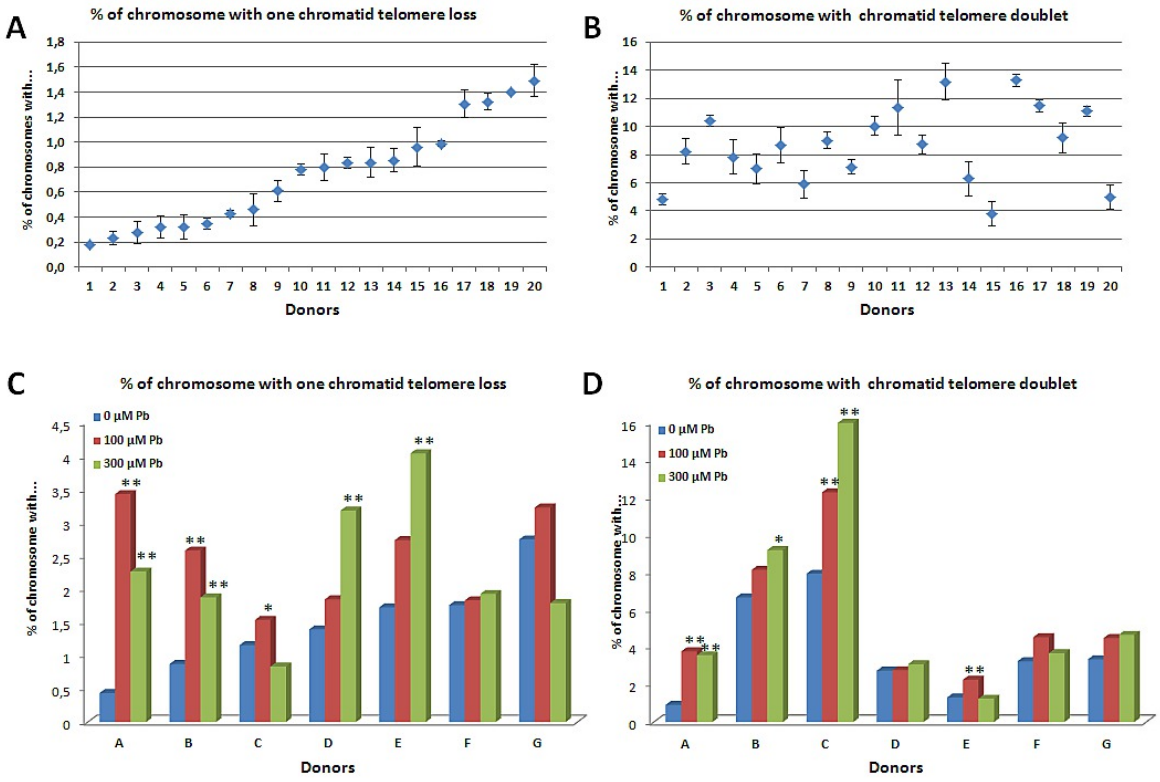

Figure S2. Lead induces telomere instability in primary human blood lymphocytes. To measure inter-individual variability, the spontaneous level of telomere loss and doublet formation were measured in the blood lymphocytes of 20 healthy donors (Panels A and B). The values represent the mean of the independent analyses of 3 different evaluators. The effect of Pb on telomere loss and doublet formation were measured in human blood lymphocytes of 7 donors after 24 h exposure with the indicated $Pb(NO_3)_2$ concentrations (Panels C and D). *p<0.05, ** p<0.01. In all cases, 50 metaphase spreads were analyzed.

REFERENCES

Advisory Group on Ionising Radiation (2013). "Human radiosensitivity", in: *Report of the Independent Advisory Group on Ionising Radiation.* (Chilton: Health Protection Agency).

Ainsbury, E.A., Al-Hafidh, J., Bajinskis, A., Barnard, S., Barquinero, J.F., Beinke, C., De Gelder, V., Gregoire, E., Jaworska, A., Lindholm, C., Lloyd, D., Moquet, J., Nylund, R., Oestreicher, U., Roch-Lefevre, S., Rothkamm, K., Romm, H., Scherthan, H., Sommer, S., Thierens, H., Vandevoorde, C., Vral, A., and Wojcik, A. (2014a). Inter- and intra-laboratory comparison of a multibiodosimetric approach to triage in a simulated, large scale radiation emergency. *Int J Radiat Biol* 90**,** 193-202. doi: 10.3109/09553002.2014.868616.

Ainsbury, E.A., Bakhanova, E., Barquinero, J.F., Brai, M., Chumak, V., Correcher, V., Darroudi, F., Fattibene, P., Gruel, G., Guclu, I., Horn, S., Jaworska, A., Kulka, U., Lindholm, C., Lloyd, D., Longo, A., Marrale, M., Monteiro Gil, O., Oestreicher, U., Pajic, J., Rakic, B., Romm, H., Trompier, F., Veronese, I., Voisin, P., Vral, A., Whitehouse, C.A., Wieser, A., Woda, C., Wojcik, A., and Rothkamm, K. (2011). Review of retrospective dosimetry techniques for external ionising radiation exposures. *Radiat Prot Dosimetry* 147**,** 573-592. doi: 10.1093/rpd/ncq499.

Ainsbury, E.A., Barnard, S., Barrios, L., Fattibene, P., De Gelder, V., Gregoire, E., Lindholm, C., Lloyd, D., Nergaard, I., Rothkamm, K., Romm, H., Scherthan, H., Thierens, H., Vandevoorde, C., Woda, C., and Wojcik, A. (2014b). Multibiodose radiation emergency triage categorization software. *Health Phys* 107**,** 83-89. doi: 10.1097/HP.0000000000000049.

Aksenova, A.Y., Greenwell, P.W., Dominska, M., Shishkin, A.A., Kim, J.C., Petes, T.D., and Mirkin, S.M. (2013). Genome rearrangements caused by interstitial telomeric sequences in yeast. *Proc Natl Acad Sci U S A* 110**,** 19866-19871. doi: 10.1073/pnas.1319313110.

Al-Achkar, W., Sabatier, L., and Dutrillaux, B. (1988). Transmission of radiation-induced rearrangements through cell divisions. *Mutat Res* 198**,** 191-198. doi: 0027-5107(88)90054-1 [pii].

Amis, E.S., Jr., Butler, P.F., Applegate, K.E., Birnbaum, S.B., Brateman, L.F., Hevezi, J.M., Mettler, F.A., Morin, R.L., Pentecost, M.J., Smith, G.G., Strauss, K.J., Zeman, R.K., and American College Of, R. (2007). American College of Radiology white paper on radiation dose in medicine. *J Am Coll Radiol* 4**,** 272-284. doi: 10.1016/j.jacr.2007.03.002.

Anderson, R.M., Marsden, S.J., Wright, E.G., Kadhim, M.A., Goodhead, D.T., and Griffin, C.S. (2000). Complex chromosome aberrations in peripheral blood lymphocytes as a potential biomarker of exposure to high-LET alpha-particles. *Int J Radiat Biol* 76**,** 31-42.

Andreassen, C.N., Dikomey, E., Parliament, M., and West, C.M. (2012). Will SNPs be useful predictors of normal tissue radiosensitivity in the future? *Radiother Oncol* 105**,** 283-288. doi: 10.1016/j.radonc.2012.11.003.

Andreassi, M.G., Piccaluga, E., Gargani, L., Sabatino, L., Borghini, A., Faita, F., Bruno, R.M., Padovani, R., Guagliumi, G., and Picano, E. (2015). Subclinical carotid atherosclerosis and early vascular aging from long-term low-dose ionizing radiation exposure: a genetic, telomere, and vascular ultrasound study in cardiac catheterization laboratory staff. *JACC Cardiovasc Interv* 8**,** 616-627. doi: 10.1016/j.jcin.2014.12.233.

Andrievski, A., and Wilkins, R.C. (2009). The response of gamma-H2AX in human lymphocytes and lymphocytes subsets measured in whole blood cultures. *Int J Radiat Biol* 85**,** 369-376. doi: 10.1080/09553000902781147.

Antunes, A.C., Martins, V., Cardoso, J., Santos, L., and Monteiro Gil, O. (2014). The cytokinesis-blocked micronucleus assay: dose estimation and inter-individual differences in the response to gamma-radiation. *Mutat Res Genet Toxicol Environ Mutagen* 760**,** 17-22. doi: 10.1016/j.mrgentox.2013.09.012.

Armanios, M., and Blackburn, E.H. (2012). The telomere syndromes. *Nat Rev Genet* 13**,** 693-704. doi: 10.1038/nrg3246.

Avondoglio, D., Scott, T., Kil, W.J., Sproull, M., Tofilon, P.J., and Camphausen, K. (2009). High throughput evaluation of gamma-H2AX. *Radiat Oncol* 4**,** 31. doi: 10.1186/1748-717X-4-31.

Ayouaz, A., Raynaud, C., Heride, C., Revaud, D., and Sabatier, L. (2008). Telomeres: hallmarks of radiosensitivity. *Biochimie* 90**,** 60-72. doi: 10.1016/j.biochi.2007.09.011.

Azzam, E.I., De Toledo, S.M., Waker, A.J., and Little, J.B. (2000). High and low fluences of alpha-particles induce a G1 checkpoint in human diploid fibroblasts. *Cancer Res* 60**,** 2623-2631.

Azzam, E.I., Jay-Gerin, J.P., and Pain, D. (2012). Ionizing radiation-induced metabolic oxidative stress and prolonged cell injury. *Cancer Lett* 327**,** 48-60. doi: 10.1016/j.canlet.2011.12.012.

Baca, S.C., Prandi, D., Lawrence, M.S., Mosquera, J.M., Romanel, A., Drier, Y., Park, K., Kitabayashi, N., Macdonald, T.Y., Ghandi, M., Van Allen, E., Kryukov, G.V., Sboner, A., Theurillat, J.P., Soong, T.D., Nickerson, E., Auclair, D., Tewari, A., Beltran, H., Onofrio, R.C., Boysen, G., Guiducci, C., Barbieri, C.E., Cibulskis, K., Sivachenko, A., Carter, S.L., Saksena, G., Voet, D., Ramos, A.H., Winckler, W., Cipicchio, M., Ardlie, K., Kantoff, P.W., Berger, M.F., Gabriel, S.B., Golub, T.R., Meyerson, M., Lander, E.S., Elemento, O., Getz, G., Demichelis, F., Rubin, M.A., and Garraway, L.A. (2013). Punctuated evolution of prostate cancer genomes. *Cell* 153**,** 666-677. doi: 10.1016/j.cell.2013.03.021.

Badie, C., Kabacik, S., Balagurunathan, Y., Bernard, N., Brengues, M., Faggioni, G., Greither, R., Lista, F., Peinnequin, A., Poyot, T., Herodin, F., Missel, A., Terbrueggen, B., Zenhausern, F., Rothkamm, K., Meineke, V., Braselmann, H., Beinke, C., and Abend, M. (2013). Laboratory intercomparison of gene expression assays. *Radiat Res* 180**,** 138-148. doi: 10.1667/RR3236.1.

Badie, S., Carlos, A.R., Folio, C., Okamoto, K., Bouwman, P., Jonkers, J., and Tarsounas, M. (2015). BRCA1 and CtIP promote alternative non-homologous end-joining at uncapped telomeres. *EMBO J* 34**,** 828. doi: 10.15252/embj.201570610.

Baker, J.E., Moulder, J.E., and Hopewell, J.W. (2011). Radiation as a risk factor for cardiovascular disease. *Antioxid Redox Signal* 15**,** 1945-1956. doi: 10.1089/ars.2010.3742.

Bakhmutsky, M.V., Joiner, M.C., Jones, T.B., and Tucker, J.D. (2014). Differences in cytogenetic sensitivity to ionizing radiation in newborns and adults. *Radiat Res* 181**,** 605-616. doi: 10.1667/RR13598.1.

Balajee, A.S., Bertucci, A., Taveras, M., and Brenner, D.J. (2014). Multicolour FISH analysis of ionising radiation induced micronucleus formation in human lymphocytes. *Mutagenesis* 29**,** 447-455. doi: 10.1093/mutage/geu041.

Balakrishnan, S., Shirsath, K., Bhat, N., and Anjaria, K. (2010). Biodosimetry for high dose accidental exposures by drug induced premature chromosome condensation (PCC) assay. *Mutat Res* 699**,** 11-16. doi: 10.1016/j.mrgentox.2010.03.008.

Balasubramanyam, M., Adaikalakoteswari, A., Monickaraj, S.F., and Mohan, V. (2007). Telomere shortening & metabolic/vascular diseases. *Indian J Med Res* 125**,** 441-450.

Barnard, S., Ainsbury, E.A., Al-Hafidh, J., Hadjidekova, V., Hristova, R., Lindholm, C., Monteiro Gil, O., Moquet, J., Moreno, M., Rossler, U., Thierens, H., Vandevoorde, C., Vral, A., Wojewodzka, M., and Rothkamm, K. (2015). The first gamma-H2AX biodosimetry intercomparison exercise of the developing European biodosimetry network RENEB. *Radiat Prot Dosimetry* 164**,** 265-270. doi: 10.1093/rpd/ncu259.

Beaton, L.A., Ferrarotto, C., Kutzner, B.C., Mcnamee, J.P., Bellier, P.V., and Wilkins, R.C. (2013). Analysis of chromosome damage for biodosimetry using imaging flow cytometry. *Mutat Res* 756**,** 192-195. doi: 10.1016/j.mrgentox.2013.04.002.

Beinke, C., Barnard, S., Boulay-Greene, H., De Amicis, A., De Sanctis, S., Herodin, F., Jones, A., Kulka, U., Lista, F., Lloyd, D., Martigne, P., Moquet, J., Oestreicher, U., Romm, H., Rothkamm, K., Valente, M., Meineke, V., Braselmann, H., and Abend, M. (2013). Laboratory intercomparison of the dicentric chromosome analysis assay. *Radiat Res* 180**,** 129-137. doi: 10.1667/RR3235.1.

Beinke, C., and Meineke, V. (2012). High potential for methodical improvements of FISH-based translocation analysis for retrospective radiation biodosimetry. *Health Phys* 103**,** 127-132. doi: 10.1097/HP.0b013e31824645fb.

Beinke, C., Port, M., Lamkowski, A., and Abend, M. (2015). Comparing Seven Mitogens with Pha-M for Improved Lymphocyte Stimulation in Dicentric Chromosome Analysis for Biodosimetry. *Radiat Prot Dosimetry*. doi: 10.1093/rpd/ncv286.

Belyakov, O.V., Folkard, M., Mothersill, C., Prise, K.M., and Michael, B.D. (2002). Bystander-induced apoptosis and premature differentiation in primary urothelial explants after charged particle microbeam irradiation. *Radiat Prot Dosimetry* 99**,** 249-251.

Belyakov, O.V., Mitchell, S.A., Parikh, D., Randers-Pehrson, G., Marino, S.A., Amundson, S.A., Geard, C.R., and Brenner, D.J. (2005). Biological effects in unirradiated human tissue induced by radiation damage up to 1 mm away. *Proc Natl Acad Sci U S A* 102**,** 14203-14208. doi: 10.1073/pnas.0505020102.

Berrington De Gonzalez, A., Mahesh, M., Kim, K.P., Bhargavan, M., Lewis, R., Mettler, F., and Land, C. (2009). Projected cancer risks from computed tomographic scans performed in the United States in 2007. *Arch Intern Med* 169**,** 2071-2077. doi: 10.1001/archinternmed.2009.440.

Bhatti, P., Sigurdson, A.J., and Mabuchi, K. (2008). Can low-dose radiation increase risk of cardiovascular disease? *Lancet* 372**,** 697-699. doi: 10.1016/S0140-6736(08)61285-4.

Blackburn, E.H., Greider, C.W., and Szostak, J.W. (2006). Telomeres and telomerase: the path from maize, Tetrahymena and yeast to human cancer and aging. *Nat Med* 12**,** 1133-1138. doi: 10.1038/nm1006-1133.

Blakely, W.F., Carr, Z., Chu, M.C., Dayal-Drager, R., Fujimoto, K., Hopmeir, M., Kulka, U., Lillis-Hearne, P., Livingston, G.K., Lloyd, D.C., Maznyk, N., Perez Mdel, R., Romm, H., Takashima, Y., Voisin, P., Wilkins, R.C., and Yoshida, M.A. (2009). WHO 1st consultation on the development of a global biodosimetry laboratories network for radiation emergencies (BioDoseNet). *Radiat Res* 171**,** 127-139. doi: 10.1667/RR1549.1.

Blasco, M.A. (2005). Telomeres and human disease: ageing, cancer and beyond. *Nat Rev Genet* 6**,** 611-622. doi: 10.1038/nrg1656.

Blumenthal, D.J., Sugarman, S.L., Christensen, D.M., Wiley, A.L., Livingston, G.K., Glassman, E.S., Koerner, J.F., Sullivan, J.M., and Hinds, S. (2014). Role of dicentric analysis in an overarching biodosimetry strategy for use following a nuclear detonation in an urban environment. *Health Phys* 106**,** 516-522. doi: 10.1097/HP.0b013e3182a5f94f.

Bocker, W., and Iliakis, G. (2006). Computational Methods for analysis of foci: validation for radiation-induced gamma-H2AX foci in human cells. *Radiat Res* 165**,** 113-124.

Bolognesi, C., Abbondandolo, A., Barale, R., Casalone, R., Dalpra, L., De Ferrari, M., Degrassi, F., Forni, A., Lamberti, L., Lando, C., Migliore, L., Padovani, P., Pasquini, R., Puntoni, R., Sbrana, I., Stella, M., and Bonassi, S. (1997). Age-related increase of baseline frequencies of sister chromatid exchanges, chromosome aberrations, and micronuclei in human lymphocytes. *Cancer Epidemiol Biomarkers Prev* 6**,** 249-256.

Bolognesi, C., and Fenech, M. (2013). Micronucleus assay in human cells: lymphocytes and buccal cells. *Methods Mol Biol* 1044**,** 191-207. doi: 10.1007/978-1-62703-529-3_10.

Bolognesi, C., Knasmueller, S., Nersesyan, A., Thomas, P., and Fenech, M. (2013). The HUMNxl scoring criteria for different cell types and nuclear anomalies in the buccal micronucleus cytome assay - an update and expanded photogallery. *Mutat Res* 753**,** 100-113. doi: 10.1016/j.mrrev.2013.07.002.

Bolognesi, C., Roggieri, P., Ropolo, M., Thomas, P., Hor, M., Fenech, M., Nersesyan, A., and Knasmueller, S. (2015). Buccal micronucleus cytome assay: results of an intra- and inter-laboratory scoring comparison. *Mutagenesis* 30**,** 545-555. doi: 10.1093/mutage/gev017.

Bonassi, S., Fenech, M., Lando, C., Lin, Y.P., Ceppi, M., Chang, W.P., Holland, N., Kirsch-Volders, M., Zeiger, E., Ban, S., Barale, R., Bigatti, M.P., Bolognesi, C., Jia, C., Di Giorgio, M., Ferguson, L.R., Fucic, A., Lima, O.G., Hrelia, P., Krishnaja, A.P., Lee, T.K., Migliore, L., Mikhalevich, L., Mirkova, E., Mosesso, P., Muller, W.U., Odagiri, Y., Scarffi, M.R., Szabova, E., Vorobtsova, I., Vral, A., and Zijno, A. (2001). HUman MicroNucleus project: international database comparison for results with the cytokinesis-block micronucleus assay in human lymphocytes: I. Effect of laboratory protocol, scoring criteria, and host factors on the frequency of micronuclei. *Environ Mol Mutagen* 37**,** 31-45.

Branzei, D., and Foiani, M. (2008). Regulation of DNA repair throughout the cell cycle. *Nat Rev Mol Cell Biol* 9**,** 297-308. doi: 10.1038/nrm2351.

Brenner, D.J., Doll, R., Goodhead, D.T., Hall, E.J., Land, C.E., Little, J.B., Lubin, J.H., Preston, D.L., Preston, R.J., Puskin, J.S., Ron, E., Sachs, R.K., Samet, J.M., Setlow, R.B., and Zaider, M. (2003). Cancer risks attributable to low doses of ionizing radiation: assessing what we really know. *Proc Natl Acad Sci U S A* 100**,** 13761-13766. doi: 10.1073/pnas.2235592100.

Brenner, D.J., and Hall, E.J. (2007). Computed tomography--an increasing source of radiation exposure. *N Engl J Med* 357**,** 2277-2284. doi: 10.1056/NEJMra072149.

Bryan, T.M., Englezou, A., Gupta, J., Bacchetti, S., and Reddel, R.R. (1995). Telomere elongation in immortal human cells without detectable telomerase activity. *EMBO J* 14**,** 4240-4248.

Brzoska, K., and Kruszewski, M. (2015). Toward the development of transcriptional biodosimetry for the identification of irradiated individuals and assessment of absorbed radiation dose. *Radiat Environ Biophys* 54**,** 353-363. doi: 10.1007/s00411-015-0603-8.

Burnet, N.G., Barnett, G.C., Elliott, R.M., Dearnaley, D.P., Pharoah, P.D., Dunning, A.M., West, C.M., and Investigators, R. (2013). RAPPER: the radiogenomics of radiation toxicity. *Clin Oncol (R Coll Radiol)* 25**,** 431-434. doi: 10.1016/j.clon.2013.04.001.

Buseman, C.M., Wright, W.E., and Shay, J.W. (2012). Is telomerase a viable target in cancer? *Mutat Res* 730**,** 90-97. doi: 10.1016/j.mrfmmm.2011.07.006.

Carroll, K.A., and Ly, H. (2009). Telomere dysfunction in human diseases: the long and short of it! *Int J Clin Exp Pathol* 2**,** 528-543.

Cartwright, I.M., Genet, M.D., and Kato, T.A. (2013). A simple and rapid fluorescence in situ hybridization microwave protocol for reliable dicentric chromosome analysis. *J Radiat Res* 54**,** 344-348. doi: 10.1093/jrr/rrs090.

Castellino, S.M., Geiger, A.M., Mertens, A.C., Leisenring, W.M., Tooze, J.A., Goodman, P., Stovall, M., Robison, L.L., and Hudson, M.M. (2011). Morbidity and mortality in long-term survivors of Hodgkin lymphoma: a report from the Childhood Cancer Survivor Study. *Blood* 117**,** 1806-1816. doi: 10.1182/blood-2010-04-278796.

Cho, M.S., Lee, J.K., Bae, K.S., Han, E.A., Jang, S.J., Ha, W.H., Lee, S.S., Barquinero, J.F., and Kim, W.T. (2015). Retrospective biodosimetry using translocation frequency in a stable cell of occupationally exposed to ionizing radiation. *J Radiat Res* 56**,** 709-716. doi: 10.1093/jrr/rrv028.

Chou, W.C., Hu, L.Y., Hsiung, C.N., and Shen, C.Y. (2015). Initiation of the ATM-Chk2 DNA damage response through the base excision repair pathway. *Carcinogenesis* 36**,** 832-840. doi: 10.1093/carcin/bgv079.

Christie, D.H., Chu, M.C., and Carr, Z. (2010). Global networking for biodosimetry laboratory capacity surge in radiation emergencies. *Health Phys* 98**,** 168-171. doi: 10.1097/HP.0b013e3181abaad4.

Chua, M.L., and Rothkamm, K. (2013). Biomarkers of radiation exposure: can they predict normal tissue radiosensitivity? *Clin Oncol (R Coll Radiol)* 25**,** 610-616. doi: 10.1016/j.clon.2013.06.010.

Counter, C.M., Avilion, A.A., Lefeuvre, C.E., Stewart, N.G., Greider, C.W., Harley, C.B., and Bacchetti, S. (1992). Telomere shortening associated with chromosome instability is arrested in immortal cells which express telomerase activity. *EMBO J* 11**,** 1921-1929.

Counter, C.M., Botelho, F.M., Wang, P., Harley, C.B., and Bacchetti, S. (1994). Stabilization of short telomeres and telomerase activity accompany immortalization of Epstein-Barr virus-transformed human B lymphocytes. *J Virol* 68**,** 3410-3414.

Cucinotta, F.A., Nikjoo, H., and Goodhead, D.T. (2000). Model for radial dependence of frequency distributions for energy imparted in nanometer volumes from HZE particles. *Radiat Res* 153**,** 459-468.

Cucinotta, F.A., Wu, H., Shavers, M.R., and George, K. (2003). Radiation dosimetry and biophysical models of space radiation effects. *Gravit Space Biol Bull* 16**,** 11-18.

D'adda Di Fagagna, F., Reaper, P.M., Clay-Farrace, L., Fiegler, H., Carr, P., Von Zglinicki, T., Saretzki, G., Carter, N.P., and Jackson, S.P. (2003). A DNA damage checkpoint response in telomere-initiated senescence. *Nature* 426**,** 194-198. doi: 10.1038/nature02118.

De Amicis, A., De Sanctis, S., Di Cristofaro, S., Franchini, V., Regalbuto, E., Mammana, G., and Lista, F. (2014). Dose estimation using dicentric chromosome assay and cytokinesis block micronucleus assay: comparison between manual and automated scoring in triage mode. *Health Phys* 106**,** 787-797. doi: 10.1097/HP.0000000000000097.

De Lange, T. (2004). T-loops and the origin of telomeres. *Nat Rev Mol Cell Biol* 5**,** 323-329. doi: 10.1038/nrm1359.

De Lange, T. (2005). Shelterin: the protein complex that shapes and safeguards human telomeres. *Genes Dev* 19**,** 2100-2110. doi: 10.1101/gad.1346005.

De Lange, T. (2009). How telomeres solve the end-protection problem. *Science* 326**,** 948-952. doi: 10.1126/science.1170633.

De Pagter, M.S., Van Roosmalen, M.J., Baas, A.F., Renkens, I., Duran, K.J., Van Binsbergen, E., Tavakoli-Yaraki, M., Hochstenbach, R., Van Der Veken, L.T., Cuppen, E., and Kloosterman, W.P. (2015). Chromothripsis in healthy individuals affects multiple protein-coding genes and can result in severe congenital abnormalities in offspring. *Am J Hum Genet* 96**,** 651-656. doi: 10.1016/j.ajhg.2015.02.005.

De Sanctis, S., De Amicis, A., Di Cristofaro, S., Franchini, V., Regalbuto, E., Mammana, G., and Lista, F. (2014). Cytokinesis-block micronucleus assay by manual and automated scoring: calibration curves and dose prediction. *Health Phys* 106**,** 745-749. doi: 10.1097/HP.0000000000000052.

De Toledo, S.M., Buonanno, M., Li, M., Asaad, N., Qin, Y., Gonon, G., Shim, G., Galdass, M., Boateng, Y., Zhang, J., and Azzam, E.I. (2011). The impact of adaptive and non-targeted effects in the biological responses to low dose/low fluence ionizing radiation: the modulating effect of linear energy transfer. *Health Phys* 100**,** 290-292. doi: 10.1097/HP.0b013e31820832d8.

Decordier, I., Papine, A., Vande Loock, K., Plas, G., Soussaline, F., and Kirsch-Volders, M. (2011). Automated image analysis of micronuclei by IMSTAR for biomonitoring. *Mutagenesis* 26**,** 163-168. doi: 10.1093/mutage/geq063.

Decottignies, A. (2013). Alternative end-joining mechanisms: a historical perspective. *Front Genet* 4**,** 48. doi: 10.3389/fgene.2013.00048.

Denekamp, J., Waites, T., and Fowler, J.F. (1997). Predicting realistic RBE values for clinically relevant radiotherapy schedules. *Int J Radiat Biol* 71**,** 681-694.

Desmaze, C., Alberti, C., Martins, L., Pottier, G., Sprung, C.N., Murnane, J.P., and Sabatier, L. (1999). The influence of interstitial telomeric sequences on chromosome instability in human cells. *Cytogenet Cell Genet* 86**,** 288-295. doi: 15321.

Di Giorgio, M., Barquinero, J.F., Vallerga, M.B., Radl, A., Taja, M.R., Seoane, A., De Luca, J., Oliveira, M.S., Valdivia, P., Lima, O.G., Lamadrid, A., Mesa, J.G., Aguilera, I.R., Cardoso, T.M., Carvajal, Y.C., Maldonado, C.A., Espinoza, M.E., Martinez-Lopez, W., Mendez-Acuna, L., Di Tomaso, M.V., Roy, L., Lindholm, C., Romm, H., Guclu, I., and Lloyd, D.C. (2011). Biological dosimetry intercomparison exercise: an evaluation of triage and routine mode results by robust methods. *Radiat Res* 175**,** 638-649. doi: 10.1667/RR2425.1.

Dianov, G.L., and Parsons, J.L. (2007). Co-ordination of DNA single strand break repair. *DNA Repair (Amst)* 6**,** 454-460. doi: 10.1016/j.dnarep.2006.10.009.

Diaz De Leon, A., Cronkhite, J.T., Katzenstein, A.L., Godwin, J.D., Raghu, G., Glazer, C.S., Rosenblatt, R.L., Girod, C.E., Garrity, E.R., Xing, C., and Garcia, C.K. (2010). Telomere lengths, pulmonary fibrosis and telomerase (TERT) mutations. *PLoS One* 5**,** e10680. doi: 10.1371/journal.pone.0010680.

Doksani, Y., and De Lange, T. (2014). The role of double-strand break repair pathways at functional and dysfunctional telomeres. *Cold Spring Harb Perspect Biol* 6**,** a016576. doi: 10.1101/cshperspect.a016576.

Ducray, C., Pommier, J.P., Martins, L., Boussin, F.D., and Sabatier, L. (1999). Telomere dynamics, end-to-end fusions and telomerase activation during the human fibroblast immortalization process. *Oncogene* 18**,** 4211-4223. doi: 10.1038/sj.onc.1202797.

Edwards, A.A., Lindholm, C., Darroudi, F., Stephan, G., Romm, H., Barquinero, J., Barrios, L., Caballin, M.R., Roy, L., Whitehouse, C.A., Tawn, E.J., Moquet, J., Lloyd, D.C., and Voisin, P. (2005). Review of translocations detected by FISH for retrospective biological dosimetry applications. *Radiat Prot Dosimetry* 113**,** 396-402. doi: 10.1093/rpd/nch452.

Fenech, M. (2007). Cytokinesis-block micronucleus cytome assay. *Nat Protoc* 2**,** 1084-1104. doi: 10.1038/nprot.2007.77.

Fenech, M. (2010). The lymphocyte cytokinesis-block micronucleus cytome assay and its application in radiation biodosimetry. *Health Phys* 98**,** 234-243. doi: 10.1097/HP.0b013e3181b85044.

Fenech, M., and Bonassi, S. (2011). The effect of age, gender, diet and lifestyle on DNA damage measured using micronucleus frequency in human peripheral blood lymphocytes. *Mutagenesis* 26**,** 43-49. doi: 10.1093/mutage/geq050.

Fenech, M., Holland, N., Zeiger, E., Chang, W.P., Burgaz, S., Thomas, P., Bolognesi, C., Knasmueller, S., Kirsch-Volders, M., and Bonassi, S. (2011a). The HUMN and HUMNxL international collaboration projects on human micronucleus assays in lymphocytes and buccal cells--past, present and future. *Mutagenesis* 26**,** 239-245. doi: 10.1093/mutage/geq051.

Fenech, M., Kirsch-Volders, M., Natarajan, A.T., Surralles, J., Crott, J.W., Parry, J., Norppa, H., Eastmond, D.A., Tucker, J.D., and Thomas, P. (2011b). Molecular mechanisms of micronucleus,

nucleoplasmic bridge and nuclear bud formation in mammalian and human cells. *Mutagenesis* 26**,** 125-132. doi: 10.1093/mutage/geq052.

Fenech, M., Kirsch-Volders, M., Rossnerova, A., Sram, R., Romm, H., Bolognesi, C., Ramakumar, A., Soussaline, F., Schunck, C., Elhajouji, A., Anwar, W., and Bonassi, S. (2013). HUMN project initiative and review of validation, quality control and prospects for further development of automated micronucleus assays using image cytometry systems. *Int J Hyg Environ Health* 216**,** 541-552. doi: 10.1016/j.ijheh.2013.01.008.

Fernet, M., and Hall, J. (2004). Genetic biomarkers of therapeutic radiation sensitivity. *DNA Repair (Amst)* 3**,** 1237-1243. doi: 10.1016/j.dnarep.2004.03.019.

Flegal, F.N., Devantier, Y., Marro, L., and Wilkins, R.C. (2012). Validation of QuickScan dicentric chromosome analysis for high throughput radiation biological dosimetry. *Health Phys* 102**,** 143-153. doi: 10.1097/HP.0b013e3182307758.

Flegal, F.N., Devantier, Y., Mcnamee, J.P., and Wilkins, R.C. (2010). Quickscan dicentric chromosome analysis for radiation biodosimetry. *Health Phys* 98**,** 276-281. doi: 10.1097/HP.0b013e3181aba9c7.

Foray, N., Colin, C., and Bourguignon, M. (2012). 100 years of individual radiosensitivity: how we have forgotten the evidence. *Radiology* 264**,** 627-631. doi: 10.1148/radiol.12112560.

Foray, N., Colin, C., and Bourguignon, M. (2013). [Radiosensitivity: evidence of an individual factor]. *Med Sci (Paris)* 29**,** 397-403. doi: 10.1051/medsci/2013294013.

Francois, M., Hochstenbach, K., Leifert, W., and Fenech, M.F. (2014). Automation of the cytokinesis-block micronucleus cytome assay by laser scanning cytometry and its potential application in radiation biodosimetry. *Biotechniques* 57**,** 309-312. doi: 10.2144/000114239.

Frenzel, M., Cuceu, C., Shim, G., Ricoul, M., and Sabatier, L. (2014). "Telomere", in: *Encyclopedia of Pathology.* (ed.) H.V. Krieken. Springer-Verlag Berlin Heidelberg).

Friedrich, T., Scholz, U., Durante, M., and Scholz, M. (2014). RBE of ion beams in hypofractionated radiotherapy (SBRT). *Phys Med* 30**,** 588-591. doi: 10.1016/j.ejmp.2014.04.009.

Fumagalli, M., Rossiello, F., Clerici, M., Barozzi, S., Cittaro, D., Kaplunov, J.M., Bucci, G., Dobreva, M., Matti, V., Beausejour, C.M., Herbig, U., Longhese, M.P., and D'adda Di Fagagna, F. (2012). Telomeric DNA damage is irreparable and causes persistent DNA-damage-response activation. *Nat Cell Biol* 14**,** 355-365. doi: 10.1038/ncb2466.

Fumagalli, M., Rossiello, F., Mondello, C., and D'adda Di Fagagna, F. (2014). Stable cellular senescence is associated with persistent DDR activation. *PLoS One* 9**,** e110969. doi: 10.1371/journal.pone.0110969.

Garcia, O., Di Giorgio, M., Vallerga, M.B., Radl, A., Taja, M.R., Seoane, A., De Luca, J., Stuck Oliveira, M., Valdivia, P., Lamadrid, A.I., Gonzalez, J.E., Romero, I., Mandina, T., Pantelias, G., Terzoudi, G., Guerrero-Carbajal, C., Arceo Maldonado, C., Espinoza, M., Oliveros, N., Martinez-Lopez, W., Di Tomaso, M.V., Mendez-Acuna, L., Puig, R., Roy, L., and Barquinero, J.F. (2013). Interlaboratory comparison of dicentric chromosome assay using electronically transmitted images. *Radiat Prot Dosimetry* 154**,** 18-25. doi: 10.1093/rpd/ncs139.

Garcia, O.F., Ramalho, A.T., Di Giorgio, M., Mir, S.S., Espinoza, M.E., Manzano, J., Nasazzi, N., and Lopez, I. (1995). Intercomparison in cytogenetic dosimetry among five laboratories from Latin America. *Mutat Res* 327**,** 33-39.

Garty, G., Bigelow, A.W., Repin, M., Turner, H.C., Bian, D., Balajee, A.S., Lyulko, O.V., Taveras, M., Yao, Y.L., and Brenner, D.J. (2015). An automated imaging system for radiation biodosimetry. *Microsc Res Tech* 78**,** 587-598. doi: 10.1002/jemt.22512.

Garty, G., Chen, Y., Salerno, A., Turner, H., Zhang, J., Lyulko, O., Bertucci, A., Xu, Y., Wang, H., Simaan, N., Randers-Pehrson, G., Yao, Y.L., Amundson, S.A., and Brenner, D.J. (2010). The RABIT: a rapid automated biodosimetry tool for radiological triage. *Health Phys* 98**,** 209-217. doi: 10.1097/HP.0b013e3181ab3cb6.

Genesca, A., Martin, M., Latre, L., Soler, D., Pampalona, J., and Tusell, L. (2006). Telomere dysfunction: a new player in radiation sensitivity. *Bioessays* 28**,** 1172-1180. doi: 10.1002/bies.20501.

Gilson, E., and Londono-Vallejo, A. (2007). Telomere length profiles in humans: all ends are not equal. *Cell Cycle* 6**,** 2486-2494.

Girinsky, T., M'kacher, R., Lessard, N., Koscielny, S., Elfassy, E., Raoux, F., Carde, P., Santos, M.D., Margainaud, J.P., Sabatier, L., Ghalibafian, M., and Paul, J.F. (2014). Prospective coronary heart disease screening in asymptomatic Hodgkin lymphoma patients using coronary computed tomography angiography: results and risk factor analysis. *Int J Radiat Oncol Biol Phys* 89**,** 59-66. doi: 10.1016/j.ijrobp.2014.01.021.

Gonzalez, J.E., Romero, I., Gregoire, E., Martin, C., Lamadrid, A.I., Voisin, P., Barquinero, J.F., and Garcia, O. (2014). Biodosimetry estimation using the ratio of the longest:shortest length in the premature chromosome condensation (PCC) method applying autocapture and automatic image analysis. *J Radiat Res* 55**,** 862-865. doi: 10.1093/jrr/rru030.

Goodhead, D.T. (1994). Initial events in the cellular effects of ionizing radiations: clustered damage in DNA. *Int J Radiat Biol* 65**,** 7-17.

Gotoh, E., and Tanno, Y. (2005). Simple biodosimetry method for cases of high-dose radiation exposure using the ratio of the longest/shortest length of Giemsa-stained drug-induced prematurely condensed chromosomes (PCC). *Int J Radiat Biol* 81**,** 379-385. doi: 10.1080/09553000500147667.

Gotoh, E., Tanno, Y., and Takakura, K. (2005). Simple biodosimetry method for use in cases of high-dose radiation exposure that scores the chromosome number of Giemsa-stained drug-induced prematurely condensed chromosomes (PCC). *Int J Radiat Biol* 81**,** 33-40.

Graakjaer, J., Bischoff, C., Korsholm, L., Holstebroe, S., Vach, W., Bohr, V.A., Christensen, K., and Kolvraa, S. (2003). The pattern of chromosome-specific variations in telomere length in humans is determined by inherited, telomere-near factors and is maintained throughout life. *Mech Ageing Dev* 124**,** 629-640.

Granzotto, A., Joubert, A., Viau, M., Devic, C., Maalouf, M., Thomas, C., Vogin, G., Malek, K., Colin, C., Balosso, J., and Foray, N. (2011). [Individual response to ionising radiation: What predictive assay(s) to choose?]. *C R Biol* 334**,** 140-157. doi: 10.1016/j.crvi.2010.12.018.

Greider, C.W., and Blackburn, E.H. (1985). Identification of a specific telomere terminal transferase activity in Tetrahymena extracts. *Cell* 43**,** 405-413.

Greider, C.W., and Blackburn, E.H. (1987). The telomere terminal transferase of Tetrahymena is a ribonucleoprotein enzyme with two kinds of primer specificity. *Cell* 51**,** 887-898.

Griffith, J.D., Comeau, L., Rosenfield, S., Stansel, R.M., Bianchi, A., Moss, H., and De Lange, T. (1999). Mammalian telomeres end in a large duplex loop. *Cell* 97**,** 503-514. doi: S0092-8674(00)80760-6 [pii].

Gruel, G., Gregoire, E., Lecas, S., Martin, C., Roch-Lefevre, S., Vaurijoux, A., Voisin, P., Voisin, P., and Barquinero, J.F. (2013). Biological dosimetry by automated dicentric scoring in a simulated emergency. *Radiat Res* 179**,** 557-569. doi: 10.1667/RR3196.1.

Guan, J.Z., Guan, W.P., Maeda, T., and Makino, N. (2014). Changes in telomere length distribution in low-dose X-ray-irradiated human umbilical vein endothelial cells. *Mol Cell Biochem* 396**,** 129-135. doi: 10.1007/s11010-014-2149-5.

Guo, Z., Shu, Y., Zhou, H., Zhang, W., and Wang, H. (2015). Radiogenomics helps to achieve personalized therapy by evaluating patient responses to radiation treatment. *Carcinogenesis* 36**,** 307-317. doi: 10.1093/carcin/bgv007.

Hall, E.J. (1984). *Radiation and life.* New York: Pergamon.

Hall, E.J. (2006). *Radiobiology for the radiologist.* Philadelphia: Lippincott Williams & Wilkins.

Hamasaki, K., Imai, K., Nakachi, K., Takahashi, N., Kodama, Y., and Kusunoki, Y. (2007). Short-term culture and gammaH2AX flow cytometry determine differences in individual radiosensitivity in human peripheral T lymphocytes. *Environ Mol Mutagen* 48**,** 38-47. doi: 10.1002/em.20273.

Hanahan, D., and Weinberg, R.A. (2011). Hallmarks of cancer: the next generation. *Cell* 144**,** 646-674. doi: 10.1016/j.cell.2011.02.013.

Harley, C.B. (1991). Telomere loss: mitotic clock or genetic time bomb? *Mutat Res* 256**,** 271-282.

Harley, C.B., Futcher, A.B., and Greider, C.W. (1990). Telomeres shorten during ageing of human fibroblasts. *Nature* 345**,** 458-460. doi: 10.1038/345458a0.

Hartel, C., Nikoghosyan, A., Durante, M., Sommer, S., Nasonova, E., Fournier, C., Lee, R., Debus, J., Schulz-Ertner, D., and Ritter, S. (2010). Chromosomal aberrations in peripheral blood lymphocytes of prostate cancer patients treated with IMRT and carbon ions. *Radiother Oncol* 95**,** 73-78. doi: 10.1016/j.radonc.2009.08.031.

Hatch, E.M., and Hetzer, M.W. (2015). Chromothripsis. *Curr Biol* 25**,** R397-399. doi: 10.1016/j.cub.2015.02.033.

Hayflick, L., and Moorhead, P.S. (1961). The serial cultivation of human diploid cell strains. *Exp Cell Res* 25**,** 585-621.

Hei, T.K., Zhou, H., Chai, Y., Ponnaiya, B., and Ivanov, V.N. (2011). Radiation induced non-targeted response: mechanism and potential clinical implications. *Curr Mol Pharmacol* 4**,** 96-105.

Henle, E.S., Han, Z., Tang, N., Rai, P., Luo, Y., and Linn, S. (1999). Sequence-specific DNA cleavage by Fe2+-mediated fenton reactions has possible biological implications. *J Biol Chem* 274**,** 962-971.

Hernandez, L., Terradas, M., Camps, J., Martin, M., Tusell, L., and Genesca, A. (2015). Aging and radiation: bad companions. *Aging Cell* 14**,** 153-161. doi: 10.1111/acel.12306.

Ho, A.Y., Atencio, D.P., Peters, S., Stock, R.G., Formenti, S.C., Cesaretti, J.A., Green, S., Haffty, B., Drumea, K., Leitzin, L., Kuten, A., Azria, D., Ozsahin, M., Overgaard, J., Andreassen, C.N., Trop, C.S., Park, J., and Rosenstein, B.S. (2006). Genetic predictors of adverse radiotherapy effects: the Gene-PARE project. *Int J Radiat Oncol Biol Phys* 65**,** 646-655. doi: 10.1016/j.ijrobp.2006.03.006.

Holland, A.J., and Cleveland, D.W. (2012). Chromoanagenesis and cancer: mechanisms and consequences of localized, complex chromosomal rearrangements. *Nat Med* 18**,** 1630-1638. doi: 10.1038/nm.2988.

Holohan, B., Wright, W.E., and Shay, J.W. (2014). Cell biology of disease: Telomeropathies: an emerging spectrum disorder. *J Cell Biol* 205**,** 289-299. doi: 10.1083/jcb.201401012.

Horn, S., Barnard, S., and Rothkamm, K. (2011). Gamma-H2AX-based dose estimation for whole and partial body radiation exposure. *PLoS One* 6**,** e25113. doi: 10.1371/journal.pone.0025113.

Hou, Y.N., Lavaf, A., Huang, D., Peters, S., Huq, R., Friedrich, V., Rosenstein, B.S., and Kao, J. (2009). Development of an automated gamma-H2AX immunocytochemistry assay. *Radiat Res* 171**,** 360-367. doi: 10.1667/RR1349.1.

Houtgraaf, J.H., Versmissen, J., and Van Der Giessen, W.J. (2006). A concise review of DNA damage checkpoints and repair in mammalian cells. *Cardiovasc Revasc Med* 7**,** 165-172. doi: 10.1016/j.carrev.2006.02.002.

Hu, S., Blakely, W.F., and Cucinotta, F.A. (2015). HEMODOSE: A Biodosimetry Tool Based on Multi-type Blood Cell Counts. *Health Phys* 109**,** 54-68. doi: 10.1097/HP.0000000000000295.

Huppert, J.L. (2008). Hunting G-quadruplexes. *Biochimie* 90**,** 1140-1148. doi: 10.1016/j.biochi.2008.01.014.

IAEA (2002). "Preparedness and response for a nuclear or radiological emergency", in: *IAEA Safety Standards Series* (Vienna: International Atomic Energy Agency).

IAEA (2011). "Cytogenetic dosimetry: Applications in preparedness for and response to radiation emergencies", in: *Emergency Preparedness and Response Series.* (Vienna).

ICRP (2007). "The 2007 Recommendations of the International Commission on Radiological Protection", in: *ICRP Publication 103.*).

Il'yasova, D., Kinev, A., Melton, C.D., and Davis, F.G. (2014). Donor-specific cell-based assays in studying sensitivity to low-dose radiation: a population-based perspective. *Front Public Health* 2**,** 244. doi: 10.3389/fpubh.2014.00244.

Ilnytskyy, Y., and Kovalchuk, O. (2011). Non-targeted radiation effects-an epigenetic connection. *Mutat Res* 714**,** 113-125. doi: 10.1016/j.mrfmmm.2011.06.014.

Ismail, I.H., Wadhra, T.I., and Hammarsten, O. (2007). An optimized method for detecting gamma-H2AX in blood cells reveals a significant interindividual variation in the gamma-H2AX response among humans. *Nucleic Acids Res* 35**,** e36. doi: 10.1093/nar/gkl1169.

ISO (2008). "Radiation protection - Performance criteria for service laboratories performing cytogenetic triage for assessment of mass casualties in radiological or nuclear emergencies -- General principles and application to dicentric assay". (Geneva: International Organization for Standardization).

ISO (2014a). "Radiation protection - Performance criteria for service laboratories performing biological dosimetry by cytogenetics". (Geneva: International Organization for Standardization).

ISO (2014b). "Radiological protection -- Performance criteria for laboratories using the cytokinesis block micronucleus (CBMN) assay in peripheral blood lymphocytes for biological dosimetry". (Geneva: International Organization for Standardization).

Iwakawa, M., Imai, T., Harada, Y., Ban, S., Michikawa, Y., Saegusa, K., Sagara, M., Tsuji, A., Noda, S., and Ishikawa, A. (2002). [RadGenomics project]. *Nihon Igaku Hoshasen Gakkai Zasshi* 62**,** 484-489.

Iyer, R., and Lehnert, B.E. (2002). Low dose, low-LET ionizing radiation-induced radioadaptation and associated early responses in unirradiated cells. *Mutat Res* 503**,** 1-9.

Jackson, S.P., and Bartek, J. (2009). The DNA-damage response in human biology and disease. *Nature* 461**,** 1071-1078. doi: 10.1038/nature08467.

Jaworska, A., Ainsbury, E.A., Fattibene, P., Lindholm, C., Oestreicher, U., Rothkamm, K., Romm, H., Thierens, H., Trompier, F., Voisin, P., Vral, A., Woda, C., and Wojcik, A. (2015). Operational guidance for radiation emergency response organisations in Europe for using biodosimetric tools developed in EU MULTIBIODOSE project. *Radiat Prot Dosimetry* 164**,** 165-169. doi: 10.1093/rpd/ncu294.

Jaworska, A., Wojcik, A., Ainsbury, E.A., Fattibene, P., Lindholm, C., Oestreicher, U., Rothkamm, K., Romm, H., Thierens, H., Trompier, F., Voisin, P., Vral, A., and Woda, C. (2013). "Guidance for using MULTIBIODOSE Tools in Emergencies". (Oslo: MULTIBIODOSE consortium).

Jermann, M. (2014). Particle Therapy Statistics in 2013. *International Journal of Particle Therapy* 1**,** 40-43. doi: 10.14338/IJPT.14-editorial-2.1.

Johnston, M.L., Young, E.F., and Shepard, K.L. (2015). Whole-blood immunoassay for gammaH2AX as a radiation biodosimetry assay with minimal sample preparation. *Radiat Environ Biophys* 54**,** 365-372. doi: 10.1007/s00411-015-0595-4.

Jones, M.J., and Jallepalli, P.V. (2012). Chromothripsis: chromosomes in crisis. *Dev Cell* 23**,** 908-917. doi: 10.1016/j.devcel.2012.10.010.

Joubert, A., and Foray, N. (2007). [Intrinsic radiosensitivity and DNA double-strand breaks in human cells]. *Cancer Radiother* 11**,** 129-142. doi: 10.1016/j.canrad.2007.01.003.

Joubert, A., Vogin, G., Devic, C., Granzotto, A., Viau, M., Maalouf, M., Thomas, C., Colin, C., and Foray, N. (2011). [Radiation biology: major advances and perspectives for radiotherapy]. *Cancer Radiother* 15**,** 348-354. doi: 10.1016/j.canrad.2011.05.001.

Joubert, A., Zimmerman, K.M., Bencokova, Z., Gastaldo, J., Chavaudra, N., Favaudon, V., Arlett, C.F., and Foray, N. (2008). DNA double-strand break repair defects in syndromes associated with acute radiation response: at least two different assays to predict intrinsic radiosensitivity? *Int J Radiat Biol* 84**,** 107-125. doi: 10.1080/09553000701797039.

Journy, N., Laurier, D., and Bernier, M.O. (2015a). Comment on: Are the studies on cancer risk from CT scans biased by indication? Elements of answer from a large-scale cohort study in France. *Br J Cancer* 112**,** 1843-1844. doi: 10.1038/bjc.2015.105.

Journy, N., Rehel, J.L., Ducou Le Pointe, H., Lee, C., Brisse, H., Chateil, J.F., Caer-Lorho, S., Laurier, D., and Bernier, M.O. (2015b). Are the studies on cancer risk from CT scans biased by indication? Elements of answer from a large-scale cohort study in France. *Br J Cancer* 112**,** 185-193. doi: 10.1038/bjc.2014.526.

Kacprzak, J., Kuszewski, T., Lankoff, A., Muller, W.U., Wojcik, A., and Lisowska, H. (2013). Individual variations in the micronucleus assay for biological dosimetry after high dose exposure. *Mutat Res* 756**,** 196-200. doi: 10.1016/j.mrgentox.2013.04.017.

Kadhim, M.A., Hill, M.A., and Moore, S.R. (2006). Genomic instability and the role of radiation quality. *Radiat Prot Dosimetry* 122**,** 221-227. doi: 10.1093/rpd/ncl445.

Kamada, T., Tsujii, H., Blakely, E.A., Debus, J., De Neve, W., Durante, M., Jakel, O., Mayer, R., Orecchia, R., Potter, R., Vatnitsky, S., and Chu, W.T. (2015). Carbon ion radiotherapy in Japan: an assessment of 20 years of clinical experience. *Lancet Oncol* 16**,** e93-e100. doi: 10.1016/S1470-2045(14)70412-7.

Kanda, R., Hayata, I., and Lloyd, D.C. (1999). Easy biodosimetry for high-dose radiation exposures using drug-induced, prematurely condensed chromosomes. *Int J Radiat Biol* 75**,** 441-446.

Kaul, Z., Cesare, A.J., Huschtscha, L.I., Neumann, A.A., and Reddel, R.R. (2012). Five dysfunctional telomeres predict onset of senescence in human cells. *EMBO Rep* 13**,** 52-59. doi: 10.1038/embor.2011.227.

Kerns, S.L., De Ruysscher, D., Andreassen, C.N., Azria, D., Barnett, G.C., Chang-Claude, J., Davidson, S., Deasy, J.O., Dunning, A.M., Ostrer, H., Rosenstein, B.S., West, C.M., and Bentzen, S.M. (2014a). STROGAR - STrengthening the Reporting Of Genetic Association studies in Radiogenomics. *Radiother Oncol* 110**,** 182-188. doi: 10.1016/j.radonc.2013.07.011.

Kerns, S.L., Ostrer, H., and Rosenstein, B.S. (2014b). Radiogenomics: using genetics to identify cancer patients at risk for development of adverse effects following radiotherapy. *Cancer Discov* 4**,** 155-165. doi: 10.1158/2159-8290.CD-13-0197.

Khvostunov, I.K., Ivannikov, A.I., Skvortsov, V.G., Nugis, V.Y., and Golub, E.V. (2015). Review of the correlation between results of cytogenetic dosimetry from blood lymphocytes and EPR dosimetry from tooth enamel for victims of radiation accidents. *Radiat Prot Dosimetry* 163**,** 399-408. doi: 10.1093/rpd/ncu203.

Kloosterman, W.P., Guryev, V., Van Roosmalen, M., Duran, K.J., De Bruijn, E., Bakker, S.C., Letteboer, T., Van Nesselrooij, B., Hochstenbach, R., Poot, M., and Cuppen, E. (2011). Chromothripsis as a mechanism driving complex de novo structural rearrangements in the germline. *Hum Mol Genet* 20**,** 1916-1924. doi: 10.1093/hmg/ddr073.

Kloosterman, W.P., Koster, J., and Molenaar, J.J. (2014). Prevalence and clinical implications of chromothripsis in cancer genomes. *Curr Opin Oncol* 26**,** 64-72. doi: 10.1097/CCO.0000000000000038.

Komarova, E.A., Diatchenko, L., Rokhlin, O.W., Hill, J.E., Wang, Z.J., Krivokrysenko, V.I., Feinstein, E., and Gudkov, A.V. (1998). Stress-induced secretion of growth inhibitors: a novel tumor suppressor function of p53. *Oncogene* 17**,** 1089-1096. doi: 10.1038/sj.onc.1202303.

Komarova, N.L., and Wodarz, D. (2004). The optimal rate of chromosome loss for the inactivation of tumor suppressor genes in cancer. *Proc Natl Acad Sci U S A* 101**,** 7017-7021. doi: 10.1073/pnas.0401943101.

Kulka, U., Ainsbury, L., Atkinson, M., Barnard, S., Smith, R., Barquinero, J.F., Barrios, L., Bassinet, C., Beinke, C., Cucu, A., Darroudi, F., Fattibene, P., Bortolin, E., Monaca, S.D., Gil, O., Gregoire, E., Hadjidekova, V., Haghdoost, S., Hatzi, V., Hempel, W., Herranz, R., Jaworska, A., Lindholm, C., Lumniczky, K., M'kacher, R., Mortl, S., Montoro, A., Moquet, J., Moreno, M., Noditi, M., Ogbazghi, A., Oestreicher, U., Palitti, F., Pantelias, G., Popescu, I., Prieto, M.J., Roch-Lefevre, S., Roessler, U., Romm, H., Rothkamm, K., Sabatier, L., Sebastia, N., Sommer, S., Terzoudi, G., Testa, A., Thierens, H., Trompier, F., Turai, I., Vandevoorde, C., Vaz, P., Voisin, P., Vral, A., Ugletveit, F., Wieser, A., Woda, C., and Wojcik, A. (2015). Realising the European network of biodosimetry: RENEB-status quo. *Radiat Prot Dosimetry* 164**,** 42-45. doi: 10.1093/rpd/ncu266.

Kulka, U., Ainsbury, L., Atkinson, M., Barquinero, J.F., Barrios, L., Beinke, C., Bognar, G., Cucu, A., Darroudi, F., Fattibene, P., Gil, O., Gregoire, E., Hadjidekova, V., Haghdoost, S., Herranz, R., Jaworska, A., Lindholm, C., Mkacher, R., Mortl, S., Montoro, A., Moquet, J., Moreno, M., Ogbazghi, A., Oestreicher, U., Palitti, F., Pantelias, G., Popescu, I., Prieto, M.J., Romm, H., Rothkamm, K., Sabatier, L., Sommer, S., Terzoudi, G., Testa, A., Thierens, H., Trompier, F., Turai, I., Vandersickel, V., Vaz, P., Voisin, P., Vral, A., Ugletveit, F., Woda, C., and Wojcik, A. (2012). Realising the European Network of Biodosimetry (RENEB). *Radiat Prot Dosimetry* 151**,** 621-625. doi: 10.1093/rpd/ncs157.

Lacombe, J., Riou, O., Solassol, J., Mange, A., Bourgier, C., Fenoglietto, P., Pelegrin, A., Ozsahin, M., and Azria, D. (2013). [Intrinsic radiosensitivity: predictive assays that will change daily practice]. *Cancer Radiother* 17**,** 337-343. doi: 10.1016/j.canrad.2013.07.137.

Lamadrid Boada, A.I., Romero Aguilera, I., Terzoudi, G.I., Gonzalez Mesa, J.E., Pantelias, G., and Garcia, O. (2013). Rapid assessment of high-dose radiation exposures through scoring of cell-fusion-induced premature chromosome condensation and ring chromosomes. *Mutat Res* 757**,** 45-51. doi: 10.1016/j.mrgentox.2013.06.021.

Lapham, K., Kvale, M.N., Lin, J., Connell, S., Croen, L.A., Dispensa, B.P., Fang, L., Hesselson, S., Hoffmann, T.J., Iribarren, C., Jorgenson, E., Kushi, L.H., Ludwig, D., Matsuguchi, T., Mcguire, W.B., Miles, S., Quesenberry, C.P., Jr., Rowell, S., Sadler, M., Sakoda, L.C., Smethurst, D., Somkin, C.P., Van Den Eeden, S.K., Walter, L., Whitmer, R.A., Kwok, P.Y., Risch, N., Schaefer, C., and Blackburn, E.H. (2015). Automated Assay of Telomere Length Measurement and Informatics for 100,000

Subjects in the Genetic Epidemiology Research on Adult Health and Aging (GERA) Cohort. *Genetics* 200**,** 1061-1072. doi: 10.1534/genetics.115.178624.

Larrea, A.A., Lujan, S.A., and Kunkel, T.A. (2010). SnapShot: DNA mismatch repair. *Cell* 141**,** 730 e731. doi: 10.1016/j.cell.2010.05.002.

Lieber, M.R. (2008). The mechanism of human nonhomologous DNA end joining. *J Biol Chem* 283**,** 1-5. doi: 10.1074/jbc.R700039200.

Lin, J., Epel, E., and Blackburn, E. (2012). Telomeres and lifestyle factors: roles in cellular aging. *Mutat Res* 730**,** 85-89. doi: 10.1016/j.mrfmmm.2011.08.003.

Lipps, H.J., and Rhodes, D. (2009). G-quadruplex structures: in vivo evidence and function. *Trends Cell Biol* 19**,** 414-422. doi: 10.1016/j.tcb.2009.05.002.

Lisowska, H., Wegierek-Ciuk, A., Banasik-Nowak, A., Braziewicz, J., Wojewodzka, M., Wojcik, A., and Lankoff, A. (2013). The dose-response relationship for dicentric chromosomes and gamma-H2AX foci in human peripheral blood lymphocytes: influence of temperature during exposure and intra- and inter-individual variability of donors. *Int J Radiat Biol* 89**,** 191-199. doi: 10.3109/09553002.2013.741284.

Little, J.B. (2003). Genomic instability and bystander effects: a historical perspective. *Oncogene* 22**,** 6978-6987. doi: 10.1038/sj.onc.1206988.

Little, M.P., Tawn, E.J., Tzoulaki, I., Wakeford, R., Hildebrandt, G., Paris, F., Tapio, S., and Elliott, P. (2008). A systematic review of epidemiological associations between low and moderate doses of ionizing radiation and late cardiovascular effects, and their possible mechanisms. *Radiat Res* 169**,** 99-109. doi: 10.1667/RR1070.1.

Litvinchuk, A.V., Vachelova, J., Michaelidesova, A., Wagner, R., and Davidkova, M. (2015). Dose-dependent micronuclei formation in normal human fibroblasts exposed to proton radiation. *Radiat Environ Biophys* 54**,** 327-334. doi: 10.1007/s00411-015-0598-1.

Liu, P., Erez, A., Nagamani, S.C., Dhar, S.U., Kolodziejska, K.E., Dharmadhikari, A.V., Cooper, M.L., Wiszniewska, J., Zhang, F., Withers, M.A., Bacino, C.A., Campos-Acevedo, L.D., Delgado, M.R., Freedenberg, D., Garnica, A., Grebe, T.A., Hernandez-Almaguer, D., Immken, L., Lalani, S.R., Mclean, S.D., Northrup, H., Scaglia, F., Strathearn, L., Trapane, P., Kang, S.H., Patel, A., Cheung, S.W., Hastings, P.J., Stankiewicz, P., Lupski, J.R., and Bi, W. (2011). Chromosome catastrophes involve replication mechanisms generating complex genomic rearrangements. *Cell* 146**,** 889-903. doi: 10.1016/j.cell.2011.07.042.

Livingston, G.K., Wilkins, R.C., and Ainsbury, E.A. (2011). Pilot website to support international collaboration for dose assessments in a radiation emergency. *Radiation Measurements* 46**,** 912-915. doi: 10.1016/j.radmeas.2011.04.006.

Lloyd, D.C., Edwards, A.A., Moquet, J.E., and Guerrero-Carbajal, Y.C. (2000). The role of cytogenetics in early triage of radiation casualties. *Appl Radiat Isot* 52**,** 1107-1112.

Lopez, M., and Martin, M. (2011). Medical management of the acute radiation syndrome. *Rep Pract Oncol Radiother* 16**,** 138-146. doi: 10.1016/j.rpor.2011.05.001.

Loucas, B.D., and Cornforth, M.N. (2001). Complex chromosome exchanges induced by gamma rays in human lymphocytes: an mFISH study. *Radiat Res* 155**,** 660-671.

Loucas, B.D., Durante, M., Bailey, S.M., and Cornforth, M.N. (2013). Chromosome damage in human cells by gamma rays, alpha particles and heavy ions: track interactions in basic dose-response relationships. *Radiat Res* 179**,** 9-20. doi: 10.1667/RR3089.1.

M'kacher, R., El Maalouf, E., Terzoudi, G., Ricoul, M., Heidingsfelder, L., Karachristou, I., Laplagne, E., Hempel, W.M., Colicchio, B., Dieterlen, A., Pantelias, G., and Sabatier, L. (2015a). Detection and automated scoring of dicentric chromosomes in nonstimulated lymphocyte prematurely condensed chromosomes after telomere and centromere staining. *Int J Radiat Oncol Biol Phys* 91**,** 640-649. doi: 10.1016/j.ijrobp.2014.10.048.

M'kacher, R., Girinsky, T., Colicchio, B., Ricoul, M., Dieterlen, A., Jeandidier, E., Heidingsfelder, L., Cuceu, C., Shim, G., Frenzel, M., Lenain, A., Morat, L., Bourhis, J., Hempel, W.M., Koscielny, S., Paul, J.F., Carde, P., and Sabatier, L. (2015b). Telomere shortening: a new prognostic factor for cardiovascular disease post-radiation exposure. *Radiat Prot Dosimetry* 164**,** 134-137. doi: 10.1093/rpd/ncu296.

M'kacher, R., Maalouf, E.E., Ricoul, M., Heidingsfelder, L., Laplagne, E., Cuceu, C., Hempel, W.M., Colicchio, B., Dieterlen, A., and Sabatier, L. (2014). New tool for biological dosimetry: reevaluation and automation of the gold standard method following telomere and centromere staining. *Mutat Res* 770**,** 45-53. doi: 10.1016/j.mrfmmm.2014.09.007.

Macia, I.G.M., Lucas Calduch, A., and Lopez, E.C. (2011). Radiobiology of the acute radiation syndrome. *Rep Pract Oncol Radiother* 16**,** 123-130. doi: 10.1016/j.rpor.2011.06.001.

Macphail, S.H., Banath, J.P., Yu, T.Y., Chu, E.H., Lambur, H., and Olive, P.L. (2003). Expression of phosphorylated histone H2AX in cultured cell lines following exposure to X-rays. *Int J Radiat Biol* 79**,** 351-358.

Maeda, T., Nakamura, K., Atsumi, K., Hirakawa, M., Ueda, Y., and Makino, N. (2013). Radiation-associated changes in the length of telomeres in peripheral leukocytes from inpatients with cancer. *Int J Radiat Biol* 89**,** 106-109. doi: 10.3109/09553002.2013.734945.

Mancuso, M., Pasquali, E., Giardullo, P., Leonardi, S., Tanori, M., Di Majo, V., Pazzaglia, S., and Saran, A. (2012). The radiation bystander effect and its potential implications for human health. *Curr Mol Med* 12**,** 613-624.

Manning, G., and Rothkamm, K. (2013). Deoxyribonucleic acid damage-associated biomarkers of ionising radiation: current status and future relevance for radiology and radiotherapy. *Br J Radiol* 86**,** 20130173. doi: 10.1259/bjr.20130173.

Martins, M.B., Sabatier, L., Ricoul, M., Pinton, A., and Dutrillaux, B. (1993). Specific chromosome instability induced by heavy ions: a step towards transformation of human fibroblasts? *Mutat Res* 285**,** 229-237. doi: 0027-5107(93)90111-R [pii].

Massard, C., Zermati, Y., Pauleau, A.L., Larochette, N., Metivier, D., Sabatier, L., Kroemer, G., and Soria, J.C. (2006). hTERT: a novel endogenous inhibitor of the mitochondrial cell death pathway. *Oncogene* 25**,** 4505-4514. doi: 10.1038/sj.onc.1209487.

Maznyk, N.A., Wilkins, R.C., Carr, Z., and Lloyd, D.C. (2012). The capacity, capabilities and needs of the WHO BioDoseNet member laboratories. *Radiat Prot Dosimetry* 151**,** 611-620. doi: 10.1093/rpd/ncs156.

Mcnamee, J.P., Flegal, F.N., Greene, H.B., Marro, L., and Wilkins, R.C. (2009). Validation of the cytokinesis-block micronucleus (CBMN) assay for use as a triage biological dosimetry tool. *Radiat Prot Dosimetry* 135**,** 232-242. doi: 10.1093/rpd/ncp119.

Meyerson, M., and Pellman, D. (2011). Cancer genomes evolve by pulverizing single chromosomes. *Cell* 144**,** 9-10. doi: 10.1016/j.cell.2010.12.025.

Mirjolet, C., Boidot, R., Saliques, S., Ghiringhelli, F., Maingon, P., and Crehange, G. (2015). The role of telomeres in predicting individual radiosensitivity of patients with cancer in the era of personalized radiotherapy. *Cancer Treat Rev* 41**,** 354-360. doi: 10.1016/j.ctrv.2015.02.005.

Miura, T., Nakata, A., Kasai, K., Nakano, M., Abe, Y., Tsushima, E., Ossetrova, N.I., Yoshida, M.A., and Blakely, W.F. (2014). A novel parameter, cell-cycle progression index, for radiation dose absorbed estimation in the premature chromosome condensation assay. *Radiat Prot Dosimetry* 159**,** 52-60. doi: 10.1093/rpd/ncu126.

Mocellin, S., Pooley, K.A., and Nitti, D. (2013). Telomerase and the search for the end of cancer. *Trends Mol Med* 19**,** 125-133. doi: 10.1016/j.molmed.2012.11.006.

Moquet, J., Barnard, S., and Rothkamm, K. (2014). Gamma-H2AX biodosimetry for use in large scale radiation incidents: comparison of a rapid '96 well lyse/fix' protocol with a routine method. *PeerJ* 2**,** e282. doi: 10.7717/peerj.282.

Morgan, W.F. (2003a). Non-targeted and delayed effects of exposure to ionizing radiation: I. Radiation-induced genomic instability and bystander effects in vitro. *Radiat Res* 159**,** 567-580.

Morgan, W.F. (2003b). Non-targeted and delayed effects of exposure to ionizing radiation: II. Radiation-induced genomic instability and bystander effects in vivo, clastogenic factors and transgenerational effects. *Radiat Res* 159**,** 581-596.

Morgan, W.F., and Bair, W.J. (2013). Issues in low dose radiation biology: the controversy continues. A perspective. *Radiat Res* 179**,** 501-510. doi: 10.1667/RR3306.1.

Morgan, W.F., Hartmann, A., Limoli, C.L., Nagar, S., and Ponnaiya, B. (2002). Bystander effects in radiation-induced genomic instability. *Mutat Res* 504**,** 91-100.

Morgan, W.F., and Sowa, M.B. (2015). Non-targeted effects induced by ionizing radiation: mechanisms and potential impact on radiation induced health effects. *Cancer Lett* 356**,** 17-21. doi: 10.1016/j.canlet.2013.09.009.

Mosse, I.B. (2012). Genetic effects of ionizing radiation--some questions with no answers. *J Environ Radioact* 112**,** 70-75. doi: 10.1016/j.jenvrad.2012.05.009.

Mothersill, C.E., Moriarty, M.J., and Seymour, C.B. (2004). Radiotherapy and the potential exploitation of bystander effects. *Int J Radiat Oncol Biol Phys* 58**,** 575-579.

Muraki, K., Han, L., Miller, D., and Murnane, J.P. (2013). The role of ATM in the deficiency in nonhomologous end-joining near telomeres in a human cancer cell line. *PLoS Genet* 9**,** e1003386. doi: 10.1371/journal.pgen.1003386.

Muraki, K., Han, L., Miller, D., and Murnane, J.P. (2015). Processing by MRE11 is involved in the sensitivity of subtelomeric regions to DNA double-strand breaks. *Nucleic Acids Res*. doi: 10.1093/nar/gkv714.

Muraki, K., Nyhan, K., Han, L., and Murnane, J.P. (2012). Mechanisms of telomere loss and their consequences for chromosome instability. *Front Oncol* 2**,** 135. doi: 10.3389/fonc.2012.00135.

Murnane, J.P. (2012). Telomere dysfunction and chromosome instability. *Mutat Res* 730**,** 28-36. doi: 10.1016/j.mrfmmm.2011.04.008.

Nam, E.A., and Cortez, D. (2011). ATR signalling: more than meeting at the fork. *Biochem J* 436**,** 527-536. doi: 10.1042/BJ20102162.

National Research Council (2006). *Health Risks from Exposure to Low Levels of Ionizing Radiation: BEIR VII Phase 2*. Washington, DC: The National Academies Press.

Nergadze, S.G., Santagostino, M.A., Salzano, A., Mondello, C., and Giulotto, E. (2007). Contribution of telomerase RNA retrotranscription to DNA double-strand break repair during mammalian genome evolution. *Genome Biol* 8**,** R260. doi: 10.1186/gb-2007-8-12-r260.

Newhauser, W.D., and Durante, M. (2011). Assessing the risk of second malignancies after modern radiotherapy. *Nat Rev Cancer* 11**,** 438-448. doi: 10.1038/nrc3069.

Nieri, D., Berardinelli, F., Antoccia, A., Tanzarella, C., and Sgura, A. (2013). Comparison between two FISH techniques in the in vitro study of cytogenetic markers for low-dose X-ray exposure in human primary fibroblasts. *Front Genet* 4**,** 141. doi: 10.3389/fgene.2013.00141.

Nussenzweig, A., and Nussenzweig, M.C. (2007). A backup DNA repair pathway moves to the forefront. *Cell* 131**,** 223-225. doi: 10.1016/j.cell.2007.10.005.

Olaussen, K.A., Dubrana, K., Domont, J., Spano, J.P., Sabatier, L., and Soria, J.C. (2006). Telomeres and telomerase as targets for anticancer drug development. *Crit Rev Oncol Hematol* 57**,** 191-214. doi: 10.1016/j.critrevonc.2005.08.007.

Opresko, P.L., Fan, J., Danzy, S., Wilson, D.M., 3rd, and Bohr, V.A. (2005). Oxidative damage in telomeric DNA disrupts recognition by TRF1 and TRF2. *Nucleic Acids Res* 33**,** 1230-1239. doi: 10.1093/nar/gki273.

Pajic, J., Rakic, B., Rovcanin, B., Jovicic, D., Novakovic, I., Milovanovic, A., and Pajic, V. (2015). Inter-individual variability in the response of human peripheral blood lymphocytes to ionizing radiation: comparison of the dicentric and micronucleus assays. *Radiat Environ Biophys* 54**,** 317-325. doi: 10.1007/s00411-015-0596-3.

Palm, W., and De Lange, T. (2008). How shelterin protects mammalian telomeres. *Annu Rev Genet* 42**,** 301-334. doi: 10.1146/annurev.genet.41.110306.130350.

Panier, S., and Boulton, S.J. (2014). Double-strand break repair: 53BP1 comes into focus. *Nat Rev Mol Cell Biol* 15**,** 7-18. doi: 10.1038/nrm3719.

Park, S.H., and Kang, J.O. (2011). Basics of particle therapy I: physics. *Radiat Oncol J* 29**,** 135-146. doi: 10.3857/roj.2011.29.3.135.

Paulasova, P., and Pellestor, F. (2004). The peptide nucleic acids (PNAs): a new generation of probes for genetic and cytogenetic analyses. *Ann Genet* 47**,** 349-358. doi: 10.1016/j.anngen.2004.07.001.

Pernot, E., Hall, J., Baatout, S., Benotmane, M.A., Blanchardon, E., Bouffler, S., El Saghire, H., Gomolka, M., Guertler, A., Harms-Ringdahl, M., Jeggo, P., Kreuzer, M., Laurier, D., Lindholm, C., Mkacher, R., Quintens, R., Rothkamm, K., Sabatier, L., Tapio, S., De Vathaire, F., and Cardis, E. (2012). Ionizing radiation biomarkers for potential use in epidemiological studies. *Mutat Res* 751**,** 258-286. doi: 10.1016/j.mrrev.2012.05.003.

Petruseva, I.O., Evdokimov, A.N., and Lavrik, O.I. (2014). Molecular mechanism of global genome nucleotide excision repair. *Acta Naturae* 6**,** 23-34.

Pijls-Johannesma, M., Grutters, J.P., Verhaegen, F., Lambin, P., and De Ruysscher, D. (2010). Do we have enough evidence to implement particle therapy as standard treatment in lung cancer? A systematic literature review. *Oncologist* 15**,** 93-103. doi: 10.1634/theoncologist.2009-0116.

Pinto, M.M., Santos, N.F., and Amaral, A. (2010). Current status of biodosimetry based on standard cytogenetic methods. *Radiat Environ Biophys* 49**,** 567-581. doi: 10.1007/s00411-010-0311-3.

Pirzio, L.M., Freulet-Marriere, M.A., Bai, Y., Fouladi, B., Murnane, J.P., Sabatier, L., and Desmaze, C. (2004). Human fibroblasts expressing hTERT show remarkable karyotype stability even after exposure to ionizing radiation. *Cytogenet Genome Res* 104**,** 87-94. doi: 10.1159/000077470.

Plaisancie, J., Kleinfinger, P., Cances, C., Bazin, A., Julia, S., Trost, D., Lohmann, L., and Vigouroux, A. (2014). Constitutional chromoanasynthesis: description of a rare chromosomal event in a patient. *Eur J Med Genet* 57**,** 567-570. doi: 10.1016/j.ejmg.2014.07.004.

Pommier, J.P., Lebeau, J., Ducray, C., and Sabatier, L. (1995). Chromosomal instability and alteration of telomere repeat sequences. *Biochimie* 77**,** 817-825. doi: 0300-9084(96)88201-0 [pii].

Pommier, J.P., and Sabatier, L. (2002). Telomere length distribution. Digital image processing and statistical analysis. *Methods Mol Biol* 191**,** 33-63. doi: 10.1385/1-59259-189-2:33.

Postel-Vinay, S., Vanhecke, E., Olaussen, K.A., Lord, C.J., Ashworth, A., and Soria, J.C. (2012). The potential of exploiting DNA-repair defects for optimizing lung cancer treatment. *Nat Rev Clin Oncol* 9**,** 144-155. doi: 10.1038/nrclinonc.2012.3.

Pottier, G., Viau, M., Ricoul, M., Shim, G., Bellamy, M., Cuceu, C., Hempel, W.M., and Sabatier, L. (2013). Lead Exposure Induces Telomere Instability in Human Cells. *PLoS One* 8**,** e67501. doi: 10.1371/journal.pone.0067501.

Prasanna, P.G., Escalada, N.D., and Blakely, W.F. (2000). Induction of premature chromosome condensation by a phosphatase inhibitor and a protein kinase in unstimulated human peripheral blood lymphocytes: a simple and rapid technique to study chromosome aberrations using specific whole-chromosome DNA hybridization probes for biological dosimetry. *Mutat Res* 466**,** 131-141.

Preston, R.J. (2003). The LNT model is the best we can do--today. *J Radiol Prot* 23**,** 263-268.

Price, L.H., Kao, H.T., Burgers, D.E., Carpenter, L.L., and Tyrka, A.R. (2013). Telomeres and early-life stress: an overview. *Biol Psychiatry* 73**,** 15-23. doi: 10.1016/j.biopsych.2012.06.025.

Prise, K.M., and O'sullivan, J.M. (2009). Radiation-induced bystander signalling in cancer therapy. *Nat Rev Cancer* 9**,** 351-360. doi: 10.1038/nrc2603.

Pujol, M., Barquinero, J.F., Puig, P., Puig, R., Caballin, M.R., and Barrios, L. (2014). A new model of biodosimetry to integrate low and high doses. *PLoS One* 9**,** e114137. doi: 10.1371/journal.pone.0114137.

Rai, R., Zheng, H., He, H., Luo, Y., Multani, A., Carpenter, P.B., and Chang, S. (2010). The function of classical and alternative non-homologous end-joining pathways in the fusion of dysfunctional telomeres. *EMBO J* 29**,** 2598-2610. doi: 10.1038/emboj.2010.142.

Rausch, T., Jones, D.T., Zapatka, M., Stutz, A.M., Zichner, T., Weischenfeldt, J., Jager, N., Remke, M., Shih, D., Northcott, P.A., Pfaff, E., Tica, J., Wang, Q., Massimi, L., Witt, H., Bender, S., Pleier, S., Cin, H., Hawkins, C., Beck, C., Von Deimling, A., Hans, V., Brors, B., Eils, R., Scheurlen, W., Blake, J., Benes, V., Kulozik, A.E., Witt, O., Martin, D., Zhang, C., Porat, R., Merino, D.M., Wasserman, J., Jabado, N., Fontebasso, A., Bullinger, L., Rucker, F.G., Dohner, K., Dohner, H., Koster, J., Molenaar, J.J., Versteeg, R., Kool, M., Tabori, U., Malkin, D., Korshunov, A., Taylor, M.D., Lichter, P., Pfister, S.M., and Korbel, J.O. (2012). Genome sequencing of pediatric medulloblastoma links catastrophic DNA rearrangements with TP53 mutations. *Cell* 148**,** 59-71. doi: 10.1016/j.cell.2011.12.013.

Ray, F.A., Robinson, E., Mckenna, M., Hada, M., George, K., Cucinotta, F., Goodwin, E.H., Bedford, J.S., Bailey, S.M., and Cornforth, M.N. (2014). Directional genomic hybridization: inversions as a potential biodosimeter for retrospective radiation exposure. *Radiat Environ Biophys* 53**,** 255-263. doi: 10.1007/s00411-014-0513-1.

Ray, F.A., Zimmerman, E., Robinson, B., Cornforth, M.N., Bedford, J.S., Goodwin, E.H., and Bailey, S.M. (2013). Directional genomic hybridization for chromosomal inversion discovery and detection. *Chromosome Res* 21**,** 165-174. doi: 10.1007/s10577-013-9345-0.

Raynaud, C.M., Hernandez, J., Llorca, F.P., Nuciforo, P., Mathieu, M.C., Commo, F., Delaloge, S., Sabatier, L., Andre, F., and Soria, J.C. (2010). DNA damage repair and telomere length in normal breast, preneoplastic lesions, and invasive cancer. *Am J Clin Oncol* 33**,** 341-345. doi: 10.1097/COC.0b013e3181b0c4c2.

Raynaud, C.M., Jang, S.J., Nuciforo, P., Lantuejoul, S., Brambilla, E., Mounier, N., Olaussen, K.A., Andre, F., Morat, L., Sabatier, L., and Soria, J.C. (2008a). Telomere shortening is correlated with the DNA damage response and telomeric protein down-regulation in colorectal preneoplastic lesions. *Ann Oncol* 19**,** 1875-1881. doi: 10.1093/annonc/mdn405.

Raynaud, C.M., Mercier, O., Commo, F., Dartevelle, P., Gomez-Roca, C., De Montpreville, V., Sabatier, L., and Soria, J.C. (2009). Telomere length, telomeric proteins and DNA damage repair proteins are differentially expressed between primary lung tumors and their adrenal metastases. *Lung Cancer* 65**,** 144-149. doi: 10.1016/j.lungcan.2008.10.030.

Raynaud, C.M., Sabatier, L., Philipot, O., Olaussen, K.A., and Soria, J.C. (2008b). Telomere length, telomeric proteins and genomic instability during the multistep carcinogenic process. *Crit Rev Oncol Hematol* 66**,** 99-117. doi: 10.1016/j.critrevonc.2007.11.006.

Rea, M.E., Gougelet, R.M., Nicolalde, R.J., Geiling, J.A., and Swartz, H.M. (2010). Proposed triage categories for large-scale radiation incidents using high-accuracy biodosimetry methods. *Health Phys* 98**,** 136-144. doi: 10.1097/HP.0b013e3181b2840b.

Rebuzzini, P., Khoriauli, L., Azzalin, C.M., Magnani, E., Mondello, C., and Giulotto, E. (2005). New mammalian cellular systems to study mutations introduced at the break site by non-homologous end-joining. *DNA Repair (Amst)* 4**,** 546-555. doi: 10.1016/j.dnarep.2004.12.011.

Repin, M., Turner, H.C., Garty, G., and Brenner, D.J. (2014). Next generation platforms for high-throughput biodosimetry. *Radiat Prot Dosimetry* 159**,** 105-110. doi: 10.1093/rpd/ncu161.

Roch-Lefevre, S., Mandina, T., Voisin, P., Gaetan, G., Mesa, J.E., Valente, M., Bonnesoeur, P., Garcia, O., Voisin, P., and Roy, L. (2010). Quantification of gamma-H2AX foci in human lymphocytes: a method for biological dosimetry after ionizing radiation exposure. *Radiat Res* 174**,** 185-194. doi: 10.1667/RR1775.1.

Roch-Lefèvre, S., Valente, M., Voisin, P., and Barquinero, J.F. (2012). *Suitability of the γ-H2AX Assay for Human Radiation Biodosimetry.* InTech.

Rodrigues, M.A., Beaton-Green, L.A., Kutzner, B.C., and Wilkins, R.C. (2014a). Automated analysis of the cytokinesis-block micronucleus assay for radiation biodosimetry using imaging flow cytometry. *Radiat Environ Biophys* 53**,** 273-282. doi: 10.1007/s00411-014-0525-x.

Rodrigues, M.A., Beaton-Green, L.A., Kutzner, B.C., and Wilkins, R.C. (2014b). Multi-parameter dose estimations in radiation biodosimetry using the automated cytokinesis-block micronucleus assay with imaging flow cytometry. *Cytometry A* 85**,** 883-893. doi: 10.1002/cyto.a.22511.

Romero, I., Lamadrid, A.I., Gonzalez, J.E., Garcia, O., Voisin, P., and Roy, L. (2015). Shortening the culture time in cytogenetic dosimetry using PCC-R assay. *Radiat Prot Dosimetry* 163**,** 424-429. doi: 10.1093/rpd/ncu258.

Romm, H., Ainsbury, E., Bajinskis, A., Barnard, S., Barquinero, J.F., Barrios, L., Beinke, C., Puig-Casanovas, R., Deperas-Kaminska, M., Gregoire, E., Oestreicher, U., Lindholm, C., Moquet, J., Rothkamm, K., Sommer, S., Thierens, H., Vral, A., Vandersickel, V., and Wojcik, A. (2014a). Web-based scoring of the dicentric assay, a collaborative biodosimetric scoring strategy for population triage in large scale radiation accidents. *Radiat Environ Biophys* 53**,** 241-254. doi: 10.1007/s00411-014-0519-8.

Romm, H., Ainsbury, E., Barnard, S., Barrios, L., Barquinero, J.F., Beinke, C., Deperas, M., Gregoire, E., Koivistoinen, A., Lindholm, C., Moquet, J., Oestreicher, U., Puig, R., Rothkamm, K., Sommer, S., Thierens, H., Vandersickel, V., Vral, A., and Wojcik, A. (2013a). Automatic scoring of dicentric chromosomes as a tool in large scale radiation accidents. *Mutat Res* 756**,** 174-183. doi: 10.1016/j.mrgentox.2013.05.013.

Romm, H., Ainsbury, E., Barnard, S., Barrios, L., Barquinero, J.F., Beinke, C., Deperas, M., Gregoire, E., Koivistoinen, A., Lindholm, C., Moquet, J., Oestreicher, U., Puig, R., Rothkamm, K., Sommer, S., Thierens, H., Vandersickel, V., Vral, A., and Wojcik, A. (2014b). Validation of semi-automatic scoring of dicentric chromosomes after simulation of three different irradiation scenarios. *Health Phys* 106**,** 764-771. doi: 10.1097/HP.0000000000000077.

Romm, H., Barnard, S., Boulay-Greene, H., De Amicis, A., De Sanctis, S., Franco, M., Herodin, F., Jones, A., Kulka, U., Lista, F., Martigne, P., Moquet, J., Oestreicher, U., Rothkamm, K., Thierens, H., Valente, M., Vandersickel, V., Vral, A., Braselmann, H., Meineke, V., Abend, M., and Beinke, C. (2013b). Laboratory intercomparison of the cytokinesis-block micronucleus assay. *Radiat Res* 180**,** 120-128. doi: 10.1667/RR3234.1.

Romm, H., Wilkins, R.C., Coleman, C.N., Lillis-Hearne, P.K., Pellmar, T.C., Livingston, G.K., Awa, A.A., Jenkins, M.S., Yoshida, M.A., Oestreicher, U., and Prasanna, P.G. (2011). Biological dosimetry by the triage dicentric chromosome assay: potential implications for treatment of acute radiation syndrome in radiological mass casualties. *Radiat Res* 175**,** 397-404. doi: 10.1667/RR2321.1.

Rosenstein, B.S., West, C.M., Bentzen, S.M., Alsner, J., Andreassen, C.N., Azria, D., Barnett, G.C., Baumann, M., Burnet, N., Chang-Claude, J., Chuang, E.Y., Coles, C.E., Dekker, A., De Ruyck, K., De Ruysscher, D., Drumea, K., Dunning, A.M., Easton, D., Eeles, R., Fachal, L., Gutierrez-Enriquez, S., Haustermans, K., Henriquez-Hernandez, L.A., Imai, T., Jones, G.D., Kerns, S.L., Liao, Z., Onel, K., Ostrer, H., Parliament, M., Pharoah, P.D., Rebbeck, T.R., Talbot, C.J., Thierens, H., Vega, A., Witte, J.S., Wong, P., Zenhausern, F., and Radiogenomics, C. (2014). Radiogenomics: radiobiology enters the era of big data and team science. *Int J Radiat Oncol Biol Phys* 89**,** 709-713. doi: 10.1016/j.ijrobp.2014.03.009.

Rossnerova, A., Spatova, M., Schunck, C., and Sram, R.J. (2011). Automated scoring of lymphocyte micronuclei by the MetaSystems Metafer image cytometry system and its application in studies of human mutagen sensitivity and biodosimetry of genotoxin exposure. *Mutagenesis* 26**,** 169-175. doi: 10.1093/mutage/geq057.

Rothkamm, K., Barnard, S., Ainsbury, E.A., Al-Hafidh, J., Barquinero, J.F., Lindholm, C., Moquet, J., Perala, M., Roch-Lefevre, S., Scherthan, H., Thierens, H., Vral, A., and Vandersickel, V. (2013a). Manual versus automated gamma-H2AX foci analysis across five European laboratories: can this assay be used for rapid biodosimetry in a large scale radiation accident? *Mutat Res* 756**,** 170-173. doi: 10.1016/j.mrgentox.2013.04.012.

Rothkamm, K., Beinke, C., Romm, H., Badie, C., Balagurunathan, Y., Barnard, S., Bernard, N., Boulay-Greene, H., Brengues, M., De Amicis, A., De Sanctis, S., Greither, R., Herodin, F., Jones, A., Kabacik, S., Knie, T., Kulka, U., Lista, F., Martigne, P., Missel, A., Moquet, J., Oestreicher, U., Peinnequin, A., Poyot, T., Roessler, U., Scherthan, H., Terbrueggen, B., Thierens, H., Valente, M., Vral, A., Zenhausern, F., Meineke, V., Braselmann, H., and Abend, M. (2013b). Comparison of established and emerging biodosimetry assays. *Radiat Res* 180**,** 111-119. doi: 10.1667/RR3231.1.

Rothkamm, K., and Horn, S. (2009). gamma-H2AX as protein biomarker for radiation exposure. *Ann Ist Super Sanita* 45**,** 265-271.

Rothkamm, K., Horn, S., Scherthan, H., Rossler, U., De Amicis, A., Barnard, S., Kulka, U., Lista, F., Meineke, V., Braselmann, H., Beinke, C., and Abend, M. (2013c). Laboratory intercomparison on the gamma-H2AX foci assay. *Radiat Res* 180**,** 149-155. doi: 10.1667/RR3238.1.

Rothkamm, K., and Lobrich, M. (2003). Evidence for a lack of DNA double-strand break repair in human cells exposed to very low x-ray doses. *Proc Natl Acad Sci U S A* 100**,** 5057-5062.

Ruhm, W., Fantuzzi, E., Harrison, R., Schuhmacher, H., Vanhavere, F., Alves, J., Bottollier Depois, J.F., Fattibene, P., Knezevic, Z., Lopez, M.A., Mayer, S., Miljanic, S., Neumaier, S., Olko, P., Stadtmann, H., Tanner, R., and Woda, C. (2015). Eurados Strategic Research Agenda: Vision for Dosimetry of Ionising Radiation. *Radiat Prot Dosimetry*. doi: 10.1093/rpd/ncv018.

Runge, R., Hiemann, R., Wendisch, M., Kasten-Pisula, U., Storch, K., Zophel, K., Fritz, C., Roggenbuck, D., Wunderlich, G., Conrad, K., and Kotzerke, J. (2012). Fully automated interpretation of ionizing radiation-induced gammaH2AX foci by the novel pattern recognition system AKLIDES(R). *Int J Radiat Biol* 88**,** 439-447. doi: 10.3109/09553002.2012.658468.

Sabatier, L., Al Achkar, W., Hoffschir, F., Luccioni, C., and Dutrillaux, B. (1987). Qualitative study of chromosomal lesions induced by neutrons and neon ions in human lymphocytes at G0 phase. *Mutat Res* 178**,** 91-97. doi: 0027-5107(87)90090-X [pii].

Sabatier, L., Dutrillaux, B., and Martin, M.B. (1992). Chromosomal instability. *Nature* 357**,** 548. doi: 10.1038/357548a0.

Sabatier, L., Lebeau, J., and Dutrillaux, B. (1995). Radiation-induced carcinogenesis: individual sensitivity and genomic instability. *Radiat Environ Biophys* 34**,** 229-232.

Sabatino, L., Picano, E., and Andreassi, M.G. (2012). Telomere shortening and ionizing radiation: a possible role in vascular dysfunction? *Int J Radiat Biol* 88**,** 830-839. doi: 10.3109/09553002.2012.709307.

Sasaki, M.S. (2009). Advances in the biophysical and molecular bases of radiation cytogenetics. *Int J Radiat Biol* 85**,** 26-47. doi: 10.1080/09553000802641185.

Schlaff, C.D., Krauze, A., Belard, A., O'connell, J.J., and Camphausen, K.A. (2014). Bringing the heavy: carbon ion therapy in the radiobiological and clinical context. *Radiat Oncol* 9**,** 88. doi: 10.1186/1748-717X-9-88.

Schmid, T.E., and Multhoff, G. (2012). Non-targeted effects of photon and particle irradiation and the interaction with the immune system. *Front Oncol* 2**,** 80. doi: 10.3389/fonc.2012.00080.

Schmitz, A., Bayer, J., Dechamps, N., Goldin, L., and Thomas, G. (2007). Heritability of susceptibility to ionizing radiation-induced apoptosis of human lymphocyte subpopulations. *Int J Radiat Oncol Biol Phys* 68**,** 1169-1177. doi: 10.1016/j.ijrobp.2007.03.050.

Schmitz, A., Bayer, J., Dechamps, N., and Thomas, G. (2003). Intrinsic susceptibility to radiation-induced apoptosis of human lymphocyte subpopulations. *Int J Radiat Oncol Biol Phys* 57**,** 769-778.

Schultz-Hector, S., and Trott, K.R. (2007). Radiation-induced cardiovascular diseases: is the epidemiologic evidence compatible with the radiobiologic data? *Int J Radiat Oncol Biol Phys* 67**,** 10-18. doi: 10.1016/j.ijrobp.2006.08.071.

Scully, R., and Xie, A. (2013). Double strand break repair functions of histone H2AX. *Mutat Res* 750**,** 5-14. doi: 10.1016/j.mrfmmm.2013.07.007.

Seymour, C.B., and Mothersill, C. (1997). Delayed expression of lethal mutations and genomic instability in the progeny of human epithelial cells that survived in a bystander-killing environment. *Radiat Oncol Investig* 5**,** 106-110. doi: 10.1002/(SICI)1520-6823(1997)5:3<106::AID-ROI4>3.0.CO;2-1.

Sfeir, A., and De Lange, T. (2012). Removal of shelterin reveals the telomere end-protection problem. *Science* 336**,** 593-597. doi: 10.1126/science.1218498.

Shah, N.R., and Mahmoudi, M. (2015). The role of DNA damage and repair in atherosclerosis: A review. *J Mol Cell Cardiol* 86**,** 147-157. doi: 10.1016/j.yjmcc.2015.07.005.

Shao, C., Folkard, M., Michael, B.D., and Prise, K.M. (2004). Targeted cytoplasmic irradiation induces bystander responses. *Proc Natl Acad Sci U S A* 101**,** 13495-13500. doi: 10.1073/pnas.0404930101.

Sharma, P.M., Ponnaiya, B., Taveras, M., Shuryak, I., Turner, H., and Brenner, D.J. (2015). High throughput measurement of gammaH2AX DSB repair kinetics in a healthy human population. *PLoS One* 10**,** e0121083. doi: 10.1371/journal.pone.0121083.

Shay, J.W., and Bacchetti, S. (1997). A survey of telomerase activity in human cancer. *Eur J Cancer* 33**,** 787-791. doi: 10.1016/S0959-8049(97)00062-2.

Shen, M.M. (2013). Chromoplexy: a new category of complex rearrangements in the cancer genome. *Cancer Cell* 23**,** 567-569. doi: 10.1016/j.ccr.2013.04.025.

Shi, L., Fujioka, K., Sun, J., Kinomura, A., Inaba, T., Ikura, T., Ohtaki, M., Yoshida, M., Kodama, Y., Livingston, G.K., Kamiya, K., and Tashiro, S. (2012). A modified system for analyzing ionizing radiation-induced chromosome abnormalities. *Radiat Res* 177**,** 533-538.

Shiloh, Y., and Ziv, Y. (2013). The ATM protein kinase: regulating the cellular response to genotoxic stress, and more. *Nat Rev Mol Cell Biol* 14**,** 197-210.

Shim, G., Ricoul, M., Hempel, W.M., Azzam, E.I., and Sabatier, L. (2014). Crosstalk between telomere maintenance and radiation effects: A key player in the process of radiation-induced carcinogenesis. *Mutat Res Rev Mutat Res*. doi: 10.1016/j.mrrev.2014.01.001.

Sorzano, C.O., Pascual-Montano, A., Sanchez De Diego, A., Martinez, A.C., and Van Wely, K.H. (2013). Chromothripsis: breakage-fusion-bridge over and over again. *Cell Cycle* 12**,** 2016-2023. doi: 10.4161/cc.25266.

Specht, L., Yahalom, J., Illidge, T., Berthelsen, A.K., Constine, L.S., Eich, H.T., Girinsky, T., Hoppe, R.T., Mauch, P., Mikhaeel, N.G., Ng, A., and Ilrog (2014). Modern radiation therapy for Hodgkin lymphoma: field and dose guidelines from the international lymphoma radiation oncology group (ILROG). *Int J Radiat Oncol Biol Phys* 89**,** 854-862. doi: 10.1016/j.ijrobp.2013.05.005.

Speicher, M.R., Gwyn Ballard, S., and Ward, D.C. (1996). Karyotyping human chromosomes by combinatorial multi-fluor FISH. *Nat Genet* 12**,** 368-375. doi: 10.1038/ng0496-368.

Spitz, D.R., Azzam, E.I., Li, J.J., and Gius, D. (2004). Metabolic oxidation/reduction reactions and cellular responses to ionizing radiation: a unifying concept in stress response biology. *Cancer Metastasis Rev* 23**,** 311-322. doi: 10.1023/B:CANC.0000031769.14728.bc.

Sproull, M., Kramp, T., Tandle, A., Shankavaram, U., and Camphausen, K. (2015). Serum Amyloid A as a Biomarker for Radiation Exposure. *Radiat Res* 184**,** 14-23. doi: 10.1667/RR13927.1.

Stephens, P.J., Greenman, C.D., Fu, B., Yang, F., Bignell, G.R., Mudie, L.J., Pleasance, E.D., Lau, K.W., Beare, D., Stebbings, L.A., Mclaren, S., Lin, M.L., Mcbride, D.J., Varela, I., Nik-Zainal, S., Leroy, C., Jia, M., Menzies, A., Butler, A.P., Teague, J.W., Quail, M.A., Burton, J., Swerdlow, H., Carter, N.P., Morsberger, L.A., Iacobuzio-Donahue, C., Follows, G.A., Green, A.R., Flanagan, A.M., Stratton, M.R., Futreal, P.A., and Campbell, P.J. (2011). Massive genomic rearrangement acquired in a single catastrophic event during cancer development. *Cell* 144**,** 27-40. doi: 10.1016/j.cell.2010.11.055.

Sullivan, J.M., Prasanna, P.G., Grace, M.B., Wathen, L.K., Wallace, R.L., Koerner, J.F., and Coleman, C.N. (2013). Assessment of biodosimetry methods for a mass-casualty radiological incident: medical response and management considerations. *Health Phys* 105**,** 540-554. doi: 10.1097/HP.0b013e31829cf221.

Suto, Y., Akiyama, M., Gotoh, T., and Hirai, M. (2013). A Modified Protocol for Accurate Detection of Cell Fusion-Mediated Premature Chromosome Condensation in Human Peripheral Blood Lymphocytes. *Cytologia* 78**,** 97-103. doi: 10.1508/cytologia.78.97.

Suto, Y., Gotoh, T., Noda, T., Akiyama, M., Owaki, M., Darroudi, F., and Hirai, M. (2015). Assessing the applicability of FISH-based prematurely condensed dicentric chromosome assay in triage biodosimetry. *Health Phys* 108**,** 371-376. doi: 10.1097/HP.0000000000000182.

Swartz, H.M., Flood, A.B., Williams, B.B., Meineke, V., and Dorr, H. (2014a). Comparison of the needs for biodosimetry for large-scale radiation events for military versus civilian populations. *Health Phys* 106**,** 755-763. doi: 10.1097/HP.0000000000000069.

Swartz, H.M., Williams, B.B., and Flood, A.B. (2014b). Overview of the principles and practice of biodosimetry. *Radiat Environ Biophys* 53**,** 221-232. doi: 10.1007/s00411-014-0522-0.

Symington, L.S., and Gautier, J. (2011). Double-strand break end resection and repair pathway choice. *Annu Rev Genet* 45**,** 247-271. doi: 10.1146/annurev-genet-110410-132435.

Szalai, V.A., Singer, M.J., and Thorp, H.H. (2002). Site-specific probing of oxidative reactivity and telomerase function using 7,8-dihydro-8-oxoguanine in telomeric DNA. *J Am Chem Soc* 124**,** 1625-1631.

Takahashi, A., and Ohnishi, T. (2005). Does gammaH2AX foci formation depend on the presence of DNA double strand breaks? *Cancer Lett* 229**,** 171-179. doi: 10.1016/j.canlet.2005.07.016.

Takai, H., Smogorzewska, A., and De Lange, T. (2003). DNA damage foci at dysfunctional telomeres. *Curr Biol* 13**,** 1549-1556.

Tchirkov, A., and Lansdorp, P.M. (2003). Role of oxidative stress in telomere shortening in cultured fibroblasts from normal individuals and patients with ataxia-telangiectasia. *Hum Mol Genet* 12**,** 227-232.

Terzaghi, M., and Little, J.B. (1976). X-radiation-induced transformation in a C3H mouse embryo-derived cell line. *Cancer Res* 36**,** 1367-1374.

Terzoudi, G.I., and Pantelias, G.E. (2006). Cytogenetic methods for biodosimetry and risk individualisation after exposure to ionising radiation. *Radiat Prot Dosimetry* 122**,** 513-520. doi: 10.1093/rpd/ncl509.

Testard, I., Dutrillaux, B., and Sabatier, L. (1997). Chromosomal aberrations induced in human lymphocytes by high-LET irradiation. *Int J Radiat Biol* 72**,** 423-433.

Testard, I., and Sabatier, L. (2000). Assessment of DNA damage induced by high-LET ions in human lymphocytes using the comet assay. *Mutat Res* 448**,** 105-115.

Thierens, H., Vral, A., Vandevoorde, C., Vandersickel, V., De Gelder, V., Romm, H., Oestreicher, U., Rothkamm, K., Barnard, S., Ainsbury, E., Sommer, S., Beinke, C., and Wojcik, A. (2014). Is a semi-automated approach indicated in the application of the automated micronucleus assay for triage purposes? *Radiat Prot Dosimetry* 159**,** 87-94. doi: 10.1093/rpd/ncu130.

Thompson, L.H. (2012). Recognition, signaling, and repair of DNA double-strand breaks produced by ionizing radiation in mammalian cells: the molecular choreography. *Mutat Res* 751**,** 158-246. doi: 10.1016/j.mrrev.2012.06.002.

Tommasino, F., and Durante, M. (2015). Proton radiobiology. *Cancers (Basel)* 7**,** 353-381. doi: 10.3390/cancers7010353.

Tubiana, M., and Aurengo, A. (2005). "La relation dose-effet et l'estimation des effets cancérogènes des faibles doses de rayonnements ionisants". Rapport commun de l'Académie Nationale de Médecine et de l'Académie des Sciences).

Tubio, J.M., and Estivill, X. (2011). Cancer: When catastrophe strikes a cell. *Nature* 470**,** 476-477. doi: 10.1038/470476a.

Tucker, J.D. (2008). Low-dose ionizing radiation and chromosome translocations: a review of the major considerations for human biological dosimetry. *Mutat Res* 659**,** 211-220. doi: 10.1016/j.mrrev.2008.04.001.

Tucker, J.D., Vadapalli, M., Joiner, M.C., Ceppi, M., Fenech, M., and Bonassi, S. (2013). Estimating the lowest detectable dose of ionizing radiation by the cytokinesis-block micronucleus assay. *Radiat Res* 180**,** 284-291. doi: 10.1667/RR3346.1.

Turinetto, V., and Giachino, C. (2015). Multiple facets of histone variant H2AX: a DNA double-strand-break marker with several biological functions. *Nucleic Acids Res* 43**,** 2489-2498. doi: 10.1093/nar/gkv061.

UNSCEAR (2010). "Sources and effects of ionizing radiation", in: *UNSCEAR 2008 Report to the General Assembly.* (New York: United Nations Scientific Committee on the Effects of Atomic Radiation).

Valdiglesias, V., Giunta, S., Fenech, M., Neri, M., and Bonassi, S. (2013). gammaH2AX as a marker of DNA double strand breaks and genomic instability in human population studies. *Mutat Res* 753**,** 24-40. doi: 10.1016/j.mrrev.2013.02.001.

Vaurijoux, A., Gregoire, E., Roch-Lefevre, S., Voisin, P., Martin, C., Voisin, P., Roy, L., and Gruel, G. (2012). Detection of partial-body exposure to ionizing radiation by the automatic detection of dicentrics. *Radiat Res* 178**,** 357-364.

Vaurijoux, A., Gruel, G., Pouzoulet, F., Gregoire, E., Martin, C., Roch-Lefevre, S., Voisin, P., Voisin, P., and Roy, L. (2009). Strategy for population triage based on dicentric analysis. *Radiat Res* 171**,** 541-548. doi: 10.1667/RR1664.1.

Viau, M., Testard, I., Shim, G., Morat, L., Normil, M.D., Hempel, W.M., and Sabatier, L. (2015). Global quantification of gammaH2AX as a triage tool for the rapid estimation of received dose in the event of accidental radiation exposure. *Mutat Res Genet Toxicol Environ Mutagen* 793**,** 123-131. doi: 10.1016/j.mrgentox.2015.05.009.

Vral, A., Fenech, M., and Thierens, H. (2011). The micronucleus assay as a biological dosimeter of in vivo ionising radiation exposure. *Mutagenesis* 26**,** 11-17. doi: 10.1093/mutage/geq078.

Wang, Z.Z., Li, W.J., Zhi, D.J., Jing, X.G., Wei, W., Gao, Q.X., and Liu, B. (2007). Biodosimetry estimate for high-LET irradiation. *Radiat Environ Biophys* 46**,** 229-235. doi: 10.1007/s00411-007-0110-7.

Watson, G.E., Lorimore, S.A., Macdonald, D.A., and Wright, E.G. (2000). Chromosomal instability in unirradiated cells induced in vivo by a bystander effect of ionizing radiation. *Cancer Res* 60**,** 5608-5611.

West, C., Azria, D., Chang-Claude, J., Davidson, S., Lambin, P., Rosenstein, B., De Ruysscher, D., Talbot, C., Thierens, H., Valdagni, R., Vega, A., and Yuille, M. (2014). The REQUITE project: validating predictive models and biomarkers of radiotherapy toxicity to reduce side-effects and improve quality of life in cancer survivors. *Clin Oncol (R Coll Radiol)* 26**,** 739-742. doi: 10.1016/j.clon.2014.09.008.

West, C., Rosenstein, B.S., Alsner, J., Azria, D., Barnett, G., Begg, A., Bentzen, S., Burnet, N., Chang-Claude, J., Chuang, E., Coles, C., De Ruyck, K., De Ruysscher, D., Dunning, A., Elliott, R., Fachal, L., Hall, J., Haustermans, K., Herskind, C., Hoelscher, T., Imai, T., Iwakawa, M., Jones, D., Kulich, C., Equal, E., Langendijk, J.H., O'neils, P., Ozsahin, M., Parliament, M., Polanski, A., Rosenstein, B., Seminara, D., Symonds, P., Talbot, C., Thierens, H., Vega, A., West, C., and Yarnold, J. (2010). Establishment of a Radiogenomics Consortium. *Int J Radiat Oncol Biol Phys* 76**,** 1295-1296. doi: 10.1016/j.ijrobp.2009.12.017.

WHO (2015). *Ionizing radiation: medical radiation exposure* [Online]. World Health Organization. Available: http://www.who.int/ionizing_radiation/about/med_exposure/en/ [Accessed June 10 2015].

Wieser, A., and Darroudi, F. (2014). EPRBioDose 2013: EPR applications and biological dosimetry. *Radiat Environ Biophys* 53**,** 217-220. doi: 10.1007/s00411-014-0535-8.

Wilkins, R.C., Beaton-Green, L.A., Lachapelle, S., Kutzner, B.C., Ferrarotto, C., Chauhan, V., Marro, L., Livingston, G.K., Boulay Greene, H., and Flegal, F.N. (2015). Evaluation of the annual Canadian biodosimetry network intercomparisons. *Int J Radiat Biol* 91**,** 443-451. doi: 10.3109/09553002.2015.1012305.

Wilkins, R.C., Romm, H., Kao, T.C., Awa, A.A., Yoshida, M.A., Livingston, G.K., Jenkins, M.S., Oestreicher, U., Pellmar, T.C., and Prasanna, P.G. (2008). Interlaboratory comparison of the dicentric chromosome assay for radiation biodosimetry in mass casualty events. *Radiat Res* 169**,** 551-560. doi: 10.1667/RR1272.1.

Wilkins, R.C., Romm, H., Oestreicher, U., Marro, L., Yoshida, M.A., Suto, Y., and Prasanna, P.G. (2011). Biological Dosimetry by the Triage Dicentric Chromosome Assay - Further validation of International Networking. *Radiat Meas* 46**,** 923-928. doi: 10.1016/j.radmeas.2011.03.012.

Wong, K.F., Siu, L.L., Ainsbury, E., and Moquet, J. (2013). Cytogenetic biodosimetry: what it is and how we do it. *Hong Kong Med J* 19**,** 168-173.

Wright, W.E., Piatyszek, M.A., Rainey, W.E., Byrd, W., and Shay, J.W. (1996). Telomerase activity in human germline and embryonic tissues and cells. *Dev Genet* 18**,** 173-179. doi: 10.1002/(SICI)1520-6408(1996)18:2<173::AID-DVG10>3.0.CO;2-3.

Yi, C., and He, C. (2013). DNA repair by reversal of DNA damage. *Cold Spring Harb Perspect Biol* 5**,** a012575. doi: 10.1101/cshperspect.a012575.

Yoshida, M.A., Hayata, I., Tateno, H., Tanaka, K., Sonta, S., Kodama, S., Kodama, Y., and Sasaki, M.S. (2007). The Chromosome Network for biodosimetry in Japan. *Radiation Measurements* 42**,** 1125-1127. doi: 10.1016/j.radmeas.2007.05.047.

Zhang, C.Z., Spektor, A., Cornils, H., Francis, J.M., Jackson, E.K., Liu, S., Meyerson, M., and Pellman, D. (2015). Chromothripsis from DNA damage in micronuclei. *Nature* 522**,** 179-184. doi: 10.1038/nature14493.

Zhang, J., Buonanno, M., Gonon, G., Li, M., Galdass, M., Shim, G., De Toledo, S.M., and Azzam, E.I. (2012). "Bystander effects and adaptive responses modulate in vitro and in vivo biological responses to low dose ionizing radiation," in *Radiobiology and environmental security,* eds. C.E. Mothershill, V. Korogodina & C.B. Seymour. (Netherlands: Springer).